UNCLASSIFIED

AD 275 857

reproduced
by the

ARMED SERVICES TECHNICAL INFORMATION AGENCY
ARLINGTON HALL STATION
ARLINGTON 12, VIRGINIA

$62-3-4$

275 857

Air force surveys in geophysics

No. 140

Proceedings of the national symposium on winds for aerospace vehicle design
Volume I

Norman Sissenwine

H.G. Kasten

(Co-Chairmen)

March 1962

ASTIA

GRD

AFCRL-62-273 (I)

PROCEEDINGS OF THE NATIONAL SYMPOSIUM ON
WINDS FOR AEROSPACE VEHICLE DESIGN

VOLUME I

N. Sissenwine and H. G. Kasten
Co-Chairmen

March 1962

Foreword

A Symposium on Winds for Aerospace Vehicle Design was held on 27-28 September 1961 at Laurence G. Hanscom Field, Bedford, Massachusetts. Cosponsors were the Geophysics Research Directorate, Air Force Cambridge Research Laboratories, Office of Aerospace Research; and the Deputy for Technology, Aeronautical Systems Division, Air Force Systems Command.

All papers stressed application of wind information to design problems. The audience was composed primarily of Air Force designers and contractors sent by the major design groups to hear and discuss these papers.

A review of hundreds of geophysical consultations with Air Force engineering interests shows that the behavior of atmospheric winds receives more consideration in aerospace vehicle design than any other geophysical element. Interactions on the aerospace vehicle due to departures of the wind from normal can result in aborted missions; they sometimes prove disastrous.

In the Symposium, five general design problem areas were discussed:

1. Launch pad stand-by and launch problems;
2. Boost wind profile problems;
3. Staging altitude wind profile problems;
4. Cruise altitude wind field problems;
5. Reentry and ballistic wind problems.

Discussions on these problems were oriented toward:

1. Descriptive material of the wind in forms applicable to design investigations;
2. Predictability of the winds (persistence, friendly area, silent area) in forms applicable to design consideration;
3. Measurability of the winds (surface, balloons, rockets);
4. Results of engineering studies of interactions of the wind with vehicles.

This Symposium had two purposes:

1. To bring the latest scientific information on wind behavior before the working-level designers and, through discussions among the various designer teams, to develop better understanding of the application and utilization of this information;
2. To provide research geophysicists with a better understanding of current and future design problems so that these scientists can orient their experimental and theoretical work toward necessary extension of knowledge of the wind field.

iii

Scientific papers describing the wind features were presented by scientists of the Geophysics Research Directorate and the national scientific community, based on the various interactions of the wind field on aerospace vehicles were programmed in the Air Force Systems Command aerospace, and

NORMAN SISSENWINE
Geophysics Research Directorate
Air Force Cambridge Research Laboratories

Aeronau...
Air Force Syst..

Acknowledgments

This symposium could not have been a success, nor even a Symposium, without the contributions of the men and engineers who presented papers, the panelists who took part in the last session, and chairmen of the various sessions who so capably kept the meeting on schedule. To all these, we extend our sincere appreciation.

We should also like to express our gratitude to Mrs. Lenora A. Baltimore and Mr. George S. McLean, Jr. of the Meteorological Development Laboratory for their accomplishments in arranging for the Symposium. These people worked strenuously for long hours through the summer preceding the Symposium and climaxed this effort by monitoring the orderly physical running of the meetings. Thanks are also tendered to Mrs. Helen Ross and Miss Sybil A. Berger for their aid to the team mentioned above, and to Mr. Charles Geold and Mr. John Hibbo for their operation of visual aid equipment and related arrangements.

Table of Contents
Volume I

Keynote Address

BRIGADIER GENERAL B. G. HOLZMAN, COMMANDER

AIR FORCE CAMBRIDGE RESEARCH LABORATORIES

Thirty years ago the most important concern that people had with
meteorology was whether or not it was going to rain. People wanted to
know if they should schedule a picnic, hang out the wash, or plant corn.
Weather forecasting itself was a rather primitive art.

We are all familiar with the great accumulation of meteorological
information we have gained since then. Most of this research progress
has been made since World War II. Almost all of the papers presented
at this conference are in research areas that would have been of little
interest one or two decades ago. We have examples of the great improve-
ments in the meteorological sciences that have come about only within the
past five or six years. In 1954 Hurricane Carol struck the New England
area with very little advance warning to the people of New England. Many
lives were lost that might otherwise have been saved. By contract,
Hurricane Car which struck the Galveston area was one for which those
living in the Gulf Coast region were completely prepared. It has been
estimated that a thousand lives were saved as a result of the excellent job
done of weather forecasting and in informing the people of the progress of
this hurricane.

We all know the attention given to winds before an atomic test or a
satellite launching. Detonations have been delayed sometimes for days and
at other times postponed altogether because the wind conditions on a given
day were not satisfactory. As an Air Force meteorologist, I participated
in many of the tests in the Pacific. We discovered that when detailed
measurements of the winds aloft were made, at hourly intervals, great
variations in wind speeds were noted. Accurate wind information was most
essential in calculating the differential ballistic wind for the precision
required in placing the atomic weapon over the target Zero. I have always
been disturbed by our lack of adequate wind information. The conventional
wind velocity and direction measurement made near the ground has very
little meaning without a gradient relationship.

Many years ago, I was involved in making measurements of the evaporation from land and water surfaces. In order to do this, it was essential to be able to calculate an exchange or transfer coefficient. This coefficient, frequency called the "Austausch", can be calculated by wind shear measurements, but it is necessary to have the shears known in detail along with the temperature stability relationships. I think that meteorologists can well look to improving the meteorological reporting network by incorporating gradient and detailed wind shear measurements.

We in AFCRL have had a part in many conferences devoted to research on wind and wind patterns. This is the first conference, however, that has been specifically devoted to problems of vehicle design from the standpoint of winds. At each layer of the atmosphere you have problems of turbulence and your vehicle must be built with the full knowledge of the wind structure at various altitudes within the atmosphere.

At AFCRL not only do we have the responsibility for carrying out research for the Air Force on wind and wind patterns, but we have the responsibility to disseminate our research results as widely as possible to all those who might be interested and who could make use of the work we are doing. It is this latter consideration that has caused us to sponsor this conference on winds for vehicle design. As you may know, we have only indirect interest in vehicle design as such. These are the problems of our sister organization, the Air Force Systems Command, which must be made aware of the special problems that unpredictable wind patterns might bring to bear on their missile and manned aircraft. The research information that we accummulate in these areas is made available to the Air Force Systems Command so that they might apply these to their advanced ideas in weapon systems design.

Judging from the very fine program that your Chairmen, Mr. Sissenwine and Mr. Kasten, have organized, I believe you have an extremely interesting and worthwhile conference. I hope that as a result of this conference those of you not associated with AFCRL will find that you have obtained a broader knowledge of our research program and that from this conference you will achieve a closer and more profitable work relationship with our scientists.

2

Review of USAF Wind Requirements and Related Documents for Aerospace System Design

H. G. KASTEN

C. J. SCHMID, JR.

AERONAUTICAL SYSTEMS DIVISION

AIR FORCE SYSTEMS COMMAND

ABSTRACT

This paper furnishes information that will be useful to engineers and techni-
cal personnel working in the general field of aerospace system design and
provides research geophysicists with a better understanding of the experi-
mental and theoretical work required to extend knowledge of the wind field.
The information contained in this document is concerned with general design
data to be used only for preliminary or comparative analysis of specifica-
tions or related documents to be checked for a final, detailed hardware
design investigation. It is not the intent of this paper to replace USAF
specifications and/or related documents by the text. Rather, this is an
expanded review of these documents intended to present a thumbnail sketch
of the literature. It should also be noted that this literature survey is by
no means complete.

ACKNOWLEDGMENTS

INTRODUCTION

With the advent of large ballistic guided missiles and aerospace-vehicle booster combinations, a great deal of effort must be devoted to the problem of designing weapon system equipment to withstand the atmospheric wind phenomena. Winds are one of the greatest variables in any type of flight and are often responsible for the critical design conditio. of vertically rising vehicles. It is necessary to consider the vertical and horizontal structure of the wind in detail. These design parameters are not easily predictable, however, so a sharp definition of wind phenomena effects on structural loads, vehicle motions, guidance requirements, and so on, cannot be formulated.

The phenomena has three principal characteristics: the steady wind velocity profile, the wind shears occurring in the neighborhood of jet streams, and the gust action that can take place at any time or altitude. A further problem is the possibility that combinations of these discrete phenomena might act simultaneously.

The literature on the wind problem is extensive but does not provide the vehicle designer with all the necessary requirements and data for optimum design. This paper will provide at least a partial survey of applicable documents, including specifications and specialized notes reporting the wind phenomena.

Although the data on the discrete elements of the wind phenomena are voluminous, information on simultaneous action of the wind elements is noticeably lacking. This combination data is just not available. It is hoped that the need for this knowledge will be satisfied in future years.

USAF WIND REQUIREMENTS

Current USAF wind requirements are in the form of military specifications, bulletins, standards and handbooks. Chart 1 summarizes these documents. A detailed review of these documents will show that the data available do not reflect the requirements. It is inherently difficult to inject new data into specifications on short notice. Therefore, as an interim procedure, information from Air Force Cambridge Research Laboratories' Reports has been applied directly to many hardware contracts as the design requirement.

Current philosophy on design of vertically rising vehicles is to use primarily a statistical load survey for final design. This involves the study and calculation of trajectory parameters, including vehicle loads, obtained by 'flying' through a sample of soundings on a digital computer.

The basic inability of discrete profiles to predict the one-percent peak load directly indicates that they are inadequate for final design purposes. For preliminary design analysis, however, which need not be especially accurate and which must very likely be made several times because of modifications in the vehicle, a quicker, though less accurate, method is needed. Properly designed and tested discrete profiles can fulfill this need and provide sufficiently accurate answers for preliminary design in a relatively short time.

Design requirements for combined wind, wind shear and gust loads are not currently available. Due to limitations in past measuring systems (which gathered the bulk of applicable wind data) the high frequency gust components were filtered out by the measuring system. For preliminary design an interim procedure can be used that combines the loads obtained from wind and wind shear studies with those obtained from gust studies employing a correlation coefficient of 1.0 to obtain the one-percent peak load due to combined winds, wind shear and gust loads. In this interim procedure it is assumed that the increase in load due to the gust effect is small compared with the design load contribution of the wind and shear analysis.

Hopefully the necessary measuring system and analysis tools to better define the wind phenomena will be available in the near future. Simultaneously, the development of a brief but sharply defined wind phenomena criterion for application to aerospace system design studies would fulfill the major needs of vehicle designers concerned with the contribution of the total wind phenomena.

RELATED DOCUMENTATION

At present, the most important source of up-to-date information on the wind problem is in papers and reports. Chart 2 tabulates some of these documents. Since much of this data has been collected by Air Force Cambridge Research Laboratories, many of the reports are GRD literature.

An examination of the chart will show that data for simultaneous combinations of the discrete phenomena is conspicuously absent. The non-existence of such information is due to the amount of time and cost required to gather it. Since designers must know the combined effects of winds, shears, and gusts on a structure or control system in order to progress in optimization studies on larger and more expensive weapon systems, instrumentation and techniques for determining realistic combination conditions are becoming mandatory.

CONCLUSIONS

Whether by intent or by accident, a philosophy of design criteria has been generated for the wind phenomena. As pointed out in the requirements and related documents discussions, the philosophy has been to include in hardware specifications data that is reported in related scientific literature. These data are not always entirely applicable to the specific equipment being designed.

This process of developing requirements is at best unsatisfactory. Much of the data is undoubtedly reliable, but the degree of accuracy may not be known. Difficulties arise when data is copied over and over again without any explanation or limitations placed upon it. Eventually some designer might accept the data as true instead of with the reservations and limitations the author intended.

The quality of design requirements is dependent on the knowledge of the originators. Great deficiencies can take place in requirements and thus provide the USAF with vehicles that are unnecessarily under- or over-designed. In either case the total system may be penalized--either by a catastrophic failure or through performance penalties due to excessive weight. A brief but sharply defined wind phenomena criterion applicable to aerospace system design studies is required.

FUTURE ACTIONS

1. Collect and evaluate available data on the total wind phenomena aspect.

2. Revise and improve USAF aerospace system specifications to reflect the newest reliable wind data based on required level of safety and an acceptable probability of failure.

3. Conduct applied research to determine system response to wind phenomena as related to criteria selection.

4. Coordinate with other government and industry organizations on realistic requirements for aerospace systems.

5. Initiate a program to ascertain the kinds of realistic conditions that will combine steady winds, shears and gusts.

6. Plan and implement a study to establish probabilities for all aspects of the wind phenomena at specific global locations.

7. Develop a brief but sharply defined wind phenomena criterion for application to aerospace system preliminary design studies.

6

GLOSSARY

Gusts - A sudden brief movement of air at a velocity in excess of the steady movement velocity.

Shears - (Wind Shear) The magnitude of the vector difference between the wind vectors at two altitudes divided by the thickness of the altitude interval (sec^{-1}).

Shear Angle - The angle between the upper (altitude) wind and the lower (altitude) wind vector (degrees).

Shear Thickness - The difference in height between the two winds used in a wind shear calculation (feet).

Turbulence - Turbulent flow motion is an irregular condition of flow in which the various quantities show a random variation with time and space coordinates, so that statistically distinct average values can be discerned.

Wind - Any movement of air; natural air in motion with any degree of velocity, direction, or density.

Wind Phenomena - Any facts and events of scientific interest on winds. For purposes of this paper, the elements of the phenomena are defined as steady wind velocity profiles, wind shears, and gust action.

CHART 1

SUMMARY OF USAF SPECIFICATION COVERAGE
WIND PHENOMENA

SPECIFICATION NUMBER	UPPER AIR WINDS	GROUND WINDS

USAF Specification Bulletin 106A General Environmental Criteria for Guided Missile Weapon Systems	APPLIES TO AIRBORNE VEHICLES
	
	1. Synthetic Wind Speed Profiles for Windiest U.S.A. Area
	  a. Peak Speed - 300 fps at 30-40,000 ft
	  b. Max. Shear - 45 fps/1000'
	  c. Probabilities: 1% to 50% (see bulletin)
	2. Synthetic Wind Speed Profiles for Calmest U.S.A. Area
	  a. Peak Speed - 213 fps (at 30-40,000 ft)
	  b. Max. Shear - 25 fps/1000'
	  c. Probabilities: 1% to 50% (see bulletin)
		APPLIES TO GUIDED MISSILES, SUPPORT EQUIPMENT & TEST RANGES
		
		1. Wind Data at a Point 10 Feet Above Ground (velocity in miles per hour)
		2. For Heights Other Than 10 Feet, Conversion Factors are Presented to Compensate From 2 to 100 Feet (same as MIL-STD-210A)

MIL-STD-210A 2 August 1957 Climatic Extremes for Military Equipment	APPLIES TO AIRBORNE VEHICLES
	
	1. Strong Winds: Strongest Winds to be Encountered at Altitude in Mid-Latitudes Occur Between 30,000 and 40,000 Feet
	2. Vertical Wind Profile Synthetic Wind Profile for the Windiest Area (Northeastern Part) of U.S.:
	  a. Peak Speed - 300 fps
	  b. Max. Shear - 45 fps/1000'
	  c. Probabilities: 1% only
	  d. Shear Thickness Indicated
		APPLIES TO ALL TYPES OF GROUND EQUIP.
		
		1. Wind Data for all Types of Locations:
		  a. Wind Velocities
		  b. Classes of Equipment
		  c. Gust Values
		  d. Distributions (same as USAF-106A)
		  e. Probability of Exceedance: 10%
		  f. Wind and Gust

8

CHART 1 (Cont.)

SUMMARY OF USAF SPECIFICATION COVERAGE
WIND PHENOMENA

SPECIFICATION NUMBER	UPPER AIR WINDS	GROUND WINDS
(Cont.)	APPLIES TO ALL TYPES OF AIRCRAFT	APPLIES TO ALL TYPES OF AIRCRAFT

ANC-22 Climatic and Environmental Criteria for Aircraft Design	1. Thunderstorms
	  a. Velocity
	2. Jet Streams
	  a. Velocity
	3. Hurricanes & Tornadoes
	  a. Velocity
	4. Effect of Wind on Aircraft Design
		1. Beaufort Scale of Wind Forces

	GENERAL APPLICATION TO USAF CONTRACTORS	GENERAL APPLICATION TO USAF CONTRACTORS

Handbook of Geophysics for Air Force Designers Revised Edition 1960	1. Synthetic Wind Speed Profiles Exceeding 1%, 5%, 10%, 20%, and 50% of the Winter for
	  a. the Windiest Areas of the U.S.
	  b. the Calmest Areas of the U.S.
	2. Tables of Wind Velocities, From Sea Level to 70,000 ft. which will be exceeded 10% and 50% of the time
	3. Horizontal Wind Profile Across the Jet Stream
	4. Wind Above 100,000 Feet
		1. Variation of Mean Wind Speed with Height in the Lowest 300 Feet
		2. Relation Between Surface Mean Wind Speeds and Peak Gusts
		3. Variation of Peak Gusts with Height in the Lowest 300 Feet
		4. Surface Wind Speed Probabilities 1, 2, 5, 10 & 20%
		5. Continental Wind Speeds by Month

9

CHART 1 (Cont.)

SUMMARY OF USAF SPECIFICATION COVERAGE
WIND PHENOMENA

SPECIFICATION NUMBER	UPPER AIR WINDS	GROUND WINDS
(Cont.)	APPLIES TO ALL TYPES OF AIRCRAFT	
MIL-A-8861(ASG) Airplane Strength and Rigidity, Flight Loads	1. Vertical Gusts (66, 50, 25 fps) 2. Aircraft Speed for Maximum Gust Intensity 3. Gust Load Factor (with formula) 4. Horizontal Gusts (66, 50, 25 fps) 5. Altitude Limitations (above and below 20,000 Feet)	
MIL-A-8862(ASG) Airplane Strength and Rigidity, Landplane Landing and Ground Handling Loads		APPLIES TO ALL TYPES OF AIRCRAFT 1. Mooring Gusts - Art. 3.4.4 a. Navy - 100 Knots From Any Horizontal Direction b. USAF - 65 Knots From Any Horizontal Direction
MIL-M-8856(ASG) Missiles, Guided: Strength and Rigidity Requirements	APPLIES TO GUIDED MISSILES Profiles as Outlined in AF Surveys in Geophysics No. 96 - ASTIA # AD 146870 Gusts - below 50,000 ft Probabilities of No Exceedence (Air-launched, SA, SS)	APPLIES TO GUIDED MISSILES Same as MIL-STD-210A

CHART 1 (Cont.)

SUMMARY OF USAF SPECIFICATION COVERAGE
WIND PHENOMENA

SPECIFICATION NUMBER	UPPER AIR WINDS	GROUND WINDS
	APPLIES TO AIRPLANES	APPLIES TO AIRPLANES
(Cont.)		

MIL-A-8865(ASG) Airplane Strength and Rigidity, Miscellaneous Loads	1. Probable loads due to gust
	   a. 30 fps (EAS)
	2. Parachute brake loads due to gust
	   a. 25 fps (EAS)
		1. Tail-to-wind-loads
		   a. 70 knot horizontal tail wind

CHART 2

SUMMARY OF GENERAL DOCUMENTATION
WIND PHENOMENA

DOCUMENT NUMBER	UPPER AIR WINDS	GROUND WINDS

Air Force Surveys in Geophysics No. 25 ASTIA #AD 28484 (Dec., 1952) A Survey of Available Information on the Wind Fields Between the Surface and the Lower Stratosphere by Widger	APPLIES TO AIRBORNE VEHICLES
	
	1. Background to Windfield Knowledge
	2. Charts for Air Motion in Troposphere: Position and Strength of Jet Stream
	3. Also:
	  a. Wind Variations
	  b. Vertical & Horizontal Shear
	  c. Jet Migrations
	  d. Clear Air Turbulence
		Note: Ground winds shall be considered as those occurring below 300 feet.

Air Force Surveys in Geophysics No. 57 ASTIA #AD 47816 (Nov., 1954) Windspeed Profile, Windshear, and Gusts for Design of Guidance Systems for Vertically Rising Air Vehicles by Sissenwine	APPLIES TO VERTICALLY RISING VEHICLES
	
	Wind Speed Design Profiles for Guidance System Analysis, and Qualifications to be Considered in Employing This Type of Analysis.
	1. Wind Speed Profiles for Windiest USA Area (Northeastern USA Region)
	  a. Peak Wind Speed: 300 fps at 35,000 feet
	  b. Peak Wind Shear 45 fps/1000 feet
	2. Wind Shears Due to Changes in Wind Direction
	
	ALTITUDE (10)3 ft / AVERAGE SPEED fps / DIR. SHEAR DEG/1000'
	0 to 2 — 15 — 180°
	30 to 40 — 50 — 10°
	60 to 80 — 40 — 40°	

12

CHART 2 (Cont.)

SUMMARY OF GENERAL DOCUMENTATION
WIND PHENOMENA

DOCUMENT NUMBER	UPPER AIR WINDS	GROUND WINDS
(Cont.)	3. Approximate Gust Shears GUST GRADIENT 1% PROBABLE DISTANCE: APPROX. GUST SHEAR EXCEEDING FT (SEC^{-1}) 19 0.60 39 0.56 59 0.51 79 0.45 99 0.39 4. Superposition of Maximum Wind Speed, Wind Shear, and Gust 5. Effective Gust Velocities 6. Probabilities (1 to 20%)	
Air Force Surveys in Geophysics No. 63 ASTIA #AD 59394 (Dec., 1954) Review of Time and Space Wind Fluctuations Applicable to Conventional Ballistic Determinations	APPLIES TO AIRBORNE VEHICLES 1. Short Time and Space Variations of the Wind Structure from 600 feet to 6,000 feet a. Average Change in Wind Speed for a 1 to 2 hour Period: 3 to 5 mph b. Standard Deviation of Wind Speed Difference for a 2 hour Period: 6 mph	APPLIES TO AIRBORNE VEHICLES 1. Local Wind Effects 2. Thunderstorms

CHART 2 (Cont.)

SUMMARY OF GENERAL DOCUMENTATION
WIND PHENOMENA

DOCUMENT NUMBER	UPPER AIR WINDS	GROUND WINDS
(Cont.) by Raginsky, Sissenwine Davidson Lettau	c. Average Change in Wind Direction for a 2 hour Period: 20° for Wind Velocities Less than 30 mph - 10° for Wind Velocities Greater Than 30 mph d. Average Variations Over a Distance of 20 Miles: Wind Speed: 2 mph Wind Direction: 10° to 15°	
Air Force Surveys in Geophysics No. 72 ASTIA #AD 78464 (Sep., 1955) Wind Variability as A Function of Time by Singer	**APPLIES TO AIRBORNE VEHICLES** Determination of Time Variability of the Winds to a Height of 38,000 feet for Muroc, Calif. 1. Brief Investigation of Variability of Winds Applies to Airborne Vehicles 2. Time Variability of Vector Change as a Function of Height for Time, Intervals From 30 min to 5 hours, Median Velocity Changes of: a. 2.0 mph (Time Interval of 30 min) b. 6.4 mph (Time Interval of 5 hrs)	
Air Force Surveys in Geophysics No. 96 ASTIA #AD 146870 (Mar., 1958)	**APPLIES TO AIRBORNE VEHICLES** 1. Probable Wind Speed Profile and Associated Shears for Patrick AFB, (Winter) a. Peak Speed = 298 fps at 40,000 ft b. Max. Shear - 46 fps/1000' c. Probabilities: 1% to 20%	

CHART 2 (Cont.)

SUMMARY OF GENERAL DOCUMENTATION
WIND PHENOMENA

DOCUMENT NUMBER	UPPER AIR WINDS	GROUND WINDS
(Cont.) Development of Missile Design Wind Profiles for Patrick AFB by Sissenwine	2. Probable Wind Speed and Associated Shears in the 30,000 to 40,000 foot Altitude Layer for Bedford, Mass. a. Peak Speed - 321 fps b. Max. Shear - 50 fps/1000' c. Probabilities: 1% to 20%	
Air Force Surveys in Geophysics No. 99 ASTIA #AD 152495 (April 1958) Evaluation of AN/GMD-2 Wind Shear Data for Development of Missile Design Criteria by Ivoskin & Sissenwine	APPLIES TO AIRBORNE VEHICLES Relationships between 1,000 - 3,000, and 5,000 ft Wind Shears, Wind Speeds and Altitude for Bedford, Mass. and Grenier AFB, N.H. 1. Frequency and Probabilities of 1,000, 3,000 and 5,000 foot Wind Shears for 5,000 foot Altitude Increments from Sea Level to 100,000 feet a. Peak Wind Speed - 321 fps b. Peak 1000 ft. Shear - 0.076 sec^{-1} Peak 3000 ft. Shear - 0.056 sec^{-1} Peak 5000 ft. Shear - 0.033 sec^{-1} 2. Probabilities: 1%, 5%, 10% and 20%	

15

CHART 2 (Cont.)

SUMMARY OF GENERAL DOCUMENTATION
WIND PHENOMENA

DOCUMENT NUMBER	UPPER AIR WINDS	GROUND WINDS
(Cont.) Air Force Surveys in Geophysics No. 117 ASTIA #AD 234551 AFCRC-TR 59-292 (Dec., 1959) Design Wind Profiles From Japanese Relay Sounding Data by Sissenwine, Mulkern & Salmela	**APPLIES TO AIRBORNE VEHICLES** Probability Curves of a Wind Being Exceeded at 3, 6, 9, 10, 11, 12, 13 and 15 km Levels, and Probability of the Maximum Wind Speed. Also 1% and 5% Profiles at 3, 6, 9, 12 and 15 km Levels (Japan)	
AFCRC-TR 57-288 ASTIA #AD 117228 (May, 1957) Studies of Wind Structure in the Lower Atmosphere by Blackadar & Buajitti	**APPLIES TO AIRBORNE VEHICLES** Boundary Layer Jet Profiles 1. Oklahoma 2. Texas 3. Maryland	

16

CHART 2 (Cont.)

SUMMARY OF GENERAL DOCUMENTATION
WIND PHENOMENA

DOCUMENT NUMBER	UPPER AIR WINDS	GROUND WINDS
(Cont.) Geophysical Research Papers No. 5 (Jun., 1950) Investigation of Stratosphere Winds and Temperatures From Acoustical Propagation Studies by A. P. Crary	APPLIES TO AIRBORNE VEHICLES Stratosphere Winds and Temperatures Are Obtained as Results of Summer Tests in the Canal Zone, Bermuda, and Alaska and of a Winter Test in Alaska 1. Wind Velocity vs Altitude (Sea Level to 200,000 ft) 2. Temp vs Altitude (Sea Level to 200,000 ft)	
ASTIA #AD 117177 (Apr., 1957) the Observed Mean Monthly Wind Fields in the Lower Stratosphere and Upper Troposphere Over North America by Wan-cheng Chiu	APPLIES TO AIRBORNE VEHICLES Investigation of Winds From 100,000 ft to 200,000 ft for Alaska, Canal Zone, Bermuda and New Mexico 1 Wind Velocities 2 Wind Velocity Variation with Altitude 3 Diurnal Variations	

CHART : (Cont.)

SUMMARY OF GENERAL DOCUMENTATION
WIND PHENOMENA

DOCUMENT NUMBER	UPPER AIR WINDS	GROUND WINDS
(Cont.) Air Weather Service Tech. Rep. 105-121 ASTIA #AD 60095 (Jan., 1955) Winds Over 100 Knots in the Northern Hemisphere by AWS	ALL AIRBORNE VEHICLES Directional Frequency Distribution of Winds Over 100 Knots (Tabulation) Profiles 1. Percentage Frequency of Winds Over 100 Knots by Height 2. Mean Wind Profiles and Mean Vertical Wind Shear (North America) 3. Maximum Wind Speed and the Height of its Occurrence Tabulation of Winds Over 100 Knots	
AFCRC-TN 59-496 ASTIA #AD 232529 (Nov., 1959) A Note Comparing 1-km Vertical Wind Shears Derived From Simultaneous AN/GMD-1A and AN/GMD-2 Winds-Aloft Observations by Saltmela & Sissenwine	APPLIES TO AIRBORNE VEHICLES A Comparison of 3000-ft Vertical Wind Shears Derived From Simultaneous Observations of AN/GMD-1A and AN/GMD-2 Wind Sounding Equipment	

18

CHART 2 (Cont.)

SUMMARY OF GENERAL DOCUMENTATION
WIND PHENOMENA

DOCUMENT NUMBER	UPPER AIR WINDS	GROUND WINDS
(Cont.)	APPLIES TO VERTICALLY RISING VEHICLES	
AFCRC-TN-59-652 ASTIA #AD 232530 (Dec., 1959) Space Probes and Persistence of Strong Tropopause Level Winds by Salmela & Sissenwine	Persistence of Wind Speeds Equal to or Exceeding Values of 185, 244, 274 and 303 fps at Jet Stream Levels Over Patrick AFB, Florida; Provides Information From Which the Winter Probability of Encountering Each of the Above-Mentioned Speeds for Various 12-Hour Periods Can Be Calculated Winter Frequency Distributions of Upper Winds Equal to or Exceeding 56, 74, 83, and 92 mps at Patrick AFB Between 8 km & 14 km	
NACA TN 3732 ASTIA #AD 99895 (Jul., 1956) An Investigation of Vertical-Wind-Shear Intensities From Balloon Soundings for Application to Air-plane & Missile Response Problems by H. B. Tolefson	APPLIES TO AIRBORNE VEHICLES Data Collected in Washington D.C. Vicinity 1. Profiles 2. Thickness and Velocities of Shear Layers 3. Frequency	

19

CHART 2 (Cont.)

SUMMARY OF GENERAL DOCUMENTATION
WIND PHENOMENA

DOCUMENT NUMBER	UPPER AIR WINDS	GROUND WINDS
(Cont.) AFCRC-TN 57-292 ASTIA #AD 117182 (Mar., 1957) Scientific Reports Nos 1 Thru 3 and Final Report on Wind Correlation by Arnold Court	APPLIES TO AIRBORNE VEHICLES Wind Data in Form of Statistical Arrangements for Seasons of Year and Geographical Locations	
GM-TM-0165-00258 by N. W. Trembath	APPLIES TO BALLISTIC MISSILES In Essence, Much of the Same as AFCRC-TN 57-292	
Memorandum by Sissenwine 9 Jul 1957		APPLIES TO AIRBORNE VEHICLES 1. Wind Velocities at 10 ft. Elevation 2. Calculated Risk 3. Associated Gusts
GM-42.3-17 FCR Specification No. 58-1 (Space Technology Laboratory)	APPLIES TO SOLID BALLISTIC MISSILES Same as GM-TM-0165-00258	

20

CHART 2 (Cont.)

SUMMARY OF GENERAL DOCUMENTATION
WIND PHENOMENA

DOCUMENT NUMBER	UPPER AIR WINDS	GROUND WINDS
(Cont.)	APPLIES TO GUIDED MISSILES	

NASA TN D-556 Jan., 1961 Investigation of the Cape Canaveral, Fla. Wind Magnitude and Wind Shear Characteristics in the Ten to Fourteen Kilometer Altitude Region by William W. Vaught	Cape Canaveral, Fla. (Annual Reference and March Reference)
	1. Wind Velocity Profiles
	   a. 0.1%, 2.2%, 15.9%, & 50% Probabilities
	   b. 1, 5, 10, & 50% Probabilities
	2. Wind Shear Profiles
	   a. 0.1, 1.0, 2.2, 5, 16, & 50% Probabilities
	3. Wind Velocity Change vs. Scale-of-Distance
	   a. 0.1, 1.0, 2.2, 5, 16, & 50% Probabilities	

Design Criteria for Wind Shears WADC MEMO WCLSSC-10 Sep., 1959	APPLIES TO VERTICALLY RISING VEHICLES
	1. Interim Wind Shear & Gust Load Requirements
	   a. 1% Wind Profile
	   b. Wind Shear Rates (1, 5, 10, & 20%)
	   c. Gust & Shear Requirements	

21

CHART 2 (Cont.)

SUMMARY OF GENERAL DOCUMENTATION
WIND PHENOMENA

DOCUMENT NUMBER	UPPER AIR WINDS	GROUND WINDS
(Cont.) WADC TR 59-504 Jul., 1959 Development of Interim Wind, Wind Shear, and Gust Design Criteria for Vertically-Rising Vehicles by Hobbs Criscione Mazzola Frassinelli	APPLIES TO VERTICALLY RISING VEHICLES CONTENTS SECRET Establishment of 1% Design Wind & Wind Shears From a Survey of Maximum Structural Loads Encountered in Each of 275 Winter "Flights" of a Simulated Thor Missile Fired From Patrick AFB 1. Front, Side, and Rear Winds 2. Validity of Wind Data 3. Number of Samples Required for Estimating the 1% Load Accuracy / Confidence / Level / Equal To 95% / 99% / 99.9% ± 5% / 351 / 607 / 990 ±10% / 88 / 152 / 243 4. Maximum Shear: (2,500 ft. Layer) 0.050 sec^{-1} 5. Maximum Wind Velocity: 270 fps 6. Gust Velocity + Max. Shear: 40 fps (1-cos)	

22

CHART 2 (Cont.)

SUMMARY OF GENERAL DOCUMENTATION
WIND PHENOMENA

DOCUMENT NUMBER	UPPER AIR WINDS	GROUND WINDS
(Cont.)	APPLIES TO VERTICALLY RISING VEHICLES _CONTENTS SECRET_	

WADD TR 61-99 (Dec., 1960) Wind, Wind Shear, & Gust Design Criteria for Vertically-Rising Vehicles as Recommended on the Basis of Montgomery, Alabama Wind Data by Mazzola Hobbs Criscione	_Establishment of 1% Design Winds and Wind Shears From a Survey of Maximum Structural Loads Encountered in Each of 200 "Flights" of Simulated Atlas, Minuteman, and Dyna-Soar Vehicles Fired From Montgomery, Alabama_
	1. Ratio of 1% Peak Load From Statistical Load Surveys to Maximum Load From the Discrete Profile: 1.15
	2. Percent Increase in 1% Peak Loads Due to Gust Effects:
	  a. Atlas: 7.1
	  b. Minuteman: 19.0
	  c. Dyna-Soar Booster: 2.5
	  d. Dyna-Soar Wing: 16.4
	  e. 1% Peak Wind: 260 fps
	  f. 1% Max. Shear: 0.035 sec^{-1}	

Low Altitude Jet Streams "Scientific American" Magazine (Aug., 1961) by Morton L. Barad	_GENERAL APPLICATION_ Nebraska Plains Study 1. Maximum Wind Velocity - 54 mph 2. Altitude Range to 5,000 ft 3. Day and Night Time Winds 4. Dallas Texas TV Tower Data	

CHART 2 (Cont.)

SUMMARY OF GENERAL DOCUMENTATION
WIND PHENOMENA

DOCUMENT NUMBER	UPPER AIR WINDS	GROUND WINDS
(Cont.) NACA RM L57A11 ASTIA #AD 126938 (Mar., 1957) Preliminary Measurements of Atmospheric Turbulence at High Altitude as Determined From Acceleration Measurements on Lockheed U-2 Aircraft by Coleman & Funk	APPLIES TO ALL AIRBORNE VEHICLES Data Up to 55,000 ft Over England and Western Europe Frequency Distribution of Derived Gust Velocity by Altitude	

Frequency Distribution for Altitude (in thousands of feet)

Gust Velocity U_{de} feet/sec	20 - 30	30 - 40	40 - 50	50 - 55
2 - 2.9	94	84	70	74
3 - 3.9	44	42	51	28
4 - 4.9	21	10	12	12
5 - 5.9	8	4	5	3
6 - 6.9	4	1	4	3
7 - 7.9	2	0	0	0
8 - 8.9	2	0	1	1
9 - 9.9	0	0	0	0
10 - 10.9	1	0	1	0

U_{de} = Derived Gust Velocity

CHART 2 (Cont.)

SUMMARY OF GENERAL DOCUMENTATION WIND PHENOMENA

DOCUMENT NUMBER	UPPER AIR WINDS	GROUND WINDS
(Cont.) NASA MEMO 4-17-59L, ASTIA #AD 216980 (Jun., 1959) Airplane Measurements of Atmospheric Turbulence at Altitudes Between 20,000 and 55,000 Feet for Four Geographic Areas by Coleman & Meadows	APPLIES TO ALL AIRBORNE VEHICLES Western U.S., England and Western Europe, Turkey, and Japan Results Similar to Those of NACA RM L57A11 Above; 1. Table of Derived Gust Velocity (four areas) 2. Frequency Distribution of Derived Gust Velocities by Altitude (four areas) 3. Frequency of Excedence of Given Gusts	
NACA RM L57G02 ASTIA #AD 140024 (Aug., 1957) Airplane Measurement of Atmospheric Turbulence at Altitudes Between 20,000 and 55,000 feet for Western United States by Coleman & Coe	APPLIES TO ALL AIRBORNE VEHICLES Western United States Information Similar to NACA RM L57A11 Above 1. Gust Velocities up to 13 fps Tabulated by Altitude	

CHART 2 (Cont.)

SUMMARY OF GENERAL DOCUMENTATION
WIND PHENOMENA

DOCUMENT NUMBER	UPPER AIR WINDS	GROUND WINDS
(Cont.) NACA RM L57L12 ASTIA #AD 151779 Summary of Locations, Extents and Intensities of Turbulent Areas Encountered During Flight Investigations of the Jet Stream From 7 Jan., 1957 to 28 Apr., 1957 by Mr. R. Copp	APPLIES TO ALL AIRBORNE VEHICLES Central U.S., Florida, and California Summary of Jet Stream Turbulence Data: 1. Extent of Turbulence 2. Maximum True Gust Velocity	
NACA TN 4332 ASTIA #AD 205674 (Sep., 1958) An Approach to the Problem of Estimating Severe and Repeated Gust Loads for Missile Operations by Steiner & Press	APPLIES TO ALL AIRBORNE VEHICLES Simple Methods of Estimating the Gust Loading, That will be Exceeded With a Given Probability Are Presented in Terms of Missile Response Parameters and Turbulence Parameters.	

Design Problem Analysis and Design Philosophy

NORMAN SISSENWINE

GEOPHYSICS RESEARCH DIRECTORATE

AIR FORCE CAMBRIDGE RESEARCH LABORATORIES

ABSTRACT

In arriving at a design criterion to be used in a calculated risk philosophy,
the appropriate distribution of the wind must be taken into account. The
selection of the appropriate distribution is possible only after a design
analysis is made based on a clear and detailed understanding of the problem.
A compromise may then be reached between the feasibility of design and the
risk of the various extremes in the distribution. It can be quantitatively
evaluated and decided upon by the aerospace vehicle management team, from
the evidence provided by the management's engineering design and geo-
physical consulting teams. Numerous examples of this analysis process
are given in this general discussion of wind design problems.

INTRODUCTION

The Geophysics Research Directorate of the Air Force Cambridge
Research Laboratories is responsible for extending geophysical knowledge
for the Air Force. About nine years ago, it was recognized that the
majority of potential 'customers' were designers of the future weapon
systems. A liaison was established with the Air Force design community
and a program was initiated to help engineers analyze geophysical problems,
to acquaint them with on-the-shelf geophysical information, to tailor both
specific and general solutions for them, and finally, to reorient research
where necessary. Since that time, nearly a thousand formal requests for
assistance have been recorded. Countless other requests were answered
without ever getting into the formal channels. About half of these requests
were in connection with some aspect of wind phenomena. It was found that
the problems were being defined, and the type of geophysical presentation
that was thought to be needed was being specified without consultation with
the geophysicists; design criteria were frequently being established with-

out a design philosophy--the acceptable calculated risk for the specific
areas and time periods of operation.

DESIGN PROBLEM ANALYSIS

Before turning to design philosophy, the importance of problem defini-
tion should be stressed by mentioning some of our wind problem encounters.
A unique wind problem, one of the first with which we came into contact
when we became missile minded, was related to inertial guidance platforms
being evaluated in an early version of an airborne intercontinental missile.
The problem was presented to us with the formal title, 'Air Mass Damping.'
It was related to oscillations of inertial guidance platforms that have a
natural frequency of 84 minutes, the period of a pendulum as long as the
earth's radius. Such a platform cannot sense, and consequently cannot
damp out, forcing factors to the system guidance that have a frequency of
84 minutes.

The original definition of the problem led us to believe that gust forces
(nicknamed 'air masses' despite the fact that this term has a special
meteorological meaning) would be deleterious to the system. Much digging
was required before it was determined that the pertinent wind features were
the components in the sinuous upper wind flow, which has wave lengths of
hundreds and thousands of miles instead of hundreds of feet. A Fourier
integral of the tail and cross-wind components, from intercontinental
flight level wind maps, revealed that these uncompensated winds could
create guidance errors of several miles.

The problem of choosing the stratospheric altitude at which a balloon
system can be maintained stationary with minimum power and fuel can be-
come quite tricky. The size of the power plant varies directly as the cube
of the extreme wind speed, and fuel comsumption as the cube of the average
wind. Since there is a fairly high correlation between average and extreme
wind speeds, it appears that the calmest altitude should satisfy both require-
ments.

The selection of optimum altitude, based only upon winds, can be in-
correct. Air density, which determines the buoyant force on the balloon
as well as the wind power available in a volume of wind and interrelates
the balloon design with the distribution of both wind and density, must be
considered. Larger balloons, which will have larger cross section for wind
loading, are required at higher altitudes. Despite this, until the speed at
100,000 feet exceeds the speed at 50,000 feet by 30 percent, less power and
fuel are required at 100,000 feet.

28

Getting back to earth, let us consider what appears to be a simple problem--surface winds. After all, there is nearly a century of surface wind records. Suppose a new missile is being designed. First, this vehicle must be available for its planned life as an active weapon, yet it must stand by on the launch pad in a readiness position, exposed day in and day out like a television antenna. In this instance the day-in and day-out winds are of small importance since the vehicle must withstand the extreme winds. The extremes occur with special weather situations associated with tropical or extratropical cyclones. The cleanest solution to this problem is to consider the extreme wind that occurs each year, rather than the frequency of cyclones.

Perhaps the military planners desire a readiness life of 25 years, and are willing to take a one-percent risk. The most straightforward approach is to obtain a distribution of maximum winds for a representative sample of 25-year periods. From these, the wind speed that has a one-percent probability of being exceeded in 25 years, the design criterion, can be determined. A representative sample of 100 requires a record of 2500 years. Fortunately, there are statistical theories that can be used, but the extensiveness of the effort required in applying these theories cannot be treated lightly.

A most important refinement is that each maximum-for-the-year wind speed used in the basic sample is a value obtained at a non standard height, and averaged over a time period dependent on the nature of the observing equipment and then-current observing practices. Is this time period the same time that it takes to tip over the erected missile? Is this anemometer altitude at the center of aerodynamic pressure? The gust that does the damage has a critical speed, duration and geometry that is interrelated with the down-wind and vertical dimensions of the missile. The wind data in the National Archives of the U.S., and that of other national weather services, were not collected for design problems. Some scientifically based adjustments, often somewhat arbitrary, must be made; these require serious consideration in the problem solution.

Let us now consider the launching of the missile. It has withstood these vicious cyclones for several years, but launching in a wind as strong as this stand-by design criterion, say 100 miles per hour, is not within the 'state-of-the-art.' Fortunately, the likelihood of its occurring during a launching operation will be less than one in a million. Now the day-in-day-out data become useful, but only several instead of many hundreds of years of record are needed for this part of the problem. From a distribution of hourly wind speeds, a reasonable criterion can be obtained,

29

weighing cost and complexity of design against calculated risk. Perhaps only one percent of the time will the wind gust geometry be more severe than the designer's calculations indicate would be critical for an initial design configuration. Working level designers and geophysicists therefore decide that this is a satisfactory design criterion because a one-percent risk appears reasonable.

DESIGN PHILOSOPHY

We made the transition into design philosophy as we did in the stand-by problem. Have we done a thorough job? For one, have we used the wind distribution from the worst location in which this missile may be called upon to operate? Does the operational concept include flying this vehicle under all kinds of weather, say heavy cloud cover? The wind distribution may be different in clear than in cloudy weather. How about season effects? If there are sharp seasonal variations, one percent on a year-round basis might prove to be a ten-percent risk during the windiest month, and for some military operations, this is much too great a risk to take that we will not be in business when given the order to push the button. On top of this, there is a great probability that this ten percent value, three days of the windiest month, might last for hours or days because there is quite a bit of persistence in weather. Such a delay could be fatal in a nuclear war. There is also the likelihood of other launching bases being inoperative concurrently.

Evidently, after the distribution of a critical parameter has been decided, a great deal of thought must be given to the design philosophy. However, in military circles, the design philosophy, the calculated risk decision, does not lie with designers or geophysicists. It is the prerogative of the management team who must act as expert witnesses: engineers by providing data on cost and difficulty of design, and geophysicists by indicating the risk incurred. The System Project Officer must make the final decision.

SHORT CUTS AND DIFFICULTIES

The approach thus far advocated is the following: (1) determine the critical representation of the wind from a diagnosis of the design problem; (2) develop a distribution of the critical representation of the wind; and (3) examine cost of design for various extremes of the distribution in order to arrive at a reasonable design with acceptable calculated risk. Complex statistical ways of showing this distribution are often required and many of

these will be discussed in later papers. Certain short cuts may prove helpful. One of these is to decide that there is no problem. It is quite obvious that if a surface-exposed object could withstand winds of several hundred miles per hour there is no need for a surface wind design criterion. Decisions of this type for upper winds are not as easy to make. Some decisions can cause trouble when incorrectly applied. Take a balloon system which must not be more than a certain distance from the point of release when it attains cruise altitude. A quick decision can be made as to whether or not a design problem exists. Extreme wind speed at each altitude for any given location can be estimated. These extremes will not occur simultaneously at all levels. If a simple calculation shows that the balloon is still within the acceptable distance if the extremes had occurred simultaneously and from the same direction, no design problem exists.

Unfortunately, this same treatment has been tried for missile boost wind profile design. Many will recognize that this type of wind profile, say one percent extreme at all altitudes, would create far less bending to and require less engine gimballing of vertically rising vehicles than a profile in which the wind speed is light or average at most altitudes, and one percent extreme at some critical altitude. Unfortunately, it cannot be entirely obvious, since some of the early missile designers did attempt to present design wind profiles that were synthesized from extreme speeds at all altitudes. Instead of over design, as they had intended, they had seriously under designed.

A difficulty with which we are frequently faced, after the problem is properly analyzed and the applicable wind distribution is specified, is obtaining the representative data sample. Several years ago it was quite difficult to get an acceptably accurate representative sample of 30,000-foot wind profiles for the boost problem.

Today, too late for consideration for some of our major missiles, upper air sounding equipment that will operate during the strong wind profiles of great importance in design is just coming into the inventory. But now we find there is a great need for wind profiles to four or five times this altitude. Also, details in the lower altitude profiles that had never before been considered and were hardly observed might be quite important.

It seems that we are always behind in obtaining the information required, even though we are in the forecasting business. This is not because we are poor forecasters. Several years ago we forecasted, and are continuing to forecast, the need for accurate information on wind behavior above altitudes attained by our balloon soundings, about 100,000 feet. Unfortunately, we are still having a difficult time convincing the powers that be of the need for such programs.

31

Managers in the aircraft and missile industry itself are somewhat at fault. They use the phrase 'all weather' with every system. They do not specify that they can build 'all weather' systems only if they have quantitative design information on critical weather parameters. Even today, there are urgent working level requests for information on winds and densities for boost glide vehicles, yet higher echelons in the Air Force, responsible for providing resources for geophysical programs, are unable to obtain verification of these requirements when they query the management level. Importance of the geophysical 'inputs' are deemphasized for reasons not entirely clear, yet the price of a single airplane or missile lost, or the cost of a major firing postponement due to weather, could cover much of the necessary geophysical research.

FORECASTING CAPABILITY

Forecasting should be brought into its proper perspective for design considerations. In many instances the design problem is one of reduced mission effectiveness rather than abortion of the mission due to inability to operate. In such cases, one may often compensate for the effect of the wind by using a forecast. The easiest prediction is specification of average conditions, the simplest form of climatology. For example, the average wind profile may compensate for much of the wind effect on a reentering nose cone, but the effect of the day-to-day variability around the average must be determined, perhaps by target and by season, before there is assurance that the system will operate within the accuracy called for in the Specific Operational Requirement.

It is good policy to design within this climatic variability, because a forecast is costly and its inclusion on an hourly or daily basis is sometimes difficult. If, however, the variability about the climatic average used as the prediction is too great for a reasonable configuration, the routine use of a synoptic prediction should be considered before resorting to a quantum jump in system complexity. Synoptic predictions necessitate knowledge of data on future forecasting capability. In some instances, these quantities can be estimated from current research on future forecasting techniques that have some likelihood of operational acceptance. When such research results are not available, a conservative approach (since forecasting improvements, although not negligible, are slow) is to use today's prediction capability, applied to realistic simulation of operational situations.

For silent area problems, special forecasting trials by operational forecasters are required to obtain these error data. Such tests have

been very infrequent and are limited in scope. Even nonsilent area wind
forecast accuracy data, which require no special situation simulation, are
far from extensive. The absence of forecasting accuracy data, even
though there is a real skill, can lead to design within climatic variability
in instances where it would be more desirable to use a synoptic prediction.
An unfortunate result is the deemphasis of need for a strong operational
prediction capability which would yield more effective systems. There has
been a little progress in the direction of documenting wind prediction
capability for design problems. It is hoped there will be further work along
these lines.

Global Wind Climatology

RODERICK S. QUIROZ

CLIMATIC CENTER, USAF

AIR WEATHER SERVICE

ABSTRACT

Available climatological wind data are surveyed for three realms of the
atmosphere--the air near the ground, the upper air, and the atmosphere
above 100,000 feet. Both published and unpublished sources of data are
considered, with special mention made of unpublished wind frequency dis-
tributions that have been prepared for stations throughout the world.
Wind variations not readily detectable from conventional wind summaries
are briefly discussed, namely, variations in periods less than 6 hours
and systematic seasonal and annual circulation reversals in the stratos-
phere. Deficiencies in existing coverage of wind climatology are noted.

INTRODUCTION

Over a period of many years, the Climatic Center, USAF, an organiza-
tion of the Air Weather Service, has provided climatological support to
agencies of the Air Force and Army, and to their contractors. As might
be expected, wind is among the parameters of prime concern. Much of the
work performed in the Center has had to do with the variability of wind at
the surface and in the upper air. Air route planning factors, structural
design winds, climatological fallout patterns, and runway wind distributions
are a few of the types of analyses made. Geographically, there is scarcely
an area of the world that has not been examined at one time or another. The
data input for these analyses is greatly varied. Full use is made of the re-
sources of the National Weather Records Center where the Air Weather
Service has an important component, and extensive use is made of pub-
lished and unpublished materials of foreign and domestic meteorological
services. In this brief survey of global wind climatology, a wide variety
of types of wind data will be noted.

SURFACE WIND DATA

Surface observational wind data are plentiful for most areas of the world. Since observing procedures vary, the data are not entirely homogeneous. In particular, differences in anemometer levels might make it necessary in some instances to introduce height correction factors based on knowledge of the micrometeorology of the air near the ground. Such adjustments may be particularly required in estimating the effect of wind on missiles and structures at heights between the usual observational levels.

Upper air wind observations, as recorded on punched cards in the National Weather Records Center, normally start at 150 meters above the ground in the case of observations taken by the United States weather services,* and at 500 meters above the ground at the majority of foreign-operated stations. Thus, unless special micrometeorological data are available, interpolation between the surface wind and the lowest recorded upper air wind is sometimes required. As is well known, the vertical wind gradient in the first few hundred meters above the ground depends on the roughness of the terrain, on the temperature lapse rate, and on the wind speed itself. Fortunately, the results of numerous series of micrometeorological observations taken at various places throughout the world are available to assist in making reasonable interpolations. Still, there are some situations in which, owing to the unique physical exposure of the site in question, meteorological insight is the only remaining basis for interpolation.

There are over 4000 stations for which detailed surface wind data, based on several years of observations, are available in unpublished form. Attempts to represent the earth's wind regimes have been made with much fewer data. A paper by Brose (1936) presents monthly mean wind speeds for over 300 stations evenly distributed throughout the world. For oceanic regions, the U.S. Weather Bureau's "Atlas of Climatic Charts of the Oceans" (1938) contains monthly charts of the prevailing and mean resultant winds, although more detailed data are now available in the U.S. Navy's recent (1955-59) series of climatic atlases of individual oceans of the world. In 1951, Lauscher made a further analysis of the data in the earlier sources just mentioned presenting maps of the earth's wind regimes, along with

---

*Refers to pilot balloon observations; first level of rawinsonde wind data is 1000 mb, applying to heights from the ground to about 1000 ft, depending on the synoptic situation.

special data for some of the windiest places on earth. (Lauscher also provided information that is probably totally useless in aerospace vehicle design; namely, the mean wind speed for the entire world--5.85 m/sec--which incidentally seems a little high.)

Somewhat more informative are wind probabilities and statistical estimates of maximum winds to be expected in specified numbers of years. This information has been prepared by various investigators for several areas of the globe. For example, extreme winds have been estimated by H.C.S. Thom (1959), among others, for the United States; and by Anapol'skaia and Gandin (1958) for the U.S.S.R. The question of whether to use peak gust speeds or maximum winds averaged over a minute or some other time interval has been gone into quite thoroughly by Davenport (1960), especially in relation to the dynamic response of anemometers and of the structures affected by the wind.

The approximate number of locations for which detailed surface wind statistics are available--4000--was mentioned above. These statistics consist of lengthy bivariate frequency distributions of wind speed and direction, generally arranged by months. Altogether there are close to 10,000 places in the world where wind is or has been systematically observed. These numbers are significant because they stress the fact that, although valuable data exist in published form, many more data are available in the form of unpublished machine summaries, and still more data are potentially available for summarization. Obviously, it is impractical to make these data available en masse. Aside from purely physical considerations, the intelligent use of the data depends on an awareness of the limitations in the original observations, the manner in which they were processed, and on the relation of the network of stations already summarized to the network of stations available for summarization. This knowledge can ordinarily be best communicated in the course of consultation and is most meaningful if the climatologist has a proper understanding of the client's operational or design problem.

THE UPPER AIR

In the past decade great progress has been made toward defining the detailed climatological wind patterns of the upper air. This progress has been due, in part, to the greater heights reached in rawinsonde ascents, especially since the mid-1950's. For the United States, available statistics show a steady rise in heights reached during the 1950's. For the critical area of the U.S.S.R., radio broadcast data have been the normal

37

source of upper air wind data, except for the period of the IGY and at least part of the ensuing IGC. In the early 1950's the broadcast Soviet upper air data rarely went higher than 300 mb. In January 1959, about 55 percent of these data were reaching 100 mb, but only one percent reached 25 mb (82,000 ft), as contrasted with 95 percent and 70 percent, respectively, for the United States. The Soviet IGY upper-air data received on microcards in the National Weather Records Center are much more impressive than the corresponding broadcast data. Already in July 1957, the microcards show 92 percent of the data reaching 100 mb, about 35 percent reaching 25 mb.

Upper-air flow patterns may be deduced either from the actual wind observations or from daily and monthly mean constant pressure maps. Daily hemispheric map analyses up to 100 mb are now routine. In recent years, daily analyses up to 25 and 10 mb have been drawn by several groups, notably the Stratospheric Analysis Project of the U.S. Weather Bureau, the Institut für Meteorologic at Berlin Free University, and the Arctic Meteorology Research Group at McGill University (Montreal, Canada). Hemispheric high-level mean maps from July 1955 on have been prepared by Pennsylvania State University; in the U.S.S.R., Dubentsov (1959) has reported on mean hemispheric maps at levels up to 10 mb, for individual months of the IGY.

Mean upper air charts based on several years of observations are enumerated in a Technical Memorandum of the Climatic Center (Quiroz, 1959). In this survey the discussion will be confined to several of the most outstanding compilations of upper air wind data having near-global coverage.

Major series of upper air climatological wind charts are listed in Table 1. The single source with comprehensive coverage of both hemispheres is the British Geophysical Memoir by Heastie, Stephenson, and Tucker; this is the well-known "Upper Winds over the World," in its 1960 reincarnation. At 60 mb (about 64,000 ft), Bannon and Jones (1959) also embrace both hemispheres. Two recent United States compilations, the Strategic Air Command's "Wind Factor Calculator," and Crutcher's "Upper Wind Statistics Charts of the Northern Hemisphere," are somewhat similar, yet I think their differences are more notable. One source, for example, presents seasonal data. whereas the other has monthly data. In an unpublished paper, Salmela and Sissenwine (1958) have indicated significant differences between mean vector winds computed for a season and for an individual month in that season. A further check of this point could be made by comparing

TABLE 1

PRINCIPAL SERIES OF UPPER AIR CLIMATOLOGICAL WIND CHARTS

Year	Source	Main Wind Parameters	850	700	500	300	200	150	100	50	30	15	Area and Period of Record
1960	Heastie, Stephenson, Tucker*	$\bar{V}$, σ_V		ms	ms	ms	ms	ms	ms				World (except Antarctic); 1949–53*
1960	USAF, SAC	$\bar{V}$, σ_V	m	m	m	m	m	m	m	m			Northern Hemisphere; POR varies by level, mainly 1949–53.
1959	Crutcher	$\bar{V}$, σ_V	s	s	s	s	s		s				Northern Hemisphere;† POR varies, mainly within 1948–58
1958	Wege, et al.	$\bar{V}$									s 30, 20 mb	s ††	Northern Hemisphere;§ 1955–57
1958–60	Lahey, et al.	$\bar{V}$, σ_V			m	m							Northern Hemisphere; 1945–53 (500 mb), 1950–57 (300 mb)
1957	Wege	$\bar{V}$		m	m	m	m		m	m			Northern Hemisphere; 1949–53
1955	Bannon and Jones	$\bar{V}$		m	m	m	m			ms 60			World (75°N–60°S); (data to 1953)
1961	Wiederanders	$\bar{V}$	m	m	m	m	m						Pacific Ocean (40°N–25°S); (avg of 4 yrs)
1956 –59	U. S. Navy	Wind roses	s	s	s	s	s		s				Oceans; POR varies

SYMBOLS: $\bar{V}$, mean vector wind (isotachs and streamlines); σ_V, vector standard deviation; $\bar{V}$, mean wind speed (isotachs); m, monthly; s, seasonal; ms, mid-season months. * Replaces 1950 edition. † Equatorial regions not analyzed at some longitudes. †† Summer only. § Not fully analyzed.

39

seasonal and monthly data in Volume 1 (1959) of a series of detailed machine
tabulations of upper air wind data for the United States prepared jointly by
the U.S. Weather Bureau and Sandia Corporation.

The military designer may well ask which of these documents may be
considered most reliable. The answer depends on the user's purpose and
on the statistical application he has in mind. Levels of interest, geographi-
cal coverage, period of record of the basic observations, accuracy of the
data--these factors must be taken into account in selecting the climatological
input. Beyond this, it is well to consider that the capacity for climatological
information in published documents is physically limited. The United States
weather services alone have produced, mainly by electronic means, de-
tailed upper air wind summaries for about 1000 locations throughout the
world. The more comprehensive of these contain between 100 and 200
sheets of frequency distributions per station, usually by months, and for
levels in some cases up to 10 mb (102,000 ft). It is not only impractical,
but perhaps also undesirable, for reasons mentioned earlier, to attempt
to publish these data. Meanwhile, they serve as an indispensable working
file, to be consulted in the course of finding solutions to specific design
problems.

The documents just referred to are all based on conventional wind
observations taken mainly at 12- or 24-hourly intervals by stations
oftentimes as much as 100 to 200 miles apart. Certain design problems
require knowing the manner in which wind varies in shorter intervals of
time and over shorter distances. There have been several special
observational programs emphasizing measurements at intervals of a few
minutes to several hours and over distances of a few miles to around 100
miles. Arnold and Bellucci (1957) published an excellent survey of such
data, and Elisaesser (1960) has made an even more comprehensive review.
Elisaesser shows that in general the wind variability increases with the
time interval and with the horizontal distance, maximum variability being
indicated at an altitude near 30,000 feet. For time periods less than 6
hours the wind variability is essentially independent of season and latitude.

For longer time periods, the geographical and seasonal variations become
appreciable. A further dependence on synoptic situation has been clearly
demonstrated by Eriksson (1961), in a thorough analysis of upper wind
structure as revealed by a network of Swedish stations taking approximately
hourly observations over a 4-year period.

Other aspects of wind variability* that the climatologist might well take into account are the rather systematic circulation reversals occurring in the stratosphere and mesosphere. The manner in which wintertime westerly winds are replaced by summer easterlies has been well described by Flohn (1959), Belmont (1961), and others.

Even more arresting are the stratospheric wind reversals reported at latitudes close to the equator. Here the reversals occur not seasonally but approximately once a year, actually at intervals of about 10 to 15 months. A highly detailed account of this phenomenon has been given recently by Veryard and Ebdon (1961) of England; Reed (1961), McCreary (1961), and others in the United States have also made detailed analyses. Reed's description is perhaps the most vivid yet published. His data show alternating bands of easterly and westerly winds, progressing downward from the highest level of observation (30 km), at intervals of approximately one year (Fig. 1). These bands are best defined near 25 km and become erratic near the tropopause. McCreary has shown that this phenomenon is present as far as 20° from the equator, and Veryard and Ebdon have shown that it may be detected to 30° N, although at this latitude the annual fluctuation is greatly dampened and is partly obscured by the seasonal component.

The climatological significance of these annual circulation reversals in the equatorial stratosphere is readily apparent if one is working with upper-air wind summaries based on several years of observations. In these summaries, the common practice is to combine all the observations of different years into frequency distributions representing months or seasons. Such summaries would tend to combine easterlies and westerlies, without showing the persistence of one or the other over periods of about one year. Also, a mean vector wind computed from these data would tend to have a smaller value than the mean vector wind calculated for individual years.

---

*Thus far no mention has been made of maximum wind speeds in the upper air or vertical wind shears. Wind shear has been analyzed in various published reports, for example, Dvoskin and Sissenwine (1958). Maximum winds have been tabulated by the Air Weather Service (1955), and by the Weather Bureau in an unpublished machine compilation (NWRC Job 2201). Special punched card decks documenting maximum wind speeds (> 100 mph) and maximum wind layers have been maintained by the Weather Bureau beginning with data in 1956.

41
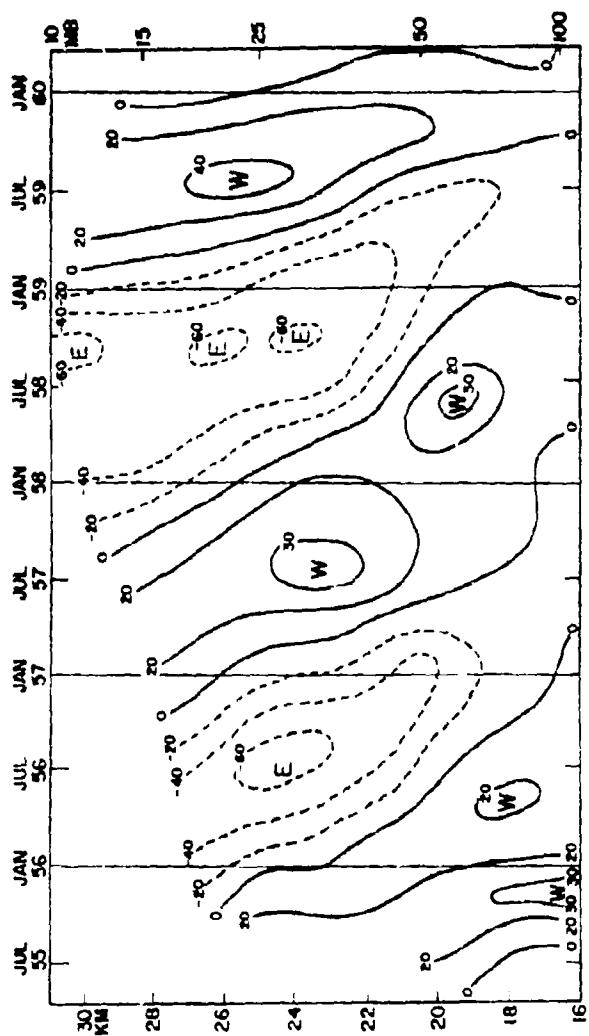
FIG. 1. Mean Monthly Zonal Wind Components, in Knots, Canton Island (3°S) Adapted from Reed (1961).

42

THE ATMOSPHERE ABOVE 100,000 FEET

Since air density decreases markedly with height, it would appear that wind would not have the same effect on a vehicle introduced into the upper atmosphere as it would farther down. Rather high wind speeds have been measured in the upper atmosphere, however, especially in the vicinity of 60 km (about 200,000 ft), so it seems appropriate to take these into account, and to consider if the data now available may be viewed climatologically.

By 1953 some 50 or 60 sets of isolated wind measurements were available for the upper atmosphere. These data, obtained by a wide variety of indirect observational techniques, were brought together by Miss H. Kallmann-Bijl at a Conference on Motions in the Upper Atmosphere (Albuquerque) in 1953, and were later issued in published form (I.U.G.G., 1954; Kaplan and Kallmann, 1957). In the period 1954-59, there was a somewhat more substantial sample of data reported in the literature, consisting primarily of:

       ~ 50   wind profiles (sound propagation measurements), at White Sands, Churchill, Denver, Guam, and in England

       ~ 50   missile measured wind profiles, at Cape Canaveral

       ~ 90   rocket chaff wind profiles, at White Sands, Tonopah, and Johnston Island

All these data refer to the period preceding the initiation of the Meteorological Rocket Network in late 1959. Since then the picture has greatly changed. In the 17-month period (October 1959 through February 1961) close to 500 wind soundings were obtained--several times the number of measurements previously available. The stations at which these soundings were taken are, in order of decreasing number of observations: Point Mugu, White Sands, Churchill, Wallops Island, Cape Canaveral, Holloman AFB, Fort Greely (Alaska), and Kauai (H.I.).

Circulation patterns in the upper atmosphere evolved from pre-1959 data have been described by Pant (1956), Murgatroyd (1957), and Attmannspacher (1959), among others. By late 1960 enough new data from the Meteorological Rocket Network had accumulated to allow a closer examination of wind behavior to moderately great heights. Batten (1961) has drawn new cross sections of the mean zonal wind up to a height of 100 km. Keegan (1961) has presented synoptic examples of wind distributions to a height of 55 km. At New York University, Bruch and Morgan (1961) have made a valuable statistical compilation, using data through September 1960.

43

Their report includes values of the mean $\underline{u}$ and $\underline{v}$ components of the wind by
months and seasons, at heights from 25 to 80 km, along with data on the
variability of wind in periods of 1 to 3 days, and data on vertical wind shears.
Data for eight stations of the rocketsonde network are presented. A maxi-
mum of wind speed occurs at around 60 to 70 km, somewhat paralleling
the maximum at jet stream level in the troposphere. Occasional westerlies
>200 knots in winter and easterlies >100 knots in summer have been
noted. The region 60 to 70 km, incidentally, is also the region of maximum
air density variability described in a recent report by the author (1961).
Further analysis of maximum winds and other aspects of wind behavior in
the mesosphere may be expected as more data are acquired by the rocket-
sonde network.

SUMMARY

Great progress in wind climatology has been made at practically all
levels of the atmosphere but certain deficiencies are still apparent. At
levels between the surface anemometer height and the first level of upper
air wind observations, our knowledge of wind behavior is far from complete.
The increased use of towers for micrometeorological observations is a
welcome trend. Modified pilot balloons for taking more detailed wind
measurements in the first thousand feet of air could also provide useful
data.

In the region of the middle stratosphere, above 50 mb (68,000 ft), the
existing climatological coverage is poor, especially in the southern hemi-
sphere. For the northern hemisphere, at least, the availability of synoptic
materials to 10 mb will undoubtedly lead to a better definition of the
climatological wind patterns. A deficiency may persist in the case of much
of Eurasia as long as we must depend on the radio broadcast version of the
upper air data. As was pointed out earlier, the Soviet IGY upper air data
received on microcards reached higher levels, but these data are for a
limited period.

At mesospheric levels, the frequency of wind soundings reaching
higher than 60 km (200,000 ft) is low. Increased coverage is needed for
the upper mesosphere and especially for the region just above the mesos-
phere (> 80 km), where indirect observational methods--for example, the
sodium cloud trail technique (Manring and others, 1961)--have indicated
erratic wind distributions and large vertical shears. Geographically, the
existing coverage is limited mainly to the North American area. Equatorial
latitudes are poorly represented. Finally, since the wind data available

44

from foreign rocket observational programs are few, the longitudinal span of wind coverage is also limited. These deficiencies, however, perhaps seem minor in the light of the tremendous progress made in recent times and the promise of further advances in observational techniques.

REFERENCES AND BIBLIOGRAPHY

Anapol'skaia, L. E. and Gandin, L. S. "Metodika opredeleniia raschetnykh skorostei vetra...." Meteorologiia i Gidrologiia, No. 10, 1958, pp. 9-17.

Arnold, A. and Bellucci, R., "Variability of ballistic meteorological parameters," U.S. Army Signal Engineering Labs., Technical Memorandum M-1913, 1957.

Attmannspacher, Walter, "On the existence of an upper stratospheric layer of maximum wind." Chapter 7 of: Cell structure of the atmosphere. Deutscher Wetterdienst, Offenbach, Contract DA/91/508/EUC/387, Final Report, 1959.

Bannon, J. K., and Jones, R. A., "The mean wind at 60 mb," Great Britain, Met. Res. Comm., MRP 925, 1955.

Batten, E. S., "Wind systems in the mesosphere and lower ionosphere," Journal of Meteorology, 18(3):283-291, June 1961.

Belmont, A. D., "The reversal of stratospheric winds over North America." General Mills, Inc. Contract AF 19(604)-6618, Final Report, 1961.

Brose, Karl, "Der jährliche Gang der Windgeschwindigkeit auf der Erde," Germany, Reichsamt fur Wetterdienst, Wiss. Abh., 1(4), 1936.

Bruch, Alvan and Morgan, G. M., "Wind variability in the mesosphere as determined by the tracking of falling objects," New York Univ. Dept. of Meteor., Contract AF 19(604)-6193, Final Report, May 1961.

Crutcher, H. L., "Upper wind statistics charts of the northern hemisphere," U. S. Office of Naval Operations, NAVAER 50-1C-535, Volumes I and II, 1959.

Davenport, A. G., "Rationale for determining design wind velocities," Proceedings of Amer. Soc. of Engineers. Journal of the Structural Division, 86(ST 5):39-68, May 1960.

Dubentsov, V. P., "Vosdushnye techeniia v stratosfere." Meteorologiia i Gidrologiia, No. 11:1-15, Nov. 1959.

Dvoskin, N. D. and Sissenwine, Norman, "Evaluation of AN/GMD-2 wind shear data for development of missile design criteria," U.S. AFCRC, AF Surveys in Geophysics, No. 99, 1958.

Ellsaesser, H. W., "Wind variability," U.S. Air Weather Service, Technical Report 105-2, 1960.

Eriksson, T.O., "Upper wind structure," Uppsala University, Meteor. Inst., Meddelande, No. 79, 1961.

Flohn, H., Holzapfel, R. and Oeckel, H., "Untersuchungen über die stratosphärische Oststromung auf der Sommerhalbkugel," Beitr, Phys. Atmos., 31:217-243, 1959.

Heastie, H. and Stephenson, P. M., "Upper winds over the world," Parts I and II, Great Britain, Met. Office, Geophysical Memoir No. 103, 1960. Tucker, G. B., Part III, Geophysical Memoir No. 105, 1960.

International Union of Geodesy and Geophysics, "Conference on motions in the upper atmosphere," I.U.G.G. Newsletter, 3(6):299-339, July 1954.

Kaplan, J. and Kallman, H. K., "Upper atmosphere research," U.C.L.A. Inst. of Geophysics, Contract AF 19(604)-111, Final Report, 1957.

Keegan, T. J., "Winds and circulations in the mesosphere," U.S. AFCRL, GRD Research Notes, No. 52, 1961.

Lahey, J. and others, Atlas of 500 mb wind characteristics. Wisconsin Univ., Dept. of Meteor., 1958. Also, Atlas of 300 mb wind characteristics, 1960.

Lauscher, Friedrich, "Über die Verteilung der Windgeschwindigkeit auf der Erde," Archiv für Meteorologie, Geophysik, und Biokl., B2(5): 427-440, 1951.

Manring, E. and others, "Upper atmospheric wind profiles determined from three rocket experiments," Geophysics Corp. of America, Contract NAS5-215, GCA Technical Report, 61-1-N, 1961.

McCreary, F. E., "Variation of the zonal winds in the equatorial stratosphere," U.S. Joint Task Force Seven, Meteorological Center, TP-20, 1961.

Murgatroyd, R. J., "Winds and temperatures between 20 km and 100 km, a review," Royal Met. Soc., Quarterly Journal, 83(358):417-458, 1957.

Quiroz, R. S., "A survey of upper air climatological information sources," U.S. Air Weather Service, Climatic Center, TM 59-4, Sept. 1959.

Quiroz, R. S., "Seasonal and latitudinal variations of air density in the mesosphere (30 to 80 kilometers)," Journal of Geophysical Research, 66(7):2129-2139, July 1961.

Reed, R. J. and others, "Evidence of a downward propagating, annual wind reversal in the equatorial stratosphere," Journal of Geophysical Research, 66(3):813-818, 1961.

Thom, H.C.S., Distributions of extreme winds in the United States. U.S. Weather Bureau, July 1959, Typescript, 23 p.

U.S.A.F. Strategic Air Command, "Climatological wind factor calculator," SAC Manual 105-2, Vol. I and II, 1960. (Standard deviation charts issued in AWS 3d Wea. Wg. Manual 55-5, 1960.)

U.S. Air Weather Service, "Winds over 100 knots in the Northern Hemisphere," AWS TR 105-121, 1955.

U.S. Office of Naval Operations, "U.S. Navy marine climatic atlas of the world," Volumes 1-5, NAVAER Publications 50-1C-528 through 50-1C-532, 1955-59.

U.S. Weather Bureau, Atlas of climatic charts of the oceans. Washington, 1938.

U.S. Weather Bureau - Sandia Corporation, Climatological data from WB-FCDA card deck. Volume I (Basic statistics), 1959.

Veryard, R. G. and Ebdon, R. A., "Fluctuations in tropical stratospheric winds," Meteorological Magazine (London), 90:125-143, 1961.

Wege, Klaus, "Druck-, Temperatur-, und Strömungsverhältnisse in der Stratosphäre über der Nordhalbkugel," Berlin Free Univ., Inst. fur Meteor., Meteor. Abh., 5(4), 1957 and 7(1), 1958. (Maps issued in English version by U.S. AWS 2d Wea. Wg.).

Wege, Klaus and others, "Mean seasonal conditions of the atmosphere at altitudes of 20 to 30 km," Berlin Free Univ., Inst. fur Meteor., Contract DA-91-508-EUC-210, Final Report, 1958.

Wiederanders, C. J., "Analyses of monthly mean resultant winds for standard pressure levels over the Pacific," Univ. of Hawaii, Meteor. Div., Contract AF 19(604)-7229, Sci. Report No. 3, 1961.

47

Applying Statistical Representations of Wind

ARNOLD COURT

GEOPHYSICS RESEARCH DIRECTORATE

AIR FORCE CAMBRIDGE RESEARCH LABORATORIES

ABSTRACT

Difficulties in the statistical description of wind, arising from its inherent vector nature and the difficulties of measuring it in the free air, are discussed. Means and standard deviations of components, their correlations, and resultant winds all are slightly underestimated in computations based on components derived from winds reported originally by speed and direction. Interpretations of time and space correlations of wind are discussed.

INTRODUCTION

Wind is the motion, in three dimensions, of air. This innate vector property makes wind much more difficult to measure, study, describe, and predict than other meteorological variables. Some of the difficulties in the description of wind vectors, and in applications of such descriptions, are the subjects of this paper.

Vertical motions of the atmosphere are, on the whole, one to three orders of magnitude smaller than horizontal motions. They may be neglected for most practical purposes, such as aerospace vehicle design. The present discussion, therefore, considers motion in only two dimensions.

Near the surface of the earth where fixed supports are available, wind is measured by the passage of air over such a fixed point, or by the pressure it exerts. Hence, variation with time at a single point, or simultaneous variations with distance, can be studied separately. But in the free air, without fixed supports, wind is measured by motion of something moving with the wind relative to a fixed point on the ground. Errors arising from failure of the balloon to follow the wind, and from the equipment used to track the balloon, will be discussed in other papers. In this paper, only certain computational errors are considered.

Because all measurements of wind in the free air are made from ob-

jects moving with or through the wind, no direct information is available on the variation of wind with time at a fixed point in the free air. Nor are truly simultaneous measurements possible of the wind speed at two points a given distance apart. In fact, none of the routine wind observations apply to a fixed point or a given instant; all are derived from balloon (or other) displacements, over intervals of time ranging from a few seconds to several minutes, and consequently are averages over that time period and over the space covered by the balloon during that period.

These basic limitations of the available wind information must be remembered by all who would compile and apply wind statistics. They are not especially inconvenient for the ordinary moments, the means and standard deviations of components of the wind for a given height interval in the general vicinity of an observing station. But these inherent limitations become progressively more restrictive as the observations are used to try to describe the simultaneous behavior of the wind in the vertical or the horizontal, or the wind variations over short time intervals.

Various tricks can be used to infer simultaneous space variations and single-point time variations of wind from the available information. Some of these will be discussed in other papers.

TRANSFORMATIONS

Whether it is measured by an instrument at a fixed point near the earth's surface or by an object (balloon) floating or rising through the free air, wind usually is reported in polar coordinates by direction and speed. But summaries and averages require conversion to rectangular (Cartesian) coordinates, causing difficulties in the statistical description and introducing biases into the means, standard deviations, and correlations.

The change from polar to rectangular coordinates, or vice versa, requires a transformation of the frequency distribution from one system to the other. Rectangular coordinates are an easier starting point than polar coordinates for discussing the general nature of bivariate frequency distributions.

Conveniently, each component of wind usually is assumed to have a normal, or Gaussian, distribution. This assumption seems to be generally acceptable, especially since no useful alternative exists. If the two components each are normally distributed, together they have a bivariate normal distribution. Such a distribution has five parameters or constants: the means and variances of the two components, and their correlation.

Unless both component means are zero, that is, the distribution is

50

centered at the origin, probabilities for specified portions such as circles of various radii cannot be evaluated directly. But graphs and tables for approximate evaluation have appeared in recent years.

Expression of this same distribution in polar coordinates is more complicated. The distribution of wind speed from any specified direction, that is, from some compass sector or from all directions combined, cannot be expressed directly; it involves an integral which can be evaluated only as a Bessel function. Despite this fact of mathematical life, many attempts have been made to describe the distribution of wind speeds by a gamma distribution (also called Pearson Type III). This would be the proper distribution if the components each had normal distributions with zero means. But since winds rarely average out to a mean of precisely zero, the gamma distribution doesn't provide a very good fit to observed wind speeds. On the whole, more satisfactory results are obtained by working with components.

BIASES

Certain biases result when component means, standard deviations, and correlations are computed from wind observations originally recorded by direction and speed. The difficulty is that the individual observations might have been recorded to the nearest degree, but usually have been grouped into sectors before averaging. The wind component means, hence the resultant wind, computed from observations grouped into sectors underestimates the true resultant (and its standard deviation) by an amount that increases as the distribution of winds becomes more and more asymmetric. For symmetric distributions, the correction factor is $\sin \phi / \phi$, when the angular width of each sector is 2ϕ.

When sectors are only ten degrees wide, so that the circle is divided into 36, no serious errors result from averaging. For wider sectors, the percentage error in the resultant is:

Number of sectors:	18	16	12	8	6	4
Sector width, deg:	20	$22\frac{1}{2}$	30	45	60	90
Resultant error, %:	0.51	0.65	1.15	2.62	4.72	11.07

Actually, these are minimum values, applicable when the basic wind distribution is symmetrical, or nearly so. The values increase with increasing asymmetry, but not very rapidly. Hence, components and resultant winds obtained from grouped data, and the standard errors of such components and resultants, should be increased by the indicated per-

centages to provide unbiased estimates of the true resultants and their variabilities.

An opposite correction is required for the standard deviations before this increase. The standard deviation computed for each component, from data originally reported in polar coordinates, is a slight overestimate. It should be reduced by an amount proportional to the mean square of the other component. The proportionality factor again increases with sector width.

The net effect of these two opposite corrections for standard deviation varies with the windiness. At places and levels where winds are predominantly zonal(west or east) and the meridional (north-south) component almost zero, the uncorrected standard error of the zonal wind is about as much an underestimate as is the uncorrected resultant, but the standard error of the meridional component is subject to two almost equal corrections. This still leaves the so-called 'standard vector deviation' underestimated by one or two percent.

Finally, the true correlation between the two components is also underestimated by the correlation computed for the components obtained by transforming from polar coordinates. The sample correlation should be increased slightly be adding an amount depending upon the means of the two components and the sector half-width ϕ, and then multiplied by another factor also depending upon ϕ. These two corrections increase the sample correlation coefficients by a few percent.

Most of the biases just discussed were found and explained by Dr. Robert Read of the Universities of California and Chicago when he was working on a research program for the Office of Civil and Defense Mobilization at the University of California. He has shown that statistics for wind components, derived initially from winds reported by speed and direction, are all biased. In general they should be increased by a few percent. This applies to component means and standard deviations, resultants, and to intercomponent correlations. However, it does not apply to time and space correlations; that is, the correlations between wind component and the same component (or the other component) at a different level, different place, or different time. But such correlations do require other corrections.

CORRELATIONS

Several years ago, when I was a consultant and contractor to GRD-AFCRL, I studied the correlations of wind components at various layers

in the atmosphere. From tabulations provided by the Air Weather Service, I extracted the statistics pertinent to such study for seven places and arranged them in a compact form, which has been used since by other groups and is familiar to most people concerned with vertical wind structure. Seasonal tables for some 60 stations have been compiled, as by-products of other studies, by the Air Weather Service's Climatic Center. Recently William W. Vaughan of NASA's Marshall Space Flight Center published monthly tables for six stations, from Panama to Berlin (NASA TN D-561), which are the most detailed and complete available at present.

In none of these tabulations have the component means and standard deviations, and the cross-component correlations, been corrected to allow for grouping bias. Read's study offers corrections for one widely used set of wind statistics. These are the once-per-day, serially complete wind records, originally compiled for the Federal Civil Defense Administration by Ben Ratner of the Weather Bureau, and analyzed in detail by Bernard Charles, then with Sandia Corporation.

The basic wind data used in this study had been grouped into 16 sectors, each 22-1/2 degrees wide, before averaging. Read's study showed that the component means and resultants should be increased by 1.3 percent, the standard deviations by varying amounts, and the cross-component correlations by 1 to 5 percent. He also showed that serial correlation causes the standard errors and all correlations to be underestimated by a few percent.

All these corrections and limitations are important to users of wind statistics in any form, including interlevel correlations. They show that, besides the deficiencies introduced by short records, missing data, errors of observation, and so on, the mechanics of computation cause serious uncertainties in the final statistics. Although most of the correlation tables offer three significant digits, the third is certainly not correct, and little reliance can be placed on the second one.

One consequence of these uncertainties concerns theoretical and empirical expressions for the manner in which the correlation between wind components at two levels decreases as the separation of the levels increases. Until more precision can be given the correlations calculated from available observations, none of the proposed models can be tested adequately. In the meantime, rather crude empirical expressions, such as those offered by Dr. Adam Kochanski (Journal of Meteorology, 18:151-159, April 1961), may be just as good as more elaborate methods, such as, for missile response computations, use of the square root of a matrix of uncorrected correlations.

53

Similar reservations apply to many other uses of wind statistics. The techniques of sampling, observation, and computation all introduce errors and biases so that the published figures are deceptive in their apparent precision. As other papers will indicate, each of these sources of error is under attack. But improvements in accuracy come slowly, and for the present the user should not place too much trust in the accuracy of the available statistics on wind.

Some Comments on the Elliptical Distribution of Wind Velocity

LEDOLPH BAER

GEORGE W. ROSENTHAL

MISSILE SYSTEMS DIVISION

LOCKHEED MISSILE AND SPACE COMPANY

ABSTRACT

Many of the meteorological problems in the aerospace industry require quick answers from general-purpose statistical summaries. Tables such as those published by Crutcher (NAVAER 50-1C-535) show that the distributions are truly elliptical as opposed to the easier-to-work-with circular. Recent publication of tables of the elliptical normal distribution allow a more exact interpretation of these summaries. Comparison is made between the results obtained under elliptical, circular, and univariate assumptions.

Large masses of wind data needed to set aerospace design requirements have been complied in recent years. Much of these data have been reduced for special problems; however, many problems arise that must be answered quickly, cheaply, and relatively accurately. This is facilitated by general purpose statistical summaries such as that published by Crutcher (1959), who presents enough information to compute the wind speed that occurs at any given probability assuming elliptical normality. This type of summary will give erroneous answers if the true wind distribution is not homogeneous and Gaussian such as occurs in a sea breeze region. In the upper air, except near the tropopause, the assumption of the elliptical normality is good for most geographical areas. Even where the assumption of normality is not valid, no general approach is yet available that is any better than computations based on the elliptical assumptions.

The purpose of this paper is to discuss the methods for using these general summaries. Four approaches have been used or advocated. These are compared in Table 1 for several examples.

TABLE 1

Comparison of the radii (in terms of σ_x) for various distribution assumptions*

PROBABILITY OF OCCURRENCE

	0.50	0.75	0.90	0.99	Condition	
1 Elliptical	1.18	1.66	2.15	3.03	$\mu_x = 0$	
2 Circular	1.18	1.66	2.15	3.03	$\mu_y = 0$	
3 'Upper Limit'	1.18	1.66	2.15	3.03	$\sigma_y = \sigma_x$	A
4. Undirectional	0.67	1.15	1.64	2.58		
1 Elliptical	0.93	1.35	1.79	2.67	$\mu_x = 0$	
2 Circular	0.97	1.37	1.77	2.50	$\mu_y = 0$	
3 'Upper Limit'	0.97	1.37	1.77	2.50	$\sigma_y = 0.6\sigma_x$	B
4 Undirectional	0.67	1.15	1.64	2.58		
1 Elliptical	0.71	1.17	1.66	2.58	$\mu_x = 0$	
2 Circular	0.85	1.20	1.55	2.18	$\mu_y = 0$	
3 'Upper Limit'	0.85	1.20	1.55	2.18	$\sigma_y = 0.2\sigma_x$	C
4 Undirectional	0.67	1.15	1.64	2.58		
1 Elliptical	2.30	2.94	3.53	4.55	$\mu_x = 2.0\sigma_x$	
2 Circular	2.30	2.94	3.53	4.55	$\mu_y = 0.5\sigma_x$	
3 'Upper Limit'	3.24	3.72	4.21	5.09	$\sigma_y = \sigma_x$	D
4 Undirectional	2.06	2.73	3.34	4.39		
1 Elliptical	2.15	2.80	3.39	4.41	$\mu_x = 2.0\sigma_x$	
2 Circular	2.22	2.76	3.24	4.09	$\mu_y = 0.5\sigma_x$	
3 'Upper Limit'	3.47	3.87	4.27	6.59	$\sigma_y = 0.6\sigma_x$	E
4 Undirectional	2.06	2.73	3.34	4.39		
1 Elliptical	2.06	2.73	3.33	4.37	$\mu_x = 2.0\sigma_x$	
2 Circular	2.18	2.66	3.09	3.81	$\mu_y = 0.5\sigma_x$	
3 'Upper Limit'	3.71	4.06	4.41	4.68	$\sigma_y = 0.2\sigma_x$	F
4 Undirectional	2.06	2.73	3.34	4.39		

μ_x = mean of the marginal distribution parallel to the major axis of the ellipse.
μ_y = mean of the marginal distribution normal to the major axis of the ellipse.
σ_x = standard deviation of the marginal distribution parallel to the major axis.
σ_y = standard deviation of the marginal distribution normal to the major axis.

The 'best' estimate is shown on the first line of each section of the table. The word 'best' is used because this was computed from tables of Rosenthal and Rodden (1961) allowing each component mean and standard deviation to vary independently. Of course, if a real case is not truly normal, neither

*Values shown are extracted from the tables of Rosenthal and Rodden (1961), Vitalis (1956), and Burington and May, (1953).

this nor any other approach discussed is correct. These tables were computed at Lockheed because no other were available. Several others (Germond, 1949; DiDonato and Jarnegin, 1960; Lowe, 1960) have had similar but non-meteorological problems and have independently computed tables so that some choice is now available. These other tables do not cover all the range of probabilities required.

The second line of each section of the table shows the speed associated with the various probabilities under the 'circular normal assumption.' This approach assumes that the variances in the two component directions are equal and independent such that

$$2\bar{\sigma}^2 = \sigma_x^2 + \sigma_y^2$$

where $\bar{\sigma}$ is a mean standard deviation equal to $1/\sqrt{2}$ times the standard vector deviation of Brooks and Carruthers (1953). For case A shown at the top of Table 1 the first and second lines are identical, but as the ratio of σ_y to σ_x decreases, and the probability increases, the circular assumption gives poorer and poorer results. At 99 percent for $\mu_x = \mu_y = 0$ and where $\sigma_y/\sigma_x = 0.2$, the circular assumption is shown to be $0.4 \sigma_x$ too small, a difference of over 15 percent!

The 'upper limit' of the wind distribution has been spoken of as synonymous with the upper limit of the circular distribution:

$$Pr\left[x \le (\mu + K\bar{\sigma})\right] = \alpha$$

where K is found by assuming $\mu = 0$ and circularity. This 'upper limit' is shown in the third line of each section of the table. In the first three sections where the means are zero, line 3 is identical to line 2 and, of course, has the same 15 percent error when $\sigma_y/\sigma_x = 0.2$. At nonzero values of the mean this varies--even going to the opposite extreme when $\sigma_y \ll \sigma_x$. For comparison, similar values are shown for a one-dimensional distribution based on the standard deviation of the major axis component as if it were oriented along the resultant mean.

In conclusion, for a truly elliptical normal distribution of winds, assumptions of circular normality are dangerous unless the ratio of σ_y to σ_x is near unity. Also, note that the errors are always biased in the same direction. Perhaps it is worth pointing out the σ_x and σ_y used here must be for independent components. If there is some correlation between the original components studied, then the axes must be rotated until they are independent before making

57

the test.* Some summaries, such as that previously referenced (Crutcher), have already rotated the axes. The most important parameter missing from such summaries is some measure of the normality of the component distributions.

REFERENCES

C.E.P. Brooks and N. Carruthers, 1953: Handbook of Statistical Methods in Meteorology. London: Her Majesty's Stationery Office.

Burington and May, 1953: Handbook of Probability and Statistics, New York, McGraw-Hill.

H. L. Crutcher, 1959: Upper Wind Statistics Charts of the Northern Hemisphere, NAVAER 50-1C-535. 2 vols. Office of the Chief of Naval Operations.

A.R. DiLonato and M.P. Jarnagin, 1960; Integration of the General Bivariate Gaussian Distribution over an Offset Ellipse, Rept. No. 1710. U.S. Naval Weapons Laboratory, Dahlgren, Va.

H.H. Germond, 1949; Integral of the Gaussian Distribution over an Offset Ellipse, Paper p-94. The Rand Corp., Santa Monica, Calif.

J.R. Lowe, 1960; Integration of the Bi-normal Distribution over an Offset Circle, ARDE Memorandum (B) 5/60, Armament Research and Development Establishment, Fort Halstead, Kent, England.

G.W Rosenthal and J.J. Rodden, 1961; Tables of the Integral of the Elliptical Bivariate Normal Distribution over Offset Circles, LMSD-800619. Lockheed Missiles and Space Division, Sunnyvale, California.

J. A. Vitalis, 1956; Table of Circular Normal Probabilities, Report No. 02-949-106. Bell Aircraft Corp., Buffalo, N.Y.

---

*The rotated means and variance can be given simply for a right-handed coordinate system as follows:

Let μ_x and μ_y denote the means, and σ_x^2 and σ_y^2 denote the variances with primes denoting the values after rotation;

then $\mu_{x'} = \mu_x \cos \Theta + \mu_y \sin \Theta$

$\mu_{y'} = -\mu_x \sin \Theta + \mu_y \cos \Theta$

and $\sigma_{x'}^2, \sigma_{y'}^2 = \dfrac{\sigma_x^2 + \sigma_y^2}{2} \pm \sqrt{\left(\dfrac{\sigma_x^2 - \sigma_y^2}{2}\right)^2 + (\rho \, \sigma_x \sigma_y)^2}$

where $\Theta = 1/2 \arctan \left(\dfrac{-2\rho \, \sigma_x \sigma_y}{\sigma_x^2 - \sigma_y^2}\right)$.

Surface Wind Observations and Anemometry

RUSSELL M. PEIRCE, JR.

GEOPHYSICS RESEARCH DIRECTORATE

AIR FORCE CAMBRIDGE RESEARCH LABORATORIES

ABSTRACT

The majority of present climatic wind surveys are based on the standard hourly weather observations made at Weather Bureau and military installations. Studies of gustiness, the calculations of gust factors, and the determination of risk quantities for the return of certain wind velocities during a given period, all based on these observations, are of meteorological interest to the designer of missile and launch pad stand-by facilities. Electrical and mechanical characteristics of present wind measuring equipment, particularly Wind Measuring Set AN/GMQ-11, are discussed and limitations are noted. Characteristics of equipment currently under development, as well as that contemplated for future development, are also discussed.

Perhaps more than any other meteorological parameter, surface winds vary greatly with time and location. In addition to the internal perturbations such as cyclonic and anticyclonic systems, fronts, squall lines, etc., effects such as thermal stratification in the lower layers, surface frictional effects and local topography contribute to the varying nature of the surface winds. Tabulations of wind direction and speed, averaged over five-minute periods, comprise the bulk of climatic data currently available. Since these values will be exceeded no more than half of the time, extrapolation beyond indicated limitations is extremely risky. As it is neither feasible nor economical to design a vehicle to be launched under extreme wind conditions, it behooves the design engineer to adopt a philosophy in which stand-by and launching wind design criteria are separated; furthermore, applicable local meteorological records should be utilized in establishing acceptable calculated risk quantities.

It must be recognized that various types of instrumentation with different mechanical and electrical characteristics, are still being used to obtain climatic information. The characteristics of the aerovane type of wind instrument used at most military sites vary from those of the three-cup anemometer used by the Weather Bureau. These different characteristics yield data that cannot be

properly correlated. Since both of these units have their limitations, development is currently underway for improved equipments having greater accuracy and the capability of operating under more severe weather conditions.

A vehicle and its associated ground support equipment, during a stand-by period of perhaps many years, would be damaged by the wind if it were designed to withstand the launch wind with only an acceptable calculated risk. To eliminate the effect of wind on a vehicle in the stand-by condition, attention must be given to the extremes of dynamic pressure caused by peak gusts superimposed on a strong wind. Rapidly amplifying self-induced vibrations can also develop when the vehicle is exposed to a steady wind of moderate speed. Thus, in the design of a vehicle and launch area facility for a given stand-by period, a knowledge is needed of the change of wind speed with height in the first 300 feet of the atmosphere as a function of the speed at anemometer height. Depending upon gust size with the downwind dimension of the vehicle, gusts can exert sufficient short-term differential wind loading to damage or destroy a structure even though steady winds may be well within design limits.

Most climatic data available at present is obtained from standard U. S. Weather Bureau and military hourly weather observations. Wind speed and direction values are obtained from anemometers located at representative sites as far from surrounding obstructions as possible. The average height of the sensor at Weather Bureau installations is twenty feet, and at military installations, thirteen feet. Reported wind speed and direction values are obtained from either direct reading indicators or stripchart recorders. In the former case, readings are made by observing and reporting the average wind speed and direction occurring in a one-minute period; an averaging period of five minutes is used when values are obtained from the recorder. In addition to wind speed, the peak gust (highest speed momentarily indicated without regard to duration) is also reported and appears in standard climatological records. This value is taken directly from the instantaneous trace on a recorder. The reported winds represent only an average, and consequently are exceeded less than half of the time, a fact that must be taken into consideration in the design of launch pad stand-by facilities.

Climatic data gathered in this manner, as well as data collected in many special studies, have yielded results of significant interest to the missile designer. It has been found that at any given time the vertical change in wind direction in the lowest 300 feet of the atmosphere is negligible, particularly when the overall airflow is strong and the location is free of major obstructions. The variation of mean wind speed V at height z, when the mean wind speed at the anemometer level is known, can be approximated by one of the following analytical expressions:

Simple Power Law:

$$V \sim z^a \tag{1}$$

Generalized Power Law:

$$V \sim \left[(z + z_o)^{1-b} - z_o^{1-b} \right]^{(1-b)} \tag{2}$$

Logarithmic Law:

$$V \sim \log (1 + z/z_o) \tag{3}$$

Extended Logarithmic Law:

$$V \sim \log (1 + z/z_o) + f(z, V_1, T') \tag{4}$$

In these expressions a and b are constants; z_o is a length known as the surface roughness parameter, and $f(z, V_1, T')$ is an analytical function of height, wind speed and the mean vertical temperature gradient at the reference level. The derivation and use of these expressions have been dealt with more extensively.[1-5]

There is evidence that the exponent a appearing in Eq. (1) is a function of topography and thermal stratification of the layers near the surface and distance above the ground, as well as the overall air flow. Its value over rough ground or at heights near the ground is greater than that over relatively smooth ground and at greater heights. Excluding cases of intense surface heating or cooling and weak overall air flow, the numerical value of a may be chosen to equal 0.20 as a good approximation. In computing wind profiles near the earth's surface, the simple power law is permissible only for crude estimates. Much of the error incurred through the use of this expression can be eliminated by use of the generalized power law and the logarithmic laws, because they have the advantage that the dependency on terrain features is incorporated in the z_o term.

It has been found that the exponent b appearing in Eq. (2) depends primarily on thermal stratification, and to a degree on height above the surface. For neutral conditions (that is, $T' = O$), the value of b is unity. Although the behavior of b and the analytical function appearing in Eq. (4) are not well known at levels above 30 feet at the present time, it has been shown[5,6] that b can be computed by combining Eqs. (2) and (4). For relatively strong air flow, it is known that intense surface heating or cooling causes only a small deviation of thermal stratification from the neutral. In such cases, the logarithmic law might represent the true conditions with a relatively high degree of accuracy. Mean numerical values of the a and b constants, determined from information gathered during the Great Plains Turbulence Field Program and other sources, are presented in the Geophysics Research Directorate's Handbook of Geophysics.[7]

If vehicles must be in a stand-by condition for any length of time in exceptionally windy areas, the designers and operators of the vehicles and related support equipment must take into account the gustiness of the wind which appears as fluctuations on a continuous trace of wind speed over a period of time. Gustiness varies with exposure and location, surrounding topography, characteristics of the upwind trajectory to a length of approximately fifty times the anemometer height, mean wind speed and vertical temperature gradient. However, relatively few weather stations record wind speed data with sufficient accuracy to permit a detailed analysis of the interrelationship of all factors.

Gustiness is referred to in terms of a gust factor or the ratio of the peak wind speed for a given duration to the mean wind speed for a five-minute averaging period. Variations in either gust duration or length of averaging period will directly affect the numerical value of the gust factor. The shorter the duration of the peak speed and/or the longer the averaging period time interval, the larger the numberical value of the gust factor. Several numerical values of average gust factors for various wind speeds and gust durations, based on the works of Deacon[2], Carruthers[8] and Sherlock[9, 10] are presented in the Handbook of Geophysics[7]. Their work also indicates that there is no real variation of gust factor with mean speeds greater than 30 knots. Data available at present point toward the fact that gust factors for peak wind speeds of two-second duration, obtained during the five-minute averaging period and from instrumentation located at a height of approximately 20 feet above the ground, remain nearly constant at 1.5 for increasing winds between 20 and 50 knots. Consequently from a design viewpoint, the 20-foot, five-minute wind speed averages should be multiplied by 1.5 to arrive at the wind criteria applicable for stand-by and launching conditions in the windiest area of North America.

The variation of peak wind speeds with height in the lowest 300 feet of the atmosphere is probably more closely related to gust duration than any other parameter. For relatively strong mean winds, gusts of a few seconds' duration arise primarily from surface frictional effects on the wind flow; gusts of a minute's duration arise primarily from internal perturbations in the air flow (vortices with vertical axes, miniature cold fronts and other thermal effects). Short duration gusts show a greater variation with height in the lower atmosphere than long duration gusts. The sparse data currently available confirm the fact that instan'aneous peak gust speeds increase with height at a substantially slower rate than mean wind speeds. As a result, gust factors show a slight decrease with height.

Calculated risk wind speeds, based on information gathered from standard climatic records, must be included in the design of vehicles and support equip-

ment for use at preselected sites. These values will give the designer a
predicted probability of the nonoperability of the equipment for periods from
two to a thousand years. For example, if a missile in its launch position is
considered as a continuously exposed, semipermanent structure with a life
expectancy of 25 years, and a 10 percent risk that it will be destroyed by the
wind during that period is acceptable, then the dormant vehicle and associated
ground equipment must be designed to withstand a wind extreme that has an
expected return period of 232 years. For land areas other than midlatitude
coastal and mountain areas, calculations indicate that a steady wind of 60
knots at the ten-foot level will be applicable to this risk. If the design must
also include these exceptionally windy areas, then the wind speed applicable
to the same calculated risk and life expectancy is 75 knots. Often auxiliary
tie-down kits or structures can be developed for military equipment assigned
to these areas so as not to increase production costs of the vast majority of
equipment that will be used in areas of light winds. These auxiliary tie downs,
if vehicles are to stand by in exceptionally windy areas, should be designed to
withstand gusts of 120 knots since the five-minute wind speed with a return
period of 232 years is 75 knots. Maps and tables of calculated risk steady
wind speed at the ten-foot level have been prepared for much of North America
and methods of obtaining values at other heights have been determined and
reported.[7]

The next logical step is to examine the configurations and characteristics
of the instrumentation with which such data is obtained. Data obtained at
U. S. Weather Bureau sites is taken from the three-cup anemometer, whereas
a majority of wind speed and direction measurements made at military installa-
tions are obtained from the Wind Measuring Set AN/GMQ-11. This set is a
permanent installation providing visual and recorded indications of wind
speeds from 0 to 240 knots and direction over the full 360-degree range. The
transmitter (see Fig. 1) is an aerovane unit composed of a three-bladed
impeller mounted on the nose and a vane tail to keep the unit facing into the
wind. The streamlined tail surface rises above the support and prevents
overswinging and underregistering which would occur if the unit were not
normal to the wind. The impeller is directly coupled to a tach generator and
turns at a speed proportional to wind speed. The generator produces a linear
DC voltage output proportional to the wind speed. As the transmitter responds
to wind shifts, a synchro vertically mounted in the vane directly above the
mounting stud creates a voltage unbalance in the system. The signals are
transmitted by cable to a voltmeter and synchro receiver located in an indi-
cator (Fig. 2). The voltmeter scale is calibrated from 0 to 120 knots. The
receiver has a scale calibrated from 0 to 360 degrees. A recorder (Fig. 3)

63

FIG. 1. AN/GMQ-11 - Transmitter Assembly.

64

FIG. 2. AN/GMQ-11 - Indicator Unit.

65
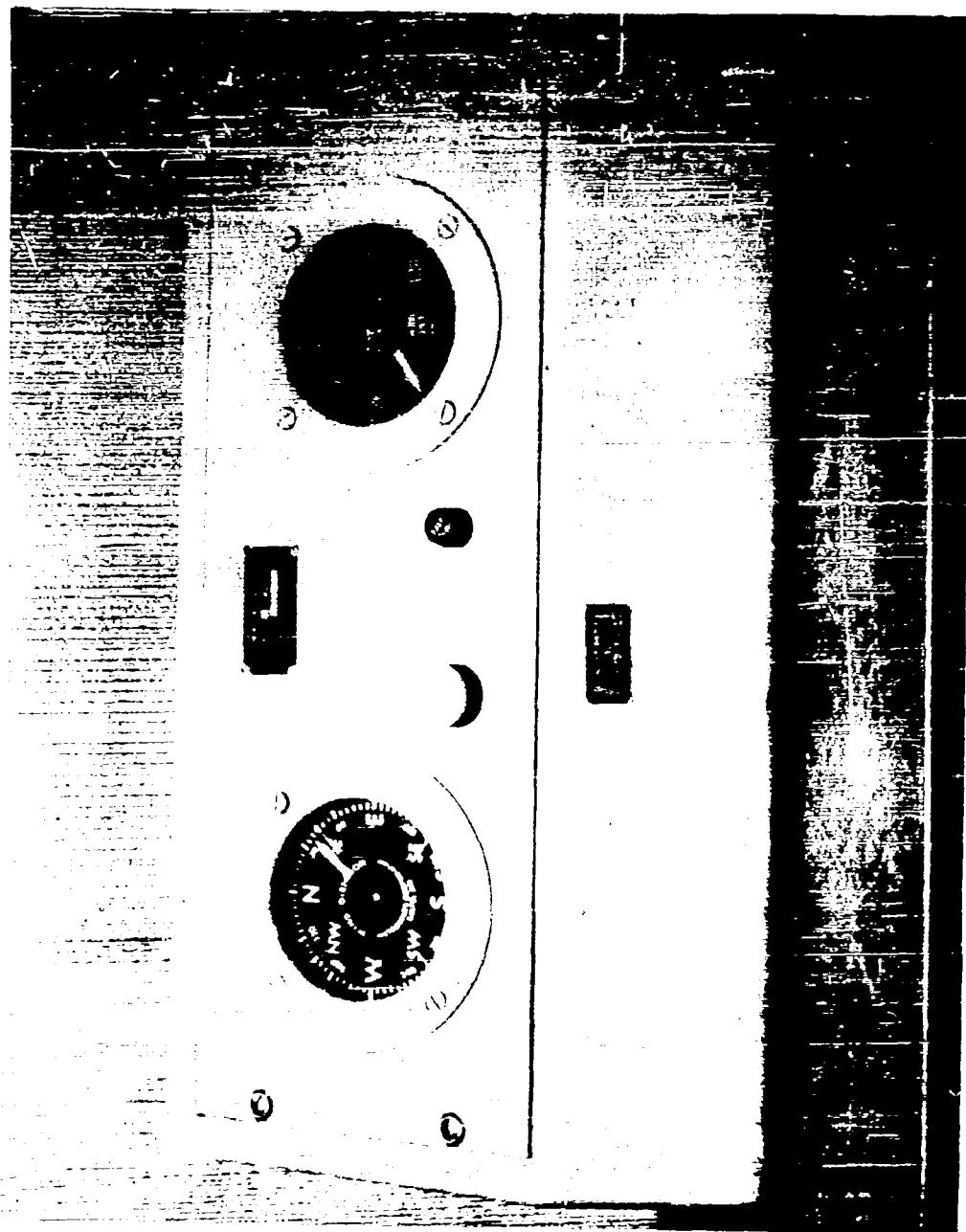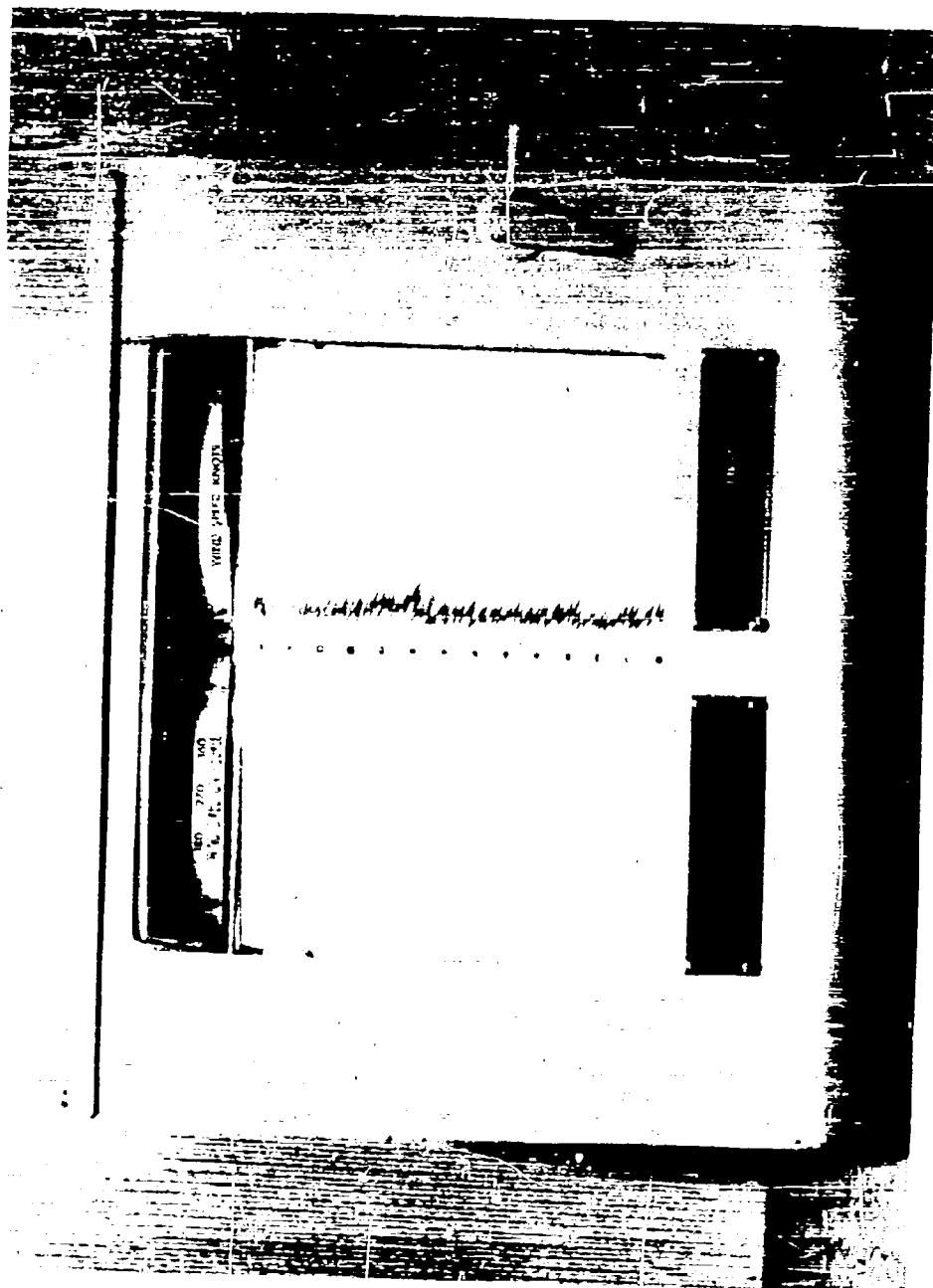
FIG. 3. AN/GMQ-11 - Recorder Unit.

with the same input signals provides a permanent record of wind speed and direction. A range doubling switch is provided to meet the 240-knot requirement.

The configuration of the set is variable and can be adapted to many situations. By the addition of a solid-state amplifier assembly, the signals can be amplified such that up to ten separate transmitters and any combination of eight indicators and recorders may be used at a single installation. A remote transfer selector switch allows the signals from any transmitter to be displayed on all indicators and recorders in the system simultaneously.

The transmitter, normally remoted from the readouts, is mounted on a thirteen-foot mast in an area free from obstructions. At most missile installations, a collapsible, lightweight crank-operated TRI-EX tower is being installed in the vicinity of each launch pad. This tower is capped by a ten-foot rigid conduit and, when fully extended, will provide a 62-foot mast for the transmitter. This type of mounting places the transmitter above many of the thermal and surface frictional wind effects encountered in the first 50 feet of the atmosphere. This provides both the designer and operator with more representative wind data at the launch pad. It must be remembered, however, that gust factors and calculated risk charts presently used are based on data obtained from an average ten-foot observing level.

The wind speed readings are accurate to plus or minus 1.5 knots in the 3 to 40 knot range; plus or minus 3 knots from 40 to 120 knots; and plus or minus ten percent of any reading above 120 knots. A wind speed of 3.4 knots is required to start the AN/GMQ-11 transmitter; stopping speed is 2.4 knots or less. Tests made by Mazzarella[11] with seven aerovanes at the Brookhaven Laboratories showed an average starting speed of 1.5 knots and a stopping speed of 2.1 knots. It should be noted that both these speeds are not only below the design limits but also in opposition to the expected condition.

As is expected in this type of system, there are two major sources of error. Mechanical errors are caused by wear over a period of time; electrical errors can be raced to a less-than-standard voltage output from the transmitter and the failure of electrical components. Since the AN/GMQ-11 system is in use throughout the world, many transmitters are directly exposed to severe weather conditions. In arctic regions, ice loading imposes severe operating restrictions on the accuracy of readings and often damages the transmitter.

The most important characteristics of the transmitter are its speed of response, damping coefficient and lag coefficient. The speed of response is defined as the time required for a transmitter and indicator or recorder combination to reach a value of $0.63u$ where u is any given wind speed in

knots. The transmitter's response to wind shift is one of periodic damped
oscillation described by a cosine function with phase displacement elimina-
ted[11]. In this case, the displacement after t seconds is directly proportional
to the product of the initial angular displacement raised to a power term con-
taining the damping coefficient γ and cos wt; it has been determined that the
damping coefficient for the transmitter is approximately 0.042. The lag
coefficient has been found to be approximately one second in a 12-knot wind
and one-half second in a 36-knot wind.

A recent survey of the manufacturers of commercial wind equipment
was conducted by the Meteorological Development Laboratory in an effort to
find a lightweight replacement for the existing tactical wind measuring set,
the AN/GMQ-1. The survey provided information concerning a commercially
available transistorized portable wind measuring system. It is believed that
this system is a follow on to the Signal Corps AN/GMQ-12 equipment but is
more rugged and is capable of measuring wind speeds up to 90 mph. This
set is currently undergoing redevelopment for use as an Air Force tactical
item. It can be used in both air drop operations and as a semipermanent
installation.

The set measures wind speed and direction at a remote location and
transmits this information to a translator and power supply unit where the
received signals are displayed on two indicating meters. A recorder can be
attached should permanent records be desired. The wind speed transmitter
of the set consists of an inertialess transducer using the light chopper tech-
nique. The wind sensor is a lightweight plastic, three-cup anemometer;
wind direction is determined by a selsyn driven by a lightweight plastic vane.
The sensors are attached to a crossarm which can be mounted on any tower
or mast; however, a standard thirteen-foot mast is provided as part of the
set; this system is powered by self-contained batteries and/or a 115-volt
50/60-cycle source; the accuracy of the system can be maintained without
the addition of extra amplifiers should the sensors be located at any distance
up to 10,000 feet from the translator and power supply unit.

The wind speed sensor of the commercial unit has an accuracy of plus
or minus one percent of true speed or 0.15 knots, whichever is greater, and
a threshold speed of 0.75 knots. The accuracy of the wind direction sensor
is plus or minus three degrees with a threshold speed of 0.75 knots. The
average transient response time of both sensors is 0.125 seconds in winds
at or greater than one knot. These same accuracies and response time values
will be maintained in the military version of this set.

As more launch facilities are constructed in regions subjected to severe
winter weather and the need for surface wind data at these locations increases,
greater demands will be placed on surface anemometry and the data obtained

68

therefrom. In anticipation of these demands, several commercial firms are currently developing various types of sonic anemometers which, it is hoped, will have greater accuracy than any of the existing equipment and will be particularly suited to conditions of severe weather as there are no exposed moving parts. Although it may be some time before the physics of the system are developed and operational anemometry are built, this type of equipment may be the answer to accuracy and continuous operation, regardless of conditions, that the designer and operator of missiles and space vehicles need.

REFERENCES

1. G. Helman, Uber die Bewegung der Luft in den untersten Schichten der Atmosphere, Meteor. Zeit., 34: 273, 1917.

2. E. L. Deacon, Vertical Diffusion in the Lowest Layers of the Atmosphere, Quarterly Journal Royal Meteorological Society, 75: 89, 1949.

3. L. Prandtl, Meteologische Anwendung der Stromungslehre, Beitr. Phys. Atmosphere, 19: 188, 1931.

4. H. Lettau, Isotropic and Non-Isotropic Turbulence in the Atmospheric Surface Layer, Geophysical Research Papers No. 1: Air Force Cambridge Research Center, 1949.

5. H. Lettau, The Present Position of Selected Turbulence Problems in the Atmospheric Surface Layer, Geophysical Research Papers No. 19: Air Force Cambridge Research Center, 1952.

6. H. Lake, A Comparison of the Power Law and a Generalized Logarithmic Formula in Micrometeorology, Trans. AGU, 33: 661, 1951.

7. Handbook of Geophysics, Rev. Ed., Geophysics Research Directorate, Air Force Cambridge Research Laboratories, 1960.

8. N. Carruthers, Variations in Wind Velocity Near the Ground, Quarterly Journal Royal Meteorological Society, 69: 289, 1943.

9. R. H. Sherlock, Variations of Wind Velocity and Gusts with Height, Paper No. 2553, Trans. American Society of Civil Engineers, 118A: 463, 1953.

10. R. H. Sherlock, Gust Factors for the Design of Buildings, Int. Assn. for Bridges and Structural Engineering, 8: 207, 1947.

11. D. A. Mazzarella, Wind Tunnel Tests on Seven Aerovanes, Review of Scientific Instruments, 25: 1, 1954.

The Low-Level Jet

YUTAKA IZUMI

GEOPHYSICS RESEARCH DIRECTORATE
AIR FORCE CAMBRIDGE RESEARCH LABORATORIES

ABSTRACT

The 1428-foot television transmitting tower located at Cedar Hill near Dallas, Texas, and mounted with instruments to make continuous measurements of wind and temperature at 12 levels from 30 feet to 1420 feet above ground, is proving to be a useful research tool for investigating low-level meteorological phenomena, especially the low-level jet. During the night of February 22-23, 1961, a pronounced low-level jet was observed. A detailed account of the orderly growth of the nocturnal jet, the accompanying temperature profiles, and the maximum wind speed and shear attained will be discussed.

INTRODUCTION

A 1428-foot tower located at Cedar Hill, Texas, approximately 20 miles south-southwest of Dallas, is serving double duty as a television transmitting tower and as the world's tallest meteorological research facility. The tower is owned jointly by KRLD-TV and WFAA-TV of Dallas and the owners have generously permitted the use of the tower facilities at no cost to the government. Structurally, the tower is triangular in cross section, 12 feet on a side, is topped with a triangular superstructure 75 feet on a side, and steadied with extensive guying. The tower is equipped with a 2,000-lb capacity elevator. The total height of 1521 feet, including the television antennas, is about 50 feet higher than the Empire State Building.

The meteorological system at the tower site was designed, assembled, and installed by the Electrical Engineering Research Laboratory of the University of Texas under contract to the Air Force Cambridge Research Laboratories with a portion of the cost of the equipment provided by the U. S. Army Signal Research and Development Laboratory. The system is designed to obtain continuous measurements of wind and temperature at twelve levels on the tower. The levels of observations are 30, 70, 150, 300, 450, 600,

71

750, 900, 1050, 1200, 1300, and 1420 feet above the ground. Measurements and recordings of the variables are done automatically. The entire meteorological system has been previously described.[1]

The principal objective of instrumenting such a tall tower is the investigation of a striking phenomenon in the lower portion of the atmosphere--the low-level jet. This jet is described as a sharply defined maximum of wind speed occurring at heights of 800 to 2000 feet above the ground with extremely high values of wind shear below the level of maximum wind speed. Low-level jets have been observed on numerous occasions in various parts of the United States, but most of the well developed jets have been found in the midwestern states, especially during the night.[2,3] Data on the development, persistence and decay of the low-level jet have been very scanty inasmuch as meteorological towers used in the past did not reach the level of the jet core, and balloon observations cannot provide enough of the continuous information required.

DISCUSSION OF DATA

Since the meteorological system on the Cedar Hill tower went into operation in late December of 1960, a number of low-level jets have been recorded. The most prominent low-level jet developed on the night of February 22-23, 1961. The surface weather maps during the period showed a cold front of moderate intensity with northeast-southwest orientation advancing from southeastern Colorado to the Texas Panhandle with no significant change of pressure gradient in the vicinity of the Cedar Hill tower. All stations surrounding the tower reported clear skies and light to moderate SSW to SW winds at the surface. There was no indication of high winds near the ground.

The data presented in this discussion are 10-minute average wind speeds from 10 levels of the tower -- the wind speeds at 600 and 900 feet were not considered because of apparent errors in the data recorded at these levels. Although the vertical temperature distribution will not be illustrated, it will be discussed together with the wind profiles because the growth of the low-level jet is intimately related to temperature inversion.

Figure 1 shows the time variation of the wind speed profiles from 1700 to 2150 hours on February 22. At 1700 hours there was nothing unusual in the temperature or in the wind profile. The temperature gradually decreased with height with an isothermal layer between 1200 and 1300 feet. The wind speed from 30 to 1300 feet varied from about 12 to 27 miles per hour. The data between the hours of 1710 to 1910 were missing, but by 1920 a strong,
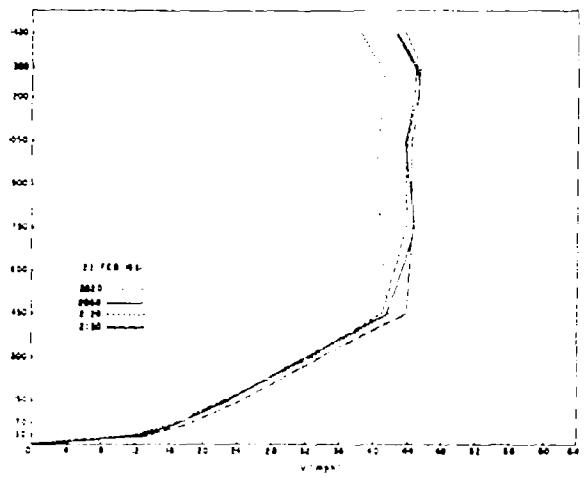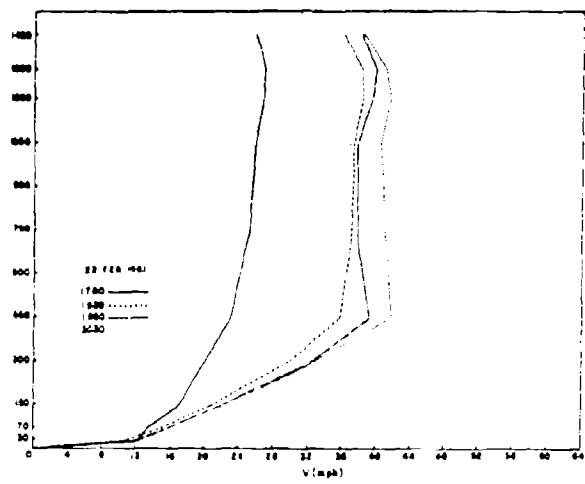
FIG. 1. Wind Profiles for the Period 1700 to 2150 CST,
22 February 1961.

73

shallow inversion existed from 30 to 450 feet. Above this inversion was a less stable layer with the temperature decreasing with height and becoming isothermal above 1300 feet. This isothermal layer between 1300 and 1420 feet persisted until 0200 hours of the next day. The wind speed increased rapidly through the inversion layer and then increased slowly up to the isothermal layer. By 1950 the surface inversion had intensified and the wind shear below 450 feet had increased. The wind speed profile at this time characterized the profiles for the next five hours with two maxima -- one at top of the inversion and the other at the bottom or immediately below the isothermal layer. By 2020 hours the wind speed at 450 feet had increased to about 42 miles per hour while at 30 feet it was only about 12 miles per hour. The temperature data at this time also showed an isothermal layer between 70 and 150 feet with a moderate inversion below and a strong inversion above to 450 feet. The isothermal layer near the surface persisted throughout the remainder of the period. By 2050 hours the inversion layer between 150 and 450 feet deepened to 600 feet and by 2120 hours to 750 feet. The top of the inversion generally remained at 750 feet for the following hour and a half with periodic drops to 600 feet. The wind speed profiles for 2050, 2120, and 2150 hours showed the level of maximum wind speed to be at 750 feet; but had the wind speed data for 600 feet been correctly recorded, the maximum wind speed level would presumably have alternated between 600 and 750 feet.

Through 2250 hours (Fig. 2) the top of the inversion remained at 750 feet. At this time the wind speed at 750 feet was over 52 miles per hour while at 30 feet it was 13 miles per hour. By 2320 hours the inversion had propagated upward to 900 feet and it remained at this height until 0100. By 2350 the inversion layer between 150 and 300 feet, which gradually decreased in intensity with time, had broken down and become isothermal. Thereafter, a weak inversion reestablished in this layer several times; but in general, the lower isothermal layer extended from 70 to 300 feet for the remainder of the period. From 2320 through 0050 hours, the maximum wind speed was observed at 750 feet; but had the correct wind data for the 900-foot level been recorded, the maximum would presumably have occurred at 900 feet.

From 0050 to 0250 hours the wind and temperature structures changed rapidly, and Fig. 3 presents the wind profiles at 20-minute intervals. At 0110 hours the inversion rose from 900 to 1050 feet and by 0130 and 0150 hours the top of the inversion was found at 1200 feet. From 0050 to 0150, marked temperature decreases were observed at all levels -- the least amount of decrease below 300 feet and above 1300 feet and the greatest decrease at about the 900-foot level. Although they were not as sharp and distinct as the preceding maxima of wind speed, it can be seen from the wind profiles that the

74
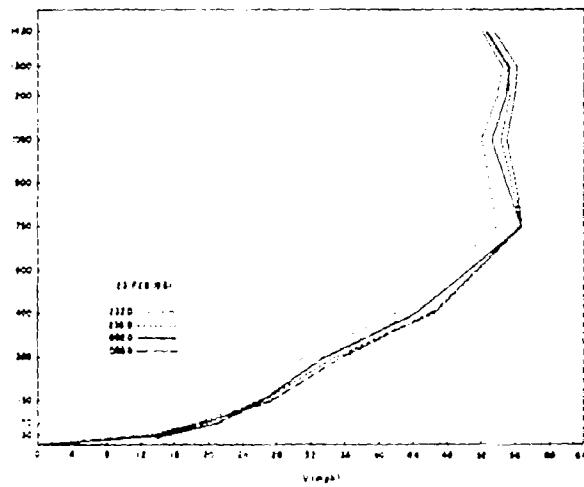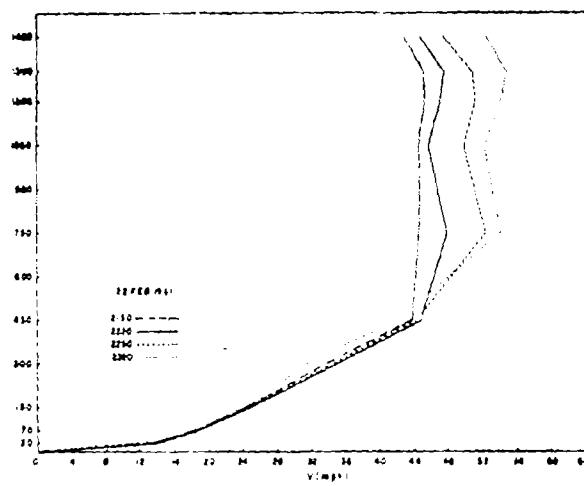
FIG. 2. Wind Profiles for the Period 2150 CST, 22 February
1961 to 0050 CST, 23 February 1961.
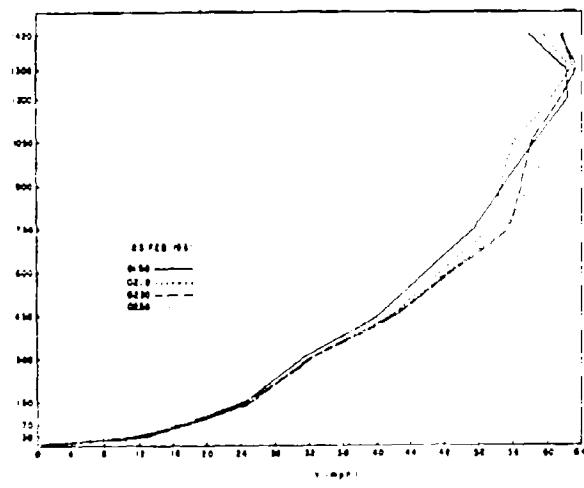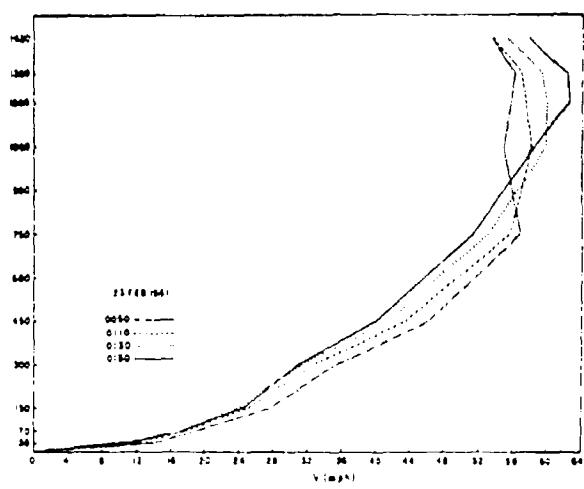
FIG. 3. Wind Profiles for the Period 0050 to 0250 CST,
          23 February 1961.

76

wind speed maxima always occurred at the top of the inversion. The wind profiles also show an orderly decrease of wind speed with time between 300 and 750 feet and an orderly increase above 1200 feet. By 0210 hours the inversion reached the uppermost level of the tower, but the temporal change in the temperature profiles from 0210 to 0250 was chaotic. The wind profiles showed that the wind speed maxima had broken through the inversion during this period. The sharp reduction of wind shear between 750 and 1050 feet at 0210 and 0230 hours coincided with the nearly isothermal to isothermal layer that existed between 900 and 1050 feet. This is evidence that mixing caused the reduction of wind as well as the temperature gradients. At 0250 hours the wind as well as the temperature gradients. At 0250 hours the wind speed at the 1200-foot level was 63.5 miles per hour while at the 30-foot level it was 12.8 miles per hour.

The temperature profiles at 0300 and 0310 hours (Fig. 4) showed that order was established with a strong inversion between 450 and 900 feet and less stable layers below and above it. At 0300, the highest wind speed value of 63.7 miles per hour was attained at 1200 feet while at the 30-foot level wind speed was 14.9 miles per hour. At 0310 hours the low-level jet showed signs of losing its intensity.

CONCLUSION

The sequence of events presented here showed the systematic and orderly growth of a low-level jet and the orderly upward growth of the nocturnal inversion despite the extremely large wind shears. It is evident that the height of the low-level jet and the height of the inversion are closely related -- in fact inseparable. It is also evident that the turbulent mixing caused by the large wind shear was responsible for the breakdown of inversion, especially in the lower layers.
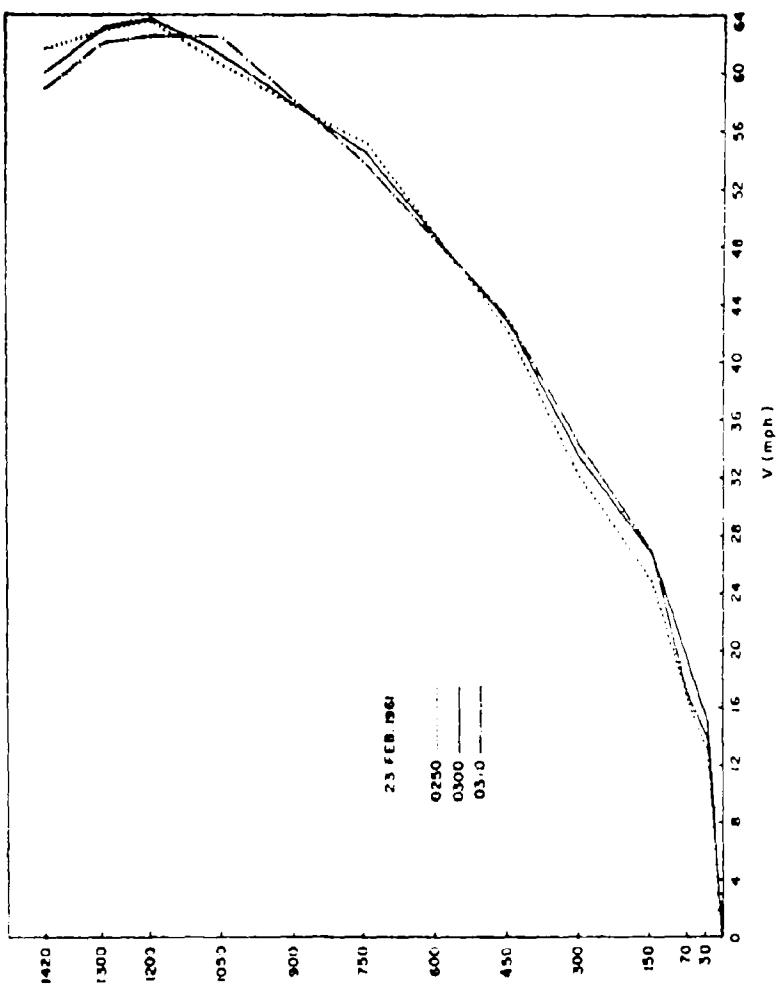
FIG. 4. Wind Profiles for the Period 0250 to 0310 CST, 23 February 1961.

REFERENCES

1. W. S. Mitchum and J. R. Gerhardt, Final Report on Research Directed Toward the Study and Application of Digital Data Processing Methods to the Problem of Sensing and Recording Meteorological Variables at Various Levels on an Existing 1400-Foot Tower, Contract AF 19(604)-3498 with the Geophysics Research Directorate, Air Force Cambridge Research Laboratories; Electrical Engineering Research Laboratory Report No. 4-03, The University of Texas, 30 April 1960.

2. H. H. Lettau and B. Davidson, Exploring the Atmosphere's First Mile, Volume 1, Instrumentation and Data Evaluation, Pergamon Press, London, 1957.

3. A. K. Blackadar, Boundary layer wind maxima and their significance for growth of nocturnal inversions, Bulletin of the American Meteorological Society, Vol. 38, No. 5, May 1957.

Power Spectral Considerations on the Launch Pad

QUENTIN R. BOHNE

AERO SPACE DIVISION

THE BOEING COMPANY

ABSTRACT

Power spectral density methods, frequently employed in the determination of flight gust loads, are shown to be useful in the solution of the nonlinear ground-wind drag problem. In the first method presented, the equations are partially linearized so that classical power spectral techniques can be employed with a spectral representation of the square of the wind speed. The second method, applicable to nonlinear systems, involves the generation of a random signal to apply to an analog simulation of the system. The random signal is fed simultaneously into quasistatic and dynamic simulations, allowing the determination of the degree of dynamic overstressing. Summary curves are presented showing typical dynamic magnification factors for various values of structural damping and frequency and various spectral representations of the wind.

SYMBOLS

C_A = aerodynamic damping coefficient = $\int_0^Y \rho\, C_D(y)D(y)\, \phi^2(y) \left[\frac{v(y)}{V} \right] dy$

C_B = $\int_0^Y \frac{\rho}{2} C_D(y)D(y)\, \phi^3(y)dy$

C_D = drag coefficient

D = dimension of the area transverse to the flow, ft

DMF = dynamic magnification factor = Q_d/Q_s

F = Force coefficient = $\int_0^Y \frac{\rho}{2} C_D(y)D(y)\, \phi(y) \left[\frac{v(y)}{V} \right]^2 dy$

f_1 = natural frequency of system, cps ($f_1 = \omega_1/2\pi$)

G = gust factor = peak wind speed/average wind speed

L = scale of turbulence, ft

$[M_i]$ = coefficient matrices in differential equations of motion, i = 1, 2, 3

81

$$M = \text{generalized mass, slugs} = \int_0^Y m(y)\, \phi^2(y)\, dy$$

m = mass distribution, slugs/ft

$P(Q_g)$ = probability that $q_g \geq Q_g$

q_i = i^{th} generalized coordinate, ft

$\bar{q}$ = mean response to design wind

q_g = quasistatic response to ground wind

q_d = dynamic response to ground wind

Q_g = quasistatic design response

Q_d = dynamic design response

t = time, seconds

$T(i\omega)$ = frequency response function

V = wind speed at reference elevation, ft/sec

V_o = mean wind speed at reference elevation, ft/sec

V_R = random windspeed fluctuation about mean V_o, ft/sec

$v(z)/V$ = wind profile

y = axial coordinate of vehicle measured from base, ft

Y = length of vehicle, ft

z = elevation above ground, ft

ζ = fraction of critical damping

ρ = air density, slugs/ft^3

σ_V^2 = variance of random function V

σ = standard deviation of random function

$\phi_i(y)$ = value of ith mode at station y

ϕ_V = power spectrum of V

ω_1 = natural frequency of system - rad/sec

ω = frequency, rad/sec

Ω = reduced frequency, rad/ft = ω/V_o .

ANALOG SYMBOLS

Summing Amplifier

$$e_0 = -(e_1 + 5e_2)$$
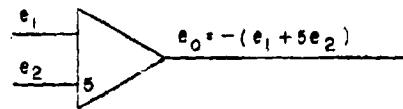
Integrating Amplifier

$$e_0 = -\int e_1 \, dt$$

Multiplier

$$e_0 = -\frac{e_1 e_2}{100}$$

Potentiometer

$$e_0 = \rho e_1$$
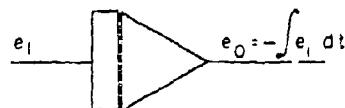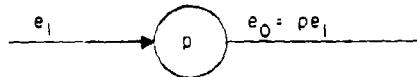
INTRODUCTION

With the advent of vertically rising high performance systems, in many cases ground wind conditions have become design conditions for a large portion of booster structures as well as for hold-down structures. The wind-induced loads consist of drag loads in the direction of the wind and oscillatory loads primarily in a plane perpendicular to the wind. The lateral oscillations due to steady winds have been the object of considerable recent research. The

work of Fung[1], Ezra[2], and Buell[3] is representative of this effort in which it has been shown that on clean cylindrical configurations the lateral loads are of the order of three to four times the drag loads. For lifting reentry vehicles, however, drag loads resulting from winds blowing normal to the lifting surface can be considerably more important that the oscillatory lateral loads. In this paper the problem of ground wind drag response is considered.

To arrive at suitable design criteria, an environment and a method of analysis must be specified. In the past, the ground wind environment has been specified in terms of an average wind speed and a gust factor. The average wind value is based upon extreme averages measured over short periods (one to five minutes) and the gust factor accounts for the fact that, for a shorter time during the averaging period, the wind must have exceeded the average by a certain factor. For example, a wind criterion of 40 to 60 mph describes a wind condition in which the average wind speed is 40 mph and the gust factor is 1.5. In the construction industry, the gust factor has been used to convert peak measured average winds to peak winds for design pressure determinations.[4]

To the aerospace industry, the gust factor is more than a means for determining a peak wind speed; it implies that a time-varying forcing function is being applied to a lightly damped flexible vehicle, and a dynamic analysis is needed to determine the resulting loads. Experience in the field of airplane gust response has shown many advantages of power spectral density analysis.[5,6] This paper presents means of applying power spectral techniques in ground wind analyses, rather than relying on a steady wind plus discrete gust solution as is now common.

There are two problems basic to the use of power spectral methods in ground wind analysis. The first is concerned with the nonlinear nature of the response equations. A method will be presented based on partial linearization of the equations to eliminate this difficulty, and an alternate method requiring no linearization will also be shown.

The second problem is basic to all spectral analyses -- namely, how are design loads determined from a power spectrum. The expected number of exceedances of various load levels, a standard product of the spectral analysis, is useful for fatigue studies but leaves the question of what probability should be selected for design load determination. It is also recognized that a rational criterion cannot be based only on the limited number of wind spectra measured, but must be primarily based upon the great volume of wind speed data that is constantly being obtained at weather stations throughout the world. The design method that is presented in this paper allows the use of the basic environmental data (average wind and gust factor) and yet also makes use of the spectral description of the wind to determine the proper dynamic effects. The method

84

involves the determination of a **dynamic magnification factor** based upon an equal probability of occurrence concept; that is, the DMF is the ratio of the dynamic load expected with a given probability to the static load expected with the same probability.

BASIC POWER SPECTRAL RELATIONSHIPS

The ground wind response of a slender vehicle cantilevered at its base is given by equations of the form*

$$\left[M_1\right]\left\{\ddot{q}_i\right\} + \left[M_2\right]\left\{\dot{q}_i\right\} + \left[M_3\right]\left\{q_i\right\} =$$

$$= \left\{\int_o^Y C_D(y)\, D(y)\, \phi_i(y)\, \frac{\rho}{2}\, \left[\frac{v(y)}{V}\, V - \sum_{j=1}^{N} \phi_j(y)\, \dot{q}_j\right]^2 dy\right\} \tag{1}$$

where the wind profile $v(y)/V$ is the ratio of the wind speed at station y to the wind speed at the reference elevation. It should be noted that Eq. (1) is based upon 'strip theory' or two-dimensional aerodynamics and that possible unsteady effects (time dependency of C_D) are not considered. The expansion of the bracket in the right member will yield a lengthy nonlinear expression involving products of the various velocities. Fortunately the aerodynamic loading is distributed continuously much like the inertial loading used to determine the normal modes. Therefore a small number of modes, possibly only one, will provide a good description of the vehicle response. For clarity of presentation only one mode will be considered in the remainder of the development, and it will be assumed that the modal displacement is the response item of interest. The conclusions that will be made are equally applicable to bending moments or other load items of interest. Eq. (1) in its simplified form is now written as

$$M\ddot{q} + 2M\zeta\omega_1\dot{q} + M\omega_1^2 q = FV^2 - C_A V\dot{q} + C_B \dot{q}^2 . \tag{2}$$

The single degree of freedom equation is still nonlinear and the usual power spectral methods of solution are not applicable. The magnitude of the nonlinear terms have been discussed in detail.[7] The term involving the square of the response velocity is very small and can be dropped at this time. The aerodynamic damping term, $C_A V\dot{q}$, in general should not be dropped, but replacing

---

*   *It is assumed throughout that $V > 0$ and $\left[V - \Sigma\, \phi_j\, \dot{q}_j\right] > 0$.

it by an equivalent damping term, $C_A V_o \dot{q}$, is suggested as a practical means of linearization. It is difficult to generalize on linearization methods for all configurations, and some thought should be given when this method is applied to a particular configuration. To the extent that the method is not exact, it is probably conservative in that the peak responses occur when $V > V_o$, or the actual time dependent damping coefficient is larger than the equivalent coefficient at that time.

The response equation is now linear, considering the forcing function to be V^2:

$$M\ddot{q} + (2M\zeta\omega_1 + C_A V_o)\dot{q} + M\omega_1^2 q = FV^2 = F(V_o^2 + 2V_o V_R + V_R^2) \quad (3)$$

where the wind speed is defined as a mean wind, V_o, plus a random wind, V_R, with zero mean.

When a time average is taken of the right member of Eq. 3, it can be seen that the mean value of the forcing function is given by

$$\overline{FV^2} = F(V_o^2 + \sigma_V^2) \quad (4)$$

where

$$\sigma_V^2 = \lim_{T \to \infty} \frac{1}{2T} \int_{-T}^{T} V_R^2(t)dt = \text{the variance of } V.$$

Power spectra of V_R have been measured and it remains only to find the power spectrum of $V^2 = (V_o + V_R)^2$. Rice[8] has developed an expression for the spectrum of the square of a sinusoidal signal plus a random signal. A similar derivation shows the desired spectrum of V^2 to be

$$\phi_{V^2}(\omega) = 4V_o^2 \phi_{V_R}(\omega) + \int_{-\infty}^{\infty} \phi_{V_R}(\xi) \phi_{V_R}(\omega - \xi) d\xi \quad (5)$$

for frequencies other than $\omega = 0$. In evaluating the convolution integral, by definition,

$$\phi_{V_R}(-\omega) = \phi_{V_R}(\omega).$$

From the usual input-output spectral relations, the power spectrum of the response item of interest can now be obtained by

$$\phi_q(\omega) = |T(i\omega)|^2 \phi_{V^2}(\omega), \quad (6)$$

where

$$T(i\omega) = \frac{F}{M(\omega_1^2 - \omega^2) + i\omega(2M\zeta\omega_1 + C_A V_0)} = \quad (7)$$

= the frequency response function.

Thus the mean response is obtained from Eqs. (3) and (4) as

$$\bar{q} = \frac{F}{M\omega_1^2}\left[V_0^2 + \sigma_V^2\right] \quad (8)$$

and the variance is given by

$$\sigma_q^2 = \int_0^\infty \phi_q(\omega)\,d\omega . \quad (9)$$

GROUND WIND SPECTRA

To conduct accurate ground wind spectral analyses, it is necessary to specify accurate wind spectra. As is the case for higher altitude gusts, only enough spectra have been obtained to fix the general shape of the spectra, and the magnitude is still quite dependent upon other measurements. The available spectra have been obtained both by tower measurements and by low flying airplane measurements. In either case, the hypothesis of G. I. Taylor[9] has been applied to convert the time spectra to space spectra by the relationships

$$\phi(\Omega) = V_0\phi(\omega)$$

$$\omega = V_0\Omega .$$

This equivalence seems valid for the airplane data, but is somewhat questionable for the low frequency end of the tower data. The applicability of Taylor's hypothesis has been discussed in detail by Henry[10] and Lappe[11] and will not be discussed here. The question is somewhat academic for the present application because most of the data were measured on stationary towers as a function of time and will be applied to a stationary vehicle as a function of time. Thus the conversion to a space spectrum could be looked upon as a convenient way to store measured spectra.

Two spectral forms are presented in this section, the first due to Henry[10], and the second the well known expression for isotropic turbulence:

93

$$\phi(\Omega) = \frac{0.0206 V_o^{5/3} \tan h \left(\frac{68.2 \, z \, \Omega}{V_o} \right)}{z^{2/3} \, \Omega^{5/3}} \tag{10}$$

$$\phi(\Omega) = 2\sigma_V^2 \frac{L}{\pi} \frac{1}{1+L^2 \Omega^2} \tag{11}$$

where L is the scale of turbulence and z is the elevation above the ground. Various values have been suggested for the scale of turbulence at low altitude, ranging in value from 200 ft to more than 1000 ft. It is not within the scope of this paper to decide what value is most appropriate. Since the response of the vehicle does depend upon the input spectrum selected, however, three spectra will be considered in the remainder of the paper (Eq. (10), and Eq. (11) with L = 400 ft and L = 1200 ft).

Henry's expression allows calculation of the variance of the turbulence in terms of V_o and z, whereas Eq. (11) gives only the frequency content. If Henry's spectrum is approximated by its asymptotes, the resulting expression can be integrated in closed form to give

$$\sigma_V^2 = 4.5 \, (.0206) \, (68.2)^{2/3} V_o . \tag{12}$$

The preceding expression will be used for σ_V^2 in Eq. (11).

Now attention will be turned to the determination of V_o. A great volume of data has been measured by weather stations and reported in terms of fastest miles of wind experienced for various observation periods. For example, Thom[12] shows fastest miles expected in the United States with return periods of 2, 50, and 100 years. Thus the most reliable data on V_o comes from records averaged over one mile, and fastest mile values are recommended in preference to five-minute averages previously used. It should be mentioned here that fastest mile averages are higher than five-minute averages and therefore a lower value of the gust factor should be used with the fastest mile average. For illustrative purposes, a value of 1.4 will be used in this paper.

Since the design wind model to be synthesized is based upon data obtained from two different sources -- average speeds from weather bureau stations and power spectra from research programs -- care must be taken neither to omit certain effects nor to include them twice. A point in question deals with the long gusts on the low frequency end of the spectrum. The random wind described by the power spectrum has by definition a zero mean, and therefore it should not contain turbulence components that are longer than the averaging period used to compute the mean. To compute a one-mile moving average, visualize a long record of random wind speed. The random fluctuations about

this average will contain only the higher frequencies which did not contribute to the moving average. In actuality, the fastest mile recorders do compute moving averages, the maximum value of the moving average being defined as the 'fastest mile.'

The spectra that describe the turbulence referred to as the one-mile moving average can be obtained by multiplying the spectra of Eqs. (10) and (11) by a function representing the moving average operation.[13] Eqs. (10) and (11) now become

$$\phi(\Omega) = \frac{0.0206 V_o^{5/3}}{2^{2/3} \Omega^{5/3}} \tanh\left(\frac{68.2\, z\Omega}{V_o}\right) \left[1 - \frac{\sin 2640}{2640}\right]^2 \tag{13}$$

$$\phi(\Omega) = 2\sigma_V^2 \frac{L}{\pi} \frac{1}{1 + L^2 \Omega^2} \left[1 - \frac{\sin 2640\Omega}{2640\Omega}\right]^2. \tag{14}$$

It should be pointed out that the attenuation function used above represents a continuous averaging process whereas the fastest mile instrument records discrete averages at one-mile intervals.

Wind speed spectra with and without the low frequency attenuation are presented in Fig. 1 for V_o = 60 ft/sec and z = 60 ft. Power spectra of V^2 from Eq. (5) are also evaluated for these conditions and are shown in Fig. 2. It should be pointed out that the convolution integral of Eq. (5) contributed very little to the spectrum of V^2 in this case. This is not true in general, but is true in this example only because $V_o^2 \gg \sigma_V^2$. It should also be pointed out that the convolution integral tends to give more power to the higher frequencies. For example, if the spectrum of V_R had a predominant spike at Ω_1, the convolution integral would produce a spike at $2\Omega_1$.

DESIGN METHOD

In this section, a method is presented whereby the power spectrum of the output can be used to determine design loads. The usual criterion of a steady wind plus gust is employed and the power spectrum is used only to determine the magnification expected due to dynamics. The steps in the solution are: (1) calculate the quasistatic* design load by a discrete analysis, (2) from the power spectrum of the quasistatic load, compute the probability of exceeding

---

*In this paper "quasistatic" refers to a response obtained from an analysis in which damping and inertia forces are omitted. Thus the response at any instant of time is directly proportioned to the forcing function at that same instant of time.

$$\Phi_v(\Omega) = 2(9.64)^2 \frac{1200}{\pi} \frac{1}{1+(1200\Omega)^2}$$

Eq. (11)

$$\Phi_v(\Omega) = 2(9.64)^2 \frac{400}{\pi} \frac{1}{1+(400\Omega)^2}$$

Eq. (11)

$$\Phi_v(\Omega) = \frac{1.236 \tanh(68.2\Omega)}{\Omega^{\frac{5}{3}}}$$

Eq. (10)
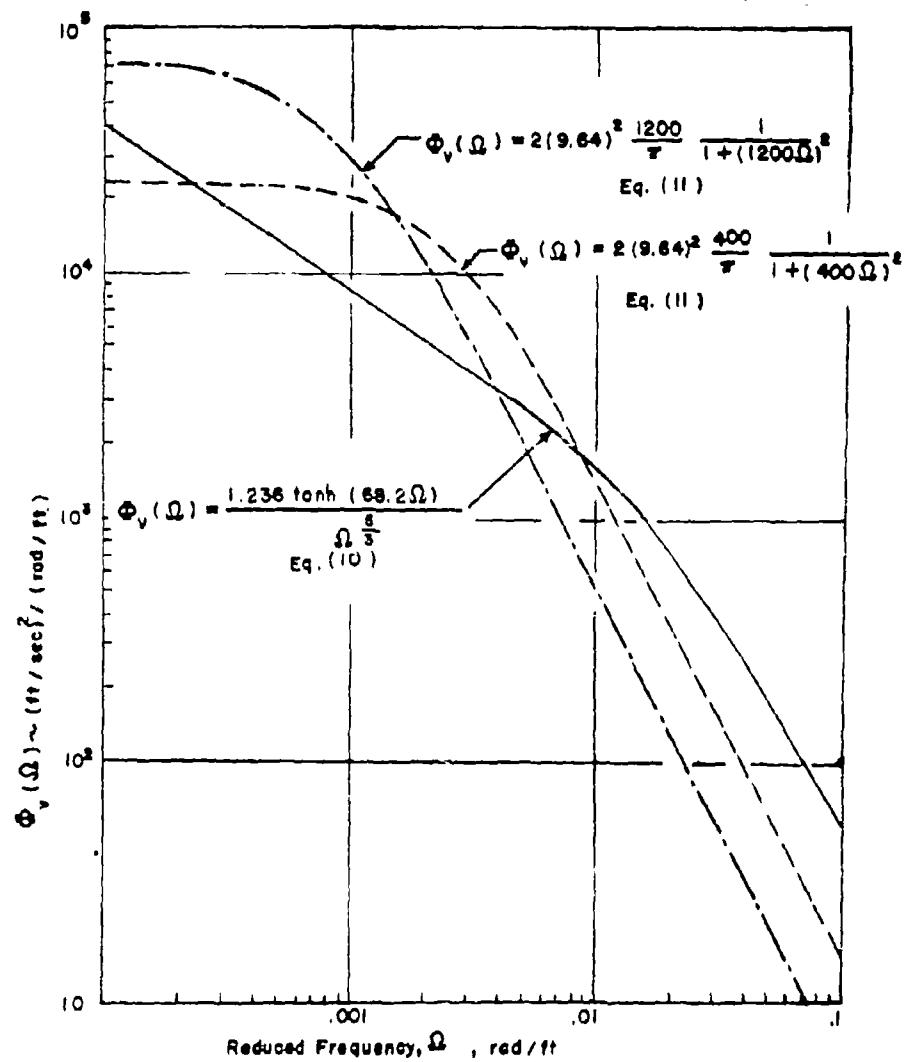
FIG. 1a. Power Spectra of Ground Wind Speed.
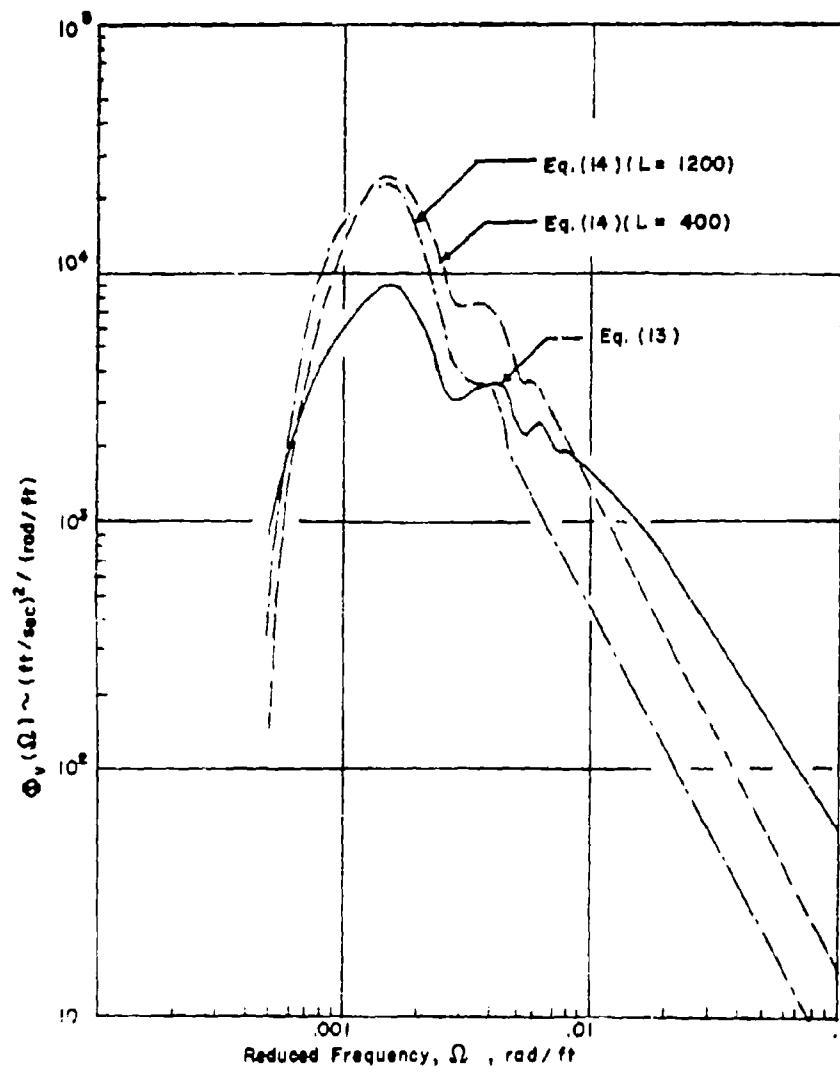
FIG. 1b. Power Spectra of Ground Wind Speed with Low Frequency Attenuation.
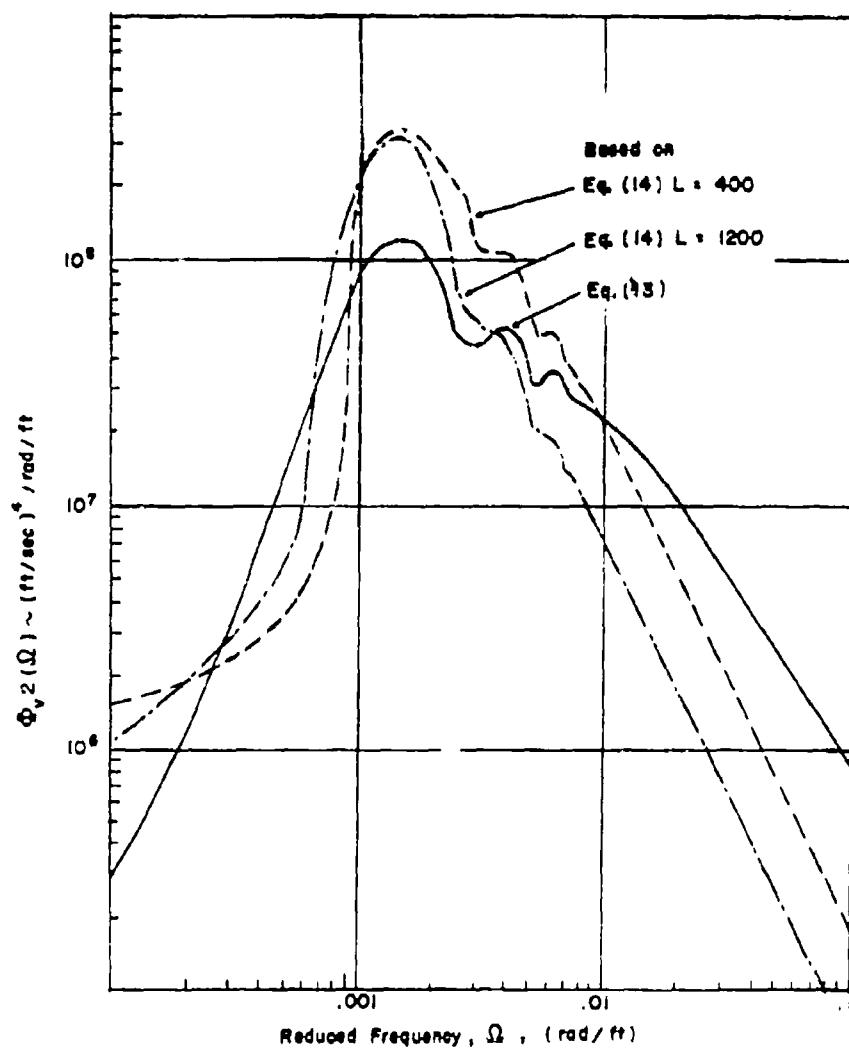
FIG. 2. Power Spectra of Square of Ground Wind Speed.

the quasistatic design load, and (3) from the power spectrum of the dynamic load compute the dynamic load that will be exceeded with that same probability. This is the design load that includes the effect of dynamics.

If dynamics are not considered, the quasistatic design response from Eq. (3) is

$$Q_s = \frac{F}{M \omega_1^2} (G \cdot V_o)^2 . \tag{15}$$

The quasistatic response can also be obtained from a power spectral solution employing Eqs. (6) through (9) by setting

$$T(i\omega) = T(i 0) \tag{16}$$

in Eq. (7).

From Eqs. (8) and (9) the mean and standard deviation of the quasistatic response are obtained and, assuming a normal distribution, the probability that the quasistatic response will exceed the quasistatic design response can be obtained by solving the following expression for $P(Q_s)$:

$$P(Q_s) = \int_{Q_s}^{\infty} \frac{1}{\sqrt{2\pi \sigma_{q_s}}} e^{-(\xi - \bar{q})^2 / 2 \sigma_{q_s}^2} d\xi . \tag{17}$$

With the substitution

$$\frac{\xi - \bar{q}}{\sigma_{q_s}} = x$$

Eq. (17) becomes

$$P(Q_s) = \int_{\frac{Q_s - \bar{q}}{\sigma_{q_s}}}^{\infty} \frac{1}{\sqrt{2\pi}} e^{-x^2/2} dx . \tag{18}$$

A similar development for the dynamic response will lead to the expression

$$P(Q_d) = \int_{\frac{Q_d - \bar{q}}{\sigma_{q_d}}}^{\infty} \frac{1}{\sqrt{2\pi}} e^{-x^2/2} dx . \tag{19}$$

93

The dynamic response that will be exceeded with the same probability as the static response ($P(Q_s) = P(Q_d)$) is found by equating the lower limits of integration of Eqs. (18) and (19), or

$$Q_d = \bar{q} + (Q_s - \bar{q}) \frac{\sigma_{q_d}}{\sigma_{q_s}} . \tag{20}$$

The dynamic magnification factor based on an equal probability concept is defined to be

$$DMF = Q_d/Q_s . \tag{21}$$

APPLICATION TO A TYPICAL MISSILE

For purpose of illustration, the method outlined in the previous section will be applied to a typical boost glide vehicle. The basic configuration[7] is shown in Fig. 3. It should be realized that the results presented are applicable only to vehicles similar to the one analyzed and are not to be used as design curves for all vehicles. For the vehicle studied, Eq. (7) has the following form:

$$T(i\omega) = \frac{0.00236}{(\omega_1^2 - \omega^2) + i\omega(2\zeta\omega_1 + 0.151)}$$

Power spectra were computed for a number of values of ω_1 and ζ and for the three input spectra defined previously. The results are shown in Table 1. The results are also plotted in Figs. 4 and 5 along with results obtained from a nonlinear study.

Effect of Natural Frequency

Equations (7) and (16) indicate that the dynamic frequency response function builds up to a peak near ω_1 and then drops off to zero, whereas the quasistatic frequency response function remains constant for all frequencies. Therefore the dynamic and quasistatic output spectra have the form shown in Fig. 6 and the variances are functions of areas I, II, and III as follows:

$$\sigma^2_{q_d} = I + II$$

$$\sigma^2_{q_s} = I + III .$$
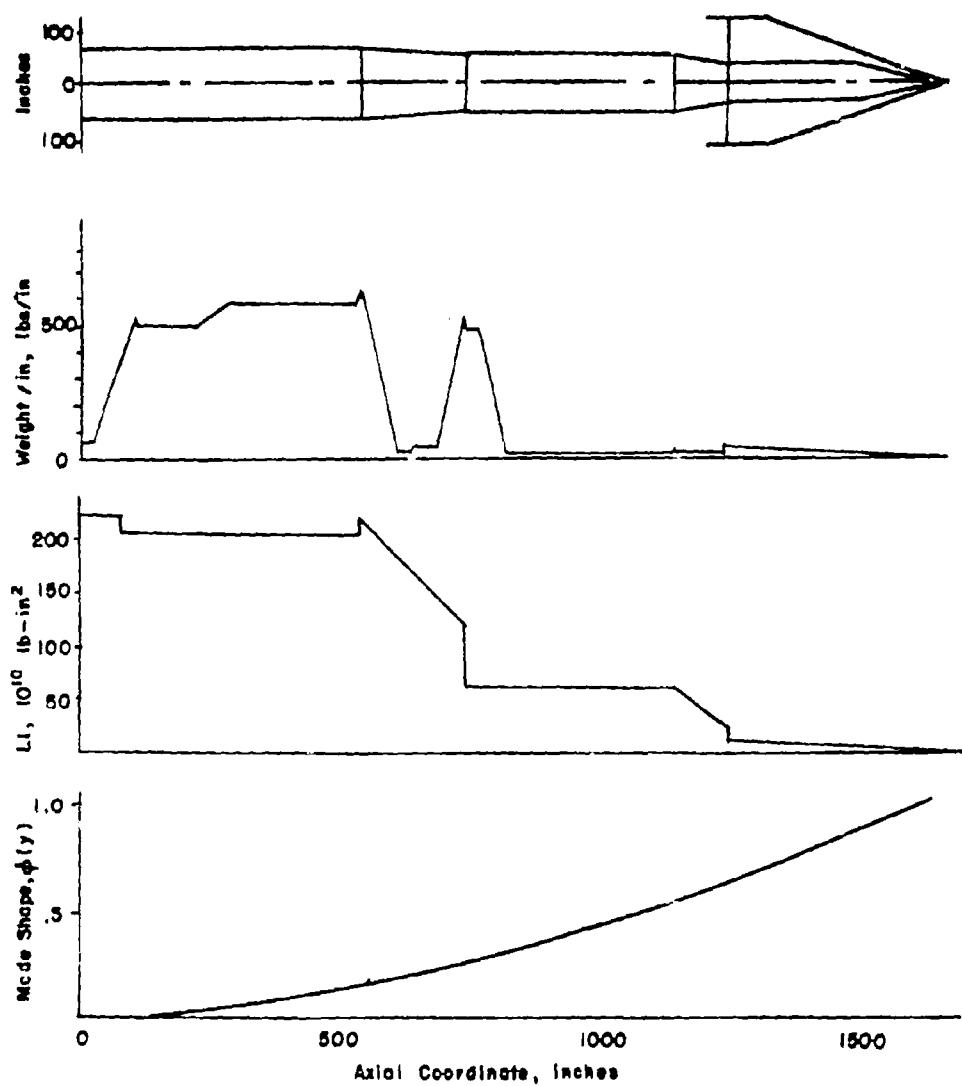
FIG. 3. Basic Configuration Analyzed.

TABLE 1

RESULTS OF LINEARIZED SPECTRAL ANALYSIS

Input Spectrum	f_1	ζ	$\bar{q}$	Q_s	q_s	q_d	IMF
Eq.(13)	.1	.1	22.1	40.3	4.99	6.00	.92
	.5	.1	.884	1.612	.282	.24	1.08
	1.0	.1	.221	.403	.0772	.060	1.13
	.1	.04	22.1	40.3	5.55	6.00	.97
	.5	.04	.884	1.612	.337	.24	1.16
	1.0	.04	.221	.403	.0866	.060	1.20
	.1	0	22.1	40.3	6.27	6.00	1.02
	.5	0	.884	1.612	.485	.24	1.46
	1.0	0	.221	.403	.145	.060	1.64
Eq.(14) L = 400	.1	.04	22.1	40.3	7.02	6.32	1.05
	.5	.04	.884	1.612	.293	.253	1.07
	1.0	.04	.221	.403	.0714	.0632	1.06
Eq.(14) L = 1200	.1	.04	22.1	40.3	5.29	4.90	1.04
	.5	.04	.884	1.612	.2145	.1960	1.04
	1.0	.04	.221	.403	.0529	.0490	1.04
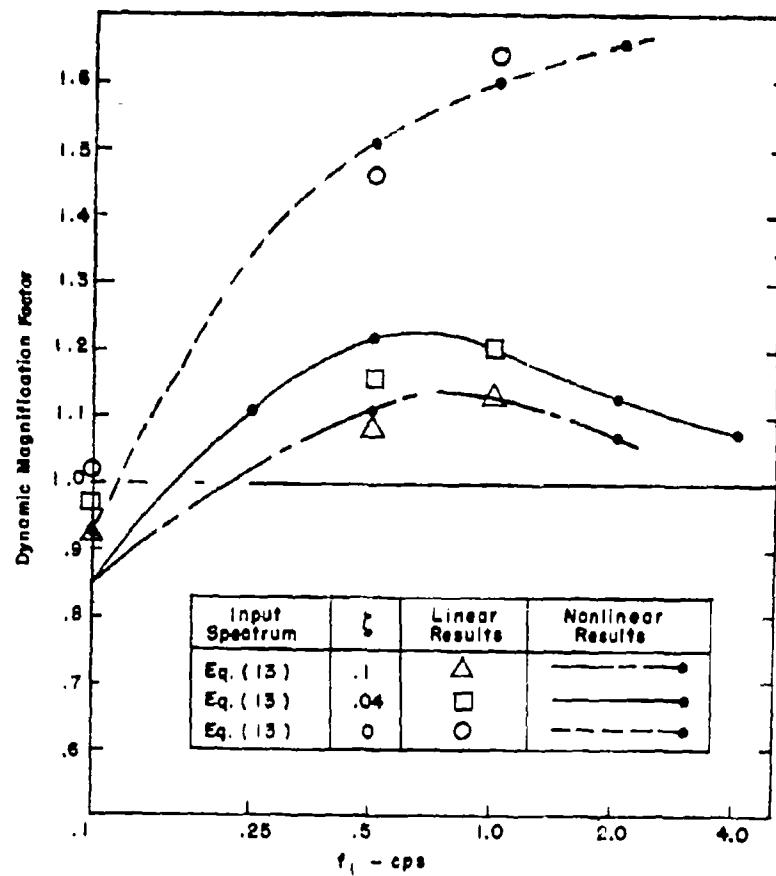
FIG. 4. DMF vs. Natural Frequency and Structural Damping.
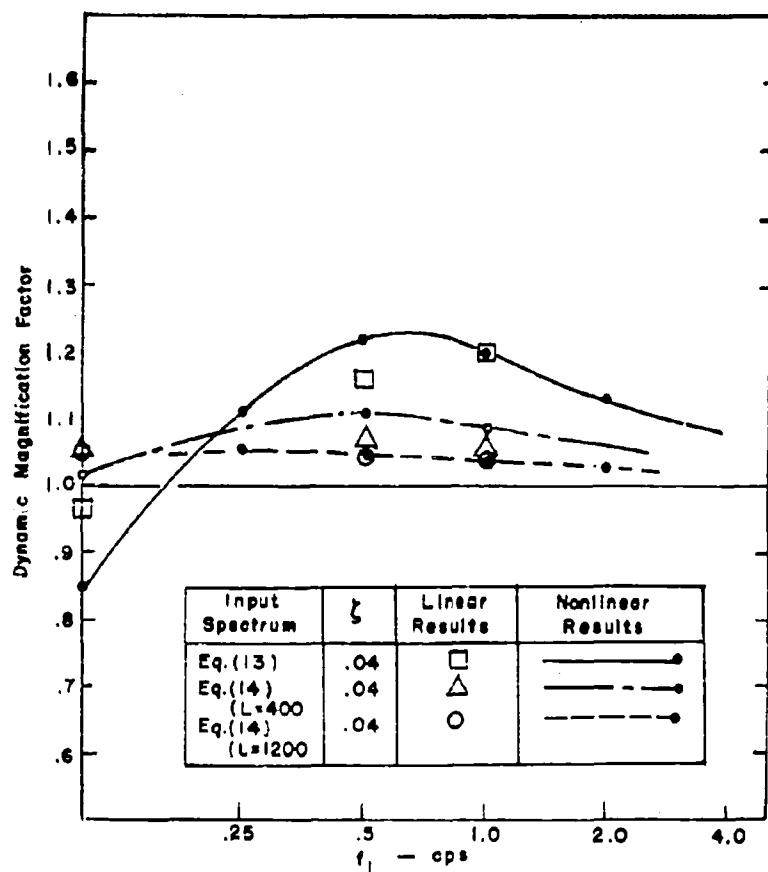
FIG. 5.   DMF vs. Natural Frequency for Various Input Spectra.
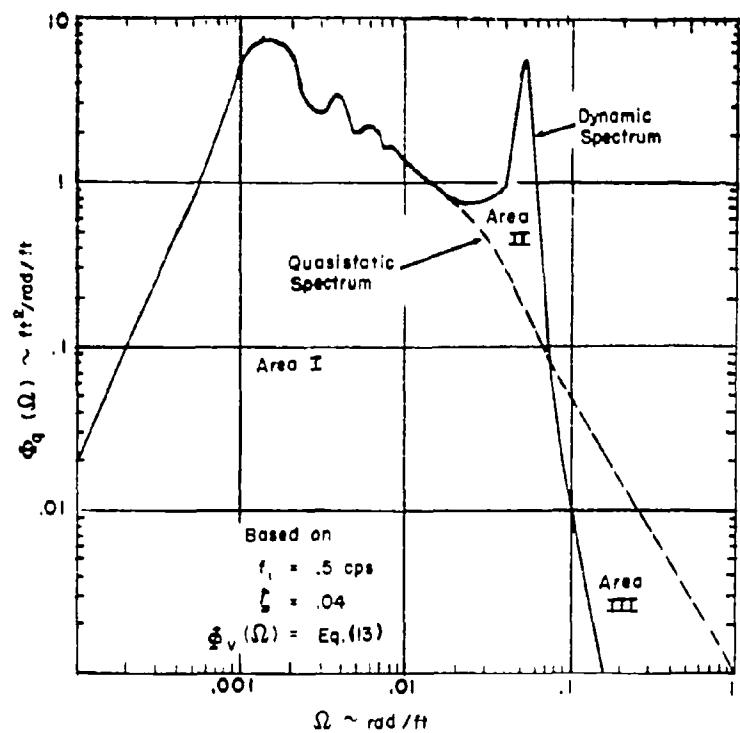
FIG. 6.   Typical Output Power Spectra.

It can be seen that for high f_1

    I $\gg$ II, III,

    DMF $\rightarrow$ 1.0 ;

for medium f_1,

    II $>$ III,

    DMF $>$ 1.0;

for very low f_1,

    III $>$ II,

    DMF $<$ 1.0.

Thus there is a critical natural frequency for ground wind drag problems which appears to be of the order of 0.5 to 1.0 cps.

Effect of Structural Damping

The effect of damping is more pronounced in spectral solutions than it is in discrete solutions. For moderate amounts of damping, the spectral method outlined in this paper will give lower magnification than would be obtained from a critically phased discrete solution. For very low damping, however, the spectral method shows higher loads than would be obtained from a discrete solution. It is felt that one of the major advantages of spectral solutions is that they show the proper effects of damping. This in turn points out the need for an accurate determination of damping.

At low natural frequencies, the effect of structural damping did not appear to be very significant. This was true because aerodynamic damping became relatively large at the low frequencies. In this regime the practice of linearizing aerodynamic damping might be questioned.

Effect of Input Spectra

The choice of the input spectrum had a significant effect on the results. Henry's spectrum in particular was most severe, because it had relatively more power in the higher frequencies which tend to phase with the vehicle response frequency. There is a need for more meteorological research in this area, with emphasis on extending the spectra to higher frequencies.

METHOD FOR NONLINEAR SYSTEMS

In this section a method is presented for computing dynamic magnification factors for systems that cannot be linearized. The assumption of normality employed in Eq. (17) is not needed, but the equal probability concept is still used.

Solution of Nonlinear Equations

The solution of the nonlinear response equation, Eq. (2), is obtained by the use of nonlinear analog equipment. A schematic diagram of the circuit used is shown in Fig. (7). A more complete description of the use of analog computers in the solution of nonlinear problems has been given.[7] The input to the problem consists of a steady wind, V_o, and a random wind V_R, defined by the power spectra of Eqs. (13) or (14). The random signal is obtained by filtering the output of a white noise generator so that it has a power spectrum equivalent to that of ground wind turbulence. The filter used to simulate the turbulence of Eq. (13) is shown in Fig. 8a. The numerical values reflect the change from a space spectrum to a time spectrum and an additional time scale change to speed up the analog operation. Less complicated filters can be used depending upon the accuracy desired. For example, the spectrum of Eq. (11) can be simulated by a simple RC circuit as shown in Fig. 8b.

Determination of Dynamic Magnification Factor

To compute the magnification factor of Eq.(21), it is necessary to compare the dynamic response with the quasistatic response obtained from the solution of

$$q_s = \frac{F V^2}{M \omega_1^2}$$

(22)

This can be accomplished by solving Eqs.(21) and (22) simultaneously on the analog computer, thus obtaining continuous traces of $q_d(t)$ and $q_s(t)$. Comparison of the dynamic and quasistatic records yields the magnification factor. The comparison is made by considering the distributions of maximum values of both the quasistatic and dynamic responses. The sets of maximum values are obtained by dividing the random records into a number of small time increments and recording the maximum value in each increment. The cumulative distributions of quasistatic and dynamic peaks can now be plotted on probability paper and the dynamic and static response peaks q_d and q_s which
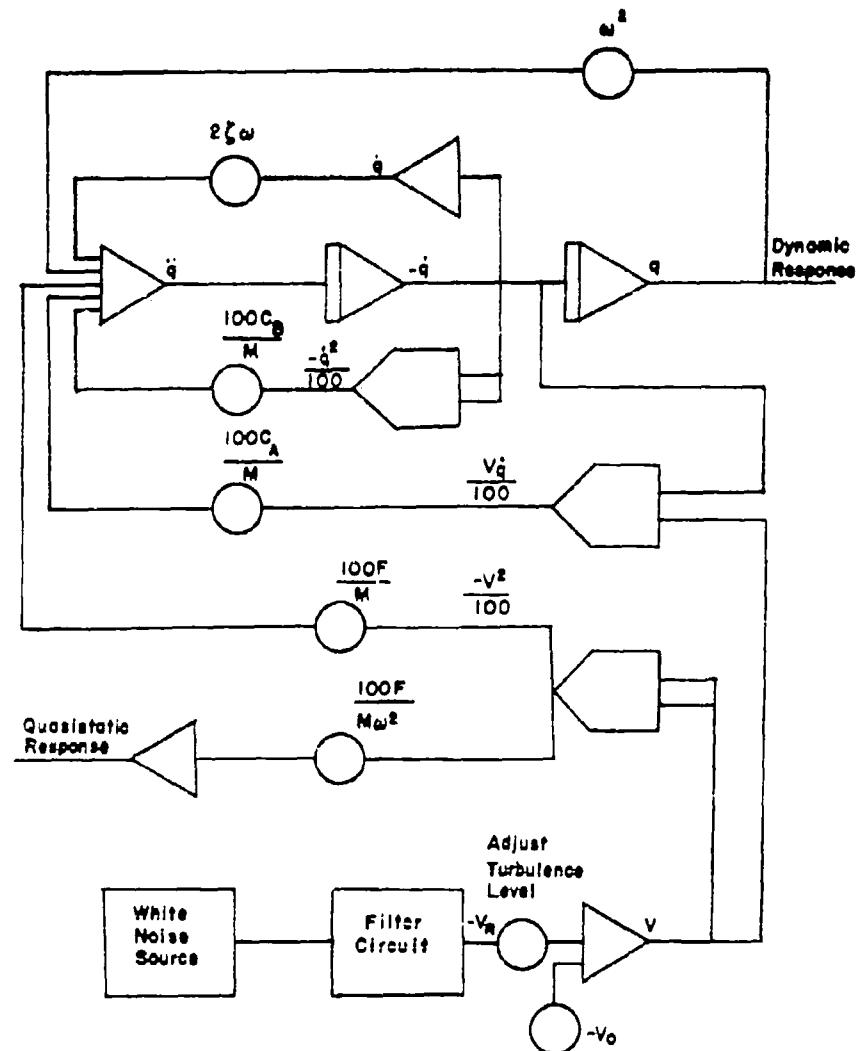
FIG. 7. Analog Circuit for Solution of
$$M\ddot{q} + 2M\zeta\omega_1\dot{q} + M\omega_1{}^2q = FV^2 - C_AV\dot{q} + C_B\dot{q}^2.$$

$$\sqrt{\frac{\tanh{(.114\,\omega)}}{\omega^{\frac{2}{3}}}}\left[1-\frac{\sin 4.4\,\omega}{4.4\,\omega}\right]$$

Desired Filter, Eq. (13)

$$\frac{E_O}{E_i}=\frac{2\,(1+12.5\,S)(1+.25\,S)\,S}{(1+50S)(1+S)(1+.067S)}\cdot\frac{1.635\,S}{1.635\,S^2+1.144S+1.0}$$

Approximating Transfer Function

FIG. 8a. Analog Filter Circuit.

$$\frac{1}{\left(1 + i \dfrac{L}{V_0} \omega\right)}$$

$$\frac{E_0}{E_i} = \frac{1}{\left(1 + \dfrac{L}{V_0} S\right)}$$

Desired Filter, Eq. (11)   Approximating Transfer Function
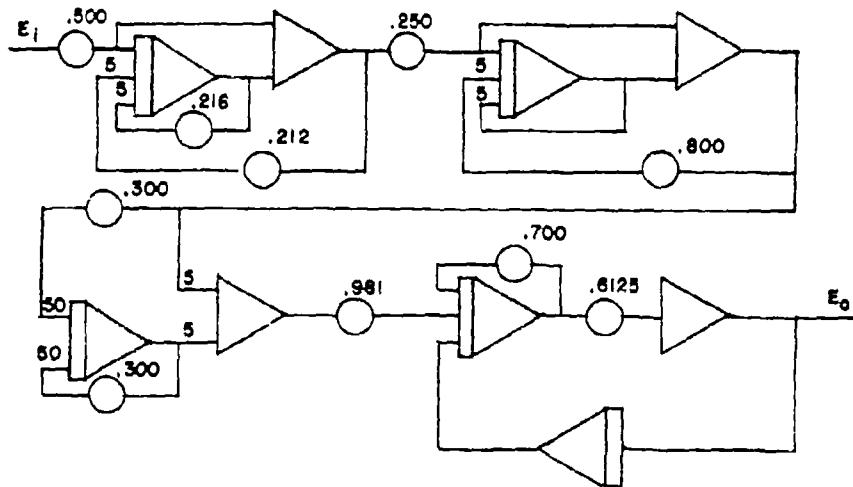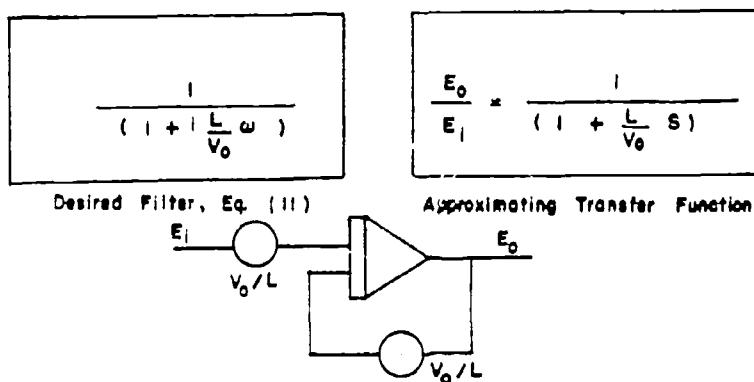
FIG. 8b. Simplified Analog Filter Circuit.

104

are expected with equal probability can be obtained for use in Eq. (21). Application of this factor to Q_s can determine the dynamic design response, Q_d, expected from the stated criterion.

It should be pointed out that this method is based upon comparing distributions of maximum values of the responses rather than distributions of the responses themselves as was done in the linear case. The maximum value comparison is more meaningful from an engineering point of view since maximum values are required for design purposes. Also it is much easier to obtain distributions of maximum values from a visual comparison of analog records than distributions of the variable itself.

Numerical Results

The nonlinear method was applied to the vehicle previously analyzed over the same general range of parameters. For each analysis, the vehicle was exposed to the random wind for 45 minutes of "real time." By a time scale change, the analog time was reduced by a factor of 10, however. The peak values were selected from one-minute time increments, or in some cases 30-second time increments. Typical distributions of peaks are shown in Fig. 9 which illustrates the computation of the magnification factor. The probability level at which to compute the ratio requires comment. The low response values (exceeded with a high probability) should not be compared because they do not represent significant loads. The highest values should not be used either, because little statistical reliability can be placed on these values. In this study, the response peaks that were exceeded 10 percent of the time were used. As can be seen from Fig. 9, there would be no difference in choosing a different probability level for this example. For some cases, however, the results would differ slightly if different probability levels were used. The results of the study are shown in Table 2 and Figs. 4 and 5.

In general, the same comments can be made as were made in discussing the linearized solutions. Certain particular comments should be made, however.

a. The two methods show remarkably good agreement. There does not appear to be any discrepancy that can be attributed to comparing responses in one case and peaks of responses in the other case.

b. The largest discrepancies occurred at $(f_1 = 0.1)$. For this case the aerodynamic damping is much more significant than the structural damping, and the damping linearization is least justified. The linear analysis gives higher values in this case for the reasons discussed earlier; that is, the time-dependent aerodynamic damping coefficient based on wind speed V is larger than the equivalent coefficient based on V_0 when the peaks occur.

105
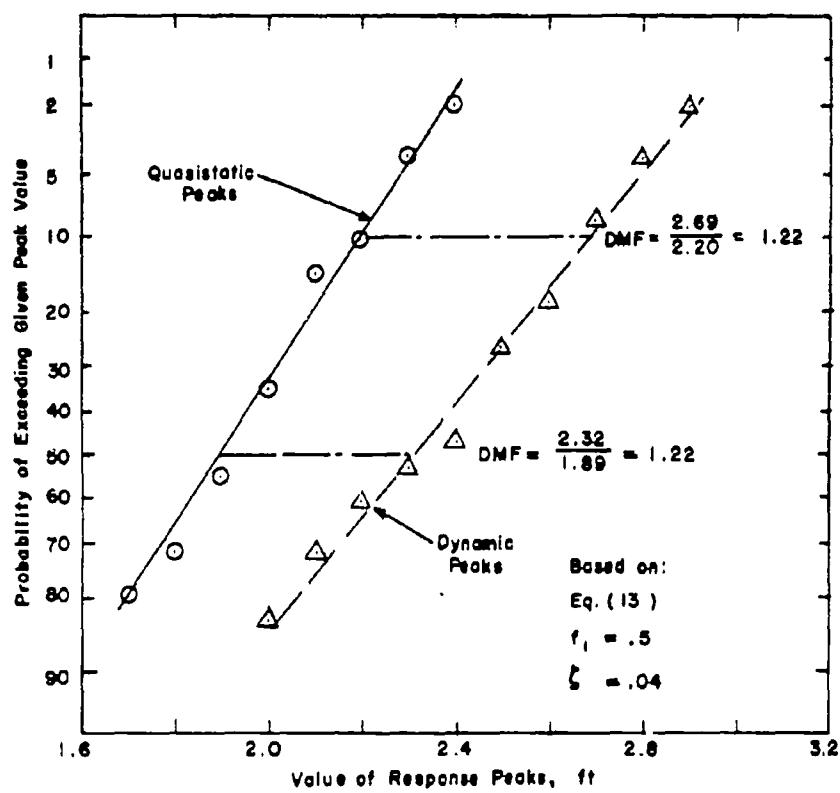
FIG. 9. Cumulative Distributions of Response Peaks.

TABLE 2

RESULTS FROM NONLINEAR ANALOG STUDY

Input Spectrum	f_1	ζ	DMF	Input Spectrum	f_1	ζ	DMF
Eq. (13)	.1	.1	.85	Eq. (14) L = 400			
	.5	.1	1.11		.1	.04	1.02
	1.0	.1	1.13		.5	.04	1.11
	2.0	.1	1.07		1.0	.04	1.09
					2.0	.04	1.06
	.1	.04	.85				
	.25	.04	1.11	Eq. (14) L = 1200			
	.5	.04	1.22		.25	.04	1.05
	1.0	.04	1.20		.5	.04	1.05
	2.0	.04	1.13		1.0	.04	1.04
	4.0	.04	1.08				
	.1	0	.92				
	.5	0	1.51				
	1.0	0	1.60				
	2.0	0	1.66				

CONCLUSIONS

In the determination of dynamic drag response of a slender flexible vehicle to ground wind, power spectral density techniques offer the best method of evaluating the effects of the natural frequency and structural damping of the system. It is felt that wind spectra are not well enough defined so that one could specify an average wind plus a gust spectrum to be used for design in place of the average wind and gust factor now specified. Wind spectra, however, can be used to define the frequency content of the gust and thus permit a more accurate determination of the dynamic effects.

In view of the effect that the choice of the input spectrum has on the DMF, more research work is needed to fix the form of the input spectrum, especially at high frequencies. In particular, this spectral information should be gathered under conditions of the highest wind speed possible.

Linearization of aerodynamic damping appears to be justified except in cases where the aerodynamic damping is large compared to structural damping. In these cases, the linearization method suggested is conservative.

REFERENCES

1. Y. C. Fung, Fluctuating lift and drag acting on a cylinder in a flow at supercritical Reynolds number, Journal of the Aerospace Sciences, November 1960.

2. A. A. Ezra and S. Birnbaum, Design criteria for space vehicles to resist wind induced oscillations, ARS Preprint 1081-60, April 1960.

3. D. A. Buell and G. C. Kenyon, The Wind Induced Loads on a Dynamically Scaled Model of a Large Missile in Launching Position, NASA TMX109, December 1959 (Confidential).

4. G. N. Brekke, Wind pressures in various areas of the United States, U.S. Department of Commerce, National Bureau of Standards, Building Materials and Structures Report 152, April 1959.

5. H. Press, M. T. Meadows and I. Hadlock, A reevaluation of data on atmospheric turbulence and airplane gust loads for application in spectral calculations, NACA Report 1272, 1956.

6. K. R. Thorson and Q. R. Bohne, Application of power spectral methods in airplane and missile design, Journal of Aerospace Sciences, February 1960.

7. Q. R. Bohne, B. E. Clingan, C. W. deCeault, and P. C. Deutschle, The dynamic response of advanced vehicles, WADD TR 60-518, September 1960.

8. S. O. Rice, Mathematical analysis of random noise, Parts I and II, Bell System Technical Journal, Vol. XXIII, No. 3, July 1944; Parts III and IV, Vol. XXIV, No. 1, January 1945.

9. G. I. Taylor, The spectrum of turbulence, Proceedings of the Royal Society (London), 164(a), 1938

10. R. M. Henry, A study of the effects of wind speed, lapse rate, and altitude on the spectrum of atmospheric turbulence at low altitude, IAS Preprint 59-43, January 1959.

11. U. O. Lappe, B. Davidson, and C. B. Notess, Analysis of atmospheric turbulence spectra obtained from concurrent airplane and tower measurements, IAS Preprint 59-44, January 1959.

12. H. C. S. Thom, Distribution of extreme winds in the United States, Journal of the Structural Division, Proceedings of ASCE, April 1960.

13. J. H. Walls, J. C. Houbolt, and H. Press, Some measurements and power spectra of runway roughness, NACA TN3305, November 1954.

Problems Associated with Launch of Wind-Limited Space Boosters

SOL LUTWAK

SPACE TECHNOLOGY LABORATORIES

ABSTRACT

Space boosters that are combinations of existing stages often must be launched under restricted altitude wind conditions because of structural or control limitations. The problems associated with specifying wind limitations and defining the 'probability of launching' for these vehicles are discussed in general terms. The necessity for operational prelaunch procedures to insure that the wind or angle of attack limitations are not exceeded on a given flight is also discussed. Prelaunch procedures for the Able-5 Lunar Probe launch are described briefly, and altitude wind forecasts and the results of prelaunch trajectory simulations are presented.

NOTATION

M_{all} Limit allowable bending moment, in. lbs = ultimate moment divided by factor of safety = M_{ult}/FS

M_{avail} Limit moment capability = $M_{all} - \frac{R}{2} P$

M_{equiv} Bending moment that produces the same stress as an axial load = $P \times \frac{R}{2}$ for a thin-walled cylinder

M_{buffet} Bending moment due to buffeting or unsteady aerodynamic effects

M_{gust} Bending moment due to gusts

M_{slosh} Bending moment due to sloshing

M_c Bending moment due to 'steady state' angle of attack

P Axial load, lbs

R Radius of vehicle, in.

q	Dynamic pressure $= \frac{1}{2} \rho V^2$, psf
V	Vehicle velocity, fps
α	Angle of attack, deg
ρ	Atmospheric density, slugs/ft^3.

INTRODUCTION

The purpose of this paper is to discuss the problems associated with the launch of a space vehicle booster that must be restricted with respect to the altitude winds through which it can fly because of structural or control limitations. An altitude wind operating limitation is often one of the restrictions for space booster vehicle systems that use combinations of existing stages. These stages were originally designed for other missions, particularly weapon systems applications, and are not optimum designs for the space booster mission. Specification of altitude wind operating limits for these space boosters will often eliminate the requirement for extensive modification to the structure or other hardware, which in turn will save money and expedite the schedules for the development of the vehicle.

It is apparent that the operating limits must not impair the operational capability to the extent that they cause very great probability of delaying or postponing the launch of a space booster whose mission requires launching during a limited time interval. In addition, the actual launch operation for a wind-limited booster will require altitude wind soundings and launch-time wind forecasts. Procedures for rapidly evaluating these wind data must be part of the prelaunch operations.

The paper will point out some of the problems involved in establishing the wind limitation, specifying the 'probability of launching' and providing prelaunch support for a space vehicle that is wind limited. These problems differ from those encountered when a weapon system is designed to a low-risk wind specification. The weapon system, which must be designed to conservatively defined altitude winds, can be launched at any time without a requirement for prelaunch wind information, and its probability of surviving the altitude wind environment, for present systems, will be at least 99 percent. For a wind-limited space booster, the 'probability of launch' must be determined early in the design phase; this probability is, of necessity, based on higher-risk wind specifications and may not be overly conservative. Then just prior to launch, when the approximate wind environment for the launch is known, it is necessary to establish with high confidence that the probability of successfully flying through the known winds is very high--approaching 100 percent.

110

DISCUSSION

Design Approach for a New System

The ideal approach to design of a new ballistic missile or rocket booster vehicle to survive altitude winds is first to select a wind criteria with a very low design risk. As an example, the wind profile used for ballistic missile design[1] is based on wind shears and velocities that are expected to be exceeded only one percent of the time during the windiest season of the year in the windiest area of the continental United States. The vehicle structure and control system are designed to these conservative criteria. And, presumably, if this design is within the overall system limitations of cost and performance, the vehicle system will have a probability of launching of nearly 100 percent with respect to altitude winds.

Design Approach for a Combination of Existing Stages

If existing stages are incorporated in a space booster, it is very likely that the strength of the vehicle will not allow use of the first approach without extensive structural modifications. The problems are similar if a control system limitation exists. To avoid making structural modifications to the vehicle, it is expedient to specify an altitude wind operating limitation for the system. The altitude wind limitation for the vehicle is based on the capability of the minimum strength portion of the structure.

Procedures for defining the wind limitation and specifying the probability of launching for the vehicle must consider the strength capability of the structure, the applied loads, the variation of load with angle of attack, and the correlation between the wind velocities and the vehicle angle of attack. The various aspects of the problem are discussed in detail below:

Strength capability of the structure

The ultimate strength of the structure can be defined as the load at which the structure will collapse or rupture. The ultimate load is generally determined from analyses and tests. The limit allowable load is the ultimate load divided by a factor of safety. In an efficient design the applied load will equal the limit allowable load. When the operating limit is established, the angle of attack is predicated on achieving the limit allowable load.

The limit allowable moment will be defined as M_{all}. For a thin-walled cylinder, which is typical of missile structures, the equivalent moment that produces the same stress as an applied axial load, P, load is given by

$$M_{equiv} = \frac{R}{2} P$$

where R is the radius of the vehicle at the appropriate station.

At any time in flight the structural capability that is available to sustain bending moment is

$$M_{avail} = M_{all} - \frac{R}{2} P .$$

The moment capability varies with time because of dependence on the variable axial load, P. Additionally, if a propellant tank is critical, its capability, which is dependent on pressure, will be affected by a time-varying internal tank pressure. The external pressures and vented compartment internal pressures also vary with time. As a result of these time-varying factors, different portions of the vehicle structure may be critical at different times.

Applied bending moments

The applied bending moments that the vehicle encounters arise from winds, which cause an essentially rigid body response, and from propellant sloshing, gusts and unsteady aerodynamic excitations such as transonic buffeting that cause both rigid-body and elastic responses. To establish the bending moment due to gusts, it is necessary to select a design gust. A discrete or spectral gust approach can be used and the appropriate shapes, wave lengths and velocities defined. Since the vehicle is expected to encounter moderate winds in this application, it might be reasonable to use moderate gust velocities rather than extremes. A low-risk gust criterion at this point, however, will introduce conservatism in the analysis. The gust bending moment calculation should consider elastic body response and the control system dynamics.

The bending moments that result from unsteady aerodynamic effects are generally obtained from missile response calculations based on wind tunnel data from tests on the particular vehicle configuration. The sloshing bending moments referred to here are those that can result from a sloshing limit cycle, or oscillation that results from feedback between the sloshing and the control system. This limit cycle does not exist on all liquid propellant vehicles; however, if one is expected, the magnitude can be estimated from flight data, or analytical results. The bending moments due to any other effects should also be determined.

At a given vehicle station the moment capability that is available to carry the steady state wind moments is given by

$$\overline{M}_{\alpha} = M_{avail} - M_{gust} - M_{buff} - M_{slosh} - \text{and so on.}$$

Limiting angle of attack

Since most boost vehicles fly very nearly trimmed, the bending moment at a given flight time is a direct function of angle of attack, α, or the product

112

of dynamic pressure and angle of attack, $q\alpha$. Hence the limiting angle of attack, $\bar{\alpha}$, can be established and is given by an equation of the form

$$\bar{\alpha} = K \bar{M}_\alpha .$$

Note that it has not been necessary to make any assumptions with regard to winds in arriving at the angle of attack limitation. This limitation is primarily a function of the strength capability and the vehicle response to other than the steady state winds.

Limiting wind velocity and probability of launching

As is apparent from the previous discussion, the operating limitation for the space booster is an applied bending moment limitation, which implies an angle of attack limitation. If it were possible to establish a valid correlation between the wind velocity and the vehicle angle of attack, then the operating limit could be stated directly as a wind velocity limitation. The probability of launching the vehicle could then be determined quite accurately from available wind statistics for the launch site.

It is well known to missile designers that the vehicle response, or angle of attack, cannot be simply related to the wind velocity at a given altitude. The integrated effect of the winds below the altitude of interest, has a significant influence on the angle of attack. The use of wind profiles (which have assumed correlations between the peak wind at the altitude of interest and the winds below this altitude) to compute the vehicle angles of attack has the advantage of simplicity. It is difficult, however, to define a wind profile producing a load or angle of attack that has strict statistical meaning. A comprehensive review has been provided[2] of the wind profile design approach that has been used in the missile industry. Also presented are the results of missile load calculations with a selected group of actual wind profiles; a load history is obtained from each profile and the load statistics are based on the missile response rather than on the wind velocities.

A number of studies[2] have shown that the angle of attack associated with a low-risk design wind profile (with a peak velocity that is exceeded only one percent of the time) is generally a conservative value and is acceptable for design use. The use of profiles to establish a correlation of angle of attack with wind velocity when the peak wind velocities are high would be expected to yield reasonable results because the profiles associated with high wind velocities are usually unidirectional and have fairly typical shapes. The profile approach, however, is believed to have serious limitations in predicting the angle of attack associated with low velocity winds. When rather low peak-wind velocities are being considered, wind direction shifts below the altitude of

113

interest are very likely. The greater variability of low velocity winds makes
the task of defining a conservative, or even a typical, wind profile difficult.

To establish the correlation of velocity with angle of attack, trajectory
calculations can be performed with a number of 'synthetic' wind profiles that
peak at varying velocities. Winds that peak at several altitudes must be
considered. Experience has shown that the altitudes near maximum dynamic
pressure (30,000 to 40,000 ft) are usually critical; however, there have been
instances in which altitudes near the transonic regime of the trajectory (ap-
proximately 20,000 ft) were also critical. The trajectory calculations will
provide a variation of angle of attack with wind velocity at the altitudes consi-
dered from which the limiting wind velocity can be estimated. The probability
of launching can then be based on the probability of encountering the limiting
wind velocity. It must be recognized, however, that the results obtained from
the synthetic profile approach will be approximate; this will be particularly
true when low peak-wind velocities are being considered.

There are alternatives to the use of synthetic wind profiles in establish-
ing the probability of launching a wind limited vehicle. A procedure similar
to that described by Hobbs[2] can be used. The response of the vehicle to a
statistically significant number of actual wind profiles can be established. The
probability of launching can be based directly on the probability of encounter-
ing the limiting angle of attack. This approach, which inherently should yield
the most satisfactory results, requires that a 'typical' or proper set of actual
wind profiles be selected. The Patrick Air Force Base wind profiles and the
200 Birmingham, Alabama profiles[2] have been oriented toward low risk design
winds and might not be entirely satisfactory for design studies with wind-
limited vehicles. In addition, the amount of computation required in the past
has been inconsistent with the time scale of the space booster design studies.

Another alternative to the synthetic profile approach is a possible
modification to the response matrix procedure presented by Trembath[3]. This
procedure can be used with wind statistical data similar in form to that given
by Court[4].

No matter what approach is used to establish the probability of launching,
the results of the study must be available early in the design phase. The
launch probability must be compatible with the mission launch requirements,
otherwise the system will not be developed.

Prelaunch Procedures

Before the actual launch of a wind-limited booster, it is essential to
establish that the wind limitations, or the angle of attack limitations, will not
be exceeded during the flight. For the Able-5 lunar probe, procedures were

incorporated as part of the prelaunch operation to obtain and evaluate altitude wind forecasts and soundings. The launch of the vehicle was contingent on the results of these evaluations. The prelaunch procedures involved obtaining altitude wind forecasts for launch time, performing a trajectory simulation based on the forecast wind data to obtain the expected angle of attack, making a go-no-go decision with respect to the altitude winds, and examining wind soundings obtained just prior to launch to insure that the trajectory simulation results are valid.

The wind data supplied was wind velocity and wind azimuth at 2000-ft altitude increments from surface to 60,000 ft. The range weather office supplied altitude wind forecasts for launch time (T-0) at T-24 hrs, T-12 hrs, and T-5 hrs. Altitude wind soundings were supplied from balloons released at T-3 hrs, T-2 hrs, T-1 hrs, and T-0. The T-12 and T-5 hr forecasts referred to the time the forecast data were supplied to STL; these forecasts were based on altitude wind soundings from balloons released at approximately T-13 hrs and T-6 hrs, as well as other appropriate meteorological data. The wind sounding time refers to the time the balloon was released.

The T-24 hr forecast generally served to alert personnel. Decisions to launch could be based on the results of the T-12 and T-5 hr forecasts. Since it was necessary to have a go-no-go launch decision prior to removal of the gantry tower, and T-5 hr forecast was the latest data that could be used. The T-3 and T-2 hr wind soundings served to confirm the T-5 hr forecast. The T-1 and T-0 soundings provided wind data just prior to and after the launch, which were used for flight test evaluation.

In the preliminary planning of the prelaunch procedures for the Able-5 lunar probe, it was thought that go-no-go wind velocities could be specified for the critical altitude ranges. Use of wind velocities alone as launch criteria was expected to simplify the prelaunch operation to some extent, since the launch decision could be made quickly at the launch site. This approach, which was later abandoned, involved the following:

    (a) If the wind velocities obtained from either the T-12 or T-5 hr forecasts exceeded the specified maximum values in the critical altitude ranges (18,000 to 22,000 ft and 30,000 to 45,000 ft) the launch was postponed.

    (b) If the T-12 and T-5 hr forecast velocities were less than the specified minimum values, it was permissible to launch without further investigation.

    (c) If the forecast wind velocities were between the specified maximum and minimum values, a trajectory simulation using the forecast wind profiles would have to be performed. Launch would be contingent upon the results of the trajectory simulation; the computed angles of attack would have to be below the limiting values.

115

The go-no-go wind velocity prelaunch procedure was abandoned because the trajectory simulation, which involved a great deal of set-up time, was already available. In addition, the conservatively low minimum velocities specified for (b) were quite restrictive, especially in the 18,000- to 20,000-ft altitude range, and would have resulted in a requirement for a trajectory simulation most of the time. It was decided to perform simulations for all forecasts and rely on the computed angle of attack, rather than the wind velocity alone, to arrive at a launch decision.

The trajectory simulation used is a digital procedure that considers a rigid missile and includes the control system dynamics; pitch and yaw plane responses are computed separately. The wind azimuth and velocity at the 2000-ft altitude intervals are provided as input. The procedure resolves the wind into the pitch and yaw plane components, computes the time history of angle of attack, engine angle, and dynamic pressure in each plane, and obtains the combined angle of attack. A typical simulation of this type requires 10 to 12 minutes of machine time on the 7090 computer for 80 seconds of flight time.

Since the Able-5 vehicle was launched from the Atlantic Missile Range and the computer facilities were in Los Angeles, transcontinental communications were involved but did not pose a problem. The wind forecasts were phoned to the Space Navigation Center at STL. Input of the data, computation, and transmission of the results to the test conductor were accomplished in approximately one hour. The altitude wind go-no-go decision was made prior to the time the gantry tower was removed (approximately T-3 hr). The T-3 hr wind sounding data was supplied at T-2 hrs and provided a check of the T-5 hr forecast, but nominally no simulation was to be run with this sounding. If there was a significant change in wind velocity or direction from the forecast values, however, there was sufficient time prior to launch to run a simulation as a check on the angle of attack.

Limitations of Prelaunch Simulations

It is apparent that there are tolerances associated with the input data and with the computed results obtained from a prelaunch trajectory simulation. There will be variations in the actual flight trajectory from the nominal values used for the simulation. In addition, the assumptions used to define the vehicle properties, such as weight, aerodynamics, and control system dynamics, will affect the validity of the results. The primary tolerances are believed to be those associated with the wind forecasts. These are a result of the time lag between the forecasts and the launch, and are also influenced by the distance between the balloon and the vehicle at the altitude of interest. (This distance varied from 5 to 30 miles for the soundings obtained in this launch operation.) It is believed, however, that if the technique used to obtain

116

the wind data and the accuracies involved are understood by the engineer there should be no problem in properly (or at least safely) defining the operating limits.

The validity of results of prelaunch simulation will improve as flight experience on vehicles is gained. Improved techniques, such as rocketsondes or dropsondes, for obtaining soundings in the vicinity of the launch site might be required. The launch-wind vehicle-interaction problem still requires considerable study. An interim solution for launch of wind-limited vehicles is to specify obviously conservative operating limits; this will be a satisfactory approach so long as the operational capability of the vehicle is not significantly impaired.

RESULTS OF ABLE-5 PRELAUNCH SIMULATIONS

The Able-5 lunar probe consisted of an Atlas first stage, an Aerojet AJ-10-101 second stage, and an ABL 248 third stage. It was necessary to launch the vehicle under restricted altitude wind considerations because of structural limitations in both the first and second stages.

The prelaunch wind forecast data, wind sounding data, and trajectory simulation results that were obtained for the two launches of the Able-5 lunar probe are presented in Figs. 1 through 4. The data from the 25 September 1960 launch illustrate a condition where the winds were very low in velocity all the way up to 50,000 ft (less than 50 fps) but variable in direction near the transonic altitude (20,000 ft). The data from the 15 December launch illustrate a condition where the wind direction was relatively constant and the peak wind velocity was moderate (170 fps) at the altitude of maximum dynamic pressure (35,000 ft).

For the 25 September launch the Able-5 limiting angles of attack were 3.8° near 20,000 ft (transonic) and 5.0° near 35,000 ft (maximum dynamic pressure). A minor structural modification was made for the 15 December launch and the limiting angles were 4.5° (transonic) and 5.0° (maximum dynamic pressure). The limiting angles of attack are indicated on Figs. 2 and 4. The launch azimuths for the flights were approximately 100°.

Figure 1 shows the T-12 and T-5 hr wind forecasts, and the T-3 hr and T-0 wind soundings for the 25 September launch. The computed angles of attack based on the T-12 hr forecast, T-5 hr forecast and the T-0 wind sounding are shown in Fig. 2.

The T-12 hr forecast indicated an abrupt change in wind direction (100° to 310°) near 15,000 ft with very low wind velocities. As can be seen in Fig. 2 this direction change resulted in an angle of attack of approximately 3.3° near

117
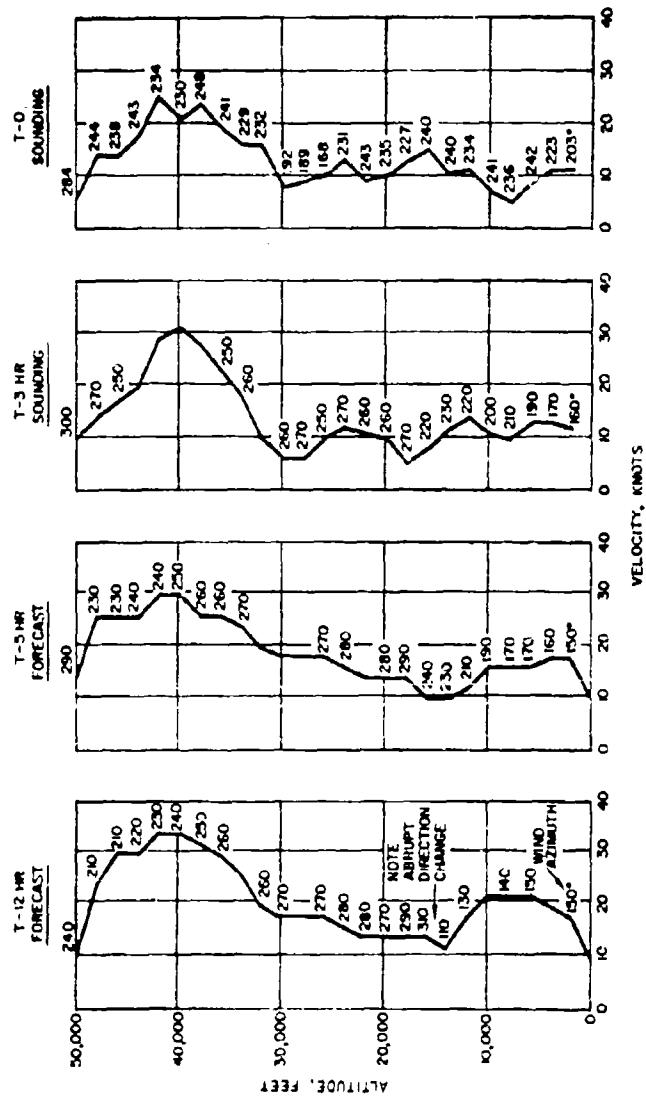
FIG. 1. Wind Forecast and Sounding Data. 25 September 1960 Launch,
Wind Velocity and Azimuth Versus Altitude.

118
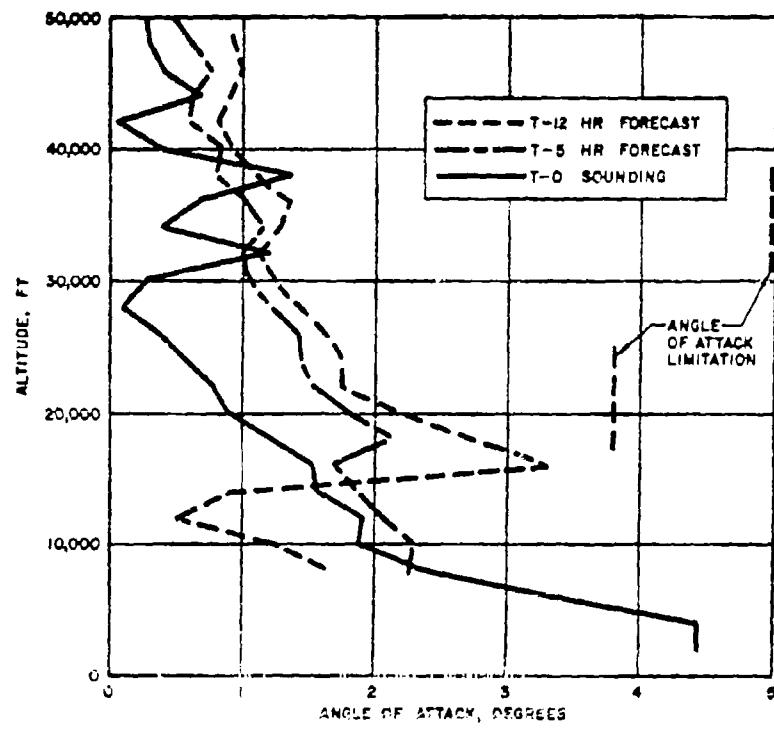
FIG. 2. Angle of Attack Based on Wind Forecasts and T-0 Sounding, 25 September 1960 Launch.

119

the transonic altitude. Since this was close to the limiting angle of attack of 3.8°, a possible flight postponement was indicated. The actual launch decision, however, was based on the T-5 hr forecast. The simulation based on this forecast resulted in angles of attack (Fig. 2) that were well below the limiting values.

It is important to point out that a prelaunch procedure based only on a go-no-go wind velocity would not have indicated that the vehicle response was approaching a limiting condition for the T-12 hr predicted winds. An an example, the T-12 hr forecast wind velocity at 20,000 ft was approximately 16 fps, while a go wind velocity may have been estimated to be 65 fps.

A further examination of the wind profiles in Fig. 1 shows that the T-3 hr sounding was in reasonable agreement with the T-5 hr forecast, but that at T-0 the wind direction did shift significantly at a number of altitudes. The wind velocities for all the forecasts and sounding were in good agreement. It is of interest to note that hurricane 'Florence' had moved inland near AMR the day before the launch. Apparently the storm conditions caused the wind direction at the lower altitudes to be quite variable.

Examination of Fig. 2 shows that the computed angles of attack at 20,000 ft for T-0 were below the T-12 hr and T-5 hr values but were approximately the same near 35,000 ft. This further illustrates the significant influence of wind direction shifts, or wind profile shape, on the vehicle response, particularly at low altitudes.

Figure 3 shows the T-12 hr and T-5 hr forecasts and the T-0 sounding for the 15 December launch of Able 5. The T-0 maximum wind velocity was in excellent agreement with the forecast values although the altitude of maximum wind varied by approximately 10,000 ft. In addition, the T-0 wind azimuth above 10,000 ft was in good agreement with the forecast data. Below 10,000 ft, however, the forecast and the T-0 wind azimuths differed significantly. The sensitivity of the missile to the wind shifts is again illustrated in Fig. 4; it can be seen that there is a great difference in the missile response in the 10,000- to 15,000-ft altitude range.

In general, the 15 December wind profiles were essentially unidirectional and monotonic up to the critical altitude, typical of most synthetic design profiles. As can be seen in Fig. 4, there is no significant difference in the maximum angle of attack in the critical altitude region of 30,000 to 45,000 ft; the result is expected since all the profiles peaked at about the same velocity.

Examination of Fig. 4 shows that the forecast angles of attack were below the limiting values of 4.5° and 5.0°. The altitude winds were not a problem for this launch.
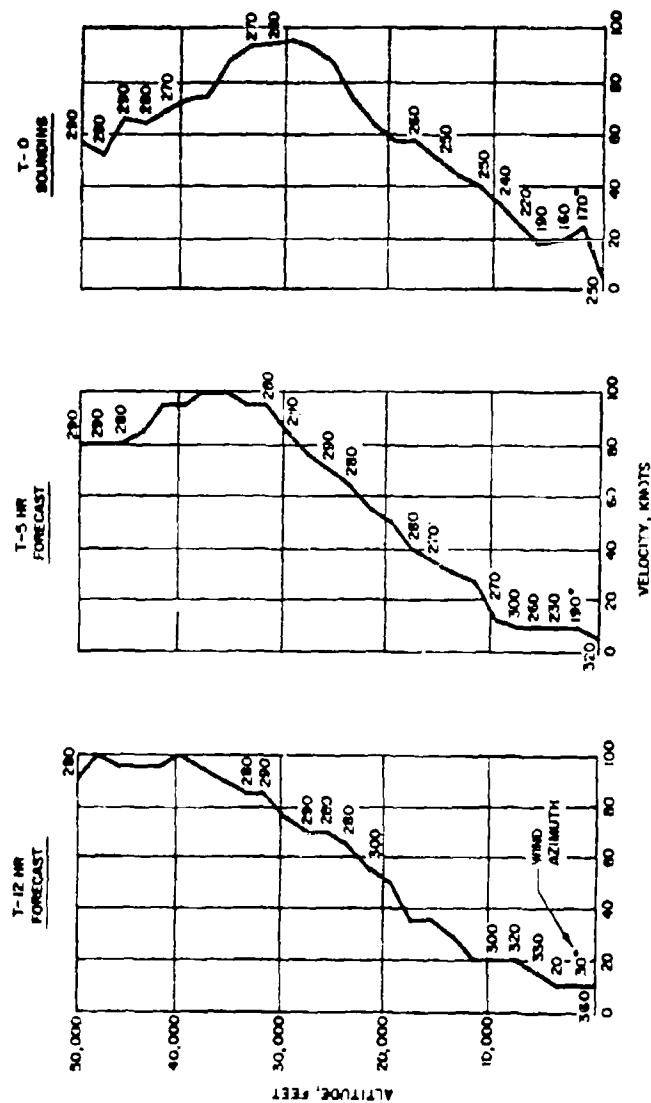
FIG. 3. Wind Forecast and Sounding Data, 15 December 1960
Launch Wind Velocity and Azimuth Versus Altitude.

121
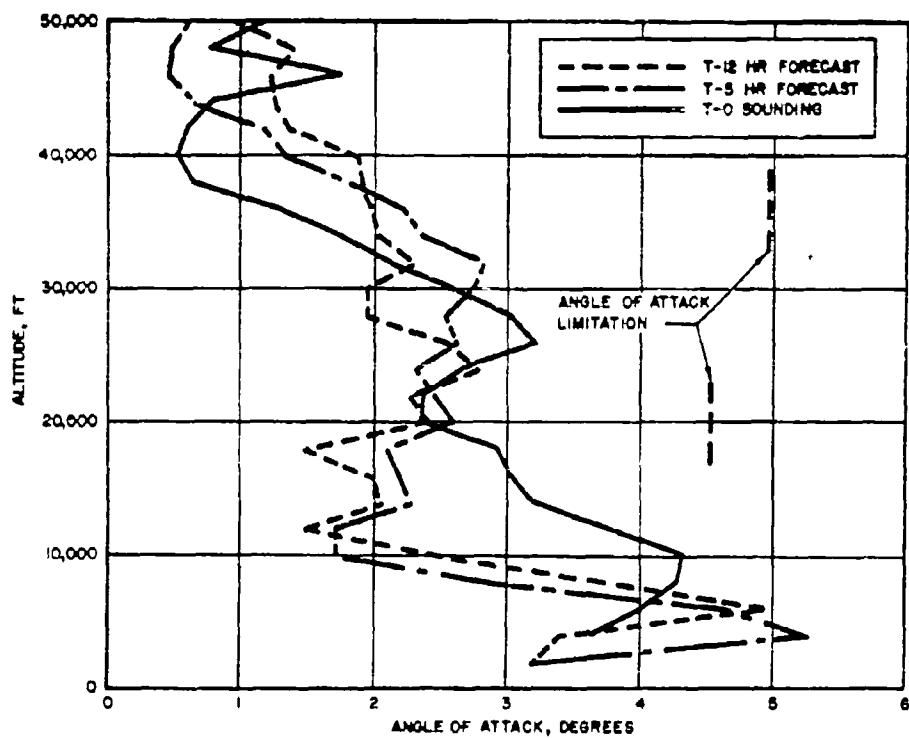
FIG. 4. Angle of Attack Based on Wind Forecasts and T-0 Sounding, 15 December 1960 Launch.

122

CONCLUSIONS

The use of moderate wind restrictions can provide savings in development time and cost for space booster vehicles that might have structural or control limitations. These moderate operational limitations can be adequately defined, and prelaunch procedures can be implemented to provide a launch decision.

If the economical development of a space booster vehicle involves severe wind limitations, the problems become more involved. Because of the variability of wind profiles associated with low velocity winds, it is difficult to define the probability of launch; in addition, it becomes more difficult to accurately preduct the vehicle response from prelaunch environment data in order to insure that the vehicle can survive the altitude winds. In general, it can be concluded that designing to severe wind limitations, even if these limitations are within the other mission requirements, is not advisable.

The use of the terms 'moderate' and 'severe' altitude wind restrictions is of course only qualitative. In an attempt to define the 'probability of launch' associated with these restrictions, however, it can be stated that vehicles that can be launched at least 80 percent of the time have moderate restrictions and vehicles that can be launched less than 80 percent of the time have severe restrictions. By comparison, a ballistic missile can be launched at least 99 percent of the time. The difference between the wind velocities and design loads associated with 99 percent winds and 80 percent winds can be appreciable.

The problem of specifying wind limitations is not peculiar to space booster systems; it is often encountered in the R and D phase of ballistic missile flight testing when a vehicle is flown to evaluate a specific problem area or must fly with components that have not been fully qualified prior to launch. Wind limitation for boost of manner space vehicles might be desirable to reduce the loads environment encountered by the crew. In addition, if significant performance benefits can be gained for very large space boosters, it might be desirable to design these vehicles to wind criteria that are less severe than those used in ballistic missile design.

In the aerospace industry the emphasis has been, until recently, on extreme or low-risk winds to be used for design purposes. It is apparent that, in the future, there will be more interest in the properties (that is, statistics and typical profiles) of moderate-risk winds, or winds that are likely to be encountered. In addition there will be a great deal of interest in wind sounding, forecasting and data reduction techniques that meet the time and accuracy requirements of operational prelaunch procedures for space booster vehicles.

REFERENCES

1. N. Sissenwine, Windspeed profile, windshear, and gusts for design of guidance systems for vertically rising air vehicles, Air Force Survey in Geophysics No. 57, AFCRC-TN-58-216, November 1954 and June 1959 Revision.

2. N. P. Hobbs, E. S. Criscione, et al., Development of Interim wind, wind shear, and gust design criteria for vertically rising vehicles, WADC Technical Report 59-504 Avidyne Research, Inc., July 1959.

3. N. W. Trembath, Control system design wind specification, No. 58-1, Space Technology Laboratories Report No. GM 42.3-17, 1 July 1959.

4. A. Court, Vertical correlations of wind components, AFCRC TN-57-292, 29 March 1957.

Random Excitation of Missiles Due to Winds

J. D. WOOD

J. G. BERRY

SPACE TECHNOLOGY LABORATORIES

ABSTRACT

The dynamic response of a large missile subjected to ground winds is
determined herein. The analysis is carried out under the assumptions that
(1) gusts persist for a time that is long compared with the longest time con-
stant of the constrained missile, that is, quasisteady winds; (2) the Reynolds
number that characterizes the flow is high, that is, 10^6. The flow phenomena
associated with the last assumption are such as to cause the response problem
to be statistical (stochastic) rather than deterministic. A numerical ex-
ample illustrates that the dynamic loads induced in a missile structure by
ground winds can be quite large. The determination of the spectral density
of lift and/or drag forces from the spectral density of gust velocity is con-
sidered in the Appendix. Certain idealized but plausible assumptions
concerning the statistical character of gusts are made in order to render
the analysis more tractable.

INTRODUCTION

A missile that is launched in a vertical position from a fixed surface
launcher is frequently subjected to significant loads as the result of the
oscillating displacements induced by the ground winds to which it is exposed
during prelaunch periods. In the case of missiles with relatively large-
diameter cylindrical sections, such ground winds can give rise to very large
Reynolds numbers R*($R > 10^6$). In such a flow condition, random vortex
shedding and consequently random lift and drag forces will result. Since the
lift forces act on the missile in a direction perpendicular to the drag forces,
large oscillating displacements and loads may result.

For Reynolds numbers in the range from 40 to 150, the shedding of
vortices is regular, and the eddying motion in the wake is periodic in both

---

*The Reynolds number R is defined to be $R = Ud/\nu$, where U is the un-
disturbed velocity of flow, d is the missile diameter, and ν is the kinematic
viscosity of the flowing liquid.

space and time. The flow under these conditions can be approximated by the well-known Kármán vortex street. Between 150 and 300 the vortex shedding is no longer so regular, while above 300, the predominant frequency of vortex shedding can be determined but the amplitude has become random. Finally, at R of order 10^5, the separation point of the boundary layer moves rearward on the cylinder and the drag coefficient drops rapidly. The exact value of this transition zone, or region of critical Reynolds numbers, depends on surface roughness, turbulence structure in the air stream, and so on. The wake for a flow below the critical Reynolds number, however, exhibits a clear periodic flow structure, with a dominant frequency at each side of the missile. The flow at Reynolds numbers above the critical point produces a much more turbulent wake in which the vortex street pattern is no longer recognizable. In such cases, it is necessary to consider a power spectrum or a correlation function rather than a single dominant frequency.

The majority of earlier research on the subject of vortex shedding in a flow around circular cylinders was concerned with the wake characteristics at subcritical Reynolds numbers. Although a limited amount of data on the shedding frequency in the supercritical range was available, the forces acting on the cylinder, other than the mean drag component, had apparently never been measured. In 1957, wind tunnel experiments were conducted by Space Technology Labs in order to measure the fluctuating lift and drag acting on a circular cylinder in a flow of an incompressible fluid at large Reynolds numbers. Data has been presented on the root-mean-square values of the lift and drag coefficients, the extreme values of these coefficients, and their power spectra at various Reynolds numbers between 330,000 and 1,390,000.[1]

THEORETICAL CONSIDERATION

The following is a derivation of the means by which the response of a large missile to ground winds, sufficient to cause random vortex shedding, may be calculated. The flow conditions for a typical missile with two distinct cylindrical sections of different diameters are depicted in Fig. 1.

Considering the lateral motion of the missile in Fig. 1, the applied lift force per unit length along the missile can be described as

$$L(x, t) = q(x) d(x) C_L(t) \tag{1}$$

where $q(x)$ is the dynamic pressure, $d(x)$ is the missile diameter at any given point along its length, and $C_L(t)$ is the lift coefficient which varies randomly
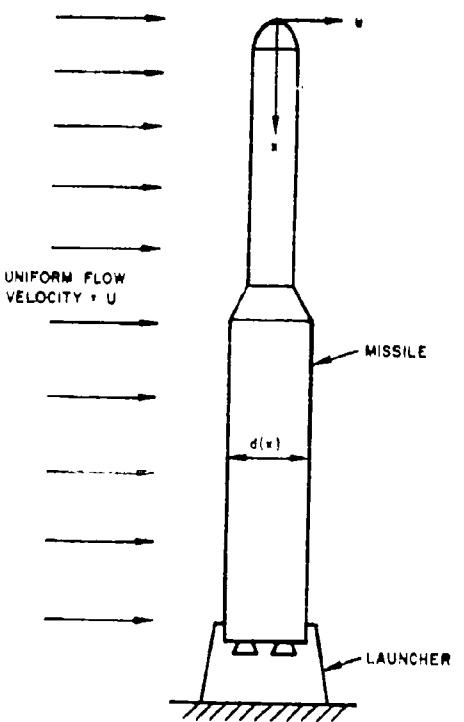
FIG. 1. Missile Exposed to Ground Winds.

with time.* Actually, C_L is a function of Reynolds number as well as of time. Therefore C_L, at each missile station, depends on the diameter of the missile at that station. The dependence of C_L on R and t is such that it is impossible, in general, to express C_L as a product or sum of a function of R and a function of t. However, the experimental data[1] indicates that C_L is not a strong function of R, at least for limited ranges of R in excess of 5×10^5. Therefore, it is reasonable to assume that a value of C_L, associated with a Reynolds number based on a representative missile diameter, should be adequate for Eq. (1). This conclusion is only valid for two-dimensional flow.[1] The three-dimensional flow characteristics around the tip of a missile have a substantial effect on the total lift and drag forces.[2,3] In the absence of detailed wind tunnel input forces on particular missiles, however, the procedure developed herein is the best available. On the basis of limited experimental data, it can be anticipated that the results obtained will be conservative.

The lift force of Eq. (1) is a random function of time since $C_L(t)$ is random in time. Problems involving random time variations are usually more conveniently treated in the frequency domain than in the time domain. The frequency representation of a random function is known as its power spectral density. Figure 2 is a typical power spectral density of lift or drag force on a uniform clyinder.[1] The frequency parameter, $S = \omega d/2\pi U$, used in Fig. 2, is known as the Strouhal number; the curve is normalized such that

$$\int_0^\infty F(S) \, dS = 1; \quad \text{or} \quad \int_0^\infty F(\omega d/2\pi U) d\omega = 2\pi U/d . \tag{2}$$

If $P_L(\omega)$ is defined as the power spectral density of the lift coefficient $C_L(t)$, the mean square value of C_L is given by

$$\int_0^\infty P_L(\omega) \, d\omega = <C_L^2> . \tag{3}$$

Comparing the latter two equations, the normalizing factor $K = P_L(\omega)/F(S)$ is evident, and

$$P_L(\omega) = \frac{d <C_L^2>}{2\pi U} F(S) , \tag{4}$$

where $<C_L^2>$ is the mean-square value of the lift coefficient observed experimentally.[1]

---

*The lift force is assumed not to vary randomly with x, that is, the spacial correlation is unity. This assumption might not be completely valid; however, no data is available concerning spacial correlation, and in any event the assumption is conservative in determining gross missile response.
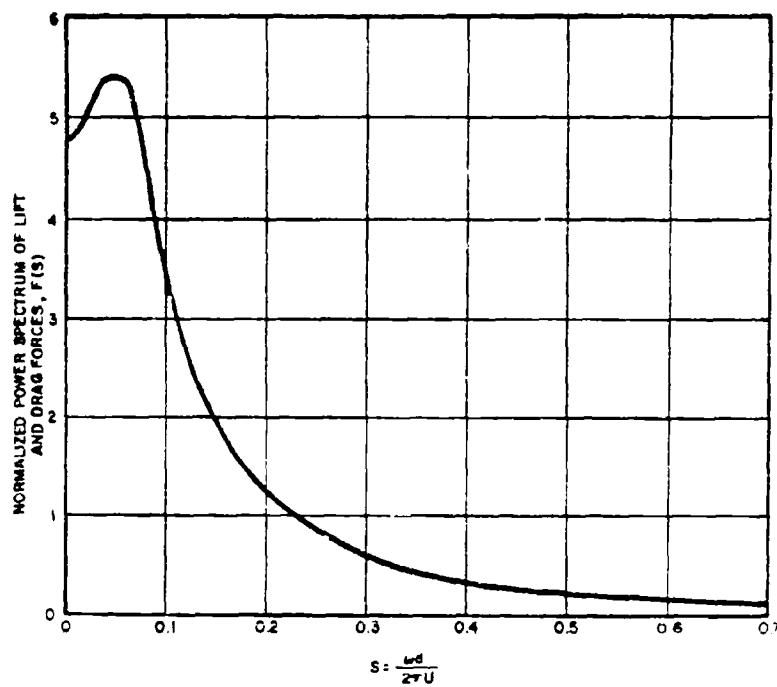
FIG. 2. Normalized Power Spectrum for the Lift Force and
Drag Force at Reynolds Number 1.39 X 10⁶.

Similarly, the power spectral density of the drag coefficient resulting from the oscillatory motion of the missile parallel to the air flow is

$$P_D(\omega) = \frac{d <C_D^2>}{2\pi U} \; F(S) \; ,$$ (5)

where $<C_D^2>$ is the mean-square value of the drag coefficient observed experimentally. [1]

The lateral displacement response of the missile, which is assumed to be a linear structure, may be expressed in terms of its normal modes as

$$u(x, t) = \sum_n \phi_n(x) \, q_n(t) \, ,$$ (6)

The generalized coordinates, $q_n(t)$, are governed by equations of motion such as,

$$\ddot{q}_n + 2 \; \zeta_n \omega_n \dot{q}_n + \omega_n^2 q_n = \frac{Q_n(t)}{M_n}$$ (7)

with certain restrictions on the modal damping, ζ_n, for example, its spacial distribution and smallness.
The generalized force is

$$Q_n(t) = \int_\ell f(x, t) \, \phi_n(x) \, dx,$$ (8)

and M_n is the generalized mass in the nth mode. [4] Since it is assumed, in the case of wind-induced oscillations, that the forcing function is $f(x, t) = F(x)T(t)$, the generalized force becomes

$$Q_n(t) = T(t) \int_\ell F(x) \, \phi_n(x) \, dx \stackrel{\Delta}{=} W_n T(t) \, ,$$ (9)

where $W_n = \int_\ell F(x) \, \phi_n(x) \, dx$, and $F(x) \cdot q(x) \, d(x)$.

The solution of Eq. (7) in terms of its indicial admittance, $h(t)$, is

$$q_n(t) = \int_0^\infty h_n(\tau) \, T(t - \tau) d\tau \; .$$ (10)

The term $T(t)$ is a random function implying that $q_n(t)$ and $u(t)$ are random functions of time. It is the nature of random processes that only a statistical description is meaningful. It is quite often impossible to construct the statistics needed for a complete description; however, the mean square value, which is the second statistical moment, is usually obtainable. If the statistics of a

random process are Gaussian, the mean square value provides a complete description. It is for these reasons that the mean square or autocorrelation function of the response is used as

$$< u^2 > \; = \; <u(x, t) \, u(x, t)> \; = \sum_n \sum_m \phi_n(x) \phi_m(x) <q_n(t) \, q_m(t + \tau)>. \qquad (11)$$

The bracket $< >$ implies an average over time only, that is, $u(x, t)$ is assumed not to vary randomly with x. The problem is to determine the quantity $<q_n(t) \, q_m(t + \tau)>$ in Eq. (11). It can be shown[5] that

$$<q_n(t) \, q_m(t + \tau)> \; = \int_{-\infty}^{\infty} \frac{P(\omega)}{Z_n(i\omega) Z_m^*(i\omega)} \, d\omega \qquad (12)$$

where $P(\omega)$ is given in Eqs. (4) and (5),

$$\frac{1}{Z_n(i\omega)} = \frac{W_n}{M_n \omega_n^2 \left\{ \left[1 - (\omega/\omega_n)^2 \right]^2 + (2\zeta_n \omega/\omega_n)^2 \right\}^{1/2}}$$

and $\dfrac{1}{Z_m^*(i\omega)}$ is the complex conjugate of

$$\frac{1}{Z_m(i\omega)} = \frac{W_m}{M_m \omega_m^2 \left[(\omega, \, m) \right]^{1/2}} \quad .$$

In evaluating the integral of Eq. (12) a simplification can be made if the damping ratios ζ_n are small and if $P(\omega)$ is a smooth function as compared with the resonant peaks of the structure. In such a case, the largest contributions to the integrand are those terms for which $n = m$, because near each resonance $\omega \approx \omega_n$ and the radicals in the denominator become very small. Neglecting the terms for which $n \neq m$, and substituting the result into Eq. (11), the mean square response is

$$<u^2(x)> \; = \int_0^{\infty} \sum_n \frac{W_n^2 \, \phi_n^2 \, P(\omega) \, d\omega}{M_n^2 \omega_n^4 \left\{ \left[1 - (\omega/\omega_n)^2 \right]^2 + \left[2\zeta_n(\omega/\omega_n) \right]^2 \right\}^2}$$

or

$$<u^2(x)> \; = \sum_n \frac{W_n^2 \, \phi_n^2}{M_n^2 \omega_n^4} \int_0^{\infty} \frac{P(\omega) \, d\omega}{\left[1 - (\omega/\omega_n)^2 \right]^2 + \left[2\zeta_n(\omega/\omega_n) \right]^2} \quad .$$

If $P(\omega) = $ const., no further assumptions need be made because each term in the foregoing equation is easily integrated. Remembering that the

131

integrand is a function with very steep peaks at each ω_n, another simplifying assumption may be made. Since the integrand has steep peaks near $\omega = \omega_n$, the main contribution to the integral comes where $P(\omega) = P(\omega_n)$ so that a good approximation can be made if $P(\omega)$ is taken as $P(\omega_n) = $ const. for each term. Then,

$$\langle u^2(x) \rangle = \sum_n \frac{W_n^2 \phi_n^2}{M_n^2 \omega_n^3} \frac{\pi}{4 \zeta_n} P(\omega_n) .$$

A similar expression has been derived.[4] Making the substitution into this equation for $P(\omega_n)$ as defined previously gives

$$\langle u^2(x) \rangle = \frac{d\langle C_L^2 \rangle}{8U} \sum_n \frac{W_n^2 \phi_n^2}{\zeta_n M_n^2 \omega_n^3} F(S_n) .$$

It follows then that the mean-square bending moment along the missile in the lift plane is

$$\langle M^2_{(x)} \rangle = \frac{d\langle C_L^2 \rangle}{8U} \sum_n \frac{W_n^2 [m_n(x)]^2}{\zeta_n M_n^2 \omega_n^3} F(S_n) ,$$

where m_n is the bending moment in the nth mode. The mean-square responses in the drag plane can be obtained from the above expressions if $\langle C_L^2 \rangle$ is replaced by $\langle C_D^2 \rangle$.

The other wind force acting per unit length along the missile is the steady state drag force which is defined as

$$F_D(x) = C_D q(x) d(x)$$

where F_D = steady state drag force

   C_D = mean steady state drag coefficient

   $q(x)$ = dynamic air pressure at station x.

For missiles exposed to a random gust environment, the relation between the spectral density of the steady state drag force and the spectral density of the gust velocity is given in the Appendix.

For purposes of analysis, assuming the air flow around the missile to be two-dimensional, the responses in the drag and lift planes are added vectorally. For example, the peak displacement of the missile at station

132

x, u(x), is defined as

$$u(x) = \left[(u_D + 3u_{oD})^2 + (3u_{oL})^2 \right]^{1/2}$$

where u_D = steady state drag displacement

   u_{oD} = rms value of the oscillatory drag displacement

   u_{oL} = rms value of the oscillatory lift displacement.

It is assumed that the oscillatory lift and drag displacements have normal distributions. The rms values of these responses are equivalent to the standard deviations (sigma) since the means are zero. Hence, a 3-sigma value of the oscillatory displacements is used in the foregoing equation, which gives a confidence level of 99.73 percent. That is, 99.73 percent of these random oscillations are within the peak displacements. Since the oscillatory components of displacement are assumed to reach their maxima at the same time, the foregoing equation should be conservative. It checks closely with the peak displacement observed in the missile model with a rounded nose cone used in the experiments reported.[2,3]

In a similar manner, the resultant bending moment, M_R, is defined as

$$M_R = \left[(M_D + 3M_{oD})^2 + (3M_{oL})^2 \right]^{1/2}$$

where M_D = steady state drag bending moment

   M_{oD} = rms value of the oscillatory drag bending moment

   M_{oL} = rms value of the oscillatory lift bending moment.

EXAMPLE

An indication of the actual full-scale order of magnitude of bending moments that can be induced by a strong ground wind (effectively steady state) acting on a large ballistic missile can be obtained from Table 1 below. In this case, a typical intercontinental type of ballistic missile is assumed to be erected on a surface launcher in the vertical position and exposed to a uniform 60 mph wind. The mean drag coefficient is taken as 0.55, and the predominant component of oscillatory response occurs at the frequency of the first bending mode of the missile, for this case, 2.4 rad/sec. The actual bending moments at several points on the missile are computed to be as follows:

133

TABLE 1

BENDING MOMENTS IN A TYPICAL MISSILE
EXPOSED TO UNIFORM 60-MPH WINDS

Distance From Missile Base, Inches	Bending Moments, in. lb X 10^{-5}			
	M_D	$3M_{oD}$	$3M_{oL}$	M_R
0	15.07	19.54	63.50	72.32
150	9.82	14.10	44.80	51.59
350	4.84	7.33	23.80	26.75
650	0.80	0.78	2.52	2.97

As can be seen from these figures, a strong ground wind can easily impose loadings on a missile that could be catastrophic if not taken into account in the structural design of the airframe or if the missile is not otherwise protected. There have been many instances in the past where research and development versions of large ballistic missiles have had to be protected from damage by raising the erector or returning the gantry to its position over the missile when heavy winds arose during prelaunch testing or flight preparations. Sufficient structural strength must be given to operational missiles to avoid restricting their use under certain wind conditions. It is common for space vehicle boosters to be ground-wind limited. After a missile is launched, the body bending mode frequencies increase sufficiently that the response due to random vortex shedding is negligible. This is due to the decrease in the power spectrum (Fig. 2) at higher frequencies.

REFERENCES

1. Y. C. Fung, Fluctuating lift and drag acting on a cylinder in a flow at supercritical Reynolds numbers, Bulletin, 26th Shock and Vibration Symposium, Department of Defense, 1958.

2. A. A. Ezra, Wind-induced oscillations of the Titan missile, WDD-M-MI-59-7, Martin Company, Denver 1, Colorado, March 1959.

3. D. A. Buell and G. C. Kenyon, The wind-induced loads on a dynamically scaled model of a large missile in launching position, NASA TM-X-109, Ames Research Center, Moffet Field, California.

4. J. G. Berry, H. E. Lindberg, and J. D. Wood, Ballistic Missiles and Space Vehicle Systems, Chapter 12, John Wiley and Sons, Inc., New York - London, 1961.

5. J. H. Laning and R. H. Battin, Control Systems Engineering, Chapter 5, McGraw-Hill Book Co., Inc., New York - Toronto - London, 1956.

6. M. V. Barton and W. T. Thomson, The response of mechanical systems to random excitation, Journal of Applied Mechanics, Vol. 24, No. 2, June 1957, p. 248.

7. H. Press, M. T. Meadows, and I. Hadlock, A re-evaluation of data on atmospheric turbulence and airplane gust loads for application in spectral calculations, NACA, Report 1272, Langley Aeronautical Lab., Langley Field, Virginia, 1956.

8. N. Wax, Noise and Stochastic Processes, Dover, 1954, p. 227.

APPENDIX

A RELATION BETWEEN SPECTRAL DENSITY OF STEADY STATE DRAG FORCE AND SPECTRAL DENSITY OF GUST VELOCITY

The problem considered herein is the determination of the spectral density of a steady state drag force from the spectral density of gust velocity. The problem is not completely trivial since the steady state drag force involves the square of the gust velocity.

Two major assumptions will be made: (1) the process is stationary, and (2) the gust velocities are distributed in a Gaussian manner. Strictly speaking, neither of these assumptions is true. The first assumption is equivalent to assuming that the gusts persist for a long time compared with any of the time constants of the system they act on, and therefore transient effects are ignored. Gusts are assumed to have greater periods than the lowest period of the missile. The second assumption is approximately true for large-scale turbulence. Since most of the energy convected by turbulence is associated with eddies of small wave number, the assumption of a Gaussian distribution is reasonable. In any event, these two assumptions allow some progress.

The steady state drag force is related to the velocity via the equation

$$F_D = 1/2 \, \rho \, C_D \, A \, U^2 \tag{A.1}$$

where the symbols have the conventional meaning. It will be assumed that C_D is effectively constant over the Reynolds number range associated with the instantaneous values of U. Otherwise, equation (A.1) is not valid. Let

$$F = \frac{F_D}{1/2 \, \rho \, C_D A} \quad , \quad \text{and } U = V + v \tag{A.2}$$

where V is the mean wind velocity and v is the random gust velocity. Then

$$F = U^2 = V^2 + 2V\ v(t) + v^2(t) \quad . \tag{A.3}$$

By virtue of the assumption of stationarity, V must be independent of time. The autocorrelation function of F is calculated first. The symbol $< >$ will denote an ensemble average,

$$< F(t)\ F(t + \tau) > = R_F(\tau) = \left\{ \left[V^2 + 2V\ v(t) + v^2(t) \right] \right.$$
$$\left. \left[V^2 + 2V\ v(t + \tau) + v^2(t + \tau) \right] \right\} \tag{A.4}$$

so that

$$R_F(\tau) = < V^4 + 2V^3\ v(t + \tau) + V^2\ v^2\ (t + \tau) + 2V^3\ v(t) + 4V^2\ v(t)$$
$$v(t + \tau) + 2V\ v(t)\ v^2(t + \tau) + V^2\ v^2(t) + 2V\ v^2(t)\ v(t + \tau)$$
$$+ v^2(t)\ v^2(t + \tau) > \quad .$$

By virtue of the definition of v from Eq. (A.2), $< v > = 0$. Thus

$$R_F(\tau) = V^4 + V^2 < v^2(t + \tau) > + 4V^2 < v(t)\ v(t + \tau) > + 2V$$
$$< v(t)\ v^2(t + \tau) > + V^2 < v^2(t) > + 2V < v^2(t)\ v(t + \tau) > \tag{A.5}$$
$$+ < v^2(t)\ v^2(t + \tau) > \quad .$$

Due to the stationarity assumption $v^2(t)$ cannot depend upon time and therefore

$$< v^2(t) > = < v^2(t + \tau) > \quad .$$

Since it is assumed that v is distributed in a Gaussian fashion and since the Gaussian distribution is symmetrical about the mean, all odd order central moments of v vanish. Therefore,

$$< v(t)\ v^2(t + \tau) > = < v^2(t)\ v(t + \tau) > = 0 \ .$$

Equation (A.5) now takes the form

$$R_F(\tau) = V^4 + 2V^2 < v^2(t) > + 4V^2 < v(t)\ v(t + \tau) > + < v^2(t)\ v^2(t + \tau) >$$
$$\tag{A.6}$$

136

and

$$< v(t)\, v(t + \tau)> = R_V(\tau)$$

is the autocorrelation function of v.

The mean square value of v is $< v^2(t)>$ and is given by

$$< v^2(t)> = R_v(o),$$

and there remains only the discovery of a form for $< v^2(t)\, v^2(t + \tau)>$. It is at this point that the assumption of a Gaussian distribution plays a crucial role. A Gaussian distribution is completely described by its first and second moments (that is, by the mean and standard deviation). Therefore, all of the higher moments are expressible in terms of the autocorrelation function R_v. As will be seen later, R_v is related to the spectral density of v.[7] The following can be written:[8]

$$< v^2(t)\, v^2(t + \tau)> = < v^2(t)> \; < v^2(t)> + 2< v(t)\, v(t + \tau)><v(t)\, v(t + \tau)>.$$

Combining all of these results, Eq. (A.6) becomes

$$R_F(\tau) = V^4 + 2V^2 R_v(o) + 4V^2 \; R_v(\tau) + R_v^{\,2}(o) + 2R_v^{\,2}(\tau). \qquad (A.7)$$

The Wiener-Khintchine theorem is used for the spectral density of F

$$P_F(f) = \int_{-\infty}^{\infty} R_F(\tau)\, e^{-i2\pi f \tau}\; d\tau = \int_{-\infty}^{\infty} V^4 + 2V^2 R_v(o) + 4V^2 R_v(\tau)$$

$$+ R_v^{\,2}(o) + 2R_v^{\,2}(\tau) \Big] e^{-i2\pi f \tau}\; d\tau$$

and

$$P_v(f) = \int_{-\infty}^{\infty} R_v(\tau)\, e^{-i2\pi f \tau}\; d\tau \; .$$

It is also noted that

$$\int_{-\infty}^{\infty} e^{-i2\pi f \tau}\, d\tau = \delta(f)$$

$$R_v(\tau) = \int_{-\infty}^{\infty} P_v(f)\, e^{i2\pi f \tau}\; df \; .$$

One more result is needed from the theory of Fourier transforms: if F(t) and

$G(t)$ are Fourier transforms of $f(x)$ and $g(x)$ respectively then

$$\int_{-\infty}^{\infty} F(t)\, G(t)\, e^{-i2\pi ft}\, dt = \int_{-\infty}^{\infty} g(\eta)\, f(x - \eta)\, d\eta$$

or the Fourier transform of the product of F and G is the convolution of f and g.

Thus

$$P_F(f) = \left[v^4 + 2v^2 R_v(o) + R_v^2(o) \right] \delta(f) + 4v^2 F_v(f)$$
$$+ 2 \int_{-\infty}^{\infty} P_v(f - \eta)\, P_v(\eta)\, d\eta \quad . \tag{A.8}$$

It is recalled that $R_v(o)$ is the mean square value of v and therefore

$$<v^2(t)> = R_v(o) = \int_{-\infty}^{\infty} P_v(f)\, df.$$

The spectral density of F is thus related to the spectral density of v.

138

The Response of a Flexible Missile to Ground Winds

L. L. FONTENOT

GENERAL DYNAMICS/ASTRONAUTICS

ABSTRACT

This paper presents techniques for estimating ground wind design loads of flexible missiles. In Section I, an expression for calculating the power spectral density of the drag force acting on the missile is formulated. In Section II the response of a flexible missile to ground winds is discussed and a simplified approach to the problem noted. In Section III, the design response of the missile to ground winds is formulated. A rational approach to combine the gust problem and the vortex shedding problem is presented.

INTRODUCTION

A missile in the prelaunch condition, that is, erected on a launch pad (Fig. 1), might be exposed to ground winds that give rise to oscillatory forces acting in a plane normal to the direction of the wind, as well as steady and oscillatory forces acting in the direction of the wind. The wind V(t) is defined as a steady mean wind V_o plus an unsteady wind v(t) which is assumed to vary randomly with time (Fig. 2).

Generally, for Reynolds numbers > 10 , the steady wind induces oscillations of the missile that are predominantly perpendicular to the direction of the flow. This in turn gives rise to large oscillating displacements and bending moments in the structure. [1,2,3]

The unsteady wind v(t) induces oscillatory forces that act on the missile in the direction of the flow. To be sure, there is an interdependence between the oscillatory forces induced by the steady wind and those generated by the unsteady wind. Unfortunately, however, nothing is known about this influence at the present time.

The problem considered in this paper is the response of a missile to ground winds. The methods employed herein can be obtained in greater detail. [4]
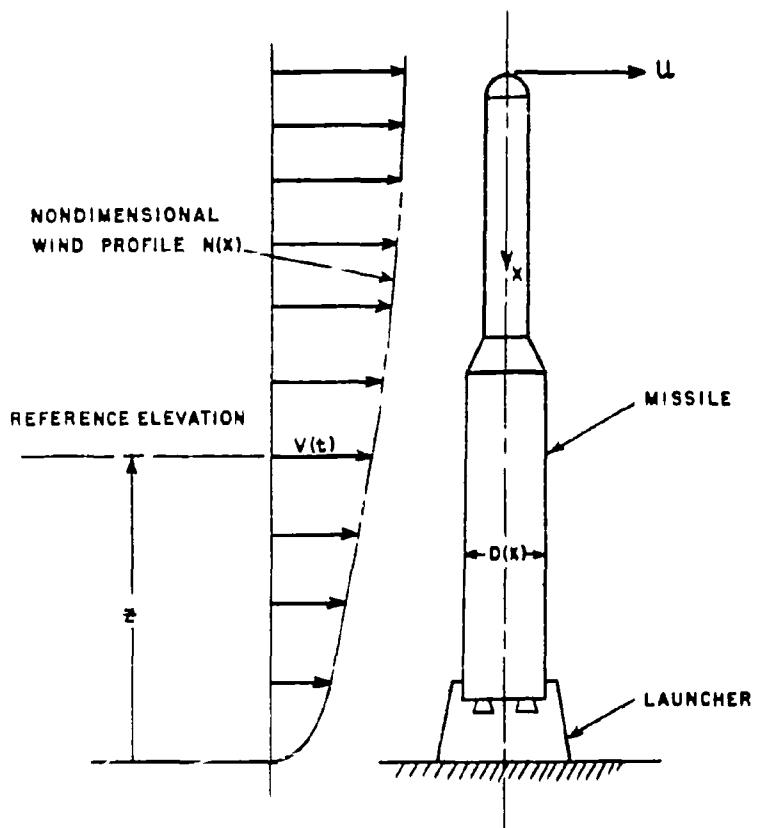
FIG. 1. Missile Exposed to Ground Winds.
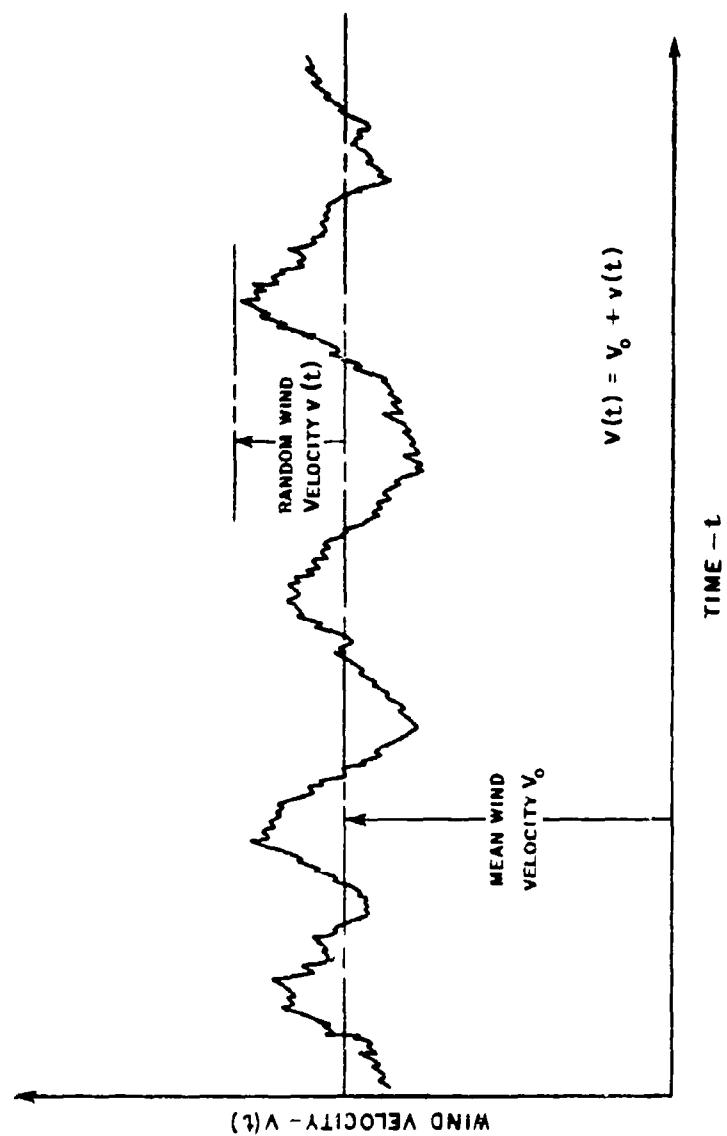
FIG. 2. A Sample Function of the Wind Velocity.

$$v(t) = V_o + v(t)$$

TIME — t

RANDOM WIND
VELOCITY v (t)

MEAN WIND
VELOCITY V_o

WIND VELOCITY— V(t)

141

THE POWER SPECTRAL DENSITY OF THE DRAG FORCE

Several authors have presented the power spectral density of the horizontal component of gust velocity at low altitudes.[5] The drag force acting on the missile, however, is a function of the square of the gust velocity. Thus, to ascertain the response of the missile in question, it is first necessary to determine the power spectral density of the drag force which is a function of the power spectral density of the gust velocity.

It will be assumed that $V(t)$ is a sample function from a random process that is stationary and ergodic, and the gust velocities are distributed in a Gaussian manner. None of these assumptions is quite true. Stationarity implies that the probability distributions of $V(t + \tau)$ in the sample space are identical with those of $V(t)$ independently of τ. This is also equivalent to assuming that the gusts persist for a long time compared with any of the time constants of the system they act on, and consequently transient effects are ignored. The ergodic property implies that a statistical average $V(t)$, or any function of $V(t)$, over a sample space can be replaced by a long time average over a single sample function. The assumption of a Gaussian distribution is approximately true for large scale turbulence.[6]

Consider the lateral motion of the missile as shown in Fig. 1. The applied drag force per unit length can be expressed as

$$f(x, t) = \frac{1}{2} \rho C_D N(x) D(x) \left[V(t) \right]^2 \tag{1}$$

where

ρ = mass density of air

$D(x)$ = missile diameter

C_D = drag coefficient

$V(t)$ = total wind velocity = $V_o + v(t)$

V_o = mean wind velocity

$v(t)$ = random gust velocity (zero mean)

$N(x)$ = nondimensional wind profile.

It will be assumed that C_D is constant over the Reynolds number range associated with the instantaneous values of $V(t)$.

Equation (1) can be rewritten in the form

$$f(x, t) = F(x) \left[V(t) \right]^2 = F(x) \left[V_o^2 + 2V_o v(t) + v^2(t) \right] \tag{2}$$

142

where

$$F(x) = \frac{1}{2} \, \rho \, N(x) \, D(x) \, C_D \, .$$

The autocorrelation function of $f(x, t)$ is defined as

$$\overline{f(x, t) \, f(x, t+\tau)}^* = R_f(\tau) = \left[F(x)\right]^2 \overline{\left[V_o^2 + 2V_o \, v(t) + v^2(t)\right]} \cdot$$
$$\overline{\left[V_o^2 + 2V_o \, v(t+\tau) + v^2(t+\tau)\right]} \, . \tag{3}$$

Expanding Eq. (3) yields

$$R_f(\tau) = \left[F(x)\right]^2 \left[V_o^4 + 2V_o^3 \, \overline{v(t+\tau)} + V_o^2 \, \overline{v^2(t+\tau)} + 2V_o^3 \, \overline{v(t)} + \right.$$
$$4V_o^2 \, \overline{v(t) \, v(t+\tau)} + 2V_o \, \overline{v(t) \, v^2(t+\tau)} + V_o^2 \, \overline{v^2(t)} + \tag{4}$$
$$\left. 2V_o \, \overline{v^2(t) \, v(t+\tau)} + \overline{v^2(t) \, v^2(t+\tau)} \right] \, .$$

But, $\overline{v(t)} = \overline{v(t+\tau)} = 0$, which follows by definition of $v(t)$ and the assumption of stationarity. Thus, Eq. (4) becomes

$$R_f(\tau) = \left[F(x)\right]^2 \left[V_o^4 + V_o^2 \, \overline{v^2(t+\tau)} + 4V_o^2 \, \overline{v(t) \, v(t+\tau)} + 2V_o \, \overline{v(t) v^2(t+\tau)} \right.$$
$$\left. + V_o \, \overline{v^2(t)} + 2V_o \, \overline{v^2(t) \, v(t+\tau)} + \overline{v^2(t) \, v^2(t+\tau)} \right] \, . \tag{5}$$

From the stationarity assumption

$$\overline{v^2(t)} = \overline{v^2(t+\tau)} \, .$$

Now $v(t)$ is assumed to have a Gaussian distribution, which is symmetrical about the mean; thus, all odd order central moments of $v(t)$ vanish. Hence

$$\overline{v(t) \, v^2(t+\tau)} = \overline{v^2(t) \, v(t+\tau)} = 0$$

which follows from the stationarity assumption.

$$* \quad \overline{(\qquad)} = \lim_{T \to \infty} \frac{1}{2T} \int_{-T}^{T} (\qquad) \, dt.$$

143

Equation (5) now assumes the form

$$R_f(\tau) = \left[F(x)\right]^2 \left[V_o^4 + 2V_o^2\,\overline{v^2(t)} + 4V_o^2\,\overline{v(t)\,v(t+\tau)} + \overline{v^2(t)\,v^2(t+\tau)}\right]$$

(6)

Now, by definition

$$R_v(\tau) = \overline{v(t)\,v(t+\tau)} = \text{autocorrelation function of } v(t):$$

$$R_v(o) = \overline{v^2(t)} = \text{the mean square value of } v(t).$$

A Gaussian distribution is completely described by its first and second moments (mean and standard deviation). Therefore all of the higher moments are expressible in terms of the first and second moments. Since the mean of $v(t)$ is zero, all of the higher moments are expressible in terms of the autocorrelation function R_v. It is easily shown that[7]

$$\overline{v^2(t)\,v^2(t+\tau)} = \overline{v^2(t)} \cdot \overline{v^2(t)} + 2\,\overline{v(t)\,v(t+\tau)} \cdot \overline{v(t)\,v(t+\tau)} \quad .$$

From the preceding properties, Eq. (6) assumes the form

$$R_f(\tau) = \left[F(x)\right]^2 \left[V_o^4 + 2V_o^2\,R_v(o) + 4V_o^2\,R_v(\tau) + R_v^2(o) + 2R_v^2(\tau)\right]$$

$$= \left[F(x)\right]^2 \left\{\left[V_o^2 + R_v(o)\right]^2 + 4V_o^2\,R_v(\tau) + 2R_v^2(\tau)\right\} \quad .$$

(7)

The power spectral density of the drag force is defined as

$$S_f(\omega) = \frac{1}{\pi} \int\limits_{-\infty}^{\infty} R_f(\tau)\,e^{-i\omega t}\,d\tau \quad .$$

(8)

Substituting Eq. (7) into Eq. (8) yields

$$S_f(\omega) = \left[F(x)\right]^2 \frac{1}{\pi} \int\limits_{-\infty}^{\infty} \left[V_o^2 + R_v(o)\right]^2 e^{-i\omega\tau}\,d\tau + 4\left[F(x)\right]^2 V_o^2$$

$$\frac{1}{\pi} \int\limits_{-\infty}^{\infty} R_v(\tau)\,e^{-i\omega\tau}\,d\tau + \frac{2}{\pi}\left[F(x)\right]^2 \int\limits_{-\infty}^{\infty} R_v^2(\tau)\,e^{-i\omega\tau}\,d\tau \quad .$$

(9)

However,

$$\int_{-\infty}^{\infty} e^{-i\omega\tau} d\tau = \delta(f) = \text{dirac delta function}$$

$$\int_{-\infty}^{\infty} (f) \, df = 1, \quad 2\pi f = \omega$$

$$\frac{1}{\pi} \int_{-\infty}^{\infty} R_v(\tau) e^{-i\omega\tau} d\tau = S_v(\omega) \quad \text{by definition}$$

$$\frac{1}{\pi} \int_{-\infty}^{\infty} R_v^2(\tau) e^{-i\omega\tau} d\tau = \frac{1}{2} \int_{-\infty}^{\infty} S_v(\omega_1) S_v(\omega - \omega_1) d\omega_1 \ .$$

Hence, Eq. (9) becomes

$$S_f(\omega) = \left[F(x) \right]^2 \left\{ \left[V_0^2 + R_v(0) \right]^2 \frac{\delta(f)}{\pi} + 4V_0^2 S_v(\omega) + \right.$$
$$\left. + \int_{-\infty}^{\infty} S_v(\omega_1) S_v(\omega - \omega_1) d\omega_1 \right\} \ , \tag{10}$$

and for frequencies other than $\omega = 0$, Eq. (10) assumes the form

$$S_f(\omega \neq 0) = \left[F(x) \right]^2 \left\{ 4V_0^2 S_v(\omega) + \int_{-\infty}^{\infty} S_v(\omega_1) S_v(\omega - \omega_1) d\omega_1 \right\} \ . \tag{11}$$

The power spectral density of the horizontal component of gust velocity is given as[5] (Fig. 3)

$$S_v(\omega) = a_1 \frac{\text{TANH } b_1 \omega}{\omega^{5/3}} \ , \tag{12}$$

where

$$a_1 = \frac{0.0206 \, V_0^{7/3}}{Z^{2/3}}$$

$$b_1 = \frac{68.2 \, Z}{V_0^2}$$

Z = elevation above the ground.

$$Sv(\omega) = a_1 \frac{Tan H \ b_1 \omega}{\omega^{5/3}}$$

$$a_1 = \frac{0.0206 V_0^{7/3}}{Z^{2/3}}$$

$$b_1 = \frac{68.2 Z}{V_0^2}$$

$$Z = 300 FT$$
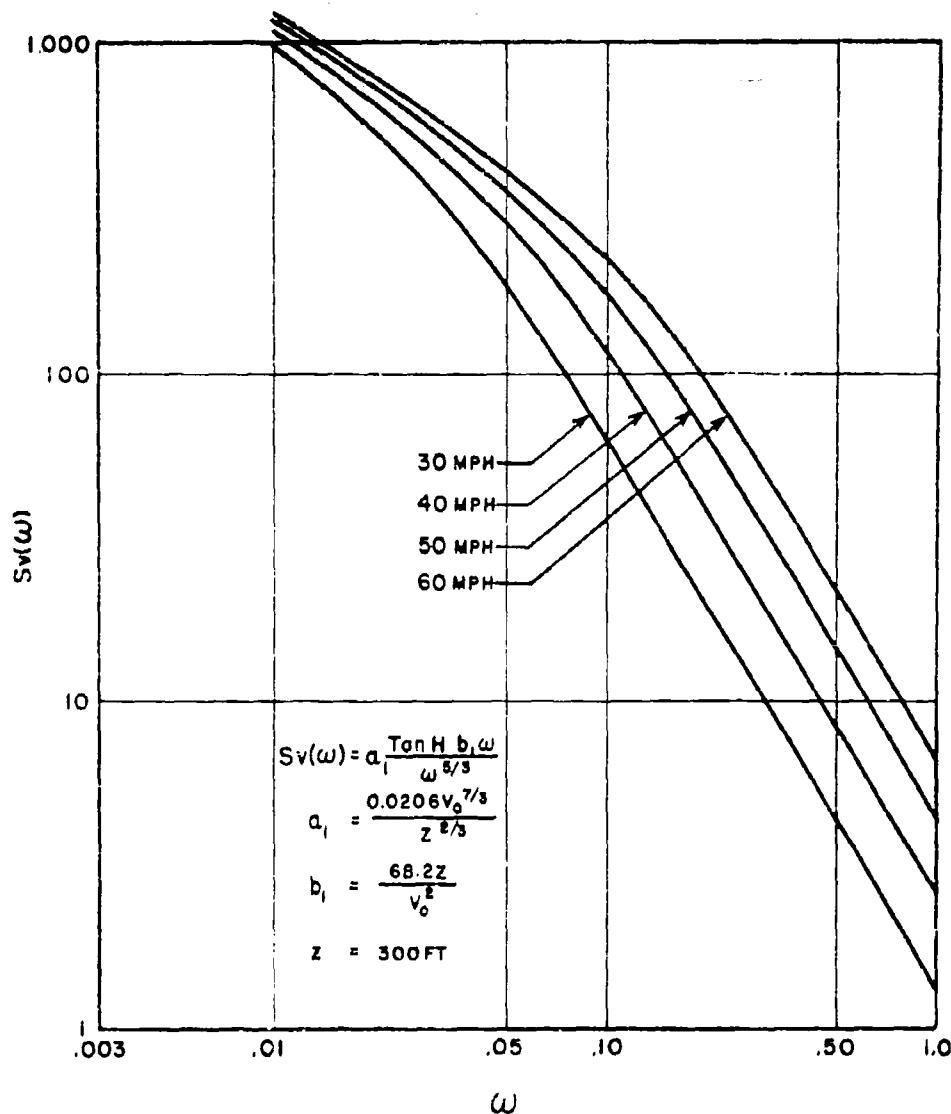
FIG. 3. Some Typical Plots of the Power Spectral Density
of Gust Velocity.

146

Another power spectral density of gust velocity that is quite useful is the well known expression for isotropic turbulence (Fig. 4)

$$S_v(\omega) = \frac{a_2 b_2}{\omega^2 + b_2^2}$$

(13)

where

$$a_2 = \frac{2\sigma_v^2}{\pi}$$

$$b_2 = \frac{V_o}{L}$$

σ_v = variance of turbulence

L = scale of turbulence.

The variance of the turbulence can be calculated in terms of V_o from Eq. (12). Equation (13) gives only the frequency content. The variance of the turbulence is defined as

$$R_v(o) = \sigma_v^2 = \frac{1}{2} \int_{-\infty}^{\infty} S_v(\omega)\, d\omega$$

(14)

Substituting Eq. (12) into Eq. (14) yields[4]

$$R_v(o) = 4.5\, a_1 b_1^{2/3} = 1.55\, V_o.$$

(15)

Note that the variance is independent of Z! The expression given by Eq. (14) will be used in Eq. (13) for subsequent calculations. Introducing Eq. (12) in Eq. (10) gives

$$S_f(\omega) = \left[F(x)\right]^2 \left\{ \frac{1}{\pi} \left[V_o^2 + R_v(o)\right]^2 \delta(f) + 4V_o^2 \frac{a_1 \text{TANH } b_1 \omega}{\omega^{5/3}} \right.$$

$$\left. + a_1^2 \int_{-\infty}^{\infty} \frac{\text{TANH } b_1 \omega_1}{\omega_1^{5/3}} \frac{\text{TANH } b_1(\omega - \omega_1)}{(\omega - \omega_1)^{5/3}}\, d\omega_1 \right\} ,$$

(16)

but the convolution integral is given as

$$a_1^2 \int_{-\infty}^{\infty} \frac{\text{TANH } b_1 \omega_1}{\omega_1^{5/3}} \frac{\text{TANH } b_1(\omega - \omega_1)}{(\omega - \omega_1)^{5/3}}\, d\omega_1$$

$$= 4\pi a_1^2 b_1^{7/3} \left(\frac{2}{b_1 \omega \pi}\right)^{5/3} \text{COTH } b_1 \omega \sum_{n=1,3,5,\ldots} \left(\frac{\text{SIN } \theta_n}{n}\right)^{5/3} \text{SIN } \frac{5}{3} \theta_n ,$$

147
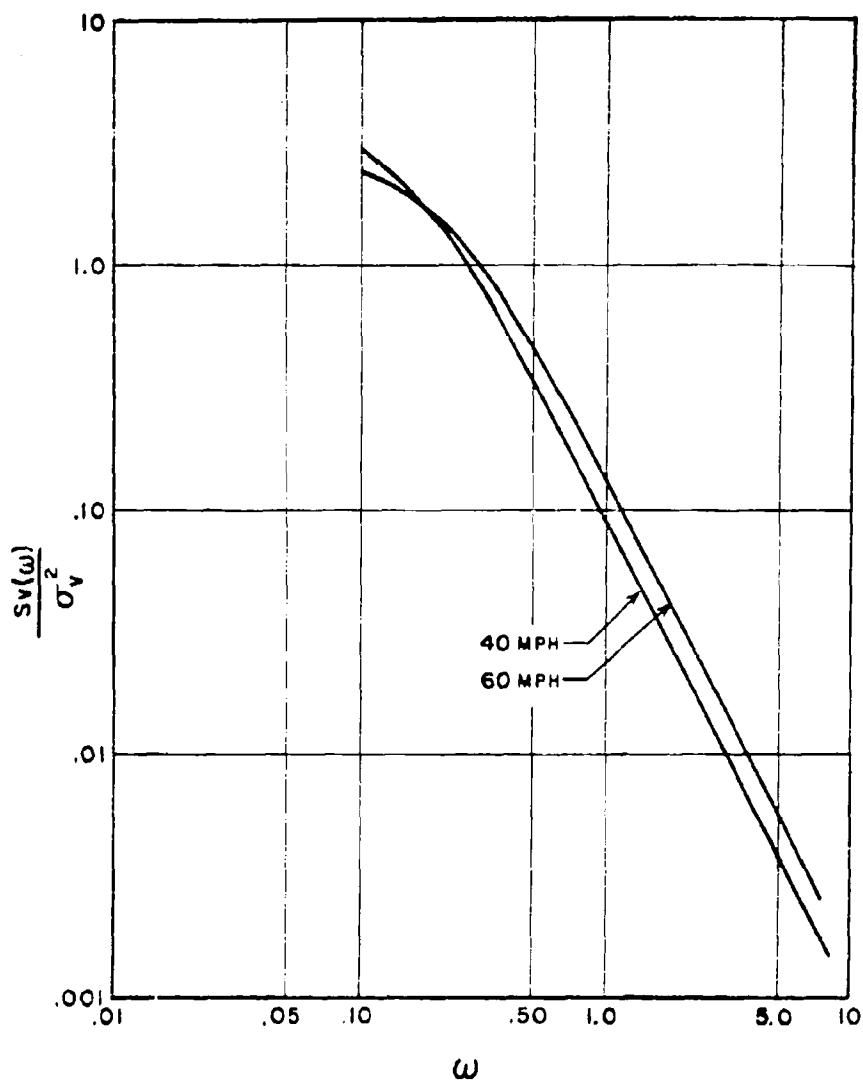
FIG. 4. Some Typical Plots of the Power Spectral Density
of Isotropic Turbulence.

where[4]

$$\text{TAN } \theta_n = \frac{2 b_1 \omega}{\pi n}$$

Hence, Eq. (16) assumes the form

$$S_f(\omega) = \left[F(x)\right]^2 \left\{ \frac{1}{\pi}\left[V_o^2 + R_v(o)\right]^2 \delta(f) + 4V_o^2 a_1 \frac{\text{TANH } b_1\omega}{\omega^{5/3}} \right.$$
$$\left. + 4\pi a_1^2 b_1^{7/3} \left(\frac{2}{b_1 \omega \pi}\right)^{5/3} \text{COTH } b_1\omega \sum_{n=1,3,5,..} \left(\frac{\text{SIN } \theta_n}{n}\right)^{5/3} \text{SIN } \frac{5}{3} \theta_n \right. \quad , \tag{17}$$

and for frequencies other than $\omega = 0$, Eq. (17) becomes

$$S_f(\omega \neq 0) = \left[F(x)\right]^2 \left\{ 4V_o^2 \frac{a_1 \text{TANH } b_1\omega}{\omega^{5/3}} + 4\pi a_1^2 b_1^{7/3} \left(\frac{2}{b_1 \omega \pi}\right)^{5/3} \right.$$
$$\left. \cdot \text{COTH } b_1\omega \sum_{n=1,3,5,..} \left(\frac{\text{SIN } \theta_n}{n}\right)^{5/3} \text{SIN } \frac{5}{3} \theta_n \right\} . \tag{18}$$

From Fig. 5, it is apparent that for mean winds between 30 and 60 mph

$$4V_o^2 a_1 \frac{\text{TANH } b_1\omega}{\omega^{5/3}} \gg 4\pi a_1^2 b_1^{7/3} \left(\frac{2}{b_1 \omega \pi}\right)^{5/3}$$
$$\cdot \text{COTH } b_1\omega \sum_{n=1,3,5,..} \left(\frac{\text{SIN } \theta_n}{n}\right)^{5/3} \text{SIN } \frac{5}{3} \theta_n$$

which is attributed mainly to the fact that $V_o^2 \gg R_v(o)$.
Therefore, Eqs. (17) and (18) can be approximated with very good accuracy
by

$$S_f(\omega) \approx \left[F(x)\right]^2 \left\{ \frac{1}{\pi}\left[V_o^2 + R_v(o)\right]^2 \delta(f) + 4V_o^2 a_1 \frac{\text{TANH } b_1\omega}{\omega^{5/3}} \right\} \tag{19}$$

and (Fig. 6)

$$S_f(\omega \neq 0) \approx \left[F(x)\right]^2 \left\{ 4V_o^2 a_1 \frac{\text{TANH } b_1\omega}{\omega^{5/3}} \right\} . \tag{20}$$
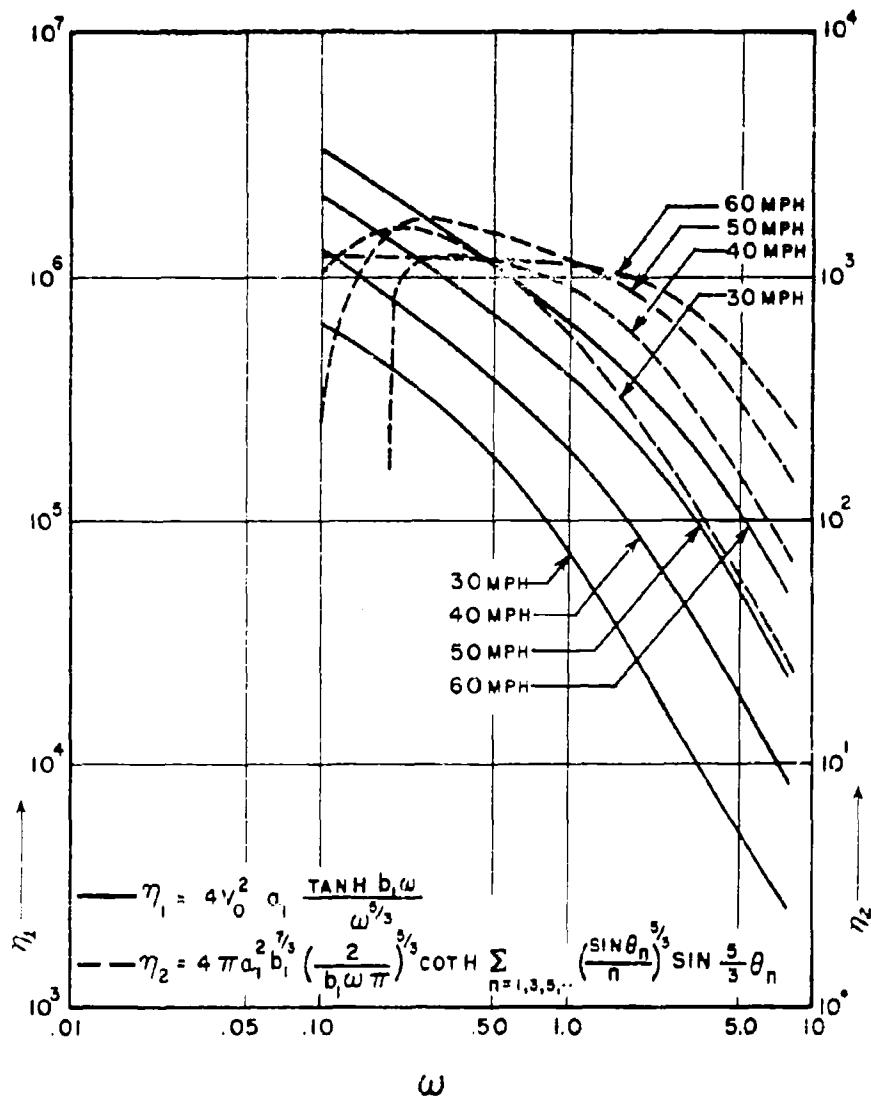
FIG. 5. Comparison of Terms of Eq. (18).

150
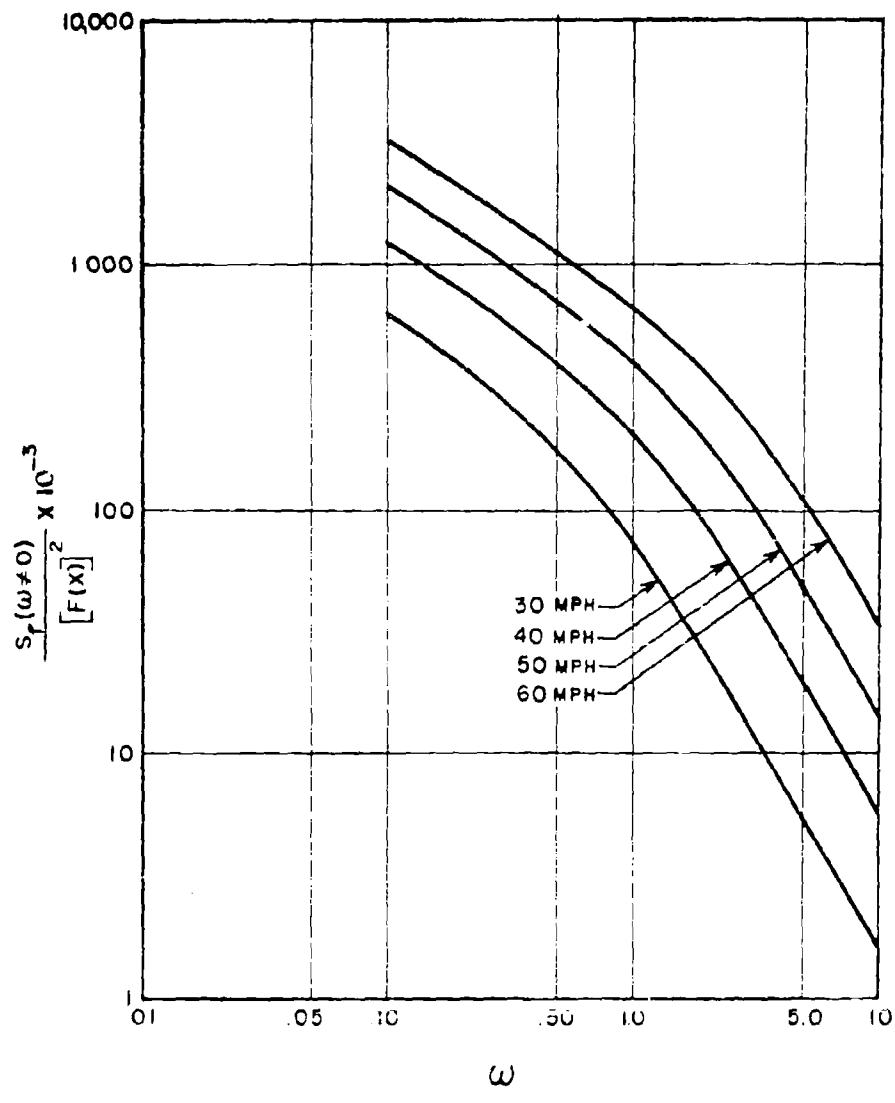
FIG. 6. Power Spectral Density of the Drag Force for
Various Mean Wind Velocities. Eq. (20).

Substituting Eq. (13) into Eq. (14) and following a similar line of reasoning, it is easily shown that the power spectral density of the drag force in terms of the isotropic turbulence spectrum is given by:

$$S_f(\omega) = \left[F(x) \right]^2 \left\{ \frac{1}{\pi} \left[V_o^2 + R_v(o) \right]^2 \delta(f) + \frac{4V_o^2 a_2 b_2}{\omega^2 + b_2^2} + \frac{2\pi a_2^2 b_2}{\omega^2 + (2b_2)^2} \right\} \quad (21)$$

and (Fig. 7)

$$S_f(\omega \neq 0) = \left[F(x) \right]^2 \left\{ \frac{4V_o^2 a_2 b_2}{\omega^2 + b_2^2} + \frac{2\pi a_2^2 b_2}{\omega^2 + (2b_2)^2} \right\} \quad . \quad (22)$$

It is quite obvious that for winds between 30 and 60 mph

$$\frac{4V_o^2 a_2 b_2}{\omega^2 + b_2^2} \gg \frac{2\pi a_2^2 b_2}{\omega^2 + (2b_2)^2} \quad .$$

This can be demonstrated in the following manner:

$$4V_o^2 a_2 b_2 \left[\omega^2 + (2b_2)^2 \right] \gg 2\pi a_2^2 b_2 \left[\omega^2 + b_2^2 \right]$$

or

$$\left[\omega^2 + (2b_2)^2 \right] V_o^2 \gg R_v(o) \left[\omega^2 + b_2^2 \right] \quad .$$

But from Eq. (15),

$$R_v(o) = 1.55 \, V_o \quad .$$

Therefore

$$V_o \gg \frac{\omega^2 + b_2^2}{\omega^2 + (2b_2)^2} \cdot (1.55)$$

since

$$\frac{\omega^2 + b_2^2}{\omega^2 + (2b_2)^2} < 1.0 \quad .$$

152
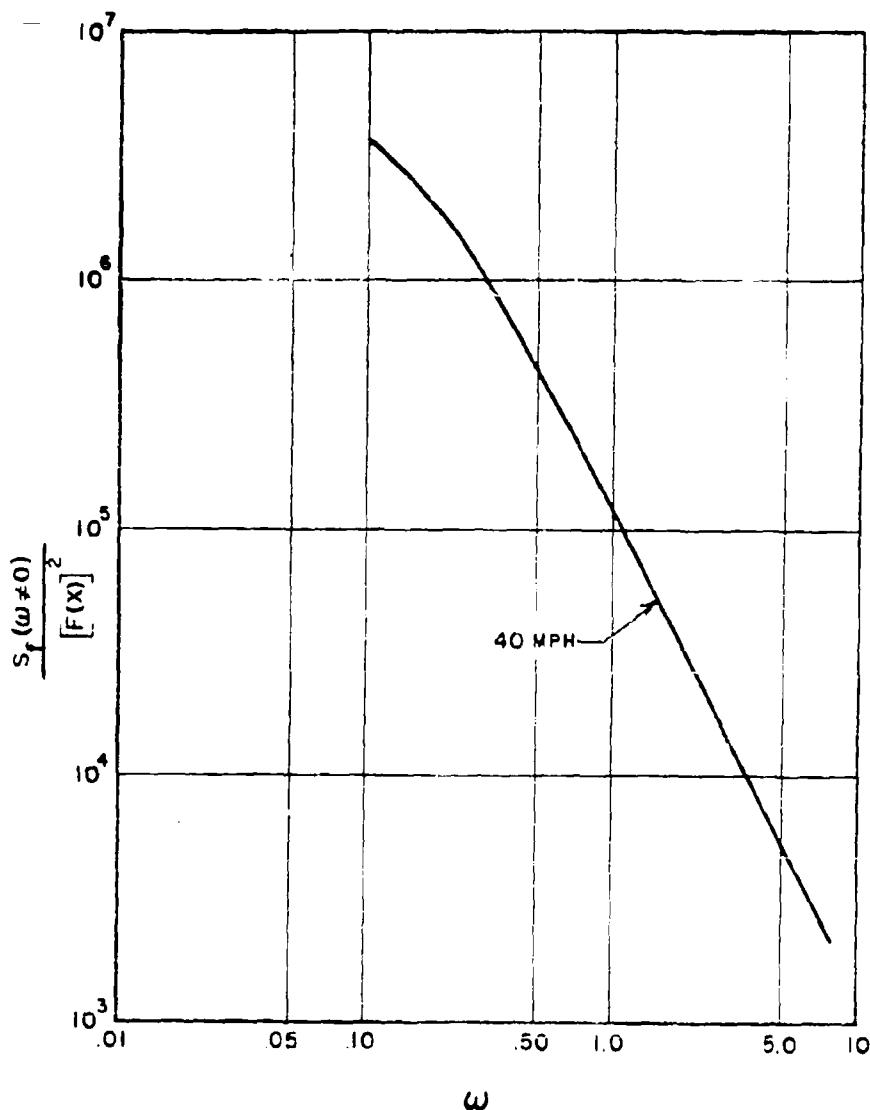
FIG. 7. Power Spectral Density of the Drag Force for a
Typical Wind Velocity. Eq. (22).

Hence Eqs. (21) and (22) can be approximated with very good accuracy by

$$S_f(\omega) \approx \left[F(x) \right]^2 \left\{ \frac{1}{\pi} \left[V_o^2 + R_v(o) \right]^2 + \frac{4V_o^2 a_2 b_2}{\omega^2 + b_2^2} \right\} . \tag{23}$$

and

$$S_f(\omega \neq 0) \approx \left[F(x) \right]^2 \left\{ \frac{4V_o^2 a_2 b_2}{\omega^2 + b_2^2} \right\} . \tag{24}$$

THE RESPONSE OF THE MISSILE

Experimental and theoretical studies indicate that the missile can be represented adequately as a nonuniform beam (in stiffness and mass distribution), for the purpose of calculating its response to ground wind turbulence. The base of the missile is supported by a torsional and a lateral spring which represent the launcher constraint (Fig. 8). In many cases, it is adequate to consider a rigid missile with flexible base constraints.

These systems, in general, are very lightly damped. Aerodynamic damping, in many instances, can assume greater values than the system damping. A conservative approximation is to neglect aerodynamic damping entirely.

The principles of the analysis of structural responses to a stochastic forcing function is well known in the literature on Brownian motion, aircraft gust loading, etc. The response of the missile to ground wind turbulence is but a short extension of these principles, and can be found in any text on generalized harmonic analysis: in particular, a closed form solution for the response using Eqs. (19) or (20), and Eqs. (21) or (22).[4] These expressions are quite lengthy and exceedingly complicated. If the damping ratios are small, a derived expression can be used for the root mean-square-response of the missile.[9]

The mean-square of the displacement response of the missile is given as[9]

$$\overline{u^2(x, t)} = \frac{\tau}{4} \sum_{r=1}^{n} \frac{\left[\phi_r(x) \right]^2 W_r^2}{M_r^2 \omega_r^3 \zeta_r} \frac{S_f(\omega_r \neq 0)}{\left[F(x) \right]^2} \tag{25}$$

where

M_r = generalized mass of the rth mode

ζ_r = modal damping ratio

ω_r = natural (angular) frequency of the rth mode

$\phi_r(x)$ = rth principle mode of oscillation

154
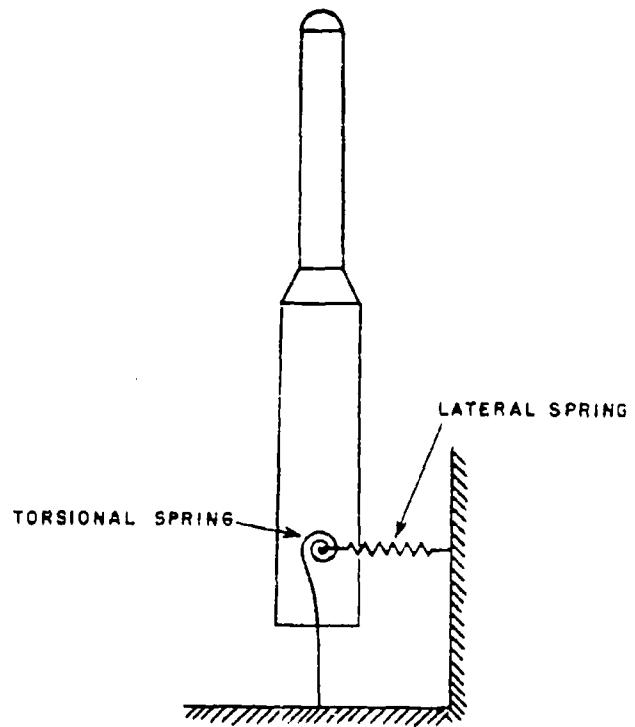
FIG. 8.   Idealization of Launcher Constraints.

and

$$W_r = \int_0^l F(x) \, \phi_r(x) \, dx$$

$$F(x) = \frac{\rho}{2} \, N(x) \, D(x) \, C_D .$$

Equation (18) or Eq. (22) yields $\dfrac{S_f(\omega \neq 0)}{[F(x)]^2}$. The mean of the displacement response is simply

$$\overline{u(x, t)} = \sum_{r=1}^{N} \frac{W_r}{M_r \omega_r^2} \, \phi_r(x) \left[V_o^2 + R_v(o) \right] . \tag{26}$$

DESIGN TECHNIQUE

It was previously customary to specify the ground wind condition in terms of a mean wind velocity and a gust factor. The mean wind velocity can be considered as the five-minute average velocity which is reported at hourly intervals by all weather stations. The turbulence is described in terms of a power spectral density and a probability distribution. Very little information is available about the latter, however. The gust factor is simply an attempt to replace the probability distribution. For example, Sissenwine[10] reports, on the basis of several special studies, that peak one-second duration gusts will not exceed velocities fifty percent higher than the steady wind. In this case, a wind criterion of 40 to 60 mph describes a wind condition in which the average wind speed is 40 mph and the gust factor is 1.5.

In the past, design information was obtained by calculating the response of the missile to mean wind values and arbitrary discrete gusts which were considered to occur rarely;[11] the inclusion of vortex shedding effects were practically nonexistent until quite recently. This was due mainly to the lack of reliable experimental data.

In this section, a method is presented whereby the design response of the missile to ground winds can be estimated. The usual criterion of a steady wind plus turbulence is employed, and the effects of random vortex shedding are included.

Consider the following definitions:

R_{us} = Quasistatic design response (acting in the direction of the fluid flow)

$$= \sum_{r=1}^{N} \frac{W_r \, \phi_r(x)}{M_r \omega_r^2} \, (G \cdot V_o)^2 , \quad [12]$$

156

G = gust factor

$R_u \sim$ = dynamic design response (acting in the direction of the fluid flow)

$R_w \sim$ = dynamic design response (acting perpendicular to the direction of the fluid flow

w = displacement of the missile normal to the direction of the fluid flow

σ_{us} = variance (root-mean-square) of the quasistatic displacement response (acting in the direction of the fluid flow)

$$= \sqrt{\left\{ \sum_{r=1}^{N} \frac{W_r W_s \phi_r(x) \phi_s(x)}{M_r M_s \omega_r^2 \omega_s^2} R_v^2(o) \right\}}$$

σ_{ug} = variance (rms) of the dynamic displacement response due to random atmospheric turbulence (acting in the direction of the fluid flow)

$$= \sqrt{\left\{ \frac{\pi}{4} \sum_{r=1}^{N} \frac{\left[\phi_r(x)\right]^2 W_r^2}{M_r^2 \omega_r^2 \zeta_r} \frac{S_f(\omega_r \neq 0)}{\left[F(x)\right]^2} \right\}}$$

σ_{uvs} = variance (rms) of the dynamic displacement response due to random vortex shedding (acting in the direction of the fluid flow) [1,2,3]

$$= \sqrt{\left\{ \frac{d\overline{C_D}^2}{8V_o} \sum_{r=i}^{N} \frac{\left[\phi_r(x)\right]^2 \overline{W}_r^2}{M_r^2 \omega_r^3 \zeta_r} F\left(\frac{\omega_r d}{2\pi V_o}\right) \right\}}$$

d = reference diameter

$\overline{C_L}^2$ = mean square lift coefficient

$\overline{C_D}^2$ = mean square drag coefficient

$F(\frac{\omega_r d}{2\pi V_o})$ = normalized power spectrum (Fig. 9)

Experimental data indicate that σ_{uvs} and σ_{wvs} are nearly in phase.[1,2,3] It will also be assumed that σ_{uG} is in phase with both σ_{uvs} and σ_{wvs}. Hence

$$\sigma_{uG} + \sigma_{uvs} = \sigma_u \sim . \tag{27}$$

157
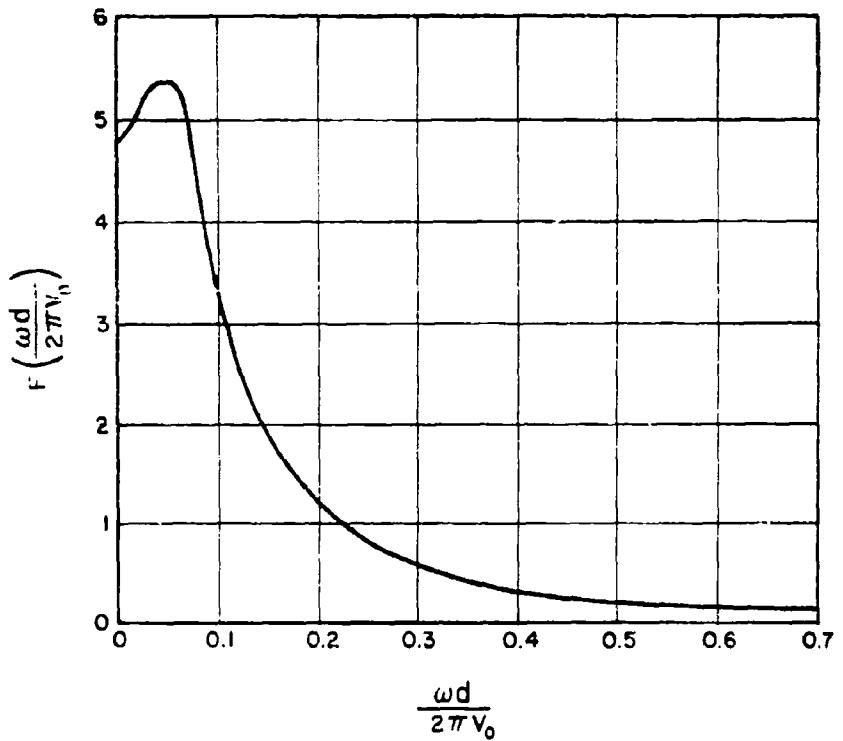
FIG. 9. Normalized Power Spectrum for the Lift Force and
Drag Force at Reynolds Number of 1.39×10^6.

Assuming that the probability of exceeding the dynamic design response $R_{w\sim}$ by $\lambda\sigma_{wvs}$ is the same as the probability of exceeding the dynamic design response $R_{u\sim}$ by $\lambda\sigma_{u\sim}$ requires that

$$R_{w\sim} = \frac{\sigma_{wvs}}{\sigma_{u\sim}} \qquad R_{u\sim} = \frac{\sigma_{wvs}}{\sigma_{us} + \sigma_{uvs}} \; R_{u\sim} \quad . \tag{28}$$

This assumption is not grossly in error since experimental data seem to indicate that the peak displacements, for uniform flow, reach their maximum at the same time.

Now assume that the probability of the quasistatic response exceeding the quasistatic design response is the same as the probability of the dynamic response $\sigma_{u\sim}$ exceeding the dynamic design response $R_{u\sim}$. This implies that

$$R_{u\sim} = m_u + (R_{us} - m_u) \; \frac{\sigma_{u\sim}}{\sigma_{us}} \quad . \tag{29}$$

A resultant dynamic design response will be defined as

$$R_{R\sim} = \left[R_{u\sim}^2 + R_w^2 \right]^{1/2} \quad . \tag{30}$$

Substituting Eqs. (28) and (29) into Eq. (30) yields

$$R_{R\sim} = \left[1 + \frac{\sigma_{wvs}^2}{(\sigma_{uG} + \sigma_{uvs})^2} \right]^{1/2} \left[m_u + (R_{us} - m_u) \frac{(\sigma_{uG} + \sigma_{uvs})}{\sigma_{us}} \right] . \tag{31}$$

The results given by Eq. (31) are based on equal probability concepts and normal distributions. [4] Figure 10 illustrates the design process considered herein.

CONCLUSIONS

A method for estimating the design response of a missile to ground winds is formulated. Also, a rational approach to combine the gust problem and the vortex shedding problem is presented. It is hoped that such an analysis will prove useful in the design of missiles and stimulate more research along these lines. It should be kept in mind that the assumptions used in the preceding analysis are due mainly to the lack of reliable or limited aerodynamic data. Nevertheless, it is believed that the analysis is conservative under these circumstances.
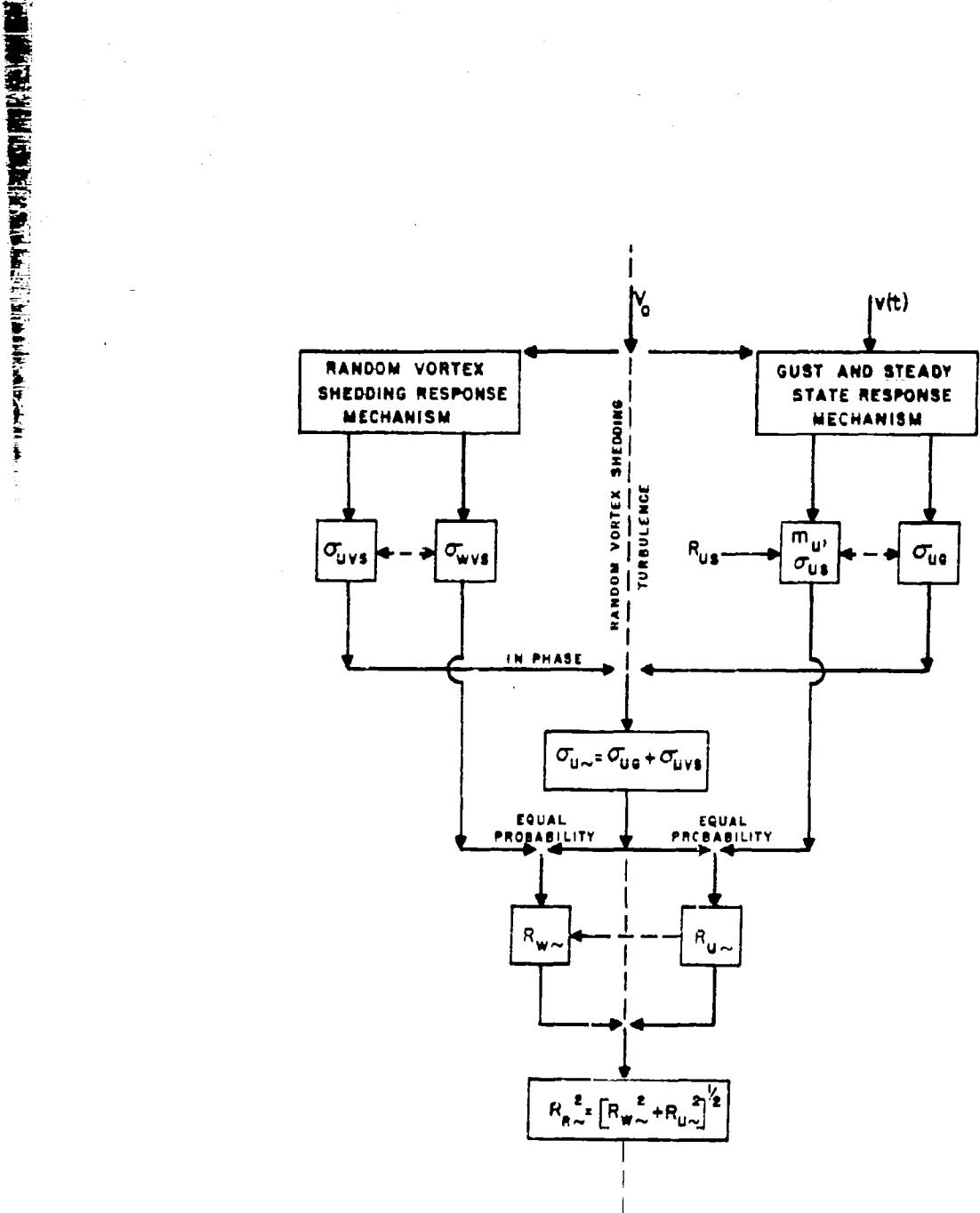
FIG. 10 Design Process.

In general, ground wind spectra are not defined to the degree that an average wind plus a gust spectrum can be used for design information in place of the average wind and gust factor. More research information is needed to ascertain the form of the input spectrum, expecially at high frequencies.

REFERENCES

1. Y. C. Fung, Fluctuating lift and drag acting on a cylinder in a flow at supercritical Reynolds numbers, Bulletin, 26th Shock and Vibration Symposium, Dept. of Defense, 1958.

2. A. A. Ezra, Wind induced oscillations of the Titan missile, WDD-M-M1-59-7, Martin Company, Denver 1, Colorado, March 1959.

3. L. L. Fontenot, The response (including effects of random vortex shedding) of the SM-65E missile erected in the launcher during a 60-mph wind, GD/A Report AE60-0233, 8 April 1960, Contract No. AF04(645)-4, Confidential.

4. L. L. Fontenot, The response of a flexible missile to ground winds, GD/A Report AE61-0943.

5. R. M. Henry, A study of the effects of wind speed, lapse rate, and altitude on the spectrum of atmospheric turbulence at low altitude, IAS Report No. 59-43, January 1959.

6. G. K. Batchelor, The Theory of Homogeneous Turbulence, Cambridge University Press, 1959.

7. S. O. Rice, Selected Papers on Noise and Stochastic Processes, Nelson Wax Ed., Dover Publications, Inc., New York.

8. S. H. Crandall, et al. Random Vibration, The Technology Press of the Massachusetts Institute of Technology, Cambridge, Mass., 1958.

9. M. V. Barton and W. T. Thomson, The response of mechanical systems to random excitation, Journal of Applied Mechanics, Vol. 24, No. 2, June 1957, p. 248.

10. Norman Sissenwine, Memorandum to AFBMD from AFCRC (Geophysics Research Directorate), Surface Wind Design Criteria for ICBM-Comments on Section B of GM45, 5-118, 9 July 1957.

11. O. Schey, Loads and ground wind criteria for erected D, E, and F Series Atlas missiles, GD/A Report AE61-0034, Contract No. AF04(647)-299, 23 May 1961, Confidential.

12. Q. R. Bohne, Power spectral density techniques in ground wind drag analyses, ARS Preprint, Lifting Re-entry Vehicles: Structures, Materials and Design Conference, April 4-6, 1961.

Persistence Factors in Serial Wind Records

B. N. CHARLES

AEROSPACE DIVISION

THE BOEING COMPANY

ABSTRACT

In applying climatology to design problems a common purpose is to estimate hardware performance under future environmental conditions. A fundamental question, therefore, concerns the extent to which a given sample of climatological data is representative of conditions to be experienced in the future. This necessitates defining the equivalent number of independent observations contained in a serial record of arbitrary length. This number can be estimated by use of a quantity termed the 'persistence factor,' S. The quantity (2S-1) is roughly equivalent to the average time span during which individual observations are statistically representative. Estimates of (2S-1) over the southeastern United States are presented herein, as derived from a serially complete collection of once-daily upper winds covering a five-year period. The results show that in the altitude range from 25,000 to 50,000 feet, the quantity (2S-1) ranges between 3 and 8, depending upon season.

In applying climatology to design problems, a common purpose is to estimate future environmental conditions for hardware. Available data collections for the parameter of interest are used to compute frequency distributions, mean values, standard deviations, etc.; and pertinent laws of mathematical statistics are used to estimate risks of encountering various large magnitudes of the parameter that are related to design or performance criteria. A fundamental question, therefore, concerns the extent to which the available data collection (which, after all, is an aggregate of hindsight) is representative of future conditions.

The mathematical statistical laws generally used are based upon random (that is, independent) events, whereas serial upper wind data exhibits the appreciable autocorrelation typical of many geophysical time series. That is, with auto- (or serial) correlation, a specific observation is partially determined by its predecessor(s), and partially determines its successor(s). The individual observations are therefore dependent, and the laws of random events cannot be legitimately applied without modification.

Since the correlation decreases with increasing time interval between observations, ultimately approaching zero, it is possible to extract suitably spaced observations from a complete time series that are indeed independent. Or alternatively, available observations during the appropriate time interval can be averaged and taken as a single observation.

These considerations have led to the concept of persistence factors[1] which relate to the equivalent number of repetitions[2] or equivalent number of independent observations[3] contained in a time series. In the notation of the latter reference, the equivalent number of independent observations is approximated by:

$$N = \frac{M}{2S - 1} \tag{1}$$

where M is the number of equispaced observations, and S is the persistence factor given by:

$$S = 1 + \sum_{j=1}^{M-1} \rho_j \tag{2}$$

where the ρ_j are the serial correlation coefficients for lags j, defined for a sample with mean $\overline{X}_M$ and standard deviation σ_x as:

$$\rho_j = \sum_{i=1}^{M-j} \frac{(X_i - \overline{X}_M)(X_{i+j} - \overline{X}_M)}{(M - j)\sigma_x^2} \tag{3}$$

The quantity (2S - 1) is approximately the average number of time units during which an individual observation is representative. Conceptually it is equivalent to Bartels' appropriate statistical time unit,[1] since observations separated by this time interval will be substantially independent.

The literature concerning the persistence of meteorological time series is substantial, but barely touches the upper wind parameter. The reasons for this deficiency include:

1) the lack of serially complete data collections covering lengthy periods of record,

2) the great magnitude of computational effort involved in analyzing even a quasiserially complete data collection, and

3) the relative arithmetic complexity of treating vector, as opposed to scalar quantities, and the unknown sampling distribution of vector correlation coefficients.[4]

The preparation of a suitable data collection by the Office of Climatology of the U. S. Weather Bureau, [5,6] and the availability of high-speed digital computers in the U.S.W.B. - Sandia Corporation Cooperative Project in Wind Climatology, [7] corrected 1) and 2) above, for much of the North American area. Further, a result of the Cooperative Project was the substantiation of the British findings [8] that wind correlations could, for all practical purposes, be considered in terms of the relatively simple stretch vector correlation coefficient up to at least the 100-mb level, without serious loss of information, [9] thus permitting minimizing of 3) above.

For present purposes, there was the additional happy circumstance that the calculations performed by Sandia Corporation included the stretch vector correlation coefficients for lags from one to ten days. They were computed from

$$\rho_j = \frac{\sum_{i=1}^{M-j} (u_i u_{i+j} + v_i v_{i+j})}{(M - j)(\sigma_u^2 + \sigma_v^2)} \qquad (4)$$

where u and v are departures of the zonal and meridional wind components from their respective mean values and σ_u and σ_v are the respective standard deviations.

The ensuing discussion is based upon these coefficients as obtained from the serially complete wind data collection ranging from 950 to 30 mb for the 51 stations shown in Fig. 1 for the period March 1951 through February 1956. We are primarily interested in Montgomery, Alabama. Although it is near the edge of the data field, it is adequately surrounded by neighboring stations for analysis of a parametric field.

Figure 2 shows isopleths of (2S - 1) for the winter season. It should be noted that although the lag correlation coefficients extended to ten days, ρ_{10} did not converge to zero in all cases. Moreover, the simple stretch vector correlation tends to underestimate the total vector correlation [9] especially at the larger lags, so these isopleth values are somewhat less than the true values. The meaning of the detail in the pattern shown is not at issue here, although the speculations of synopticians would be welcome, but the figure shows that the rather abstract parameter (2S - 1) does exhibit a fairly regular field over the region of interest, and moreover indicates an essentially continuous variation with altitude. Figures 3, 4, and 5 are similar results for the spring, summer and fall seasons.

Figure 6 shows vertical profiles of the quantity (2S - 1). It can be seen that between altitudes of 25,000 to 50,000 feet near Montgomery, the values vary between 3 and 8, depending upon the season. The horizontal gradient of

(2S - 1), moreover, appears to be relatively large in this region, suggesting possible large variations in the parameter for individual years.

With persistence present in the serial wind record, the standard errors of estimate of mean values and standard deviations are $(2S - 1)^{1/2}$ times larger than those computed by assuming the data to be independent, and the implications for reliability predictions may be significant. Where specific daily wind profiles are used to simulate missile dynamic responses, consideration should be given to adequate time separation of the profiles to avoid redundancy due to use of profiles containing identical information for statistical purposes.

REFERENCES

1. C. E. P. Brooks, and N. Carruthers, Handbook of Statistical Methods in Meteorology, Chapter 16, Air Ministry, M. O. 538. London pp. 309-329, 1953.

2. J. Bartels, Periodicities and Harmonic Analysis in Geophysics, Geomagnetism (Vol. 2), S. Chapman and J. Bartels, Clarendon Press, Oxford, 1940, Cn. XVI.

3. G. Morgan, Jr. and Major A. Bruch, Preliminary Analysis of Wind Variability at High Altitudes, Scientific Report 750-01, Contract AF 19 (604)-6193, 1961.

4. A. Court, Wind Correlation and Regression, Sci. Rep. 3, USAF Contract 19(604)-2060, AFCRC TN 58-230, 1958.

5. U. S. Weather Bureau, Reference Manual 508, Upper Winds 850-30 MB, 23 January 1957.

6. Ben Ratner, Upper-Air Climatology of the United States, Part 3 - Vector Winds and Shear, Technical paper No. 32, U. S. Dept. of Commerce, Weather Bureau.

7. B. N. Charles, U. S. Weather Bureau-Sandia Corporation Cooperative Project in Climatology (Upper Wind Statistics from USWB - FCDA Data, Final Report), Office of Climatology, U.S.W.B., Washington 25, D. C., 1958.

8. C. S. Durst, Variation of Wind with Time and Distance, Geophysical Memoirs No. 93, Met. Office, London, 1954.

9. B. N. Charles, Utility of Stretch Vector Correlation Coefficients, Quarterly Journal, Royal Meteorological Society, Vol. 85, No. 365, pp. 287-290.

10. U. S. Weather Bureau, New Study of High-Level Winds, Bulletin, American Meteorological Society, Vol. 39, p. 557, 1958.

Station Locator
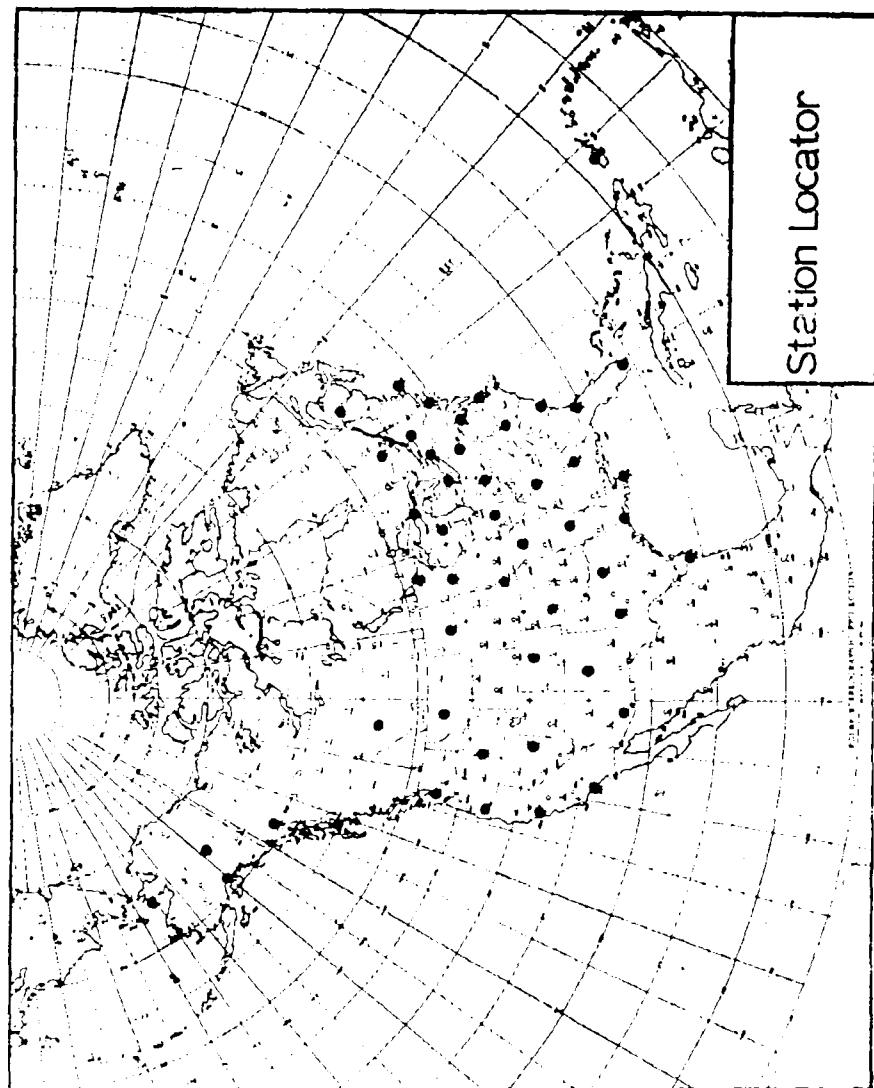
FIG. 1. Stations included in Card Deck 508.
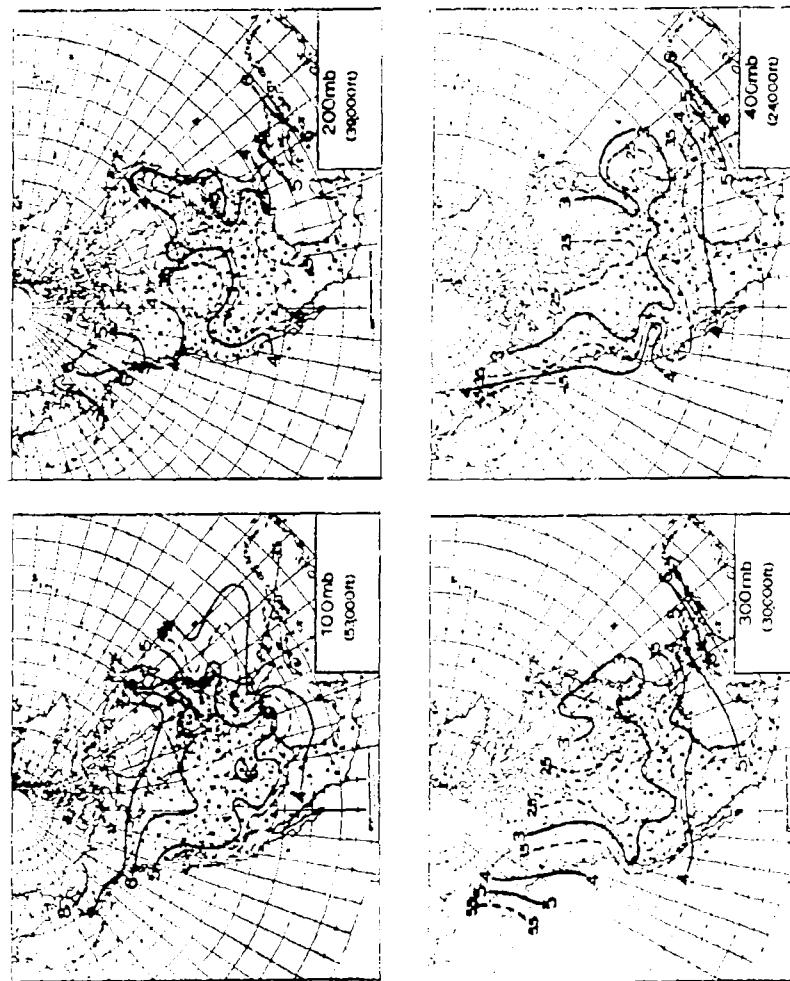
FIG. 2. Isopleths of 2S-1, December - January.
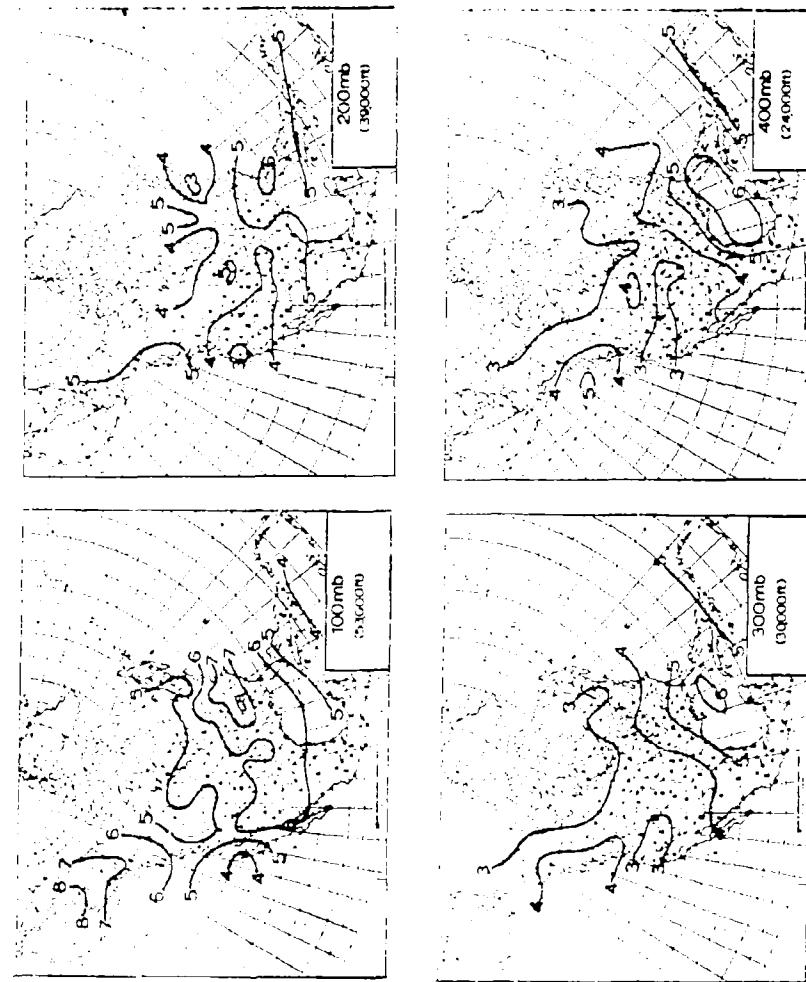
FIG. 3. Isopleths of 2S-1, March - May.
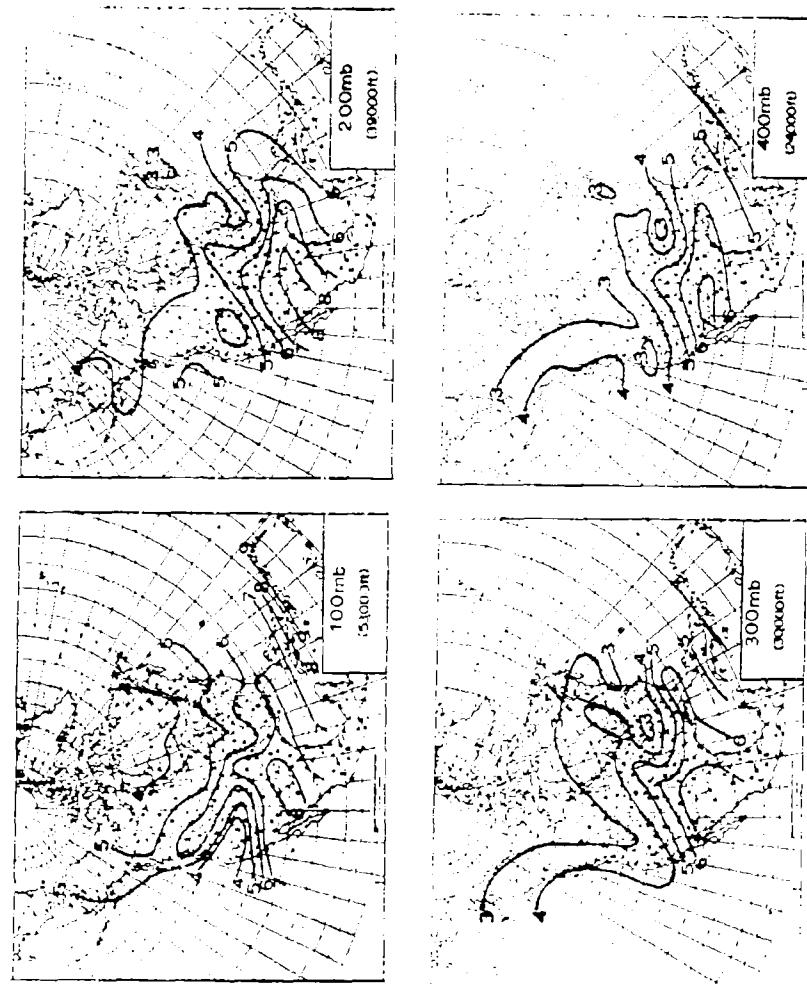
FIG. 4. Isopleths of 2S-1, June - August.
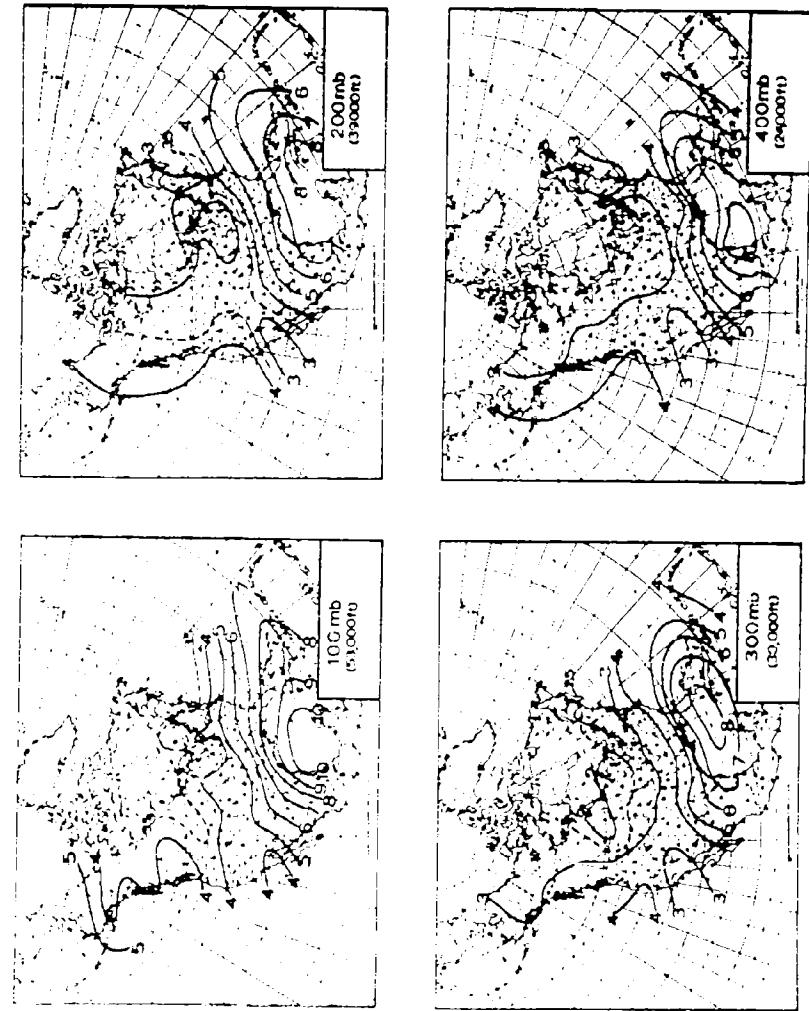
FIG. 5. Isopleths of 2S-1, September - November
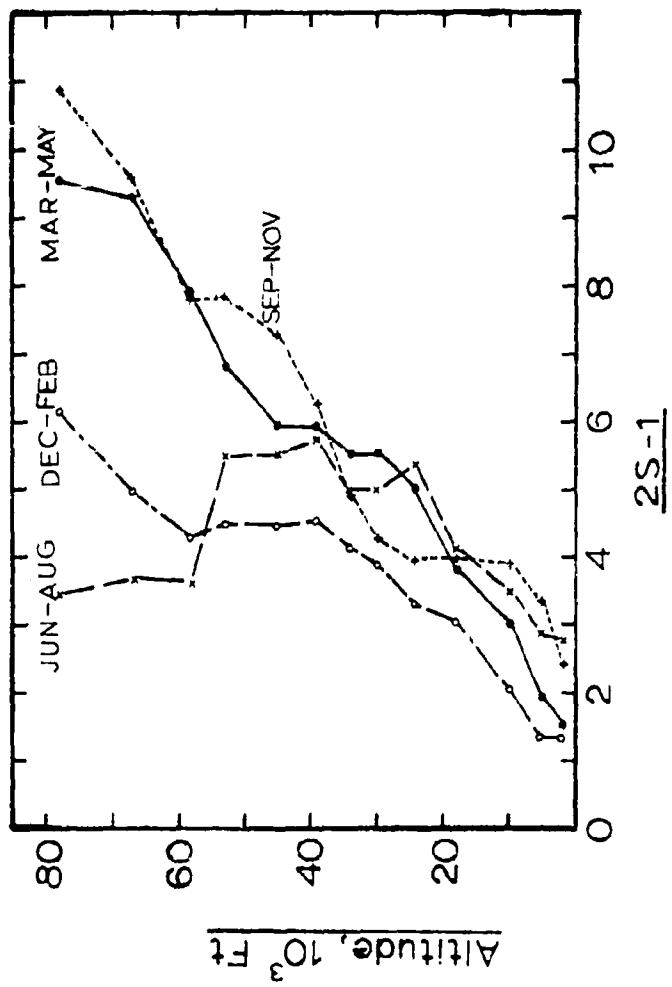
FIG. 6. Vertical Profiles of 2S-1 At Montgomery, Alabama.

Variation of Tropospheric Wind Vectors Over Short Time Intervals

ROBERT W. LENHARD, CAPTAIN, USAF

HENRY A. SALMELA

GEOPHYSICS RESEARCH DIRECTORATE

AIR FORCE CAMBRIDGE RESEARCH LABORATORIES

ABSTRACT

Wind observations from GMD-1 soundings taken at hourly intervals for an
entire week in April 1960 at Bedford, Massachusetts are being studied to ex-
plore the variability of winds over short time intervals. At 12 km (39,000 ft)
variability increases with time up to 18 hours; the rate of increase decreases
with time. Quadratic regression fits the data slightly but significantly better
than linear regression. Resultant wind during the period was 259 degrees,
36.7 m/s with a standard vector deviation of 26.8 m/s. The quadratic re-
gression indicates an rms difference of 26.8 m/s in winds observed 14 hours
apart. Hence for general purposes observed winds can be considered representa-
tive for 12 to 14 hours. Regressions indicate a residual variability at zero
lag of about 12 m/s. A sample series of observations was analyzed for the
effect of the difference in balloon positions on successive runs. During this
period of strong winds, the standard vector deviation of balloons about their
mean position was 10.6 km and the rms difference in positions of successive
balloons was 13.5 km. The contribution of this spatial separation of suc-
cessive balloons to observed wind difference is significant at the five-percent
level. Residual wind variability at zero lag appears to be due in part to the
spatial variability of winds and not solely to observational error. A series
of hourly rocket soundings made with the ARCAS-ROBIN at Eglin AFB, Florida
on 9-10 May 1961 enables a first comparison to be made of conditions at 65
km with those in the lower atmosphere. A large diurnal wind variation appears
to exist with variability reaching a maximum at a lag of 11 hours and decreasing
thereafter. Variability increases more rapidly and is greater at 65 km than
at 12 km at lags up to 12 hours.

INTRODUCTION

This study is the initial analysis of a series of observations of upper
air winds as they change over short time intervals. The main purpose of
this study was to evaluate data reduction problems and the utility of various
analyses. These topics will be discussed somewhat and preliminary findings
will be given on the variability of winds over short periods and applied to
evaluate the observations.

DATA

General

The basic data is a series of AN/GMD-1 rawinsonde observations taken at hourly intervals at Hanscom Field, 1 April through 7 April 1960. This experiment is described in detail in the forthcoming GRD Research Note No. 60, which will also contain listings of the data obtained. The winds used in this study were computed from these data.

Selection of Samples

For this analysis, a selection from the mass of data was desired. The 12-km level was chosen as one that appeared to have considerable variability and to be somewhere near the level of maximum wind on many occasions. The three-minute winds were selected for examination as being convenient for calculating; the data point chosen was that one whose central minute contained the 12-km level.

Finally, a short sequence of runs was desired and 21 soundings were selected. These were made between 0100 and 2300 on 4 April 1960 and were chosen because they formed a continuous sequence of usable runs and appeared to be in a jet stream regime.

ANALYSIS

To find the hour-to-hour change in winds, the wind speeds at 8, 10, and 12 km were plotted. A sample sequence is shown in Fig. 1. The 12 km wind is stronger and more variable than at lower levels; but, on occasion, this was not the case.

Greater changes were observed in one hour than are shown. Most of them are of questionable accuracy, as are some on the figure. Note the peak speed of 102 mps which occurred on the 1700 sounding. The elevation angle at the 35th minute of ascent, at a height of 12,330 meters, was 7 degrees. It is probable that this value contains an appreciable tracking error; a wind of 200 knots seems unlikely.

The sounding for internal consistency shows some fluctuation with altitude from minute to minute of ascent. These fluctuations move about an increasing and then decreasing trend; there is little doubt that a wind maximum existed somewhere about 12 km. The preceding and following soundings also indicate that a peak velocity occurred at about this time.
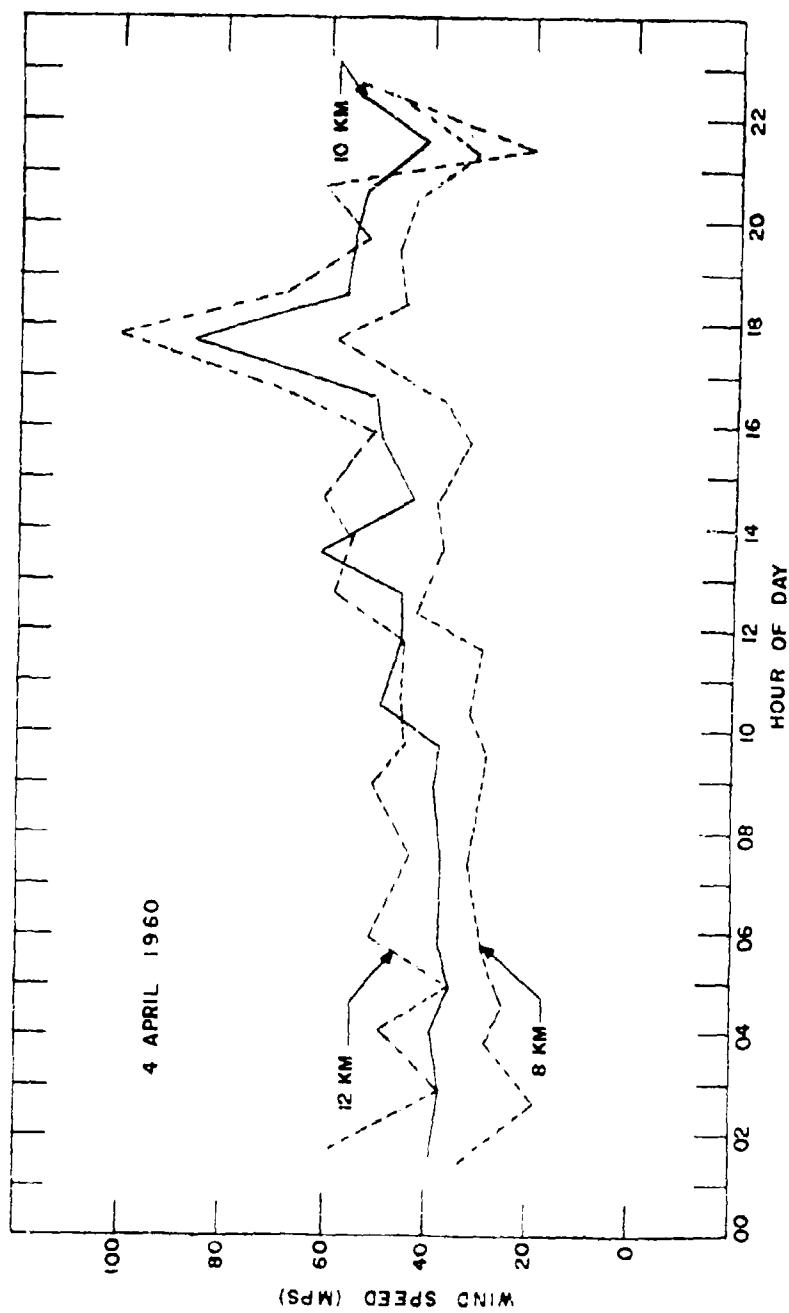
FIG. 1. Hourly Wind Speeds over Hanscom Field

175

Since a peak in the wind speed seems real, and since the exact error in
the observed magnitude is unknown, the reported value is retained. If con-
siderations of continuity and consistency had not supported the peak in the
speed, the sounding would have been regarded as erroneous and dropped from
any further calculations. This was done with several soundings, mostly
those with elevation angles as low as 3 to 5 degrees when the balloon was at a
height of 12 km.

DATA REDUCTION

Depth of Computing Layer

The dependence of the wind on the depth of the layer over which it is
averaged is a matter of some concern. To explore this, the wind speeds were
computed for one, two, three, and four minutes of balloon ascent, corresponding
to layers that are one, two, three and four thousand feet thick. To have dif-
ferences show up graphically, an average of all four estimates of the 12-km
speed was obtained for each sounding in the short sample. The speed for
each depth was then plotted as a departure from that average. These de-
partures are shown in Fig. 2.

It is expected that the mean speed and the variability would decline as the
depth of the layer over which winds are averaged increased. Within the
vagaries of sampling, this occurred. For the short sample, mean speeds
were 53.8, 52.8, 53.0 and 51.0 mps as the depth of the layer increased from
one to four thousand feet. The rms vector difference in winds one hour apart
did not behave as nicely. Values of 19.4, 17.3, 19.8 and 19.6 mps were ob-
tained as the layer thickness was increased. A larger sample showed the
expected results. For the entire week, the rms changes ran 19.6, 14.3, 12.8
and 12.1 mps with increasing layer thickness.

Deviations From Nominal Positions

It would be convenient to be able to treat successive runs as being
exactly one hour apart and as sampling essentially the same point in space.
It was primarily to see if this could be done with validity that the short one-
day sequence of 21 runs was selected. The strong wind regime with con-
siderable variability was chosen to give the maximum opportunity for sig-
nificance of effect to appear.

Considerable spatial variability existed. At the first observation point
above 12 km, the standard vector deviation of the balloons about their mean
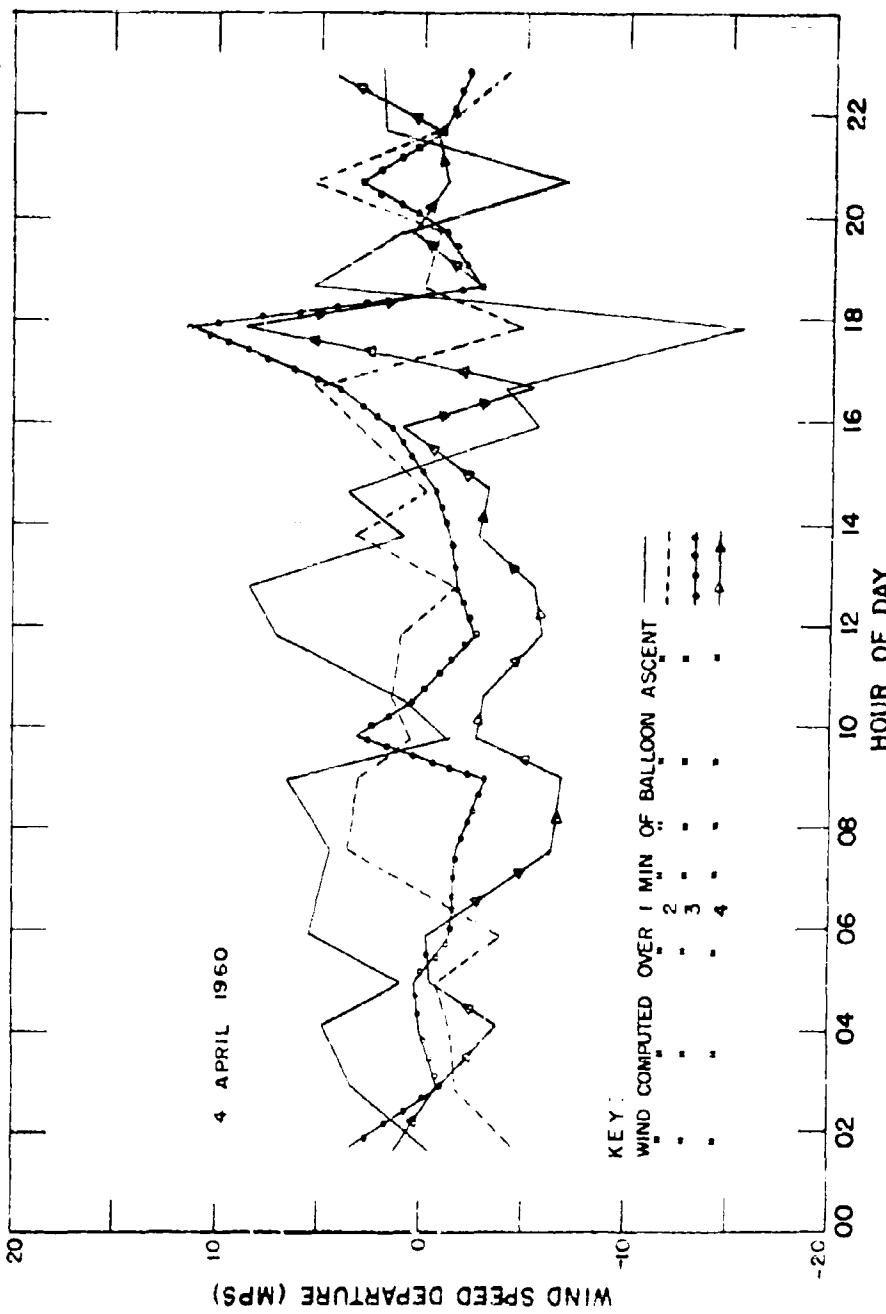
FIG. 2. Variation of 12KM Wind Speed with Depth of Computing Layer.
Departure of Computed Speeds from Their Mutual Average for Each
Sounding.

177

position was 10.6 km. The root mean square vector difference between successive positions was 13.5 km.

The vector difference in wind speeds was correlated with the difference in balloon positions and also with time differences between successive runs, assuming linear relationships. The portion of the variance of wind speed differences explained by the time interval was not significant; that explained by the space displacement was significant at the five-percent level. The linear partial correlation of wind change with time change was only 0.18; that with space variation was 0.54.

In this one-day sequence, at least, part of the observed variability must be due to space separations of the successive balloons. Further investigation of this relation is called for, and a multiple correlation of wind change against time and balloon position may be necessary.

VARIABILITY

Short Sample

The lag effect on wind variability was studied using the one-day sample as well as the entire record. The rms vector difference in three-minute 12-km winds was computed for the one-day sample for all possible lags, assuming one-hour intervals between runs. Results are shown in Fig. 3. Points beyond 17 hours are considered doubtful since only one to three observation pairs were available for their computation.

The straight line in Fig. 3 provides a fit to the 17 lag points that is significant at the five-percent level. The standard error of estimate is 2.8 mps. A quadratic relationship is slightly, but not significantly, better: the standard error is reduced only to 2.7 mps. The relation of the vector wind change to the square root of the lag is very nearly the same as the linear relationship.

These statistical fits do not necessarily reflect physical relationships. A boundary condition for the physical relationship being sought is that zero variability occurs with zero lag in both time and space. The degree to which statistical relationships conform or can be reconciled with this boundary condition is one measure of their probable reality. The most disturbing feature of the linear relationship is the zero time rms of 22 mps. Either of the curvilinear relations mentioned above reduces this to 19.5 mps; an excessively large instrument error is still implied.

The mean wind for the period was 52.5 mps and the standard deviation was 17 mps. Low-elevation angles would be expected, and did occur, so wind error should be great; but it should not be as high as $1°$ to 22 mps. An

178
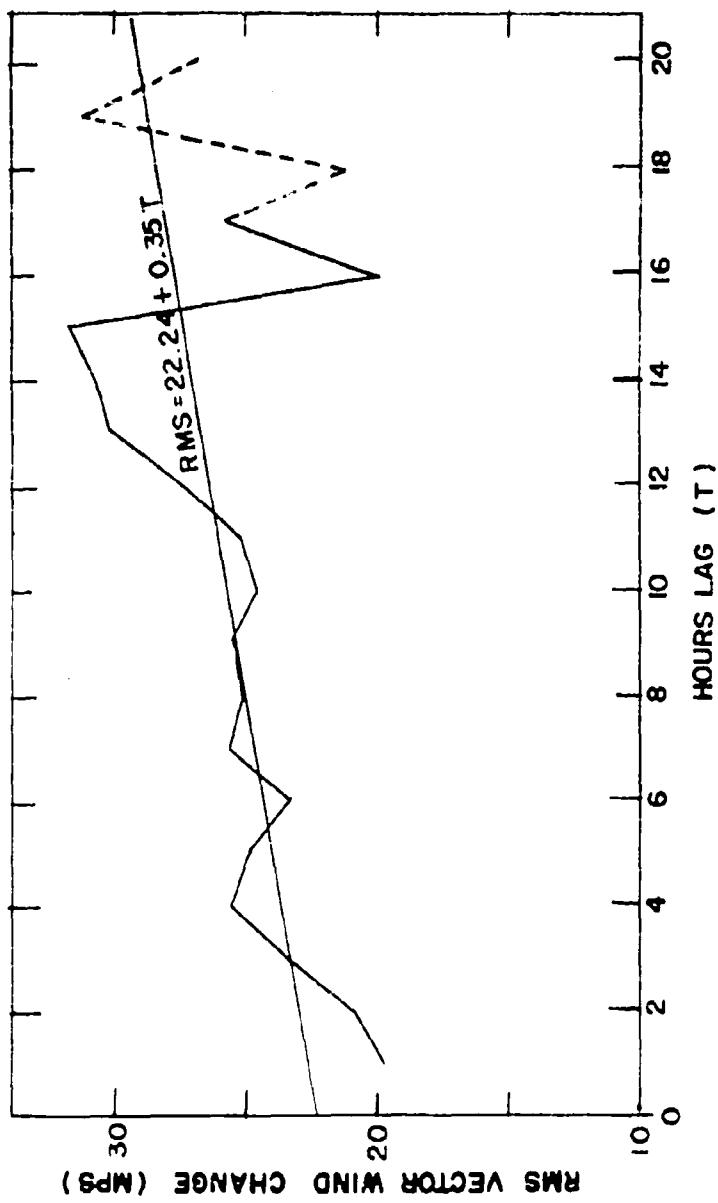
FIG. 3. Lag Variability of Winds at 12 KM over Hanscom Field on 4 April 1960.

The plot axes read: vertical axis "RMS VECTOR WIND CHANGE (MPS)" with values 10, 20, 30; horizontal axis "HOURS LAG (T)" with values 0, 2, 4, 6, 8, 10, 12, 14, 16, 18, 20. A fitted line is labeled RMS = 22.24 + 0.35 T.

approximation, based on an average height of 12 km and elevation angle of 8.5 degrees, gives an estimated rms error of 8.5 mps in wind and 12 mps in wind change. The significant spatial displacements that have been mentioned must have contributed to this zero time rms. The variability at zero time cannot be accounted for entirely by instrument error and space variability. After some rough allowances for these, the residual variability may be as small as 5 mps or as large as 15 mps. This must be due to small-scale fluctuations analogous to those observed on the continuous trace of several hours of surface anemometer records during apparently steady weather situations. Turbulence does occur in the free atmosphere, and this particular sample of wind is taken from a situation that meets many of the criteria listed by Anderson[1] for a probability of above-average turbulence.

It is difficult to resist making inferences from these results, partly because they can be so dramatic, so it is fitting to emphasize that the sample from which these results were obtained was unique. This set of only 21 soundings was made during a single day when the jet stream was certainly overhead. There was a deep trough aloft to the west, a warm front passed during the period, and a cold front and low center passed early on the following day. The analysis level was deliberately selected to show maximum variability, and on at least one sounding an observation from the core of the jet apparently was included in the sample.

These results might not describe jet stream conditions properly, since a rather extreme situation was sampled. The results do provide an illustration of the variability that can occur near the tropopause during one day. With this illustration, and with typical conditions near the jet stream in wind, it can be said that observed jet stream winds cannot be representative with any great precision. This is true with perfectly accurate observations, and the lack of precision in representation will increase with an observation that is subject to error, such as is obtained from the GMD-1A system.

Complete Series

For a more complete view, the rms vector wind differences were obtained for the week-long record at lags of 1, 2, 3, 4, 5, 6, 9, 12 and 18 hours. These values are shown as data points in Fig. 4. The mean resultant wind for the week was 259 degrees, 36.7 mps, and the standard vector deviation was 26.8 mps.

The variance explained by the linear regression shown is significant at the 0.1-percent level and better fits are possible with regressions of higher degree. The residual difference at zero lag decreases only slightly,

180
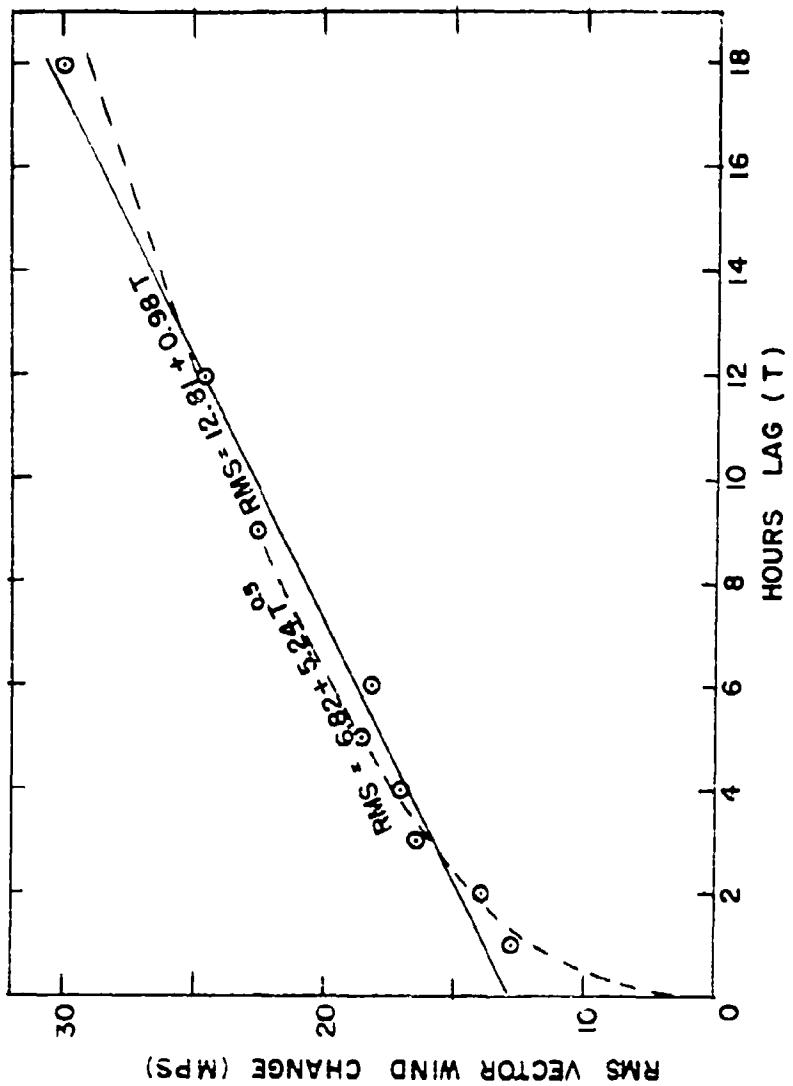
FIG. 4. Increase of Wind Variability with Time 12 KM over Hanscom Field 1-7 April 1960.

however. The third degree regression has a standard error of estimate of only 0.2 mps but the zero intercept is 11 mps. With winds of this speed and variation, it is unlikely that observational error accounts for 11 or 12 mps of the observed variability. Some of the zero time rms is probably due to differences in the balloon positions.

Durst[2], Spreen[3], and others have examined the behavior of r_t, the stretch vector lag correlation coefficient. They have provided estimates of d for use in the expression of the decay of the lag correlation $r_t = \exp(-dt)$. A least-squares estimate of d was obtained from the Hanscom data and a value of 0.5 was obtained. This is about twice the value obtained by Durst and appreciably larger than those obtained by Spreen. The uncertainty in the estimate of d from this sample is so great, however, that it cannot be said to differ significantly from the values obtained by these other investigators.

That the variability of winds increases with time proportionately to the square root of the lag has been noted. This was tested and the equation shown by the dashed line on Fig. 4 was obtained. The standard error of estimate is 0.7 mps compared with 0.9 mps for the linear regression. The difference in the explained variability is slight: 97 percent for the linear regression, 98 percent for the square root regression, and 99.8 percent for a cubic equation.

The excellent fit of the square root curve to the first four data points is of interest. The zero lag residual variability of 6.8 mps appears to be a better estimate than that given by the straight line. This comes close to the range within which the observational error might be.

Elimination of zero lag was tried by fitting an expression of the form $rms = dt^b$. The equation obtained was $rms = 11.8t^{0.3}$ and explained 96 percent of the variance. The 90-percent confidence limits for b were 0.15 and 0.43.

It seems that the square root relationship is not a good description of the observed data unless compensation is made for observing errors. Arnold and Bellucci[4] have determined the proportionality constant empirically and find $rms = 4t^{0.5}$ for lags up to 12 hours and velocity in mph. For velocity in mps this constant would be 1.79, which does not agree with the values of 5.24 and 11.8 found in this study. Expansion of the analysis to more levels might remove this discrepancy. If it does not, further investigation will be required to reconcile the difference.

REPRESENTATIVENESS

One of the ultimate goals of a study of short-term wind variability is to

be able to stipulate the observational network required for any specific purpose. The analysis made so far is not adequate for making inferences with any confidence, but the process of determining useful observational frequencies can be illustrated.

For general purposes the climatological average wind is a useful standard. The accuracy with which it estimates specific wind is measured by the standard vector deviation. The accuracy with which an observed wind estimates the wind at a later time is measured by the lag rms.

The standard vector deviation of the 12-km winds as observed was 26.8 mps. Most simply, this can be equated to the rms and the regression equations solved for time. Estimates are obtained for how old an observation is when it becomes as inaccurate as the climatic mean. The linear regression gives an estimate of 14.3 hours, the quadratic gives 13.7 hours, and the square root yields 14.5 hours. Thus, by this standard, observations appear to be representative for about 14 hours.

A more realistic approach is to use climatology appropriate to the place and season rather than from the specific sample. The standard vector deviation is 22.65 mps at 200 mb over Nantucket in March[5]. The linear regression indicates 10 hours and the square root relation 9 hours for the length of time that observations are representative. Observations would be representative for much shorter periods when the application requires greater accuracy than that obtainable from climatology.

ROCKETSONDE DATA

While this study was in progress, data became available from a series of rocket soundings made with the ARCAS ROBIN system that was comparable to some degree with the data being used herein. Details of the system and data reduction will be discussed in a later paper[6]. The data used for this comparison consisted of wind velocities, by components, at 65 km over Eglin Air Force Base, Florida, for 19 soundings taken between 1930, 9 May, and 1830, 10 May 1961. The intervals between these soundings varied between 36 and 176 minutes. By grouping according to time intervals, data pairs were obtained for time lags up to 23 hours. Beyond 18 hours, however, data pairs were too few to place much confidence in the average. Differences in rms plotted against lag are shown in Fig. 5. The variability is greater than that observed over Hanscom at 12 km and increases more rapidly with time up to 12 hours.

The maximum of variability at 11 hours lag, and the apparent minimum in the vicinity of 24 hours, indicate strong diurnal variation. This variation
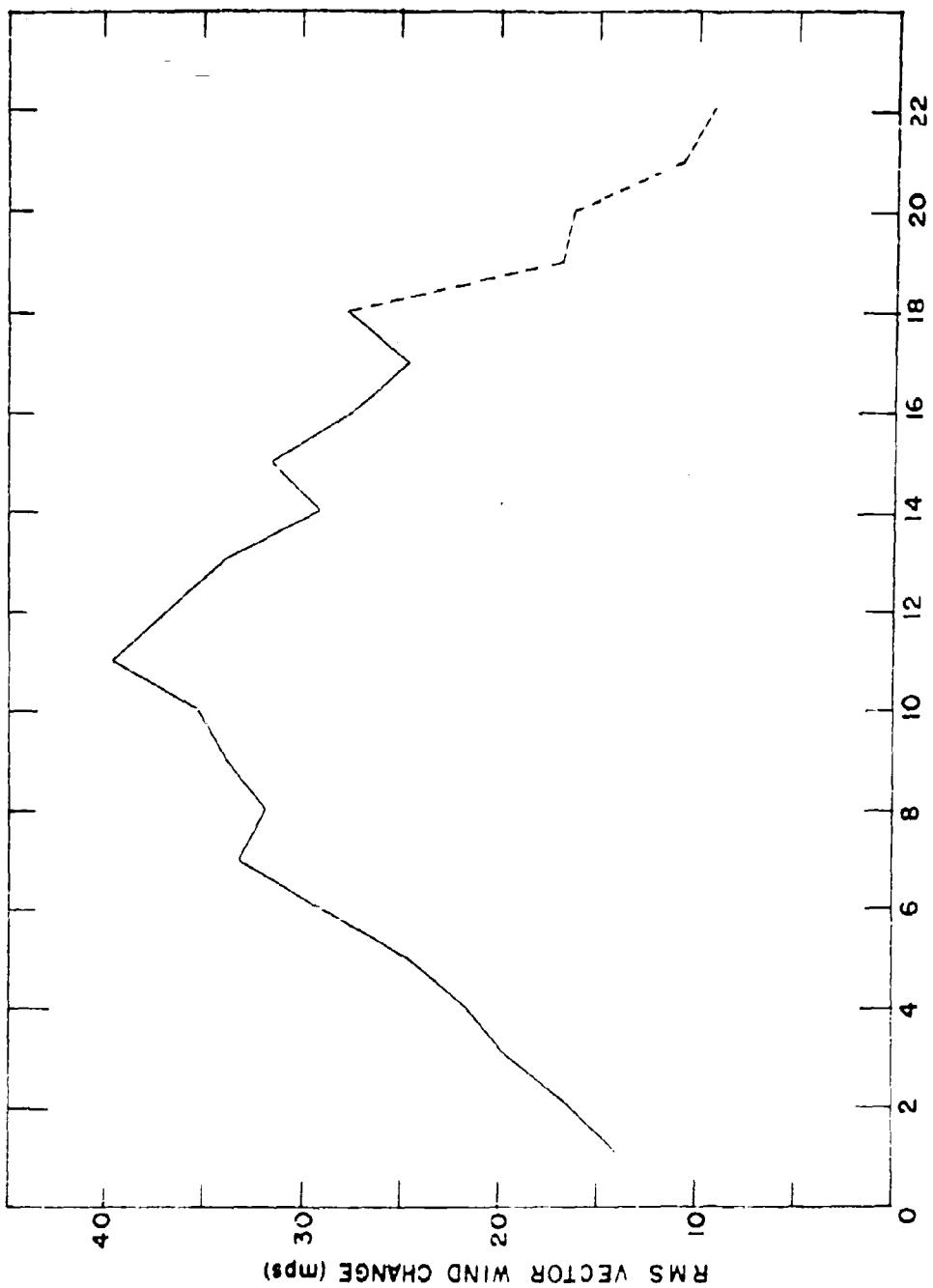
FIG. 5. Lag Variability of Winds at 65 KM over Elgin AFB, 9–10 May 1961.

was primarily directional: northeasterly winds prevailed from 2200 to 0900 and southeasterly winds the rest of the time. Such a diurnal variation of large amplitude, if real and recurrent at these levels, would be of great importance to atmospheric physicists and to missile engineers.

REFERENCES

1. A. D. Anderson, Free-Atmosphere Turbulence, NRL Report 4735, Naval Research Laboratory, Washington, D.C., 1956.

2. C. S. Durst, Variation of Wind with Time and Distance, Geophysical Memoirs No. 93, Met. Office, London, 1954.

3. W. C. Spreen, The Distribution of the Temporal Wind Variation, paper presented at 148th AMS Meeting, Ashville, N.C., 1 Nov. 56 (Unpub.)

4. A. Arnold, and R. Bellucci, Variability of Ballistic Meteorological Parameters, Tech. Memo. No. M-1913, U.S. Army Signal Corps Eng. Labs., Ft. Monmouth, N.J., August 1957.

5. Harold B. Crutcher, Upper Wind Distribution Statistical Parameter Estimates, U.S.W.B. Technical Paper No. 34, U.S.W.B., Washington, D.C., 1958.

6. J. Wright, and N. Engler, Wind Sensing Capability of the Robin, paper presented at National Symposium on Winds for Aerospace Vehicle Design, September 1961.

A Detailed Wind Profile Sounding Technique

ROBERT LEVITON

GEOPHYSICS RESEARCH DIRECTORATE

AIR FORCE CAMBRIDGE RESEARCH LABORATORIES

ABSTRACT

A method of obtaining detailed wind data from the radar track of a rising
balloon is presented. This method involves the use of the AN/FPS-16 high
precision radar and a small, rigid plastic sphere. Data errors caused by
radar tracking errors and the nonresponse of the balloon to wind shears are
analyzed. Some examples of wind profiles are shown.

INTRODUCTION

Detailed information on the structure of the wind field in the atmosphere
is of considerable importance in the design and test of missile and rocket
systems. The technique currently in field operation uses a balloon track deter-
mined from a radio direction finder. Considerable smoothing is employed in
this technique to provide information concerning the average wind through a
relatively thick layer (2000 ft) and as a result upper air wind profiles thus cal-
culated are not suitable for certain uses in missile design and testing, such
as for evaluation of responses to gust forcing of the structural vibration modes.
This paper indicates the feasibility of making precise measurements of winds
through 100-ft layers from the surface to at least 65,000 ft with a special,
passive, absolutely spherical balloon and a precision tracking radar.

TRACKING CAPABILITY

The feasibility of determining precise, detailed wind measurements by
radar track of an ascending balloon is a function of the radar tracking accuracy
and response of the balloon to the wind, in particular to extreme wind shears
such as are encountered in gusts. For extreme tracking accuracy, a radar of

the characteristics and precision of the AN/FPS-16 is desirable. The FPS-16 has a theoretical rms tracking accuracy of 0.5 yds in range and 0.05 mils (0.003°) in azimuth and elevation angles. However, operational accuracy is probably not quite that good. An AFCRL evaluation of the radar data on the ROBIN falling sphere program indicates an rms error of less than 2 yds in range and about 0.1 mils in angles to be more realistic. Assuming the existence of these errors in the radar, Table 1 shows errors in wind speed (in fps) that can be expected over a five-second interval, if a finite difference reduction method was used.

TABLE 1. RMS Speed Errors for 5-sec Time-averaged Sphere Displacement

Wind Speed Height (ft)	20,000	40,000	60,000
Light	1.0	1.6	2.0
Medium	1.6	2.0	2.3
Strong	2.0	2.3	2.6

It can be seen that the wind errors due to the tracking errors would average about 2 fps, somewhat greater at the higher altitudes and in strong winds.

The FPS-16 radar is designed to produce position information on a target at sample intervals of a period as shown as 0.1 sec, thus allowing for some position smoothing if desired, and possibly greater accuracy. The data are recorded on magnetic tape in a form suitable for processing in digital computers. Tabulated position data in component form are also available for manual data reduction. While the availability of the FPS-16 is rather limited, each U. S. missile site has at least one.

BALLOON RESPONSE

To determine how accurately a rising spherical balloon will respond to a given wind shear it is necessary to examine the forces acting on a balloon and the reaction of the balloon to these forces for any given atmospheric conditions. Balloons that are not symmetrical both in shape and weight distribution might be subjected to periodic lifting forces, giving rise to 'sailing,' so only a perfect sphere will be considered here.

A balloon in the atmosphere, whether it is rising or falling in its flight, experiences three forces; namely, the bouyant force of the displaced air mass (F_B), the weight force on the balloon itself (F_W), and the drag force due to

the balloon motion relative to the surrounding air mass (F_D). (The coriolis force is negligible.) F_B can be written as $\rho V_2 g$ where ρ is the density of air, V_2 is the volume of the balloon and g the gravitational value. F_W is expressed as mg where m is the balloon mass including its gas, and F_D equals $-1/2 \rho V^2 C_D A$ where V is the balloon velocity relative to the air mass, C_D the drag coefficient of the balloon and A the drag area. F_D is exerted in both the horizontal and vertical directions and its components can be written as $-1/2 \rho V^2 C_D A \left(\dfrac{W - \dot{X}}{V} \right)$ and $-1/2 \rho V^2 C_D A \left(\dfrac{\dot{Z}}{V} \right)$, respectively. The quantity $W - \dot{X}$ is the wind relative to the balloon in the X direction (true wind minus indicated wind), or the wind error, while $\dot{Z}$ is the vertical balloon velocity, assuming there is no vertical wind.

In the horizontal, the only force affecting the balloon is the drag force, and the equation of motion can be written as

$$m\ddot{X} = -1/2 \rho V^2 C_D A \left(\frac{\dot{X} - W}{V} \right) \quad . \tag{1}$$

In the vertical, the equation of motion becomes

$$m\ddot{Z} = -mg - 1/2 \rho V^2 C_D A \left(\frac{\dot{Z}}{V} \right) + \rho V_2 g \quad . $$

The $\ddot{X}$ and $\ddot{Z}$ terms are the horizontal and vertical accelerations, respectively. Combining these equations yields

$$W - \dot{X} = \frac{m \ddot{X} \dot{Z}}{m(\ddot{Z} + g) - \rho V_2 g} \quad . \tag{2}$$

In the case of a rising balloon where the rate of rise is relatively constant, $\ddot{Z}$ is effectively zero and the equation becomes

$$W - \dot{X} = \frac{m \ddot{X} \dot{Z}}{mg - \rho V_2 g} \quad . \tag{3}$$

For any given wind shear (S), $W - \dot{X}$ is a constant, or $W - \dot{X} = k$. Therefore the following can be written

$$\frac{dW}{dt} = \frac{d\dot{X}}{dt} = \ddot{X} \quad . \tag{4}$$

Since S is defined as the change in horizontal wind with height, then

$$S = \frac{dW}{dZ} = \frac{dW}{dt} \frac{dt}{dZ} = \frac{\ddot{X}}{\dot{Z}} \tag{5}$$

189

so long as the balloon is not floating, or $\dot{Z} \neq 0$. Substituting in Eq. (3) yields

$$W - \dot{X} = - \frac{m S \dot{Z}^2}{mg - \rho V_{2g}} .$$

(6)

For radar tracking purposes, a reflective, rigid balloon of some kind would be required. Experience has shown that a nonexpansible spherical balloon made of aluminized mylar is the optimum configuration because of weight, tensile strength and other considerations, including its ability to withstand a certain amount of superpressure without distortion. The following Table 2 shows the response error (W - X) in fps for various thicknesses and diameters of mylar balloons for a shear of 0.25 sec^{-1} at 25,000 ft. (Such a shear would result from a gust in which the wind vector changed 25 fps through a 100-ft layer.) The rate of rise was assumed to be 23 fps.

TABLE 2.   Response Errors (fps) vs Sphere Construction

Diameter Thickness	1/4 mil	1/2 mil	1 mil	2 mil
1 meter	1.6	3.1	9.3	- -
2 meter	1.1	1.7	3.0	9.4
4 meter	0.9	1.1	1.6	3.0

It can be seen that the error increases with balloon thickness and decreases with balloon size. Therefore as large and as thin a balloon as possible is desirable, taking into account its capability to reach the required height, its cost, the launching problems and trackability. The two-meter, half-mil type appears to best fit these requirements at the present time. This balloon would have an error of 1.7 fps at the very large 0.25 sec^{-1} shear.

No development effort will be necessary for these commercially available balloons. A gas valving technique, enabling the balloon to remain completely inflated up to the maximum height attainable, has been designed by the G. T. Schjeldahl Co. for a similar balloon used at the Pacific Missile Range for radar calibration work. Approximate cost of the half-mil, two-meter balloon ranges from about $50 each for a small number (under 100) to about $25 each for a large procurement (1000 or more).

Another possibility for obtaining radar wind data is with the use of an expansible neoprene balloon with chaff dipoles adhering to the inside film.

Theoretically the W - X for this balloon (800 gm standard size) at 35,000 ft, for example, would be about 1.7 fps also, and cost of such a balloon would be somewhat less than the mylar balloon described above. However, there is grave danger of such a balloon having a tendency to 'sail' under certain conditions of shape distortion and altitude, thus introducing an uncalculable error into the data.

FLIGHT DATA

A series of five balloon flights were made at Eglin AFB, Florida on 6 and 7 September 1961 with a helium-filled two-meter, half-mil mylar balloon tracked by the FPS-16 radar. Wind conditions throughout the flights were extremely light. Although time precluded a complete analysis of the data, some interesting results are evident. Figure 1 shows part of the profile of Flight No. 3. Winds calculated over 5-second intervals through that segment are shown in Table 3.

TABLE 3. Part of Wind Profile, 1706 CDT, 6 September 1961, Eglin AFB, Florida

Height (ft)	Wind Speed (fps)	Direction (° from)
36387	24	18
36493	17	352
36596	17	22
36702	15	63
36817	0	--
36924	4	152
37033	25	64
37130	17	11
37223	21	61
37348	22	29
37479	15	50
37608	18	71
37733	22	68
37852	22	25
37951	18	9
38055	10	103
38155	26	83
38252	33	63
38357	31	56
38463	26	46
38571	24	73
38695	21	94
38834	17	49

Altitude, 38,000 ft approx.
X—Y Plot 5–sec Intervals

Y, ft

X, ft
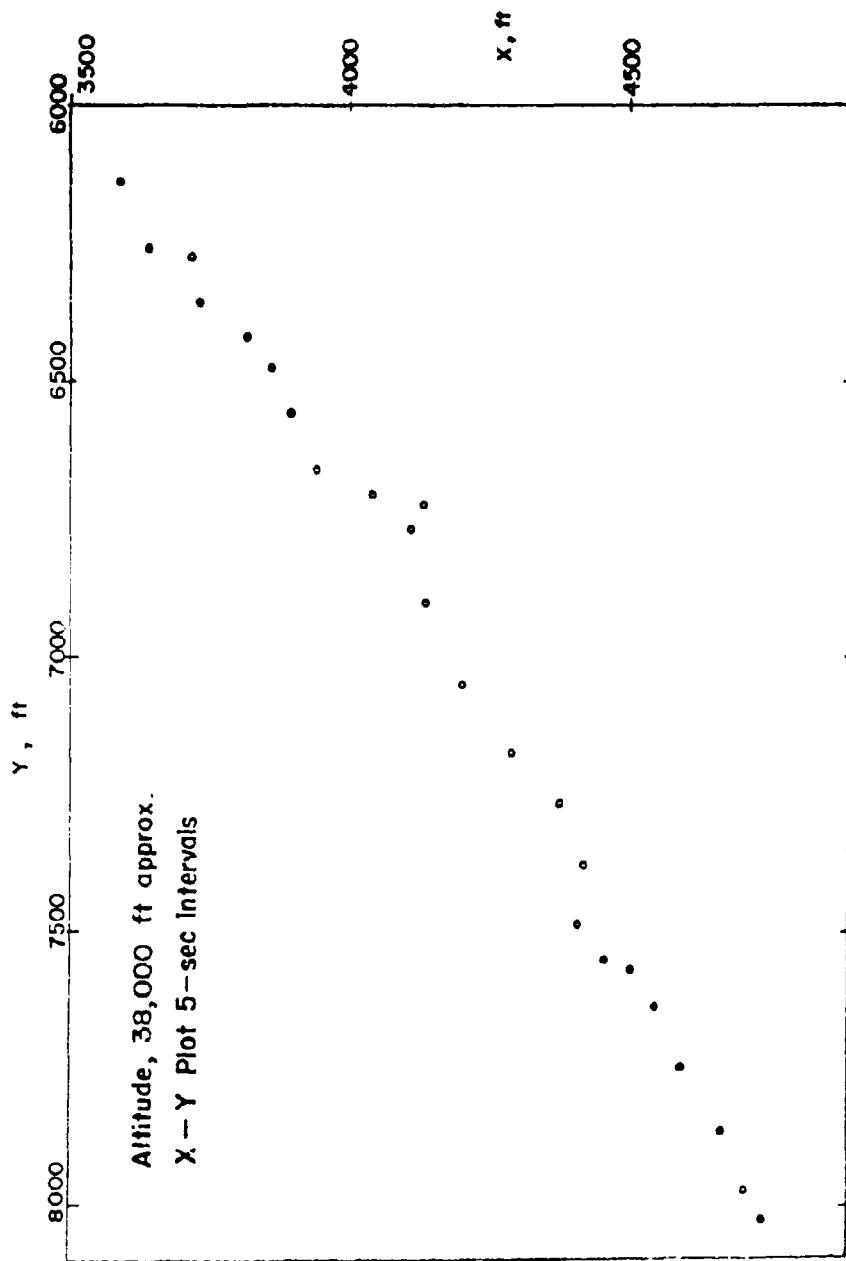
FIG. 1. Part of profile of Flight No. 3, 1706 CDT, 6 September 1961

Some rather large wind shears are to be noted. It is believed that these shears are real. Figure 2 is a position plot of part of the profile in Fig. 1 using the radar observations for each half second. The relative smoothness of this curve tends to verify the previously indicated FPS-16 tracking accuracy. Figure 3 is an altitude-time chart for the period of the flight shown in Fig. 1. Obviously, further analysis of these and subsequent flights must be made before any conclusive statements on the accuracy of the data from this tracking technique can be forthcoming

CONCLUSIONS

From the foregoing discussion it appears that the technique of tracking a two-meter, half-mil aluminized mylar sphere by an FPS-16 radar will give wind data through a strong shear to an accuracy of at least 2 to 3 fps over a five-second time interval, taking into account both the tracking and wind response errors. This accuracy can probably be improved by the use of a smoothing technique, with a somewhat more sophisticated data reduction process. Also, the wind response error can, if necessary, be evaluated and a correction made as in the case of the ROBIN falling sphere. Thus, it does not seem unreasonable that the ultimate accuracy of the radar-sphere method can approach 1 fps for the five-second interval, perhaps allowing shears to be measured over a thickness as small as 50 ft.

In summary, some of the advantages from the use of the technique are as follows:

1. The technique proposed is simple and straightforward with high reliability.

2. The instrumentation and techniques required are currently available, so that neither time nor money need be spent in design or development.

3. Necessary data are obtainable under all weather conditions, thus permitting the development of a representative climatology of precise wind measurements.

4. Operating costs are low, under $5000 for 100 flights per year.

5. Computer programs are available for automatic reduction of data.
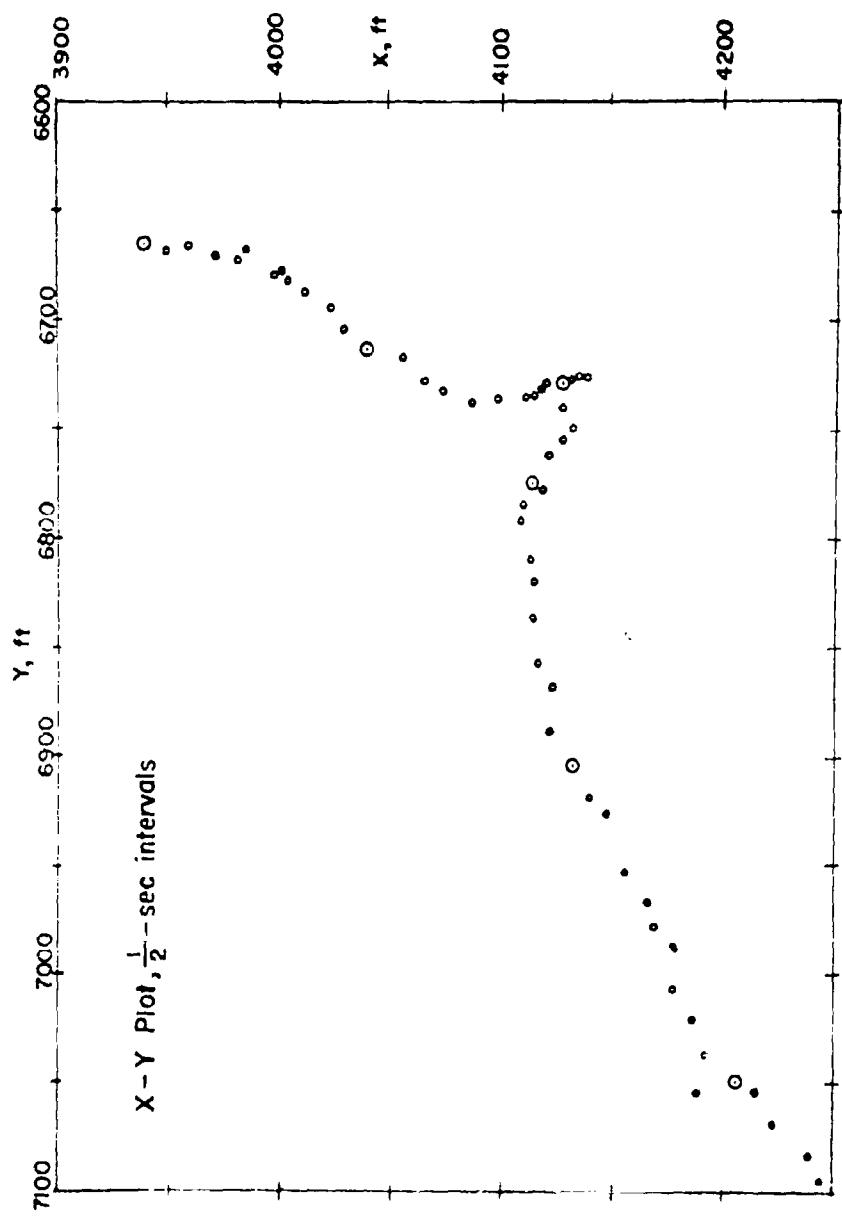
FIG. 2. Position plot of part of profile of Fig. 1.

194
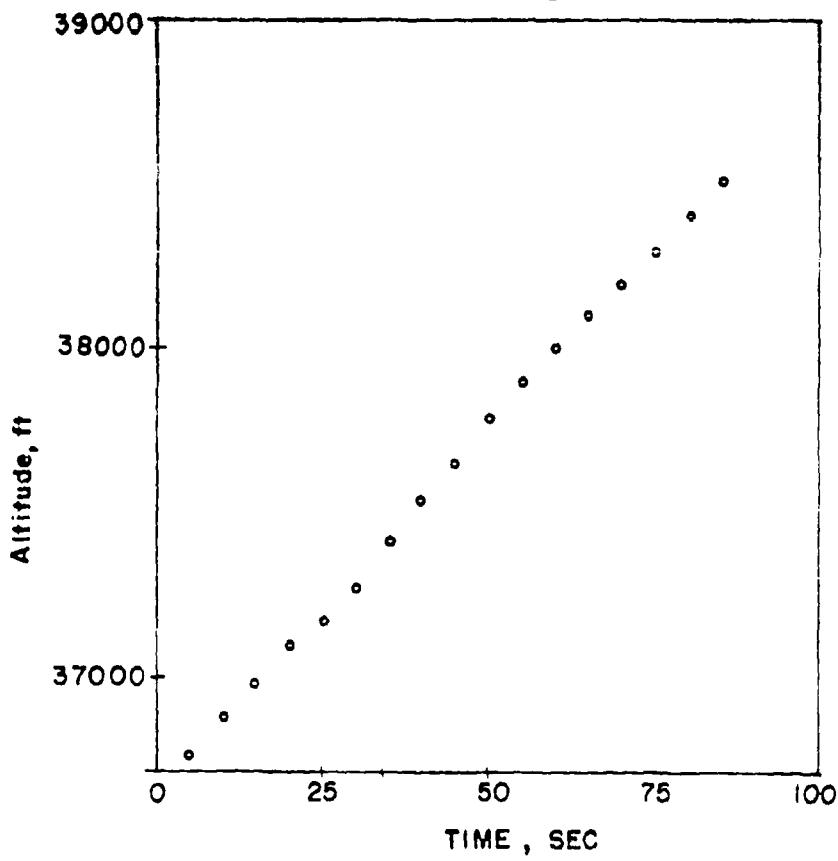
FIG. 3. Altitude time chart for period of Flight No. 3

Wind Measurement and Forecasting Problems at the Atlantic Missile Range

MAJOR ROBERT L. MILLER, USAF

ATLANTIC MISSILE RANGE

PATRICK AIR FORCE BASE, FLORIDA

ABSTRACT

A summary of the surface and upper wind launch criteria for the various missile and space systems is presented. The problems and methods of forecasting winds to 110,000 ft are discussed. The difficulties associated with wind measurements and forecasts during high winds and extreme wind shears are discussed. The accuracy requirements of wind measurements as stated by users of the Atlantic Missile Range are given.

In the consideration of wind forecasting problems at the Atlantic Missile Range (AMR), it is necessary to include the measuring problems. Missile contractors ask for general forecasts as many as 2 to 3 days in advance of launch date and continue until near launch time, wanting more detailed forecasts of the wind profile as launch hour approaches. It is obvious that errors in the observed winds will introduce similar errors in the forecasts. Under wind conditions that approach the maximum allowable for a particular launch, the go, no-go decision is based on a measurement taken as near to launch time as possible, that is, in effect, a persistence forecast. Knowledge of the trend toward improved or worse conditions is of course considered. In addition, the observed wind profile taken immediately after launch is used to determine whether or not deviations in the trajectory or performance of the missile were a result of extreme wind shears or speeds.

There are some fifteen active ballistic missile and space programs at the AMR with vehicles ranging in size from the PERSHING and BLUE SCOUT to the SATURN being prepared for launch this fall. It might be said that the designers are responsible for the fact that there are forecasting problems. If a system were designed to operate under any extreme wind conditions there would be no requirement for wind forecasts. There are several good reasons why all of the wind problems are not designed out of a particular system:

(1) the specifications do not call for designing for the most extreme conditions, (2) to design for such conditions would be costly both in money and payload capability, (3) precise meteorological data on which to base design criteria are lacking, and (4) weapons system boosters are being used in ways for which they were not originally designed, for example, the ATLAS vehicle.

Most weapons systems being tested at the Cape, including ATLAS, are designed to be launched in surface winds up to 60 knots, including gusts. Some of the complex orbital and space probe systems are much more wind sensitive. One particular vehicle launched at the Cape could theoretically have been affected by gusts with periods of the order of 0.5 sec or less when the service structure was removed. The anemometers in use at the Cape have a response time of approximately 1 to 2 seconds. For this reason, gusts 50 percent higher than the gusts measured on the anemometers were assumed to be present and the maximum allowable wind was reduced accordingly.

The levels of the maximum allowable upper wind speed and shear, as stated in AFMTC documents for most missiles, are between 25 and 45 thousand feet. The maximum speed varies from 120 knots to 180 knots and the shear from 20 knots/1,000 feet to 40 knots/1,000 feet. For some of the more sensitive vehicles, the wind effects are so complex that a computer must be used to determine if the forecast wind profile exceeds the launch criteria. The launch minima for these vehicles are not stated explicitly.

The limitations of the GMD-1A rawinsonde equipment cause uncertainties in the measurement of upper winds, especially during jet stream conditions at Cape Canaveral. The GMD-1A cannot measure winds when the elevation angle of the tracking antenna falls below 6°. At Cape Canaveral the tracking data become erratic at elevation angles less than 12 to 14°. Upper winds producing angles of 8 to 12° are quite common during the winter months and can persist for several days. These low elevation angles cause the antenna to hunt which in turn introduces fictitious shears and large errors in the observed wind profile. Unfortunately, this problem is acute at levels where the winds are strongest and real shears are greatest. During past winter seasons, up-wind balloon releases have been used to keep the elevation angles large. This has been effective in improving the data. The smoothing procedures used in the computer processing of the GMD-1A data help to reduce this source of error but also eliminate small-scale motion of the atmosphere. The winds that are computed are actually mean vectors through 2,000-foot layers or, under high wind conditions, 4,000-foot layers. The computation of winds through shallower layers is not justified because of limitations of the tracking data. An estimate of the error of GMD-1A mea-

sured winds is given by[*]

$$\sigma V = \frac{0.9h \times 10^{-2}}{\sin^2 \alpha}$$

where σV = rms vector error in knots, h = height in thousands of feet and α = elevation angle. With strong upper-levels winds, rms vector errors of 30 to 35 knots may be expected (see Fig. 1).

Table 1 shows the required accuracies (rms error) and altitude for launch-time observed wind data, as stated by the various AMR users. The wind profiles measured near launch time that are used for test evaluation purposes, with allowable rms errors as given in Table 1, are required by some range users to be given in 500-foot intervals. It is quite apparent from the previous discussion that the present wind equipment and processing procedures do not justify this much detail. The GMD-2, which is expected to be in use at the AMR by early 1962, will help to reduce the wind errors because of its capability for measuring slant range. In addition, an attempt is being made to provide more accurate wind profiles for evaluation of SATURN test-vehicle performance by tracking a 6-foot mylar sphere with FPS-16 radar.

Up to the present time at the AMR, the wind forecasts required by missile and space vehicle test agencies have been for surface (0 to 200 feet) and for wind profiles from the surface to 110,000 feet. Some of the test programs in the near future, such as SATURN and DYNASOAR, will require wind profile forecasts up to 250,000 feet.

The methods for wind forecasting for missile launches at the AMR are essentially those used for forecasting for aircraft operations, except that a vertical profile is required for the missiles, whereas the horizontal wind field is usually of more importance to aircraft. As mentioned previously, the level of critical wind speed and shear, of primary concern to the missile contractor, usually coincides with the level of the tropospheric wind maximum--25,000 to 45,000 feet. The wind maximum and shear facsimile prognostic charts from the National Weather Center are used along with the progs for the various pressure levels to arrive at a forecast profile. This method is not completely satisfactory, especially with the more wind-sensitive space vehicles which require a detailed forecast profile, with winds at close intervals, to be run through a computer to determine if launch criteria are exceeded. Our present forecast techniques do not warrant presenting wind profiles in greater detail than at 5,000-foot intervals for periods beyond 6 to 12 hours. Such a forecast profile given in 5,000-foot intervals may not portray shears which cause

_____
[*]Karl Johannessen, Accuracies of Meteorological Upper Air Data, Hq AWS, Scott AFB, Ill. Unpublished report.

ALTITUDE (Thousands of feet)

120

100

80

60

40

20

0

30-knot mean wind (a=18°)

60-knot mean wind (a=9°)

90-knot mean wind (a=6°)

10   20   30   40   50

rms error (knots)
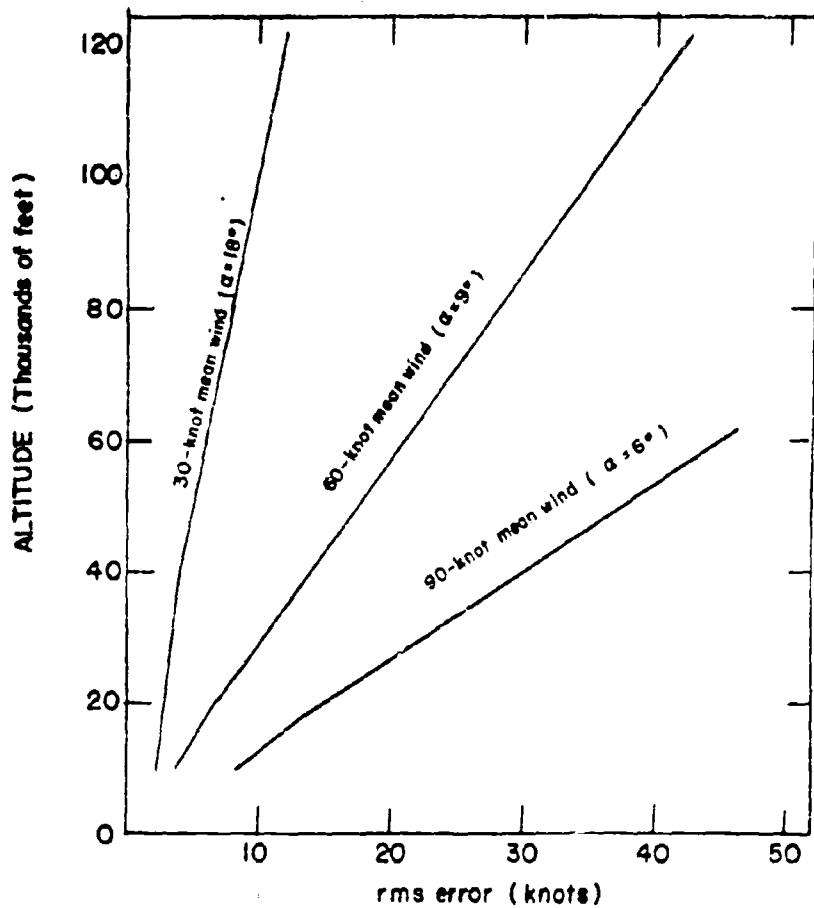
$$\sigma V = \frac{0.9h \times 10^{-2}}{\sin^2 a}$$

where : σV = rms vector error in knots

h = height in thousands of feet

a = elevation angle

FIG. 1.   From Johannessen, K., "Accuracies of Meteorological
Upper Air Data," Hq. AWS, Unpublished Report.

TABLE 1

REQUIRED ACCURACIES AND ALTITUDE FOR LAUNCH TIME
OBSERVED WIND DATA

	ALTITUDE		
	0-50,000 FT	50,000-120,000 FT	120,000-250,000 FT
POLARIS	5.0 kts, 5°	Same	-
HETS (BLUE SCOUT)	6.0 kts, (VE)	Same	-
PERSHING	0.5 kts, 5°	Same	Same
ATLAS	6.0 kts, 10°	Same	Same
TITAN	6.0 kts, 10°	Same	-
ADVENT	6.0 kts, 5°	Same	-
MERCURY	0.5 kts, 5°	Same	Same
MINUTEMAN	10.0 kts (VE)	18.0 kts (VE)	*
CENTAUR	5.0 kts, 5°	Same	-
DELTA	6.0 kts, 5°	Same	-
TRANSIT COURIER	6.0 kts, 5°	Same	-
RANGER	*	*	-
SKYBOLT	6.0 kts, 10°	Same	-
SATURN	*	*	*
DYNASOAR	*	*	*

*Data required but accuracy not stated.

concern, whereas the 'true' wind which includes vertical shears produced by motion of the scale of 1000 to 5000 feet may cause excessive wind loads especially on some of the more complex combinations of boosters and payloads. For this reason observed wind profiles are provided for unusually wind-sensitive vehicles beginning at 12 hours prior to launch and continuing at intervals, depending on the wind and shear magnitude, until launch.

As indicated by the title of this paper, only AMR problems have been discussed. The research and development agency, AFCRL for the Air Force, is well aware of these problems and is devoting considerable effort and funds toward their solution.

Smoke-Trail Measurements of the Vertical Wind Profile and Some Applications

HAROLD B. TOLEFSON

NASA LANGLEY RESEARCH CENTER

ABSTRACT

This paper discusses a method in which the detailed structure of the wind profile is determined from photographic tracking of a smoke trail left by a vertically rising rocket. The accuracy of the method is discussed and results are presented in the form of wind profile measurements. Particular attention is given to small-scale wind fluctuations which cannot be measured with conventional wind-sounding systems. The implications of these fluctuations to missile loading problems are illustrated by the results of computer studies of missile responses to different wind profiles.

INTRODUCTION

The problem of obtaining accurate measurements of the wind structure for application to flight problems has been under continuing study for a number of years. The need for improved wind measurements has been particularly emphasized by the current development and use of large and complex rocket vehicles for launch through the earth's atmosphere. For such vertically rising vehicles, the wind conditions experienced during the exiting flight phase are a major loading source and impose serious design conditions on the vehicle's structural strength capabilities and on its guidance and control system.

In an effort to provide improved wind measurements a technique based on photographs of visible trails emitted from vertically rising rockets has been under development by NASA for about a year. This technique has provided highly accurate measurements of the complete wind profile including small-scale wind fluctuations which are completely masked in conventional sounding wind measurements. It has the further advantage of providing the measurements along typical missile trajectories, thus eliminating the differences in the wind structure between the time-space path followed by balloons or other commonly used tracers and the near-vertical missile trajectory.

The purpose of this paper is twofold. First, the smoke-trail technique will be briefly described and some measured wind profiles will be discussed. Secondly, the measurements will be applied in missile response calculations as a means of highlighting some missile response problems.

NOTATION

b	length of base line between cameras, ft
f	focal length of camera, in.
x', z'	horizontal and vertical film coordinates, in.
X, Y, Z	right-hand Cartesian coordinates with origin at camera I, X axis along the camera base line, and Z axis vertical, ft
α	azimuth angle at camera from Y axis to point on smoke trail, positive clockwise, deg
ε	dihedral angle at camera base line from horizontal plane to plane containing point on smoke trail, positive upward, deg
subscript I	refers to camera I
subscript II	refers to camera II.

MEASUREMENT PRINCIPLES

The principles of the smoke-trail measurements have been described rather completely;[1,2] accordingly, only an outline sufficient to give an understanding of the basic principles is given here. A filament composed of very fine particles, or 'smoke,' provides an extremely sensitive tracer system with nearly perfect response to very small-scale atmospheric motions, at least throughout the relatively dense atmosphere below 100,000 feet. The smoke particles have essentially zero fall rate, and it is thus possible to deduce a wind velocity from a time averaging of the displacement of the trail without also being concerned with a vertical-height averaging interval. The general measurement system is illustrated in Fig. 1.

Figure 1 illustrates the trail as it is distorted by the winds a moment or so after missile passage and the two camera sites which make up the ground installation. The distance of the cameras to the launch site is about 1C miles for this particular application in which photographs of a trail up to about 100,000 feet are desired. The trail sketched in Fig. 1 may be formed either by the natural exhaust products of a solid-propellant rocket or by introducing hygroscopic particles into the wake of the rocket to induce condensation of atmospheric water vapor. In either case it is possible to obtain

204
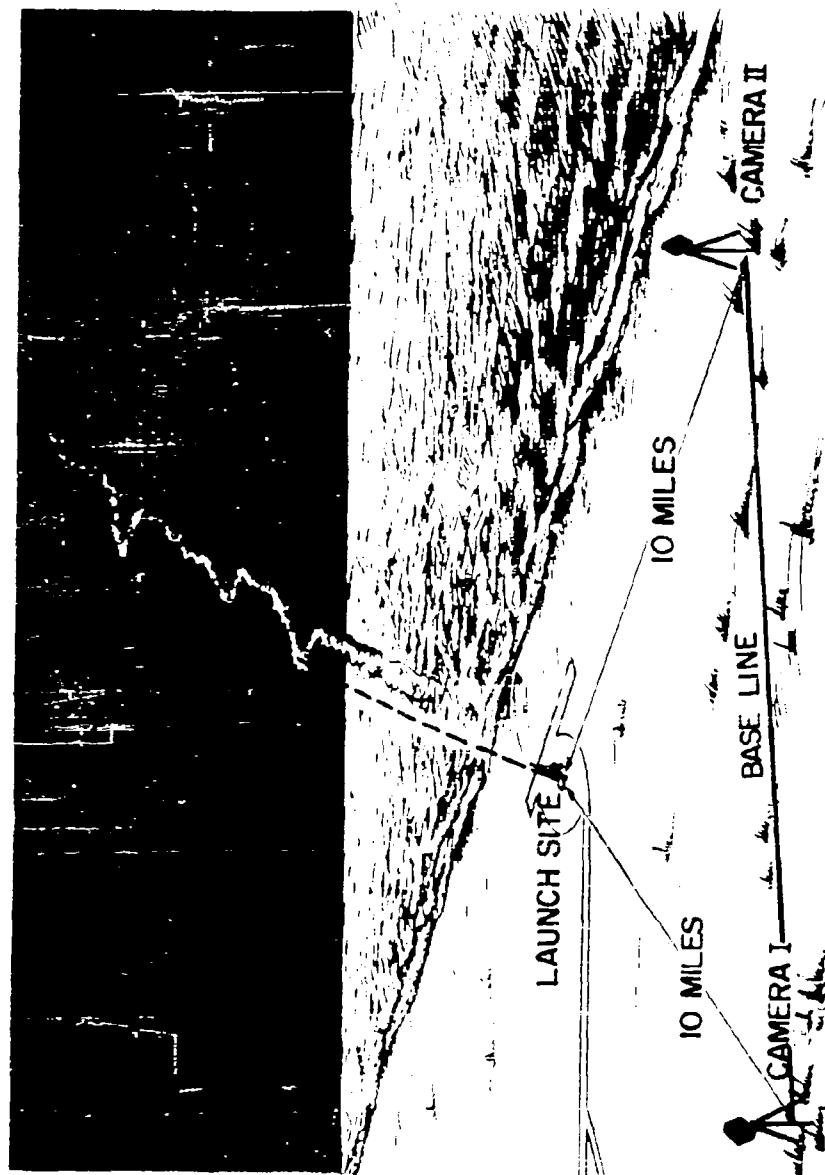
FIG. I. Camera Installation.

a highly reflective trail that persists for several minutes for photographic applications.

A set of photographs of a rocket exhaust trail as taken from the two camera sites at the Wallops station is shown in Fig. 2. These particular photographs were taken about one minute after passage of the rocket and show the distortions in the trail due to the varying winds at different altitudes.

The determination of the trail displacements over given time intervals from sets of such photographs forms the basic scheme of the smoke-trail wind measurement system. Obvious operational requirements for this system are relatively clear skies and good visibility. For some locations, these requirements may severely limit the application of photogrammetric methods of wind shear measurements.

As can be noted from an examination of Fig. 2, it is usually not possible to identify a common point on the trail in the two photographs. This identification of points is an important feature of the smoke-trail reduction procedure and is described in the following paragraphs.

Figure 3 shows the image of the smoke trail as it would be formed by a camera pointed perpendicular to the base line and in the horizontal plane. It can be seen that the following relations between the angular values and film coordinates hold for the camera system:

$$\tan \alpha = \frac{x'}{f} \tag{1}$$

$$\tan \epsilon = \frac{z'}{f} \tag{2}$$

The use of these two angles in identification of points, and in computation of the geographic position of the points, is illustrated in Fig. 4.

Notice in Fig. 4 that the elevation angle ϵ is the dihedral angle between the horizontal plane and the plane through the base line b and point (XYZ) on the smoke trail. This angle serves as a means of identification of the point on the simultaneous photographs from the two camera sites since it has a common value for any given point. The two azimuth angles α_I and α_{II} are measured from the Y-axis direction to the projection of the point (XYZ) on the horizontal plane.

From Fig. 4 it can be seen that

$$\tan \alpha_I = \frac{X}{Y} \tag{3}$$

$$\tan (-\alpha_{II}) = \frac{b - X}{Y} \tag{4}$$

CAMERA I   CAMERA II

FIG. 2. Exhaust Trail Photographs.

$$\text{TAN } \alpha = \frac{x'}{f}$$

$$\text{TAN } \epsilon = \frac{z'}{f}$$
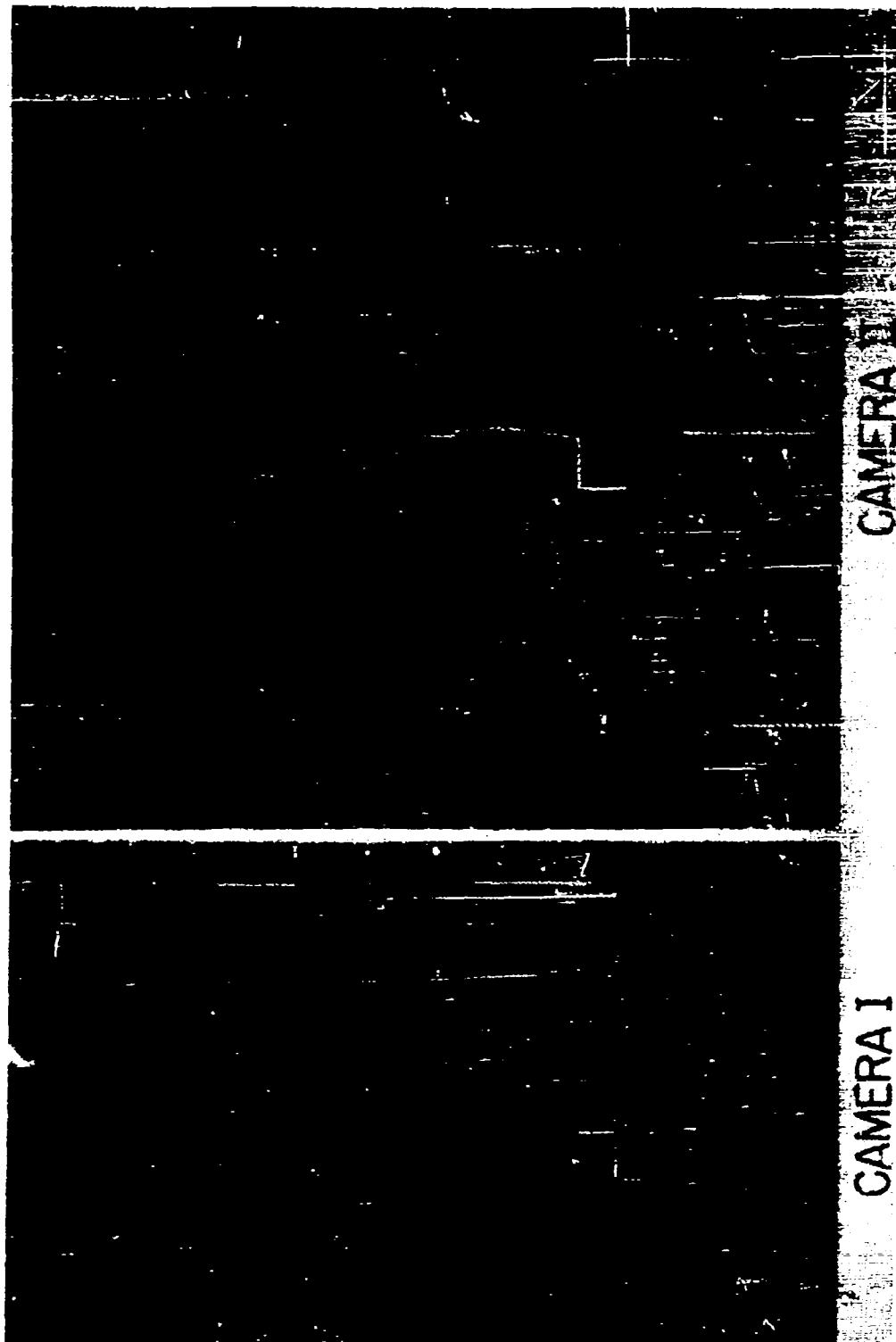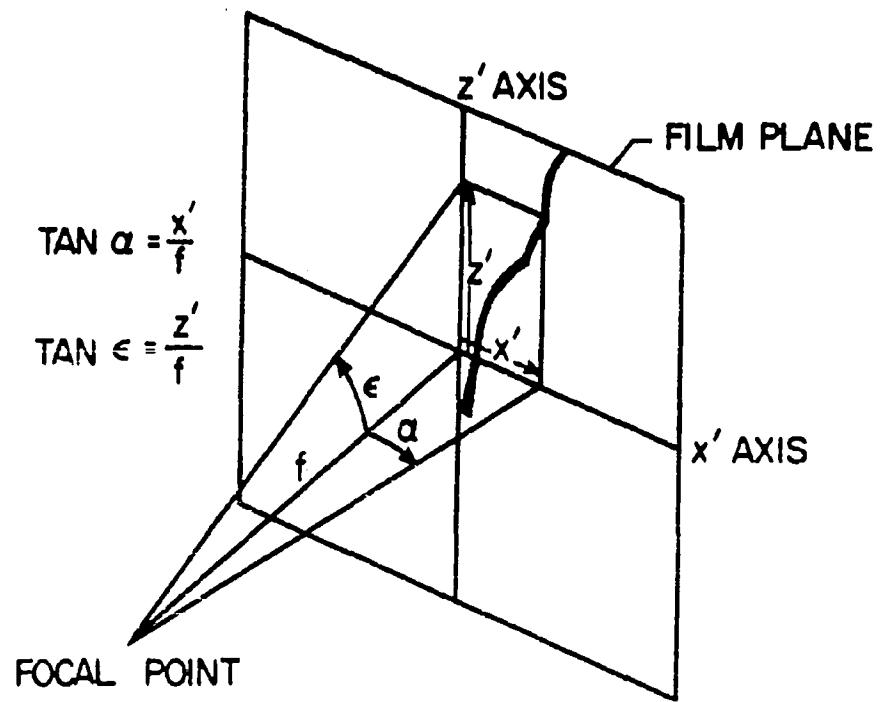
FIG. 3. Ideal Camera Relationships.

208
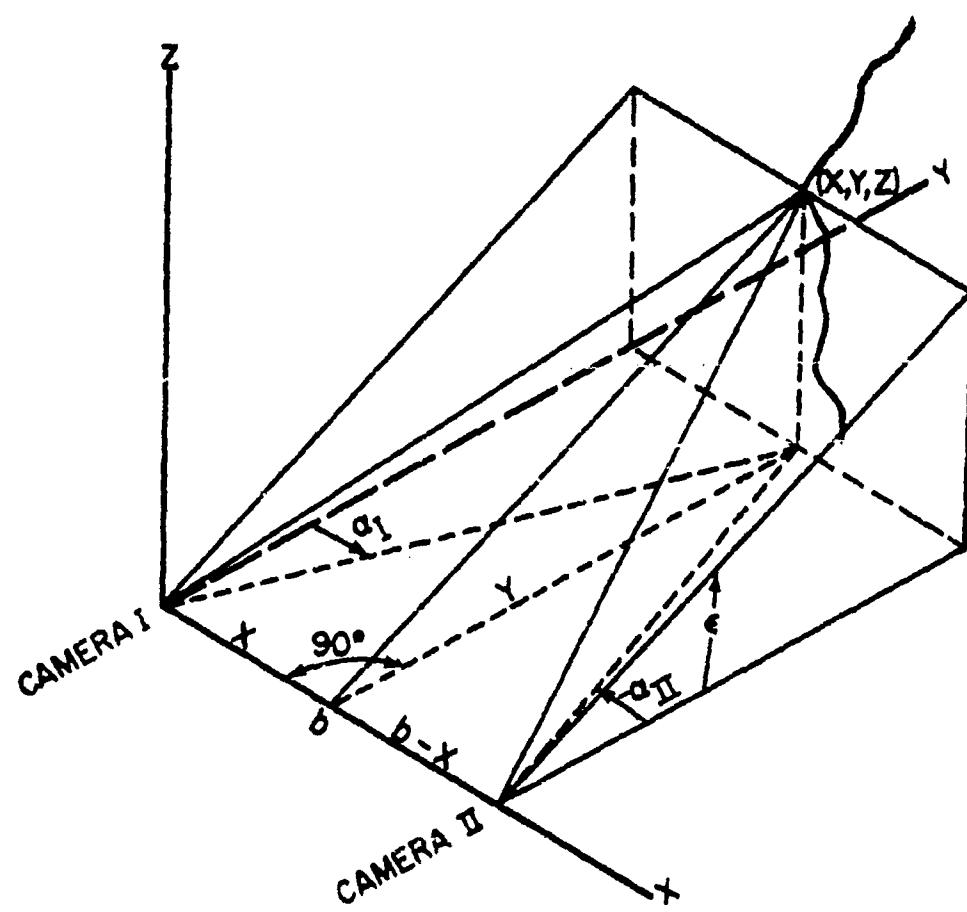
FIG. 4. Coordinate System.

$$\tan \epsilon = \frac{Z}{Y} , \tag{5}$$

and solving simultaneously:

$$X = \frac{b \tan \alpha_I}{\tan \alpha_I - \tan \alpha_{II}} \tag{6}$$

$$Y = \frac{b}{\tan \alpha_I - \tan \alpha_{II}} \tag{7}$$

$$Z = \frac{b \tan \epsilon}{\tan \alpha_I - \tan \alpha_{II}} . \tag{8}$$

Equations (6), (7), and (8) define the position in space of any given point on the trail. Repeating this procedure for a large number of points read from the film negatives defines the X-Y coordinates of the trail at closely spaced height (Z) values. The wind components along the X and Y axes at a given height Z are then found simply by subtracting the X (or Y) values determined from successive pairs of simultaneous photographs and dividing by the time interval. In practice, it is not convenient to aim the cameras perpendicular to the base line and in the horizontal plane as in this simple example, and coordinate transformations[3] are used to give equivalent results for cameras aimed toward the trail.

RESULTS OF MEASUREMENTS

As an illustration of the wind profiles measured by the smoke-trail technique, the W-E and S-N components of two measured profiles are given in Figs. 5 and 6. The profiles were measured at the NASA Wallops Station and represent light to moderate wind conditions throughout the altitudes covered. In each profile the wind velocities have been determined at altitude increments of 100 feet as given by the dotted points in the figures. This degree of detail in specifying the wind profile is considered adequate for missile response problems encountered to date, but if necessary, somewhat greater detail could be obtained.

The important feature of Figs. 5 and 6 is the continuous nature of the disturbances throughout the profile with large- and small-scale wind fluctuations following one another in altitude in an apparently random pattern. Many of the small-scale disturbances have vertical wavelengths considerably less than 1000 feet. The large number of independent data points obtained by the smoke-trail method allows even these small-scale disturbances to be traced
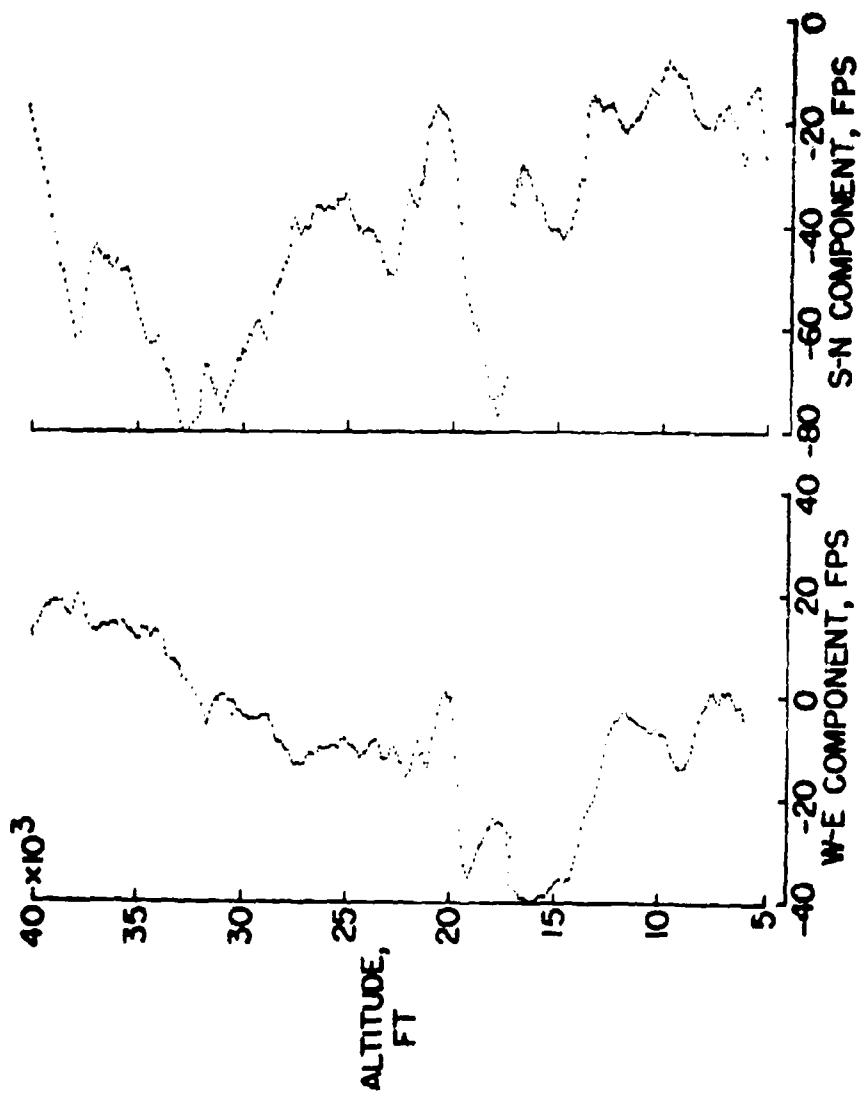
FIG. 5. Smoke-trail Winds.
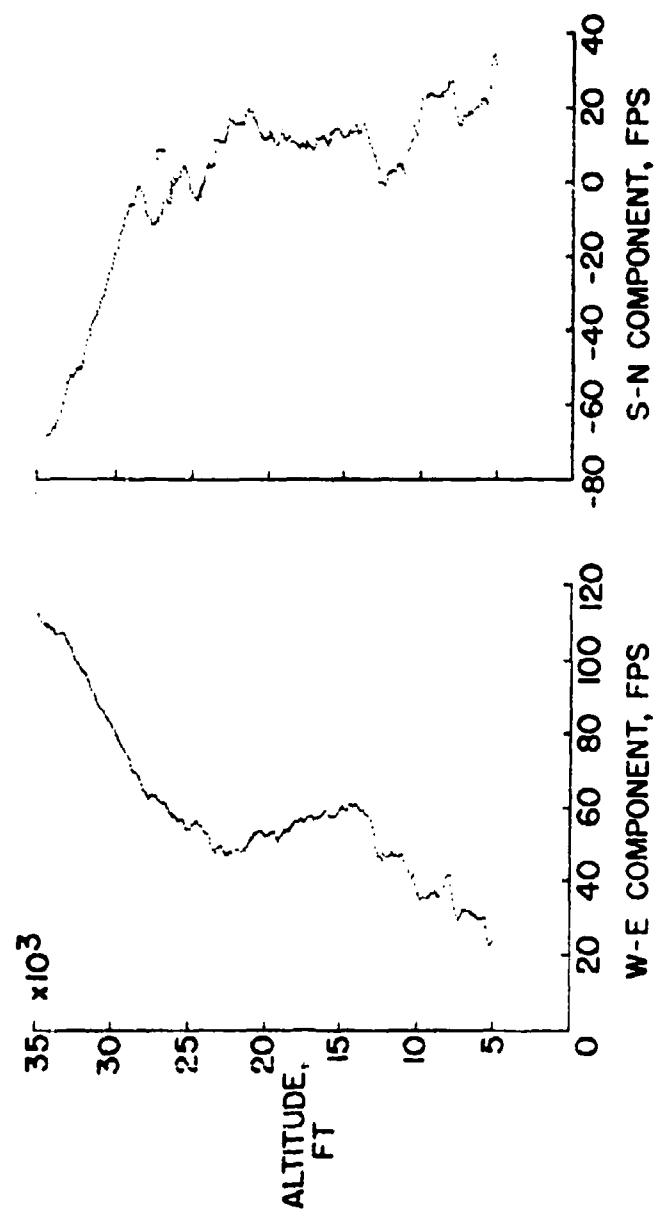
FIG. 6. Smoke-trail Winds.

out quite clearly and gives a high degree of detail in the wind profile. Although not many smoke-trail measurements have been obtained to date, the random distribution of small- and large-scale disturbances throughout the altitude range covered appears as a common feature of all measurements and is apparently typical of the wind inputs to vertically rising vehicles.

A definition of the fluctuations at the different altitudes as in Figs. 5 and 6 requires, of course, very accurate wind measurements, and it is appropriate to discuss the measurement accuracy briefly at this point. In the smoke-trail measurements relatively great errors can be tolerated in the absolute position of the trail as long as these errors are consistent from frame to frame. These systematic errors tend to cancel out in the subtraction of successive trail positions for the wind-velocity determinations and thus have little effect on the final wind measurements. Other random effects that generally do not cancel out contribute the major errors to the present system. The primary factor contributing to the overall error is reading the position of the smoke-trail image on the photographic negative. Other factors affecting the wind velocity error are the focal length of the cameras, the location and aiming of the cameras, and the position and slope of the smoke trail. Detailed error equations in terms of the factors noted above have been developed and discussed.[1,2,4]

Table 1 summarizes the rms vector wind error as a function of the altitude of the point in question and the altitude coverage afforded by the camera installation. The conditions concerning averaging time interval, random reading error, etc., are noted. The upper row illustrates the accuracy of the wind measurements for an altitude coverage up to 100,000 feet.

TABLE 1[1,2,4]

RMS VECTOR WIND VELOCITY ERROR, AS A FUNCTION OF ALTITUDE AND RANGE				
Altitude Coverage ft	Altitude of point on trail, ft			
	1000	10,000	50,000	100,000
100,000	0.141	0.178	0.330	0.525
50,000	0.073	0.107	0.262	
10,000	0.018	0.053		

Based on:
 Camera elevation and azimuth angles of 45° rms reading error of 0.001 in.
 9" by 9" film negative.
 1-minute time averaging interval

These values are representative of the camera installation at the Wallops
Island range. Notice that the wind velocity error increases with height, but
even at the top of the trail at 100,000 feet the error (0.525 fps rms) is
negligibly small. This degree of accuracy is sufficient to allow definition of
the small-scale and random fluctuation in the wind profile as previously dis-
cussed in connection with Figs. 5 and 6.

The other rows in Table 1 are indicative of the accuracy that would be
obtained with less height coverage from a similar camera arrangement. For
the lower altitude ranges of 50,000 or 10,000 feet, a much shorter averaging
time than the 1-minute interval assumed in the table might be used, and would
probably be necessary as the trail would be blown out of the field of view of
the camera in a short time.

APPLICATION OF MEASURED PROFILES TO
MISSILE RESPONSE CALCULATIONS

The unsteady aerodynamic loading conditions resulting from wind dis-
turbances as given in Figs. 5 and 6 are of great interest in connection with
response problem of large boosters. The loads from this varying wind input
when coupled with low aerodynamic and structural damping could excite the
lower frequency structural modes and thus result in severe dynamic loading
conditions. Although the wind-sounding data currently available for applica-
tion to vehicle design problems do not provide the finer details of the wind
profile, the effects of severe and sharp wind fluctuations have been allowed
for to a degree in design practices. Design procedures, for example, can
consist of superposing on the loading determined from the steady winds the
loading due to a (1-cosine) shaped wind disturbance or gust. To produce the
maximum effect, the wavelength of the gust can be adjusted to excite the
fundamental structural mode of the vehicle under consideration.

In an examination of the significance of the more complete wind profile
to missile loading histories, the bending-moment responses of the Scout
vehicle have been calculated for flight through the wind profile given in Fig. 5
and for flight through the same wind field as it might be measured with a
balloon. These two wind velocity measurements are shown in Fig. 7. In this
figure the dashed curve indicates the simulated (perfect) balloon measurement
and was obtained simply by averaging the smoke-trail winds over 2000-foot
altitude intervals. This interval corresponds to the averaging altitude usually
used in evaluating radiosonde sounding data. As can be noted in Fig. 7, this
method of simulating the balloon measurement leads to a highly smoothed
profile, the smoothing being particularly apparent at altitudes near 17,000
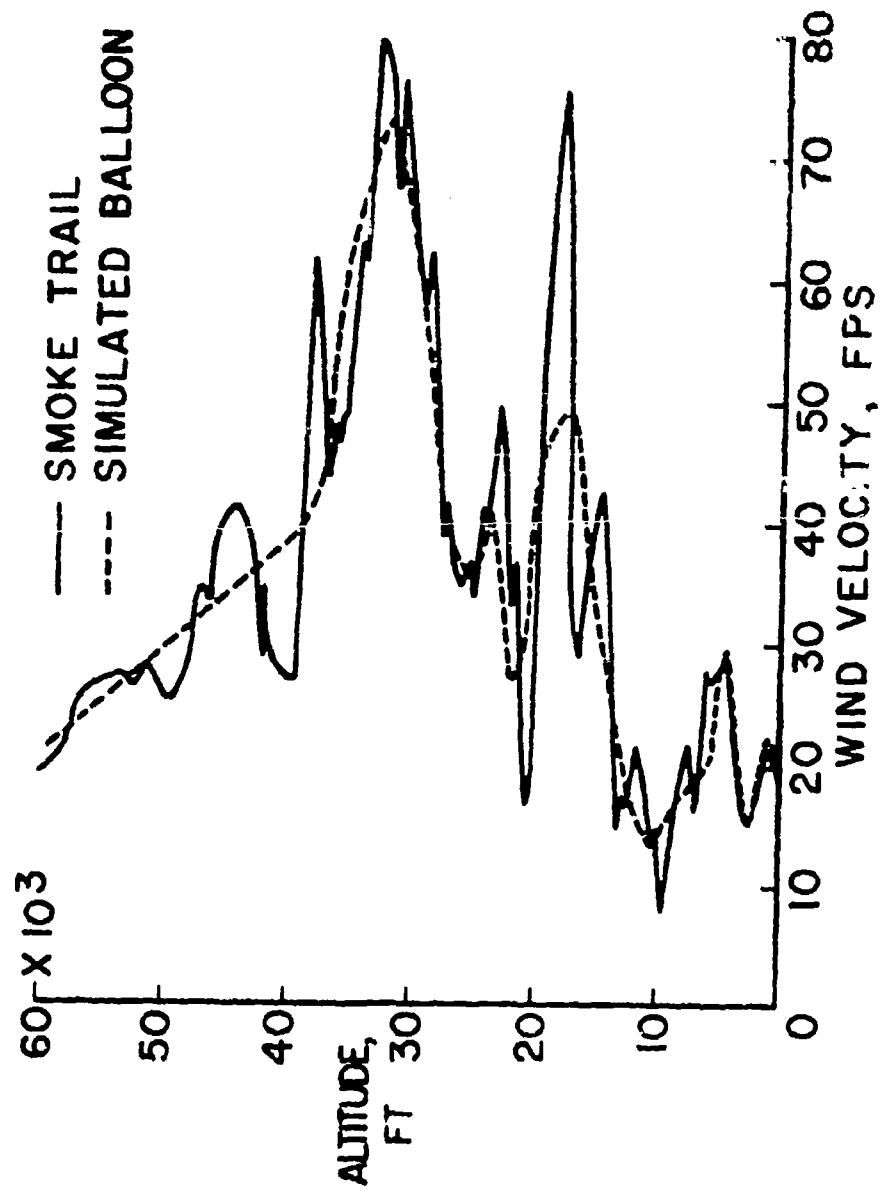
FIG. 7. Wind Velocity Measurements.

and 35,000 feet. These relatively mild winds would not be suitable for design purposes, but will serve for making the desired comparisons.

The bending-moment responses of the Scout vehicle to the wind profiles were calculated on a digital computer by a system developed by Vernon L. Alley, Jr., of the Engineering Division, LRC. The equations of motion described perturbations in the pitch plane about a reference trajectory and included three elastic bending modes. The solution to these equations was found using time-varying coefficients and included an active rate and altitude guidance system. The resulting maximum bending moments as a function of altitude are shown in Fig. 8 for flight both through the smoke trail and from simulated balloon measurements. These bending moments were calculated for a station at about the midpoint of the first stage; similar results were obtained for other stations.

The bending-moment curves illustrated are actually envelopes of the maximum bending moment. The insert in Fig. 8 shows the details of this bending moment near 35,000 feet and illustrates the cyclic characteristic of the response. The large response at the structural frequencies of the vehicle is very apparent, especially to the smoke-trail measured wind.

The significant results from Fig. 8 are the larger bending moments for the smoke-trail winds throughout all altitudes up to 50,000 feet. Near 18,000 feet and 35,000 feet, in particular, the wind fluctuations indicated by the smoke trail measurements resulted in significant increases in the bending-moment responses. The increase at 18,000 feet resulted from the large single spike in the smoke-trail wind measurement at that altitude (see Fig. 7), whereas the increase at 35,000 feet resulted from the response of the vehicle to the sequence of wind fluctuations. In both cases the increase in load comes from the response of the elastic modes which usually are not excited by the smoothed wind profiled.

As has been noted earlier, design criteria established within the aerospace industry account for sharp wind fluctuations by superposition of the loads from some gust, such as a step or a (1-cosine) shape, on the loads calculated for an averaged wind profile. In an attempt to determine if such a procedure would account for the increase in load experienced by the vehicle due to the smoke-trail profile, as compared to the averaged profile, the bending-moment response of the Scout was calculated at various altitudes for a series of step gusts. These loads were then added to the loads due to flying the simulated balloon wind profile. It was found that an 18 ft/sec step gust was required at 18,000 feet to make the total bending moment reach the level predicted by flying the smoke-trail profile. Similarly, at 35,000 feet a 6 ft/sec step gust was required. For this case of the Scout vehicle, a superposition
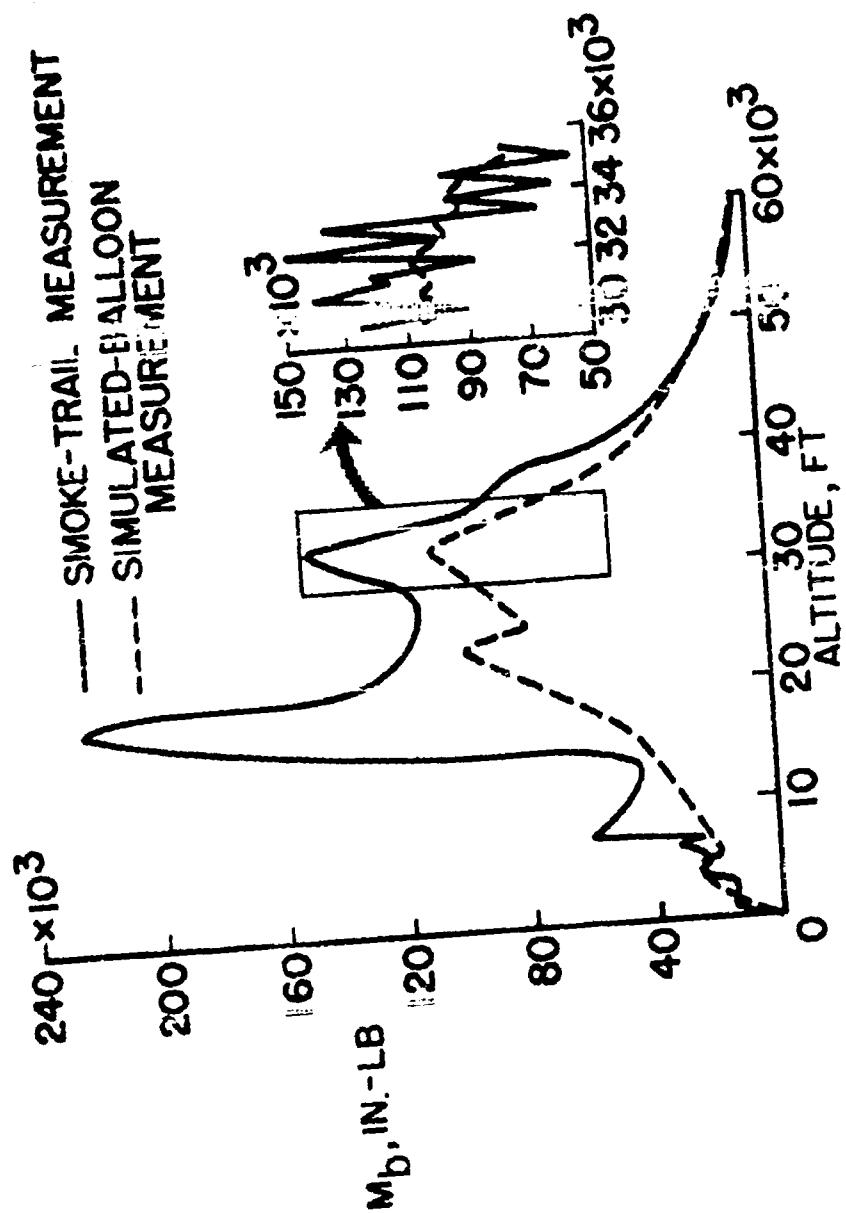
FIG. 8. Bending-moment Envelope due to Winds.

217

of loads of the type considered in the vehicle design resulted in loads as severe as those calculated for the smoke-trail winds. As has been noted, however, few smoke-trail measurements have been made and the wind speeds and wind gradients exhibited herein are by no means maximum conditions.

An additional factor of interest concerns the correlation between the steady or mean wind speeds and the higher frequency fluctuations about the mean. The wind velocities measured so far from smoke-trail soundings are relatively mild, the velocities of Fig. 7 never exceeding 80 fps. The fluctuations, on the other hand, appear quite large. In this connection it might be noted from Fig. 7 that the fluctuation from the mean is 27 fps at 18,000 feet. There appears to be no sure method of extrapolating the conditions for these relatively low wind speeds to the much higher wind speeds used in design. Although it might be expected that the fluctuations do not increase in direct proportion to the wind speed, a firmer answer to this question awaits the acquisition of higher-speed wind data. In this regard, measurements recently obtained at Wallops under considerably stronger winds at altitudes of 30,000 to 35,000 feet will be of assistance.

CONCLUSION

The smoke-trail method offers unique advantages as a wind-measuring tool for missile applications; the most important of these is the ability to obtain a precise measure of both the short- and long-wavelength wind disturbances along missile flight paths. An examination of the bending-moment responses for a missile flight through a given wind field as determined by a smoke-trail measurement and by a balloon measurement indicated considerably more severe loading conditions for the smoke-trail winds. The increased loadings are attributed to the bending-moment amplifications resulting from excitation of the structural modes by the unsteady wind input. A brief consideration of current design practices indicates that these effects of sharp wind fluctuations are allowed for to a degree by the application of varying forms of loads superposition. A significant feature of the smoke-trail measurements is that they provide a basis for evaluating the adequacy of more simplified design procedures. The smoke-trail wind measurements are being extended to the severer wind conditions for a more complete investigation of these problems.

REFERENCES

1. R. M. Henry, G. W. Brandon, H. B. Tolefson, and W. E. Lanford, The Smoke-Trail Method for Obtaining Detailed Measurements of the Vertical Wind Profile for Application to Missile-Dynamic-Response Problems, NASA TN D-976, September 1961.

2. H. B. Tolefson, and R. M. Henry, A Method for Obtaining Wind Shear Measurements for Application to Dynamic Response Problems of Missile Systems. Jour. of Geo. Res., Vol. 66, No. 9, September 1961.

3. E. L. Merritt, Analytical Photogrammetry, Pitman Publishing Corp. New York, 1958.

4. R. M. Henry and G. W. Brandon, The Use of Smoke Trails as Wind Sensors, Pres. to the Instrument Society of America and the American Meteorological Society, Los Angeles, California, September 11-15, 1961.

The Jet Stream Profile and Associated Turbulence

GEORGE S. McLEAN, JR.

GEOPHYSICS RESEARCH DIRECTORATE

AIR FORCE CAMBRIDGE RESEARCH LABORATORIES

ABSTRACT

The general discussion of turbulence is followed by a discussion of turbulence in relation to jet streams. Horizontal and vertical wind profiles are combined into a model of the jet stream. Distribution of turbulence as observed in Project Jet Stream flights around the jet stream core is shown. Observations of severe turbulence (with a maximum true gust velocity of 31 ft sec^{-1}) in convective clouds in a well developed squall line and observations of even stronger clear air turbulence (true gust velocities up to 37 ft sec^{-1}) in a jet stream situation are discussed. An estimate of the intensity of turbulence and the vertical extent of turbulent layers on a typical wind profile through a jet stream is presented. Some important considerations for the occurrence of turbulence appear to be the change of vertical wind shear with height, thermal stability, horizontal convergence in upper air troughs, and strong winds. The most severe turbulence that could have an effect on aerospace vehicles can be expected to be encountered in front of an upper air trough in the region of jet stream winds.

DISCUSSION OF TURBULENCE

Turbulence in the atmosphere is described[1] as those motions smaller in scale than the motion that is designated as the mean flow. Larger scale motions occur as drafts in convective clouds and vertical motions in such phenomena as mountain waves. Turbulent eddies with dimensions of 50 to 500 feet can cause yawing, pitching and rolling of aircraft as well as other erratic motions, and would influence any vehicle passing through the region.

Turbulence over land is dependent upon terrain only to a limited degree at altitudes of 30,000 to 40,000 feet. Overall there is more turbulence in winter than in summer (due generally to stronger winds and stronger wind shears). Maximum turbulence is found in the vicinity of jet streams. A figure of 5 percent of the time for turbulence over ground is quoted from NACA[5] and can be compared with a low occurrence of 0.2 percent[4] of time over water, but

in jet streams the overall average is about 12 percent of the time with tur-
bulence encountered up to 40 percent of the time in particular sectors near
the jet stream core.[3,4]

HORIZONTAL PROFILE THROUGH JET STREAMS

Average horizontal wind profiles through jet streams are shown in Fig.
1. This figure shows average wind speed profiles across jet streams for
various profile classes. Wind speeds are expressed in percent of the maxi-
mum wind speed. These profiles show rather smooth values on crossing the
jet stream as would any average profile, so in general smaller scale features
would be expected on an individual profile. There are not the intense varia-
tions that have been indicated in the past, however.

VERTICAL PROFILES IN JET STREAMS

A typical vertical profile of wind speed versus height through a jet
stream is shown in Fig. 2. This is an actual wind profile measured by GMD-2
equipment at Bedford, Massachusetts on 3 April 1957.[2] There are small
variations in the wind in the vertical but not the irregular profile with many
smaller maximums as have been measured by less accurate equipment.
Figure 3 shows average profiles of wind speed in the vertical measured from
the level of maximum wind. Generally, this figure shows stronger shear
with stronger wind speeds.

THE JET STREAM MODEL

The principal features of jet streams have been combined and presented
in the form of a Jet Stream Model (Fig. 4). This model is based on a com-
bination of aircraft observations made by the Geophysics Research Directorate's
Project Jet Stream over the eastern United States from 1953 to 1957.[3,4]
This is an average model of the jet stream. Particular jet streams vary in
many ways just as other meteorological phenomena differ from their ideal-
izations. Tropopause breaks vary from case to case, as do vertical and
horizontal wind shears, upper fronts, etc. The deviations of particular jet
streams from the mean structure may often be inferred from synoptic data,
if these data are plentiful. However, without clear evidence of deviations,
it must be assumed that the average structure exists.

222
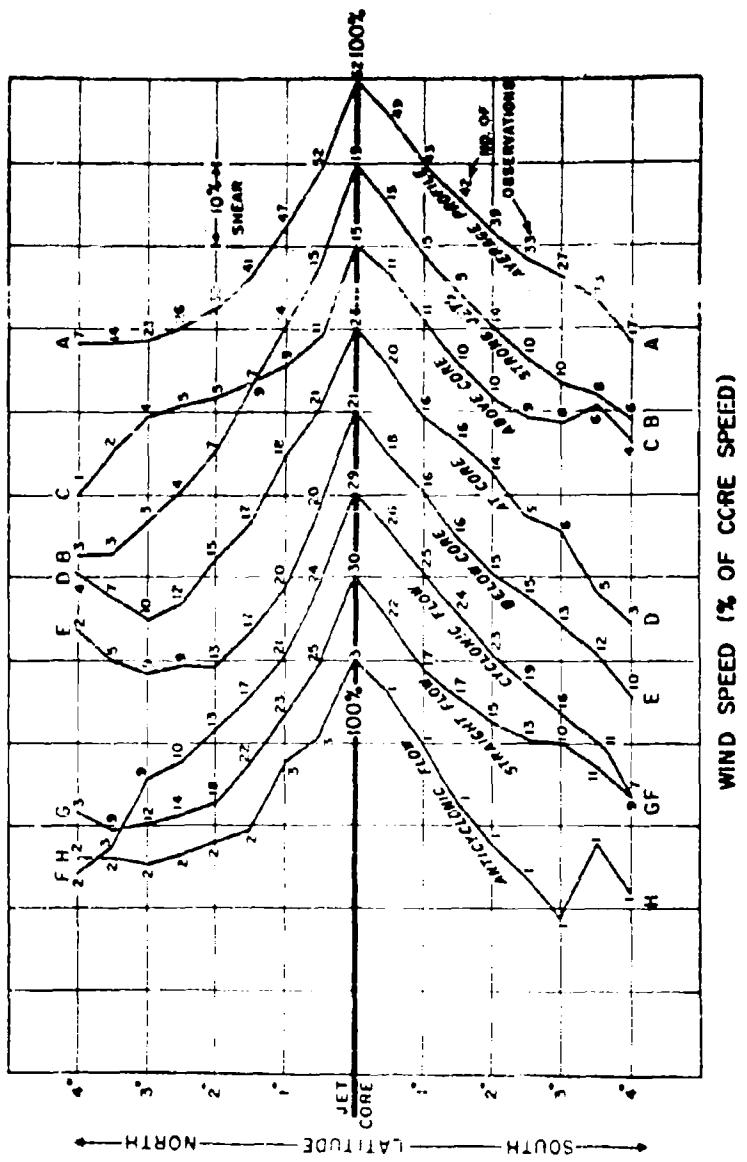
FIG. 1. Average wind speed profiles across jet stream for various profile classes. Wind speeds are expressed in percent of the maximum speed.

223
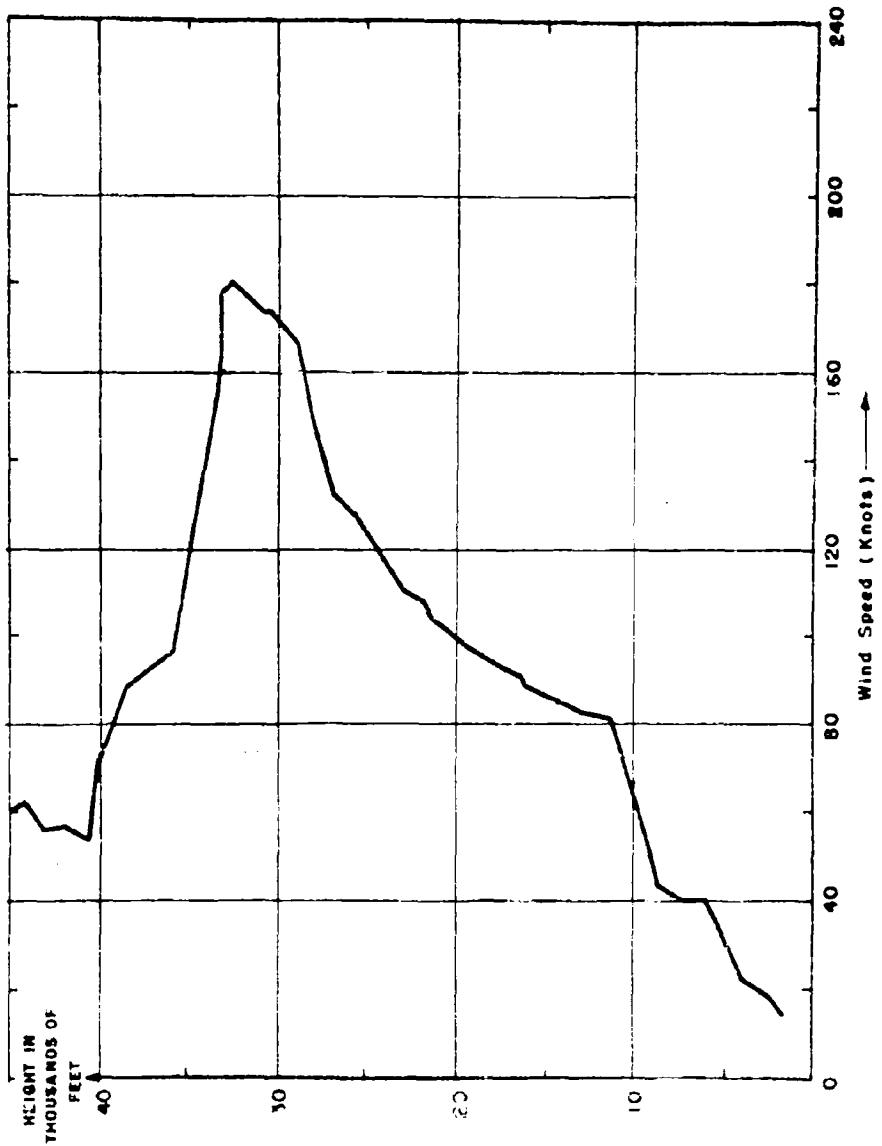
FIG. 2. Typical profile of wind speed vs height through a jet stream. (Measured by GMD-2 equipment at Bedford, Massachusetts on 3 April 1957.)
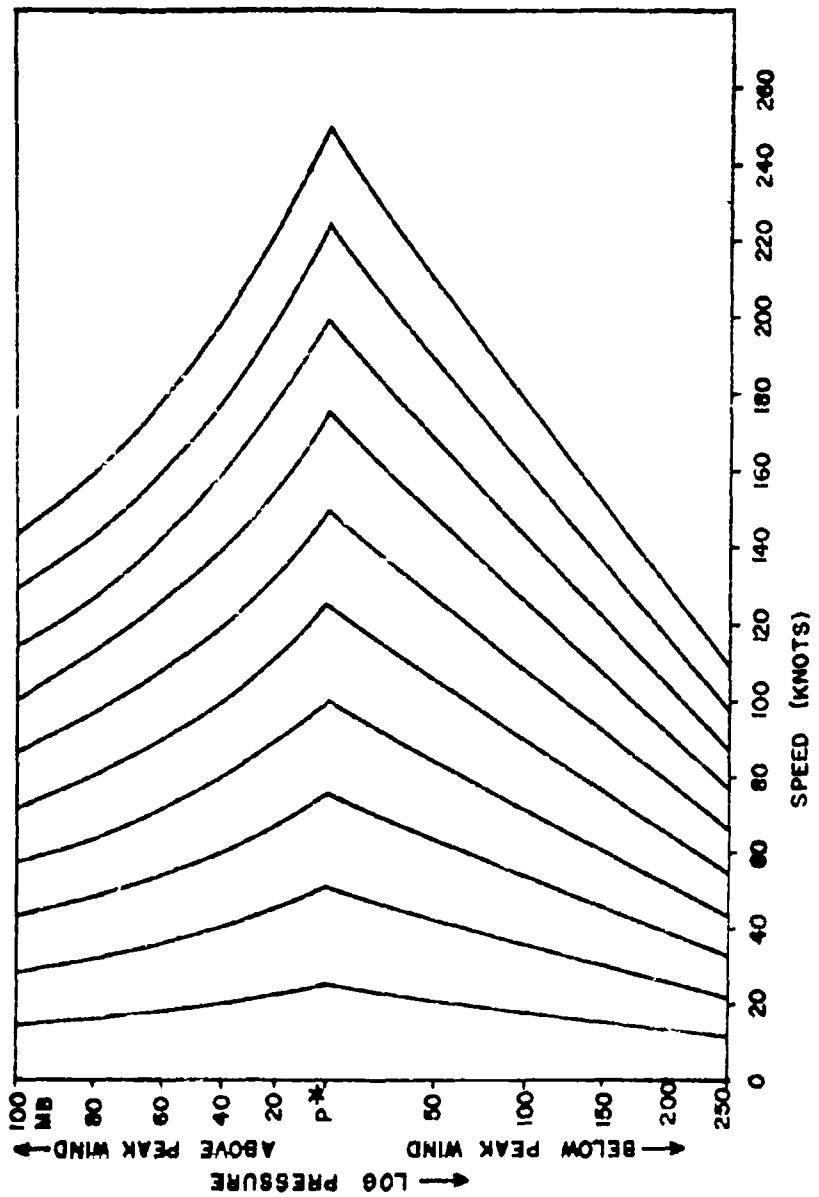
FIG. 3. Average profiles of wind speeds vs height measured from the level of maximum wind. Curves are drawn for maximum winds at 25 kt intervals.
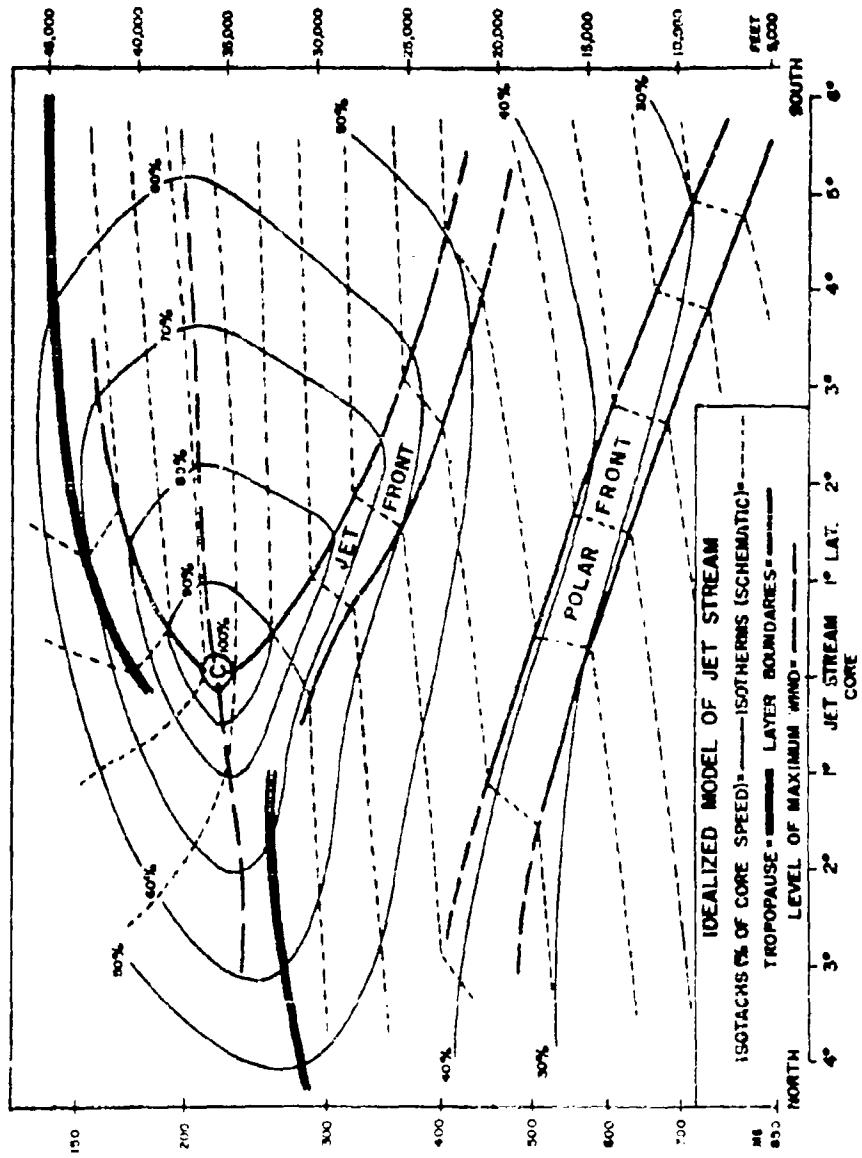
FIG. 4. Average structure of the jet stream in a cross section perpendicular to the flow.

DISTRIBUTION OF TURBULENCE ABOUT THE
CORE

The frequencies of observed turbulence (as measured by Project Jet Stream aircraft) are shown in Fig. 5. Observations of turbulence of just perceptible intensity (called 'very light' by crew members) are classed as nonexistent in this tabulation. From this figure it can be seen that turbulence is most likely to be found north of the jet stream core near the polar tropopause and above the core along the tropical tropopause.[1,7] Indication of a maximum is also found in the 'jet stream front.' There is less turbulence in the jet core itself than in the surrounding areas.

SEVERITY OF TURBULENCE

Much of the turbulence observed by Project Jet Stream aircraft was classed as light turbulence (true gusts less than 5 feet per second). A considerable amount was classed as moderate turbulence gusts (greater than 10 feet per second) and some was classed as severe turbulence (gusts greater than 20 feet per second). During one flight into a squall line, convective turbulence with gusts over 20 feet per second was encountered a good part of the time that the aircraft was in clouds and at one point measured a gust of 31 feet per second.[8] The strongest turbulence observed by Project Jet Stream, however, was observed in clear air in a moderately strong jet stream (146 knots). On this flight No. 27 (Fig. 6), the most severe turbulence encountered on each of three traverses through the same location was 32, 35, and 37 feet per second, true gust velocity, respectively. The synoptic charts and terrain in this case gave no indication of turbulence in this region.

PROPERTIES OF THE FLOW INDUCIVE
TO TURBULENCE

A combination of factors seems to be of importance in the location of clear air turbulence. There are many theories as to the best method of forecasting the occurrence of turbulence, but no one method stands out above the others. One important factor that has been studied perhaps to the greatest degree is the vertical wind shear. Even more important is the change of the vertical wind shear. Another important feature that showed up in Project Jet Stream studies is the local mesoscale horizontal convergence. This is probably a contributing factor and should be studied further.
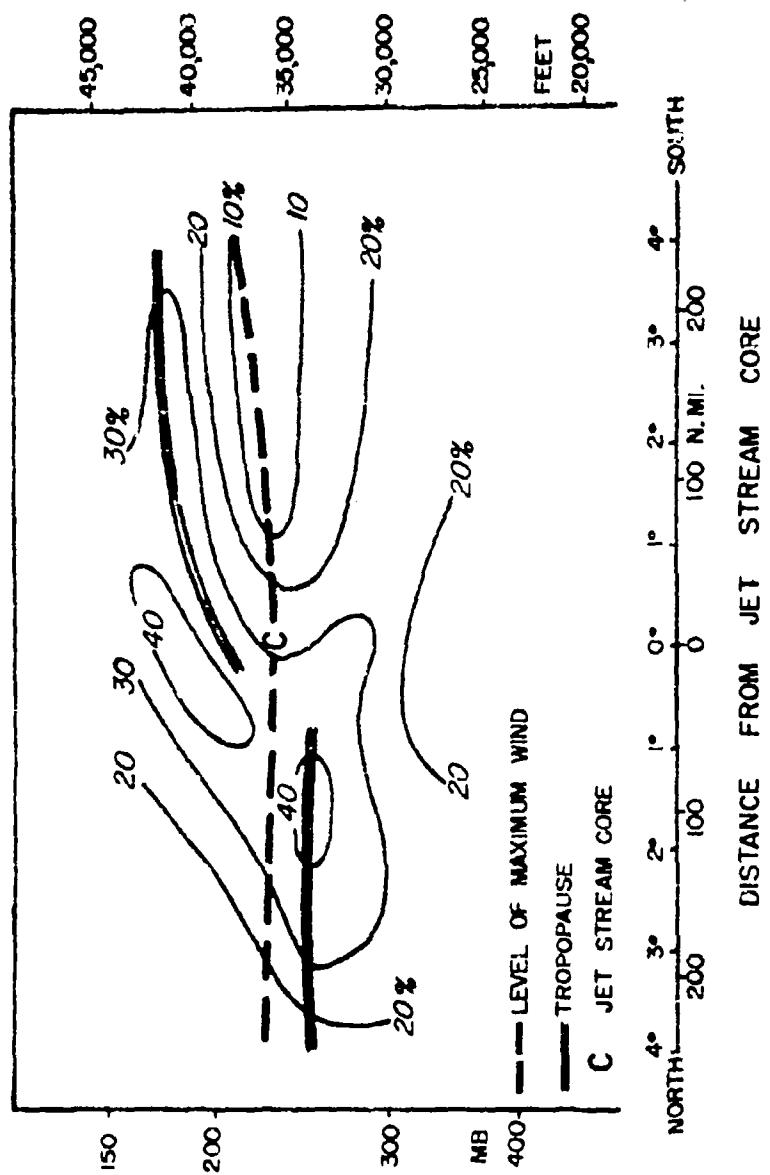
FIG. 5. Frequency (percent) of turbulence in various sectors of the jet stream cross section.
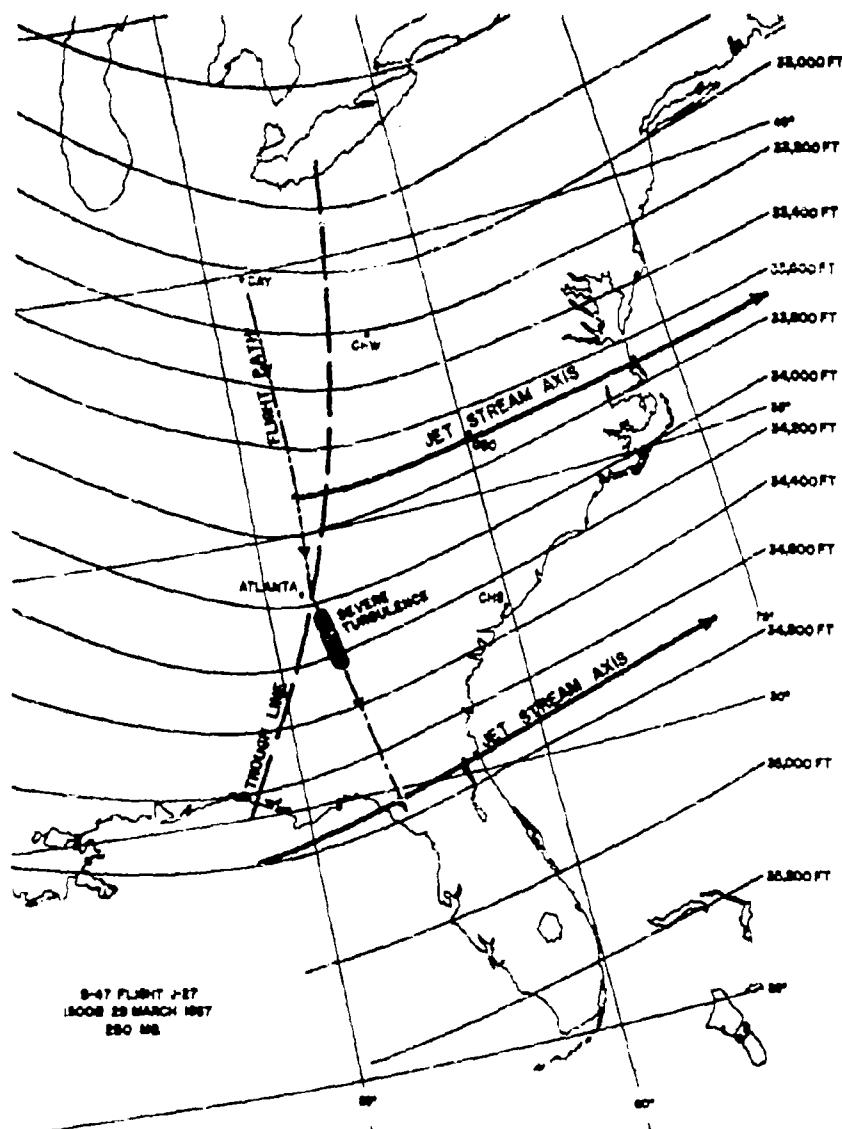
FIG. 6. Severe clear air turbulence encountered by B-47 aircraft
near intersection of trough line and strong horizontal
shear zone during traverses of double jet at 10 to 12 km
height. (H. Marx)

The curvature of the wind flow pattern at jet stream altitudes is also considered an important factor. Project Jet Stream flights, in front of troughs and at intersection of jet streams (such as Flight No. 27, Fig. 6) encountered moderate or severe turbulence in nearly every case. The severest turbulence in this situation would be found to the north and slightly below the jet stream and in the vicinity of the polar tropopause. Strong updrafts were also found in these cases.

VERTICAL SHEAR AND MICROSCALE
TURBULENT EDDIES

If a vertical sounding has many variations in the wind, such as peaks and minimums, it is difficult to describe the turbulent eddies created. On the other hand, where can turbulence be expected to be encountered in looking at a vertical wind profile through a jet stream and studying the vertical maximums and the vertical gradient of the wind shear. This has been studied extensively and principles have been theoretically derived in an effort to explain the presence of turbulence. [1,7]

Lake used a number first derived by Scorer[2] in the hopes that it would provide a criterion for estimating the intensity of clear air turbulence.

The Scorer number

$$
= \frac{V \dfrac{\Delta^2 V}{\Delta Z^2}}{\dfrac{g}{\theta} \dfrac{\Delta \theta}{\Delta Z}} \quad ,
$$

where V is the wind speed, $\dfrac{\Delta^2 V}{\Delta Z^2}$ is the vertical gradient at the wind shear, g is gravity, θ is potential temperature, and $\Delta \theta / \Delta Z$ is the vertical gradient of potential temperature.

Lake used turbulence data gathered during the U. S. Synoptic High-Altitude Gust Program in 1953 and found, generally speaking, that as the Scorer number increased from negative through zero to positive, the intensity of turbulence changed from none to slight to moderate.

In this present study, independent data from Project Jet Stream flights were used. A large number of cases were not available, but by studying cases during which ascents and descents were made through turbulent layers, relatively good agreement was found with studies by Lake.

In regions above the jet stream core, it was usually found that moderate turbulence was associated with a large negative wind shear, a positive curvature to the wind profile and a thermally stable atmosphere. In regions below

230

the jet stream core where the positive wind shear is strongly increasing with height, the vertical wind shear gradient can counteract thermal stability and cause turbulence below the core. Kuettner[6] attributes this to the existence of traveling gravitational waves in the jet stream, which will appear in a region of instability.

CONCLUSIONS

From these studies it seems probable that turbulence would be found on certain sections of a vertical profile such as the 'Sissenwine Design Criteria Profile' (Fig. 7).[10] Generally, turbulence would be expected to be observed in the regions where the shear begins to increase sharply with height (point A) with an upper limit at B, below the core, and also above the core from C to D where there is a strong positive curvature of the wind profile. These turbulent layers would be in the order to 2000 to 5000 feet in depth, dependent upon the wind speed, wind shear, curvature of the wind profile and the thermal field. Climatology of detailed wind profiles collected by the methods described in the two previous papers will undoubtedly take the guessing out of the supposition of this turbulence on these general profiles. In the meantime, for design purposes, some arbitrary gust, say at least ±20 feet per second with a half wave length of 100 feet, should be added to the critical design profile to arrive at the bending moment responses if the vehicles must fly through most of the winter situation jet streams.

REFERENCES

1.   J. Clodman, G. M. Morgan, and J. T. Ball, High Level Turbulence, Research Division, College of Engineering, New York University, Contract AF19(604)-5208, 1960.

2.   N. Dvoskin and N. Sissenwine, Evaluation of AN/GMD-2 Wind Shear Data for Development of Missile Design Criteria, Air Force Surveys in Geophysics No. 99, Geophysics Research Directorate, AFCRL, 1958.

3.   R. M. Endlich, and G. S. McLean, The Structure of the Jet Stream Core, J. Meteor. 14, 543-562, 1957.

4.   R. M. Endlich, and G. S. McLean, Analyzing and Forecasting Meteorological Conditions in the Upper Troposphere and Lower Stratosphere, Air Force Surveys in Geophysics No. 121, Geophysics Research Directorate, AFCRL, 1960.
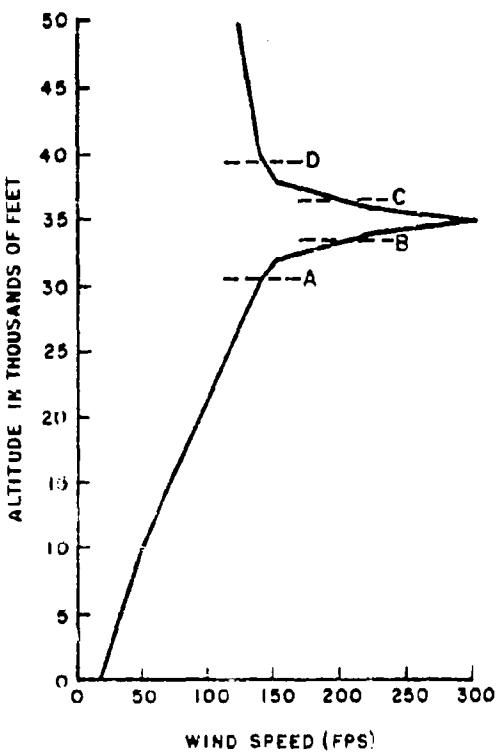
FIG. 7. Expected location of turbulence on Sissenwine Design
Criteria Profile. Sectors AB and CD are regions of
marked change in shear where severest turbulence
might normally be found.

232

5. M. W. Fetner, Summary of Locations and Extents of Turbulent Areas During Flight Investigations of the Jet Stream, NACA Research Memorandum SL55HO4a, 1955.

6. J. Kuetiner, On the Possibility of Soaring on Traveling Waves in the Jet Stream, Aero Eng. Rev. 11, No. 12, 1-7, 1952.

7. H. Lake, A Meteorological Analysis of Clear Air Turbulence, Geophysics Research Papers No. 47, Geophysics Research Directorate, AFCRL, 1956.

8. G. S. McLean, Observation of Severe Convective Activity in a Squall Line, Bull. Amer. Meteor. Soc. 42, 252-264, 1961.

9. R. S. Scorer, Theory on Waves in the Lee of Mountains, Quar. Jour. Roy. Met. Soc. 76, 323-341, 1949.

10. N. Sissenwine, Windspeed Profile, Windshear, and Gusts for Design of Guidance Systems for Vertically Rising Air Vehicles, Air Force Survey in Geophysics No. 57, Geophysics Research Directorate, AFCRL, 1954.

AIR FORCE SURVEYS IN GEOPHYSICS

No. 1. (Classified Title), *V. K. Widger, Jr.,, Mar 1952. (SECRET/RESTRICTED DATA Report)*

No. 2. Methods of Weather Presentation for Air Defense Operations *(U), V. K. Widger, Jr., Jun 1952. (CONFIDENTIAL Report)*

No. 3. Some Aspects of Thermal Radiation From the Atomic Bomb *(U), R. M. Chapman, Jun 1952. (SECRET Report)*

No. 4. Final Report on Project 8-52M-1 Tropopause *(U), S. Coroniti, Jul 1952. (SECRET Report)*

No. 5. Infrared as a Means of Identification *(U), N. Oliver and J. V. Chamberlain, Jul 1952. (SECRET Report)*

No. 6. Heights of Atomic Bomb Results Relative to Basic Thermal Effects Produced on the Ground *(U), R. M. Chapman and G. V. Vares, Jul 1952. (SECRET/RESTRICTED DATA Report)*

No. 7. Peak Over-Pressure at Ground Zero From High Altitude Bursts *(U), N. A. Haskell, Jul 1952. (SECRET Report)*

No. 8. Preliminary Data From Parachute Pressure Gauges, Operation Snapper, Project 1.1 Shots No. 5 and 8 *(U), N. A. Haskell, Jul 1952. (SECRET/RESTRICTED DATA Report)*

No. 9. Determination of the Horizontal *(U), R. M. Chapman and M. H. Seavey, Sep 1952. (SECRET Report)*

No. 10. Soil Stabilization Report, *C. Molineux, Sep 1952.*

No. 11. Geodesy and Gravimetry, Preliminary Report *(U), R. I. Ford, Sep 1952. (SECRET Report)*

No. 12. The Application of Weather Modification Techniques to Problems of Special Interest to the Strategic Air Command *(U), C. E. Anderson, Sep 1952. (SECRET Report)*

No. 13. Efficiency of Precipitation as a Scavenger *(U), C. E. Anderson, Aug 1952. (SECRET/ RESTRICTED DATA Report)*

No. 14. Forecasting Diffusion in the Lower Layers of the Atmosphere *(U), B. Davidson, Sep 1952. (CONFIDENTIAL Report)*

No. 15. Forecasting the Mountain Wave, *C. F. Jenkins, Sep 1952.*

No. 16. A Preliminary Estimate of the Effect of Fog and Rain on the Peak Shock Pressure From an Atomic Bomb *(U), H. P. Gauvin and J. H. Healy, Sep 1952. (SECRET/RESTRICTED DATA Report)*

No. 17. Operation Tumbler-Snapper Project 1.1A Thermal Radiation Measurements With a Vacuum Capacitor Microphone *(U), M. O'Day, J. L. Bohn, F. H. Nadig and R. J. Cowie, Jr., Sep 1952. (CONFIDENTIAL/RESTRICTED DATA Report)*

No. 18. Operation Snapper Project 1.1. The Measurement of Free Air Atomic Blast Pressures *(U), J. O. Vann and N. A. Haskell, Sep 1952. (SECRET/RESTRICTED DATA Report)*

No. 19. The Construction and Application of Contingency Tables in Weather Forecasting, *E. V. Vahi, R. M. White and H. A. Salmela, Nov 1952.*

No. 20. Peak Overpressure in Air Due to a Deep Underwater Explosion *(U), N. A. Haskell, Nov 1952. (SECRET Report)*

No. 21. Slant Visibility, *R. Penndorf, B. Goldberg and D. Lufkin, Dec 1952.*

No. 22. Geodesy and Gravimetry *(U), R. I. Ford, Dec 1952. (SECRET Report)*

No. 23. Weather Effects on Radar, *D. Atlas et al, Dec 1952.*

No. 24. A Survey of Available Information on Winds Above 30,000 Ft., *C. F. Jenkins, Dec 1952.*

No. 25. A Survey of Available Information on the Wind Fields Between the Surface and the Lower Stratosphere, *V. K. Widger, Jr., Dec 1952.*

No. 26. (Classified Title), *A. L. Aden and L. Katz, Dec 1952. (SECRET Report)*

No. 27. (Classified Title), *N. A. Haskell, Dec 1952 (SECRET Report)*

No. 28. A-Bomb Thermal Radiation Damage Envelopes for Aircraft *(U), R. H. Chapman, G. V. Vares and M. H. Seavey, Dec 1952, (SECRET/RESTRICTED DATA Report)*

No. 29. A Note on High Level Turbulence Encountered by a Glider, *J. Kuettner, Dec 1952.*

AIR FORCE SURVEYS IN GEOPHYSICS (Continued)

AIR FORCE SURVEYS IN GEOPHYSICS (Continued)

AIR FORCE SURVEYS IN GEOPHYSICS (Continued)

AIR FORCE SURVEYS IN GEOPHYSICS (Continued)